Structural Studies of the Corneal Stroma

Thesis

STRUCTURAL STUDIES OF THE CORNEAL STROMA

Thesis submitted for the degree of Doctor of Philosophy

in the Discipline of Biophysics

by

Julia Mary Goodfellow, BSc

Open University

October 1975

STANFORD UNIVERSITY
STANFORD, CALIFORNIA 94305

DEPARTMENT OF CHEMISTRY

9th March, 1976

Dear Mr Sullivan,

Thank you for your letter of 26th February confirming that the Senate had approved the award of Doctor of Philosophy. I am quite willing to allow my thesis to be made available to readers in the library and to be photocopied subject to the discretion of the Librarian

yours sincerely,

Julia Goodfellow

JULIA M. GOODFELLOW

Abstract.

The corneal stroma is an unusual connective tissue in that it is transparent to visible light and that it can swell to many times its original weight when placed in salt solution with a consequent loss in transparency with swelling. The stroma consists of lamellae of parallel collagen fibrils, of uniform diameter, embedded in a ground substance. It also contains glycosaminoglycans which are negatively charged at physiological pH. The organisation of the collagen fibrils and their relationship to the glycosaminoglycans are important when considering both the transparency and the ability to swell of the fresh tissue and the reason for the loss in transparency on swelling.

Experiments were undertaken to study changes in the stroma which take place on swelling as a function of the pH and the ionic strength of the bathing solution. Initially, the total water content per unit dry weight is studied as a function of the bathing solution and the time of swelling. Low-angle x-ray diffraction techniques are used to monitor the centre-to-centre distance between the collagen fibrils (the interfilament spacing) as a function of hydration as well as the reflections due to the packing of the tropocollagen molecules from which the fibrils are formed. Thirdly, the fixed charge concentration due to the polyelectrolytes in the stroma is calculated from microelectrode measurements of the potential difference which exists between the stroma and the bathing solution. Fourthly, the absorbance of the stroma to visible light is measured as a function of hydration in various solutions.

The results of these four different techniques indicate the importance of the fixed charge on the corneal macromolecules. This fixed charge must give rise to an unequal distribution of permeant ions between the stroma and the bathing solution which leads to a Donnan, osmotic, pressure. This Donnan pressure appears to be the main cause of swelling. Measurement of the fixed charge from the potential difference which also arises from the unequal distribution of permeant ions, shows similar behaviour with pH and ionic strength to that estimated from the swelling results. This dependence is also similar to the behaviour expected from polyelectrolyte gel theory. The value of the interfilament spacing, for a given hydration, is shown to depend on the pH of the bathing solution so that more fluid goes into the lattice of fibrils with some solutions that with others. The water not going into the lattice may be in the form of 'lakes' as suggested by Benedek (1971). The reflections from the packing of tropocollagen molecules along the fibrils are unusual in that, although they index on a repeat of around 66nm, the first order reflection is absent. The Patterson function from such a X-ray pattern is calculated and compared with that from scleral collagen which shows the first order reflections. Finally, the transmission of light by the stroma is shown to decrease linearly with increasing hydration, the rate of decrease being dependent on the pH of the bathing solution. Correlations between the rate of loss of transmission and the rate of swelling as well as between the percentage water in 'lakes' with the transmission of the stroma are discussed.

Acknowledgements.

I would like to thank my supervisor, Professor G.F. Elliott, for his continual help and encouragement over the past three years as well as for initiating these studies. Dr. A.E. Woolgar has kindly read through this thesis and made many helpful comments as well as taking part in many earlier discussions of my work. Dr. P. Cooke taught me all I know about electron microscopy and undertook the light diffraction studies with me. Dr. D. Gayton and Mr. G. Naylor designed and constructed the microelectrode apparatus. Members of the Molecular Biophysics Group, Oxford University, allowed me to use their apparatus and Dr. B. Doyle and Mr. D. Hulmes took part in useful discussions on the structure of collagen. I also wish to thank the many other friends and collegues who have helped in many different ways. They include Mr. P. Finnemore, Mr. P. Goodfellow, Mr. A. Guthrie, Ms R. Loving and Dr. C. Martin.

List of Contents

Chapter 2 Swelling Properties of the Corneal Stroma.

Table of Illustrations

Chapter 4.

Chapter 5.

CHAPTER 1

Introduction

I Why Study the Corneal Stroma

Unlike other connective tissues, e.g. skin and cartilage, the corneal stroma is transparent to visible light. The reason for this transparency must be found in the structure of the cornea. Similarly to other connective tissues, it is formed from collagen fibrils embedded in a ground substance. Glycosaminoglycans are also known to be present in the corneal stroma. The collagen fibrils of the cornea are arranged parallel to each other and have approximately uniform diameter. In cartilage and sclera, the collagen fibrils are not parallel to each other and their diameters range over an order of magnitude.

Several tissues are known to consist of ordered arrays of long cylindrical charged molecules. These systems have been listed by Elliott (1968) and include equilibrium gels of tobacco mosaic virus, TMV, the A-band proteins of myosin filaments in striated muscle, microtubules and the mitotic apparatus in the dividing cell. A similar list has been drawn up by Brenner and McQuarrie (1973). One of the most characteristic properties of TMV and the myosin filaments in muscle is that the interparticle distance depends on the pH and ionic strength of the external solution. (Bernal and Frankuchen, 1941; Rome, 1968).

It is suggested that the corneal stroma may be analagous to these systems in consisting essentially of ordered arrays of long cylindrical fibrils of collagen and with the glycosaminoglycans providing the fixed charge concentration at physiological pH. The cornea is a more complicated

system than muscle in that two components are present - collagen and glycosaminoglycans - and the physical relation between them is still under discussion.

The cornea has two properties which aid the investigation of its structure. First, the stroma is transparent to visible light. This occurs even though the collagen fibrils are thought to have a different refractive index to that of the ground substance (Maurice, 1957; Smith, 1969) and would be expected to scatter light. It has been suggested by Maurice (1957) that the arrangement of the fibrils is important in maintaining the transparency of the tissue. The second property related to the structure is the ease with which the corneal stroma can swell, imbibing many times its original weight in fluid. (Chapter 2). A noticeable decrease in the transparency of the tissue occurs on swelling and is presumably due to a change in the arrangement of the fibrils.

Two obvious ways of monitoring changes in the structure are thus available for the study of the cornea. We can measure the swelling properties (Chapter 2) and also the transparency of the corneal stroma and its change on swelling (Chapter 5).

II The Cornea in Relation to the Eye

The cornea and sclera form the continuous outer protective coat to the eye (Fig. 1). They must be tough to withstand pressure from within the eye, the intraocular pressure, and also to protect the eye from damage on impact. Maurice (1962) has shown that the eye globe can withstand pressures up to 5×10^4 kg m^{-2} which is the order of a hundred times larger than normal intraocular pressure. (Leydhecker et al (1958) found a distribution of pressure within human eyes. The greatest probability occured at 16 mm

Hg i.e. .02 $kgcm^{-2}$). The cornea as well as having this protective role is transparent. It refracts light falling on its curved surface helping to focus it on to the retina. It has three-quarters of the dioptric power of the eye (Maurice, 1969), the other quarter being due to the lens. It also protects the eye from harmful ultra-violet radiation with wavelength less than 300 nm which might otherwise damage the retina (Kinsey, 1948).

Detailed descriptions of the anatomy of the cornea have been given by many authors (Ranvier, 1881; Virchow, 1910; Cogan, 1951; Jakus, 1954; Maurice, 1962; Payrau et al, 1967 and Maurice, 1969). The cornea of the rabbit is approximately 4 mm thick at the centre, whereas bovine cornea is thicker at about 8mm. The cornea has several distinct layers transverse to the radial direction in the eye (Fig. 2). On the outer surface is the epithelium. This is a cellular layer consisting of five rows of cells in the rabbit but as many as ten in bovine cornea. This layer makes up about ten per cent of the corneal thickness. (For general descriptions of the epithelium see reviews by Payrau et al, 1967 and Maurice, 1969). The second layer is called Bowman's membrane and consists of a disordered array of collagen fibrils. This layer appears structureless when stained for optical microscopy (Maurice, 1969). In some species of fish (elasmobranch) there is a much larger Bowman's region, and this has provoked interest in the mechanisms of transparency of such a large disordered region (Goldman and Benedek, 1967).

The third corneal layer is the stroma, which is 90% of the total thickness of the cornea. This thesis is concerned with the stroma i.e. the cornea minus its cellular layers. The corneal stroma consists of collagen fibrils arranged in a ground substance or matrix. The tissue

is mainly extracellular but some fixed cells (keratocytes) can be seen (Jakus, 1962; Smelser and Ozanics, 1965; McTigue, 1965; Goldman et al, 1968). The fourth corneal layer is Descemet's membrane. It appears structureless in the light microscope but has been found to consist of meshes of collagen fibrils arranged in the form of an equilateral triangle of 110 nm, in ox, though not in other species (Dohlman and Balazs, 1961; Jakus, 1956; Feeney and Garron, 1961). The final corneal layer, the endothelium, is a single layer of cells which cover the entire posterior surface. These cells form a roughly hexagonal network which can be seen on staining and which is next to the aqueous humour of the eye (Speakman, 1959; Kaye et al, 1961; Jakus, 1962; Iwamoto and Smelser, 1965; Blümke and Morgenroth, 1967; Hodson, 1968; Svedburgh and Bill, 1972).

III Structure of the Corneal Stroma.

i) The Lamellae

The corneal stroma consists of many thin sheets or lamellae which always lie parallel to the surface (Fig. 3). In ordinary stained sections, in the light microscope, they appear structureless (Maurice, 1969) but Virchow (1910) found (by injection of chromic acid) that they had a fibrous structure. The fibres within each lamella are parallel to each other as seen in the electron microscope (Schwarz, 1953; Jakus, 1954, 1961; Sandler, 1974). The angle between the direction of the fibrils in neighbouring lamellae, in lower vertebrates, is 90° (Virchow, 1910; Payrau et al, 1967). Bovine and rabbit stromas are similarly made of lamellae of collagen fibrils. However, in these species, the angles made between the axes of the fibrils in neighbouring lamellae are large but not 90° (Maurice, 1969). In the polarising microscope, the lamellae have been shown to extend from one

limbus or edge of the cornea to the other (Maurice, 1969). Their breadth has been roughly estimated at 250μm (His, 1856) but Polack (1961) has shown that the lamellae are more likely 2-3 mm broad. Salzmann (1912) gives values between 1.5 and 2.5μm for the thickness of a lamella. Beef stroma of total thickness .8 mm must be approximately 350 lamellae thick. The lamellae become narrower and appear to interweave in the anterior part of the stroma as they merge into the disordered Bowman's region (Maurice, 1969).

Birefringence measurements show that for the cat cornea the birefringence of the whole cornea is half that of an individual lamella (Stanworth and Naylor, 1953). The theory of Mallard (1884) shows that if the lamellae are very thin, the birefringence of a series of lamellae will depend on the square of the cosine and sine of the angle, a, between the axes of the lamellae. If the lamellae are randomly orientated then

$$\Sigma \cos^2 a = \Sigma \sin^2 a = \tfrac{1}{2}$$

so that the birefringence of all the lamellae in series is half that of an individual lamella. Thus the cat cornea is behaving as a uniaxial crystal (Jenkins and White, 1951). However, the interference pattern between crossed polarizers from bovine stroma is different from cat cornea (Coulombre and Coulombre, 1961). Bettelheim and Vinciguerra (1969) have shown that there is a preferential orientation of the lamellae in bovine cornea using low-angle light scattering techniques. Maurice (1969) also explains the birefringence behaviour of some species as being due to the non-random orientation of the collagen fibrils in the bovine cornea superimposed over a random distribution. Thus the bovine cornea acts as a biaxial crystal i.e. there are two directions in the tissue for which the velocities of propagation of the two polarised waves are equal (Bettelheim and Vinciguerra, 1969; Maurice, 1969; Kaplan and

Bettelheim, 1972).

The sclera is also composed of lamellae or rather continuations of the stromal lamellae. They interweave with each other after dividing into several parts and become more disordered than in the stroma (Maurice, 1969).

Elastic-like fibres have been found in the stroma by Kanai and Kaufman (1973b) but were not seen by Aurell and Holmgren (1941). The presence of such fibres has not been mentioned in other electron microscopic examinations of the cornea (Jakus, 1954, 1962, 1964: Kaye et al, 1962). These fibres have been found in the sclera by Virchow (1910) and Aurell and Holmgren (1941).

(ii) Cells.

The stroma contains a few cells. These are fixed cells, keratocytes, which are flattened parallel to the surface and lie between lamellae as well as in them (Jakus, 1954, 1962). The total volume of the cornea occupied by cells is between two and three per cent in rabbit stroma (Otori, 1967). The cells in the stroma have been described by Jakus (1964) and Tripathi and Tripathi (1972). They have long thin cytoplasmic processes which are orientated parallel to the surface of the cornea. Many cells are in contact with each other but are separated by cells membranes (Jakus, 1964).

(iii) Fibrils.

Schmitt et al (1942) found that beef corneal lamellae consist of long fibrils of constant width, 50nm, embedded in a tough matrix from which it is difficult to tease out the fibrils. This matrix obscures the cross-banding usually associated with collagen fibrils. Wolpers (1944)

obtained cross-striated collagen fibrils of 20nm diameter after fixing and cleaning corneal collagen by sonification. Van den Hooff (1952) also looked at collagen from fixed and unfixed beef corneas. In osmium tetroxide stained, fixed corneas, the fibrils had diameter 35-40nm but they were 45-50nm in unfixed tissue. Both showed typical collagen banding although the ground substance was seen to adhere to the collagen. Schwarz (1953) found that fibrils from human stroma, without their coating of ground substance which had been enzymically digested, had an average diameter of 29nm. Jakus (1954) also showed that fibrils from rat cornea have a circular cross-section and appear parallel to each other within one lamella but not with neighbouring lamellae. The diameter of the fibrils from thin sections was between 20-30nm but when the fibrils were fragmented (so that flattening did not occur as it would in sections), the diameters were larger at 30-40nm. A collagen periodicity of 62.5-70nm along the fibril axis was reported. Garzino (1955) showed that on preliminary cleaning by sonification and distilled water, the fibrilshave a thick adherent coat which thickens every 64nm. With more cleaning, collars of amorphous material adhere every 21nm. François et al (1954) showed that fully cleaned fibrils have a 21nm banding with every third band intensified so that the overall repeat is 64nm. Sometimes a 13nm repeat is also seen. This last paper elucidates the differences between the collagen fibrils from the sclera and from the cornea. The 64nm periodicity is seen very clearly in fibrils from the sclera. However these fibrils have diameters varying from 40-330nm unlike corneal fibrils whose diameters are uniform between 30-35nm. The scleral fibrils are very 'pure' i.e. little or no amorphous ground substance adheres to them. The 21nm banding also appears along scleral collagen fibrils.

Later studies by Schwarz and Graf Keyserlingk (1966), on human cornea, verify the small variation in diameter of the corneal fibrils and also give estimates of the distance between the fibrils which they find to be between 10-40nm. Cox et al (1970), investigating the structure of rabbit cornea, gave the diameter between 12.5 and 32.5nm but with an average of 20.5 $\pm$ 1.5nm.

The most recent investigations using electron microscopy, concentrate on looking at the order of the fibrils as shown in fixed and stained preparations. Maurice (1957) has predicted that the fibrils are arranged in a lattice possibly hexagonal. This theory was based on the early electron microscopy of Jakus. However, Schwarz and Graf Keyserlingk (1966) found no symmetry in the arrangement of the fibrils in the human corneal stroma based on the measurement of fibril positions from electron micrographs. Farrell and Hart (1969) have shown from their electron micrographs that the arrangement of fibrils is neither completely ordered nor completely random. They measured the increase in local density of the fibrils above the average density for the bulk tissue with increasing distance from a central fibril using many fibrils as centres. Thus they generated a radial distribution function for the stroma. Maxima occured at 55nm and also at 110nm. The former peak was more distinct. No further correlations in spacing were found at distances larger than 110nm from the central fibril. These findings have been confirmed by Cox et al (1970).

(iv) Fibres and Superstructures.

Other organisations of fibres have been reported besides the fibrils and the lamellae. Kikkawa (1958) has suggested that a superlattice of

fibres about 13-15μm apart exists and gives rise to a light diffraction pattern. Bettelheim and Vinciguerra(1969) have published low-angle light scattering patterns and birefringence measurements which they suggest indicate a 'symmetric distribution of superstructures' of the size 1-20μm in the cornea. These superstructures have not been verified in the electron microscope except possibly by Schwarz (1953) who sees 'bundles' of fibrils whose size is between 2.5-8μm. Regular cross striations can be seen in the polarising microscope having a 7μm period. (Maurice, 1969). As Maurice points out these superstructures may be due to either the fine corrugation of the lamellae or to the keratocytes (Maurice, 1969).

IV Chemical Composition of the Corneal Stroma.

(i) Total Water Content.

The largest constituent of fresh stroma is water forming 75% of the weight. Exact figures are given by Duane (1949) as 77.77 $\pm$ .63% for beef stroma and 77.67 $\pm$ 1.15% for rabbit stroma. Davson (1955) reports values of between 73.7 - 77.5% with an average at 75.9% for beef cornea. Langham and Taylor's (1956) results of about 75.45% for rabbit are in agreement. Maurice and Riley (1970) review all measurements of water content since 1956 and agree on a value of 78% for beef stroma. In contrast, fresh sclera contains only 68.07 $\pm$ 1.9% water in beef and 68.3 $\pm$ 2.82% in rabbit (Duane,1949).

It is often more useful to give the water content by calculating the hydration of the tissue. The hydration is defined as the weight of water per unit dry weight. It is a ratio and has no units. From Maurice and Riley (1970), a water content of 78% was agreed for fresh

tissue. This is quivalent to a hydration of 3.5. In future, this value will be referred to as normal or physiological hydration of the cornea. The sclera has a hydration of between 2.6 and 2.1 (Fisher, 1933; Krause, 1934; Duane, 1949).

The hydration of the cornea and the corneal stroma have been found to be the same within experimental error by Ehlers (1966) and Otori (1967).

(ii) Water Associated with the Collagen Fibrils.

When dried corneal stroma rehydrates, the initial gain in water content goes to hydrate the collagen fibrils. After a certain hydration, the fibrils themselves no longer increase in size and the imbibed fluid increases the centre-to-centre distance between the fibrils or possibly forms lakes (Benedek, 1971; Kanai and Kaufman, 1973a). In the last section, I discussed the total water content of the tissue but in this section I am interested in the water associated with the fibrils i.e. that water which increases the diameter of the fibrils or fills in the gaps between the tropocollagen molecules from which the fibril is formed.

This water associated with the collagen fibrils has been measured by several different techniques which give different values. This is to be expected because each technique will be measuring a slightly different 'water' i.e. there will be layers of water bound to the collagen with different energies and each technique will measure a different number of layers. This must be kept in mind when comparing the values found for the water associated with the collagen fibrils.

Heringa et al (1940) and Leyns et al (1940) equilibrated dehydrated corneal tissue with water vapour at various degrees of saturation to obtain a sorption isotherm. This isotherm was found to be similar to that of collagen extracted from the tissue. About .8 g water/1g dry tissue was absorbed by the cornea before the isotherm became appreciably different from that of collagen.

Further measurements of the water associated with the collagen can be made using the high angle x-ray diffraction pattern. The major equatorial spacing from this pattern can vary from 10.6 A with dry tissue up to 15-16 Å for moist collagen (Bear, 1952). Maurice (1969) calculated that such a change in spacing corresponds to 120% change in volume of the fibrils if their length remains constant. This would be equivalent to an increase of .9g water per g dry tissue. However, Hertel (1933) found that the equatorial spacing from the collagen of fresh cornea could increase up to 17 Å whereas Adler et al (1949) found a value of 11.2 Å.

Birefringence measurements made by Maurice (1957) indicate that there is a minimum of .4g water / g dry tissue associated with the fibrils. Alternatively, by pressing the tissue the water content can be reduced down to a hydration of one with all water with binding energy less than 10 calories $mole^{-1}$ being removed (Maurice, 1969).

Experiments on the solubility of small molecules, arabinose and alanine, show that a weight equal to 25% of the dry weight of the cornea is not available as a solvent. The distribution of haemoglobin between the stroma and the bathing solution indicate that water amounting to two or three times the dry weight is unavailable as a solvent (Maurice, 1967).

This amount was found to be independent of the hydration of the tissue. However, this very large non-solvent volume is due to the excluded volume effect of the polysaccharide molecules (Laurent, 1968).

Further evidence about the water associated with collagen fibrils has been obtained from nuclear magnetic resonance and infrared absorption studies. These indicate that only a minor fraction of the water is behaving differently to the majority (Isayama et al,1966).

Maurice (1967) has reviewed the evidence on the physical state of water in the cornea. It is concluded that approximately 1g water/1g dried tissue is associated with the collagen fibrils before separation of the fibrils begins.

(iii) Dry Constituents - General.

The main constituent of the dry weight of the corneal stroma is collagen. Its exact percentage of the weight of the tissue can be calculated from estimates of the hydroxyproline content of the stroma. Maurice and Riley (1970) have calculated that this must be between 60% and 70% based on the data of Kapfhammer (1942) and Smits (1957). Polatnick et al (1957) also give a value of 70%. Maurice and Riley (1970) argue that the value of 70% is a minimum figure and conclude that approximately 75% of the dry weight is collagen. Approximately 4.5% of the weight is due to the presence of the glycosaminoglycan (also called acidic mucopolysaccharides), chondroitin sulphate and keratan sulphate (Anseth and Laurent,1961). Other proteins besides insoluble collagen exist. Extracellular proteins form about 20-25% of the weight of the stroma. This category includes glycoproteins (i.e. proteins containing

oligosaccharides), proteins attached to the mucopolysaccharides often called proteoglycans and soluble collagen (1% of the total collagen content). Cytoplasmic proteins form 2% of the dry weight. Salts also exist in the cornea to about 1% of the dry weight. Maurice and Riley (1970) review measurements on the concentration of sodium, potassium and chloride ions in the stroma of various species. In bovine cornea, the concentration of sodium ions is between 140-147 meq kg^{-1} H_2O, of potassium ions is 21-29 meq kg^{-1} H_2O and chloride ions 89.5-99.6 meq kg^{-1} H_2O (Fisher, 1933; and Davson, 1949).

The sclera has higher percentage of nitrogen and hydroxyproline than cornea (Krause, 1934; Kapfhammer, 1942; Polatnick et al, 1957b). It also contains a smaller percentage of soluble collagen i.e. 0.28% of the total collagen content is soluble. Mucopolysaccharides form only 1% of the dry weight i.e. a quarter the percentage in the cornea (Polatnick et al, 1957a). Half of the polysaccharide content is chondroitin-6-sulphate. The other half is due to chondroitin-4-sulphate and dermatan sulphate (Payrau et al, 1967). Approximately 6% of the weight is proteins due to a structural glycoprotein (Robert and Robert, 1967).

(iv) Collagen.

The collagen in the corneal stroma resembles that from other connective tissues but shows some particular differences when compared with non-corneal collagen from the same species. In general, it is characterised by a high percentage of glycine (forming one in every three residues), proline and hydroxyproline (forming 2/9 of the residues) and by the absence of tryptophan. It also contains hydroxylysine. (For reviews see Ramachandran (1967), Gould (1968), Kühn (1969), Yannas (1972)).

Collagen can also be recognised by its well known high angle x-ray pattern discussed in chapter 3.

Both tropocollagen(i.e. soluble collagen) and insoluble collagen have been found, the former being about 1% of the total collagen content of the stroma. Tropocollagen has a molecular weight of about 380,000 and is around 300nm long, 1.5nm in diameter. It is formed from three polypeptide chains wound in a helix about the same axis. (Gould, 1968). Macromolecular complexes of these molecules form fibrils of collagen. Each fibril contains parallel arrangements of the tropocollagen molecules. The exact way in which the molecules are arranged in order to give rise to the known 66nm banding pattern found in electron microscopy of positively and negatively stained tissue is still under discussion (Hodge and Schmitt, 1960; Cox et al 1967; Grant et al, 1967; Smith 1968; Miller and Wray, 1971; Hulmes et al 1973; Doyle et al, 1974a,b). It is assumed by most authors that the tropocollagen molecules are staggered by this repeat distance and that it is this stagger which accounts for the banding. To extend this staggering to three dimensions is not obvious. Smith (1968) has proposed that five tropocollagen molecules form a three dimensional filament in which each molecule is staggered by 1 x D, the length of each tropocollagen molecule being 4.4 x D. Then the filaments combine to give the structure compatible with the known banding patterns by staggering by n x D where n is an integer from 1-4. Other models have been suggested by Cox et al (1967) and Grant et al (1967).

Itoi (1961), using pepsin digested collagen, found that the physicochemical properties or corneal collagen treated in the same way were similar to that of limited pepsin digested collagen from other sources.

This preparation of collagen could be reconstituted into native type fibrils. Lewis et al (1967) compared calf skin and corneal collagens. They found less threonine, serine, methronine, tyrosine, hydroxlysine and lysine in the cornea but more histidine and amide ammonia. The hydrodynamic and optical rotary properties were the same. However, differences were found in the thermal behaviour which could not be explained in terms of differences in amino acid composition.

Freeman et al (1968) have shown that no difference exists between the amino acid composition of tendon collagen and corneal collagen. Their technique used bacterial amylase to free the collagen from the amorphous material which adheres to the fibrils strongly. In the electron microscope typical collagen banding could be seen from fibrils treated in this manner. Grant et al(1969) and Schofield et al (1971) have shown that there are considerable differences in the sugar content of collagens isolated from different sources. For bovine tendon, sclera and cornea, the hexosamine content per 3000 residues were .85, .66 and .3 whereas the hexose content was 6.37, 8.54 and 29.88 respectively. These authors, from studies of many types of collagen, correlated small diameter fibrils (in the cornea) with high sugar content and large average diameter of fibrils with low sugar content. They also show a high sugar content occurs in tissues showing a small range in the diameter of the fibrils and a low sugar content occurs in tissues containing widely differing collagen fibril diameters. They suggested that the high carbohydrate content may prevent hydroxylysine forming cross-links (Bailey and Peach, 1969) or may hold collagen molecules apart by the size of the hydrated sugar molecule. Studies on the collagens from chicken cornea and sclera have shown little or no difference between the collagens (Trelstad and Kang, 1974).

The banding of stained collagen seen in the electron microscope has been investigated by several authors (François et al, 1954; Garzino, 1955; Smith and Frame, 1969). Corneal collagen shows a strong 21nm repeat along the fibrils when negatively stained. Every third one of these bands is more intense leading to the 66nm banding typical of collagen. François et al (1954) have seen bands every 13nm in certain sections. Smith and Frame (1969) have compared the banding of stained fibrils from tendon and collagen (Fig 5). Using PTA at pH 7, tendon collagen shows a light (A) zone and a dark(B)zone. The B zone is longitudinally transversed by 1nm filaments (possibly those suggested by Smith (1969)). It is also crossed transversely by three asymetrically located light bands each of which contains a linear series of white spots. The A zone has five light bands but treatment with weak acid reveals the appearance of 3nm filaments (Chapman and Steven, 1966). Grant et al (1967) and Cox et al (1967) propose that each light band represents a site of cross linking between longitudinal filaments within a fibril. Similarly treated corneal collagen shows identical B zones but three of the light bands from the A zone are absent. The 3nm filaments are visible in the A zone. Smith and Frame (1969) suggest that the absence of these bands in the A zone indicates that there is a lack of cross linking in the central part of the A zone of stained corneal collagen.

(v) Glycosaminoglycans (Mucopolysaccharides).

Mucopolysaccharides are the general name given to the glycosaminoglycans associated with connective tissue. They are usually found attached to proteoglycans i.e. proteins containing sugar molecules. In the cornea the mucopolysaccharides constitute about 4% of the dry weight

(Woodin, 1952; Meyer et al, 1953; Polatnick et al, 1957a; Smits, 1957; Anseth and Laurent, 1961; Laurent and Anseth, 1961; Greilung and Stuhlsatz, 1966). The value of Anseth and Laurent (1961) (which is between 4-4.5%) is lower than that estimated by Woodin (1952) and Smits (1957) but is higher than that of Meyer et al (1953) or Polatnick et al (1957). The higher values were obtained with thorough purification of the polysaccharides (Anseth and Laurent, 1961).

Several different polysaccharides can be isolated differing in chemical composition, molecular weight and charge density. They can be divided into two main groups; galactosamines and glucosamines. The former consists of varying forms of keratan sulphate (Fig. 4). This is a polysaccharide formed from two repeating units, galactose and N-acetyglucosamino-6-sulphate linked by 1e 3e and 1e 4e glycosidic bands (Fig. 4). However, it is now known to be a more complicated structure containing small amounts of sialic acid (0.2-1%) and methyl pentose (0.7-0.1%) both of which may occupy terminal ends (Seno et al, 1965; Berman and Salit-ernik-Givant, 1968). Galactosamine may constitute up to 10% of the hexosamine units in ox-cornea. (Mathews and Cifonelli, 1965). There is some evidence that keratan sulphate has more sulphate than expected because of the presence of galactose-6-sulphate as well as the usual N-acetylglucosamine-6-sulphate (Bhavandran and Meyer, 1966). Further work has indicated the existence of 25% galactose over the amount linked to hexosamine (Bhavandran and Meyer, 1967). These authors report that 74% of the hexosamine residues were sulphated as were 40% of the galactose residues, both in the sixth position. Keratan sulphate is known to be polydisperse with molecular weights ranging between 4,200 and 19,000 (Laurent and Anseth, 1961). However, other studies indicate the existence of more than one molecular species of keratan sulphate existing in the cornea. Wortman (1964) has separated keratan sulphate

into different species on account of their sulphur content. However, Anseth and Laurent (1961) and Berman and Salternik-Givant (1968) have not detected such a low sulphur containing species.

The galactosamine is known to be chondroitin-4-sulphate (Fig. 4). This has a similar polymer structure to keratan sulphate but consists of repeating units of glucose linked by le 3e glycosidic bonds to N-acetylglucosamine-4-sulphate followed by a le 4e glycosidic bond (Fig.4). Again, varying degrees of sulphation have been reported including a species, chondroitin, which is not sulphated to any degree (Meyer et al, 1953; Polatnick et al 1957a; Laurent and Anseth, 1961; Greilung and Stuhlsatz, 1966; Fransson and Anseth, 1967). The molecular weight is around 40,000 and it does not show a large amount of polydispersity.

The distribution of the mucopolysaccharides in the stroma has been studied by Anseth (1961) who found no difference between central and peripheral areas. However, Bleckmann and Wollensak (1974) have found that the maximum concentration of glycosaminoglycans occurs at the centre and decreases to 70% of this value at the periphery.

(vi) Glycoproteins.

In 1957, Dohlman and Balazs isolated a soluble glycoprotein which they extracted by protease digestion. It was high in hexosamine but low in acid mucopolysaccharides. It also contained galactose, glucose, mannose and fucose. Robert and Dische (1963) identified a structural glycoprotein (sometimes known as a neutral glycosaminoglycan) which Robert et al (1963) named keratoglycosaminoglycan (KGAG). It was thought to be an oligosaccharide containing mannose, glucosamine, galactose, sialic acid and fucose. Robert et al (1964) suggested that it is linked covalently

to insoluble collagen. A small fraction is covalently linked to soluble collagen and a third part is freely soluble. Moczar et al (1967) have also identified an oligosaccharide containing mannose, glucosamine, galactose and glucose which may be the same as Robert's KGAG. Robert et al (1964) confirms that KGAG lies within the fibrils and probably within the collagen. It forms a major part of the amorphous material which surrounds and impregnates the fibrils and which is known to mask the electron microscope banding along corneal collagen fibrils. KGAG has been found to occupy 16-16.2% of the dry weight of calf cornea. Polatnick et al (1957b) have isolated a collagen glycoprotein complex. The soluble part was 1% of the dry weight of the stroma and the insoluble part 66%.

The glycoproteins of the cornea have been reviewed by Payrau et al (1967) and Maurice and Riley (1970).

(vii) The Linkage Between the Glycosaminoglycans and Proteoglycans.

The glycosaminoglycans do not occur freely but are found bound to proteins in most connective tissues including the cornea. Saliternik-Givant and Berman (1965) and Berman and Saliternik-Givant (1968) have isolated a native protein-polysaccharide complex from bovine stroma using mild extraction procedures. After passing through a sephadex column, two polymers, namely a glycosaminoglycan and an acid glycoprotein, were detected. Kern and Brassil (1967) obtained three principle fractions on a DEAE cellulose column, one containing high protein with little hexuronic acid or sulphate, one high in galactosamine (chondroitin sulphate) and one high in glucosamine (keratan sulphate).

Keratan sulphate is thought to be linked to the protein by either

an asparagine or a glutamine residue of the protein via a N-glycosidic linkage (Mathews and Cifonelli, 1965; Seno et al, 1965; Greilung and Stuhlsatz, 1966; and Castellani, 1967). Chondroitin sulphate is linked by an O-glycosidic linkage to serine and possibly to a few threonine residues (Muir, 1958; Anderson et al, 1963, 1965; Greilung et al, 1967). Woodin (1954) proposed an electrostatic linkage but none have been found so far.

(viii) Collagen - Glycosaminoglycan Interactions.

In cartilage, proteinpolysaccharide complexes are known to form attachments to collagen (Partridge, 1948; Mathews, 1965; Bangor, 1966; Schubert, 1966; Matthews, 1970). However, the position of the protein-polysaccharide molecules relative to the collagen fibrils is a matter for discussion in the stroma. Mathews (1965) has proposed a model involving the protein cores running parallel to the collagen fibrils and the polysaccnaride chains spreading out at right angles to the core and interacting with the collagen to form cross links. This model has been used by Farrell and Hart (1969), Hart et al (1969) and Hart and Farrell (1971) in their calculations on the structure of the stroma. However, Hodson and Meenan (1969) have demonstrated that silver staining of the cornea results in a beaded appearance of the collagen fibrils concluding that the polysaccharides may be lying around the collagen fibrils. Hodson (1971) proposes a structure of the cornea in which there are no radial cross links between the collagen fibrils. These theories are compared in more detail in chapter 2, section I,v of this thesis in relation to the origin of the swelling pressure of the stroma.

Evidence for an in vitro interaction between glycosaminoglycans and collagen (or glycosaminoglycan-protein complexes and collagen) have been

obtained by many authors (Woodin, 1954; Wood, 1960; Disalvo and Schubert, 1966; Mathews and Decker, 1968; Toole and Lowther, 1968; Lowther and Natarajan, 1972; Öbrink, 1973). Mathews (1970) reviews the literature on the interaction of proteoglycans and collagen and concludes that the interaction is partly electrostatic and partly steric. He states that there is no evidence for covalent interactions between the collagen and the proteoglycans.

Electron microscopy allows the study of the arrangement of material in the stroma but only after the stroma has been fixed and stained. It has been known for many years that the collagen banding seen along the fibrils is obscured by an amorphous material in the cornea (Section II, iii, this chapter). It may be that this is due to the structural glycosaminoglycans (Robert et al, 1964) or possibly the acidic mucopolysaccharide. Smith and Frame (1969) have noted 4.0nm diameter filaments throughout the ground substance of the cornea from araldite sections stained with lead citrate and uranyl acetate. Theses filaments run between adjacent collagen fibrils and lie tangential to the surface of the fibrils. Most filaments are related to two adjacent fibrils. Attachment to points along the fibrils is not uniform but a large number of the spacings occur at the order of 55nm apart. These authors concluded that these filaments are associated with a specific site whithin a period along one collagen fibril and from that site extend orthoganally through the ground substance until they attach to the next collagen fibrils. In mechanically disintergrated cornea stained with phosphotungstic acid at pH 7, 4.0nm filaments are again seen of which some are attached to collagen but others are free about 220nm long. The site of attachment is one of the marginal light bands in the A-zone corresponding to an A-band in positively stained collagen (Nemetschek, 1965). When bismuth nitrate is added to the

latter preparations, filaments 200nm long are seen but they have a beaded appearance. The beads are 7.0nm in diameter.

The stains used in this series of experiments are known to attach to polar amino acids so that it is suggested that the filaments are protein cores of the protein-polysaccharides complex. Bismuth nitrate is thought to cause the polysaccharide to become tightly coiled leading to a conformation resolvable in the electron microscope i.e. 7 nm beads. However, these staining methods do not show the existence of filaments in cartilage but cartilage is thought to have 5x less non-collagenous protein than cornea (Woodin, 1954). Using ruthenium red stain, filaments approximately 3.5nm in diameter have been seen in the electron microscope associated with collagen from articular cartilage and aorta (Myers et al, 1973). The filaments are thought to represent acid mucopolysaccharides (Myers et al, 1969). Both filaments and granules can be seen connecting collagen fibrils in rabbit articular cartilage. The granules can be removed by 4m guanidine chloride leaving clearly visible collagen banding. Similar treatment on rabbit cornea has not yielded any filaments between the collagen fibrils. However, the fibrils were found to be surrounded by coats of dense granules which could be partially removed by treatment with 4M guanidine chloride (Myers et al, 1973).

(V) Comparison of the Corneal Stroma with Other Connective Tissues.

The major difference between the cornea and other connective tissues containing collagen is that it is transparent to visible light. The corneal stroma is made from collagen fibrils whose diameters are small compared with those of sclera or cartilage of adult tissue. Associated

with large diameters is a large range of diameters e.g. sclera. However the corneal fibrils have approximately uniform diameters (section III, iii, this chapter). This may be due to and can be correlated with the sugar content of the tissues (section IV, iv this chapter).

The cornea can swell by taking in many times its own weight in fluid unlike the sclera and cartilage which swell only slightly (chapter 2). This may be due to the interwoven structure of the sclera and cartilage so that the swelling pressure is balanced by the elastic forces cross-linking the tissue (Maroudas, 1975).

Different polysaccharides are found in the cornea compared with those in the sclera or in cartilage. Cornea contains only chondroitin-4-sulphate and keratan sulphate. Cartilage contains both of these as well as chondroitin-6-sulphate. Sclera contains chondroitin-4-sulphate, chondroitin-6-sulphate and dermatan sulphate. Payrau et al (1967) present a table of the polysaccharides present in different connective tissues. The cornea is low in uronic acid content because of the low proportion of chondroitin sulphate (approximately $\frac{1}{3}$ total polysaccharide content). This chondroitin-4-sulphate is under sulphated with sulphate:glucosamine ratio being 1.0-.13:1 in cornea compared with 1.3-1.7 in cartilage (Mathews and Cifonelli, 1965; Seno et al, 1965). The total percentage of the dry weight which is made up of polysaccharides is less in the cornea than in cartilage (Maroudas, 1975) but more than in sclera.

In table 1, differences in composition between the corneal stroma and the sclera are summarised.

VI The Purpose of this Thesis.

The purpose of this thesis is to study the arrangement of the collagen fibrils in the stroma and properties which will influence this arrangement. Using other systems as analogies, as suggested at the beginning of this chapter, it was decided to investigate two important parameters of the external solution i.e. the pH and the ionic strength. Both of these are known to effect the distance between arrays of polyanions. The swelling, being the most noticeable of the properties of the stroma , was studied (Chapter 2) in order to investigate the total intake of water into the corneal stroma. Low-angle x-ray diffraction techniques previously used to investigate the inter-particle distance in TMV and striated muscle (Bernal and Frankucken, 1941; Rome, , 1968) were employed to measure the spacings between the collagen filaments (Chapter 3) from which the volume of water associated with the lattice of fibrils could be found. Microelectrodes were used to measure the fixed charge concentration in the stroma, a parameter which will effect the swelling and the interfilament spacings. Finally, the changes in the absorbance of visible light were investigated as the cornea was swollen in different solutions (Chapter 5).

It is hoped that a better understanding of the origin of the swelling pressure of the corneal stroma will be possible when the pH and ionic strength dependence of the swelling and the fixed charge concentration is known. Comparison of the water associated with the lattice of fibrils and the total water content of the stroma may lead to a knowledge of the amount of water not in the lattice i.e. which may be in the form of lakes as proposed by Benedek (1971) and which may correlate with an increase in the absorbance of the tissue.

Table 1.

Comparison of the Composition of the Cornea and Sclera.

Component	Cornea	Sclera
Water [1]	78%	68%
Collagen [2]	70 - 75%	75%
Glycoproteins [2] acidic	20%	10%
Glycosaminoglycans [2] (GAG)	4%	1%
Keratan sulphate	$\frac{2}{3}$ total GAG	
Chondroitin-6-sulphate	-	$\frac{1}{2}$ total GAG
Chondroitin-4-sulphate	$\frac{1}{3}$ total GAG	$\frac{1}{2}$ total GAG
Dermatan sulphate	-	
Diameter of fibrils	19-34 nm	30-300 nm
Amorphous protecting layer [3]	+ + +	+
Elastin [3]	0	+

The data is taken from Maurice (1968), Maurice and Riley (1970) and Payrau (1968). 1 indicates that the number refers to the percentage of the wet weight. 2 indicates that the number refers to the percentage of the dry weight and 3 indicates that the magnitude is given qualitatively in terms of + signs, the more + signs the higher the value.

DIAGRAM OF THE EYE SHOWING POSITION OF THE CORNEA

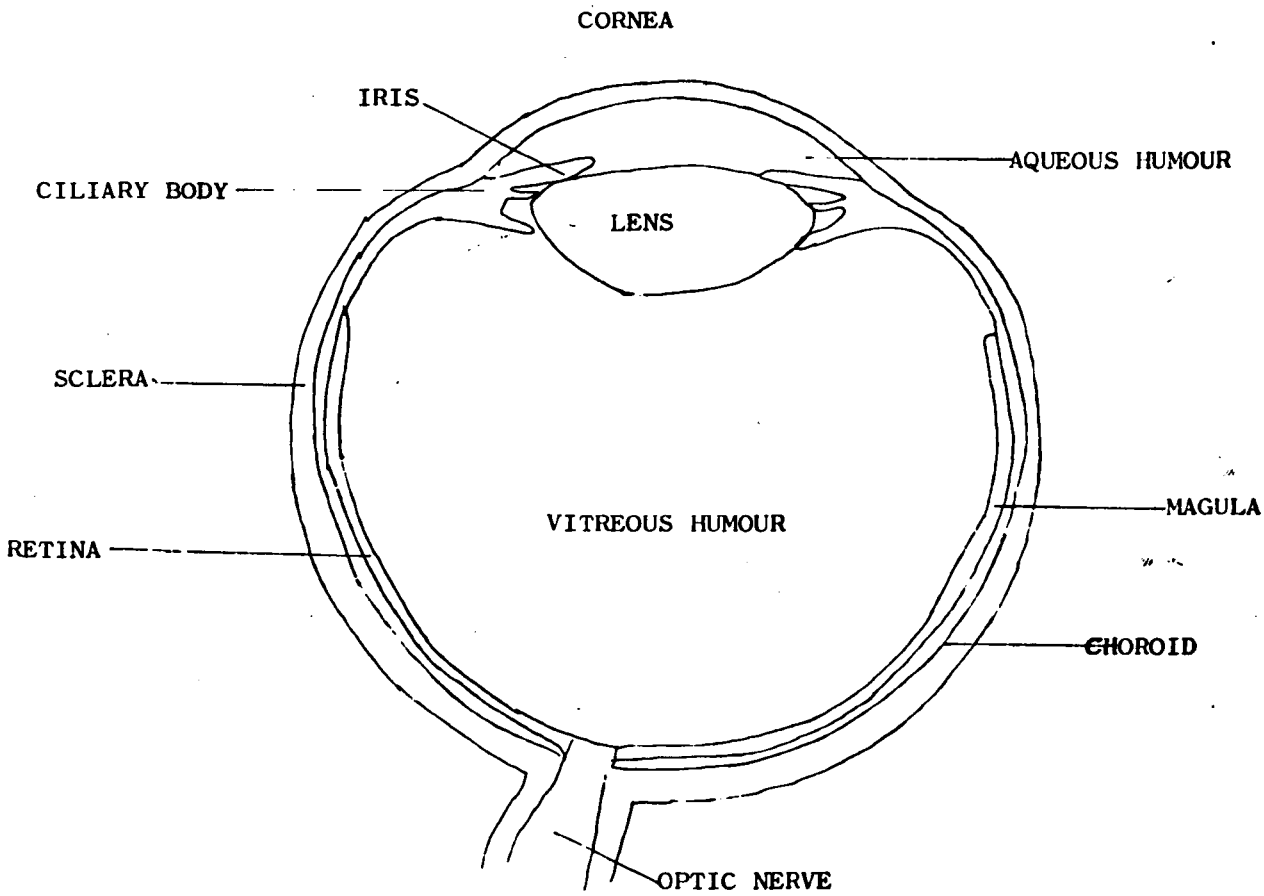

Fig. 1. Diagram of the eye showing position of the cornea relative to the other components of the eye from Krause (1934)

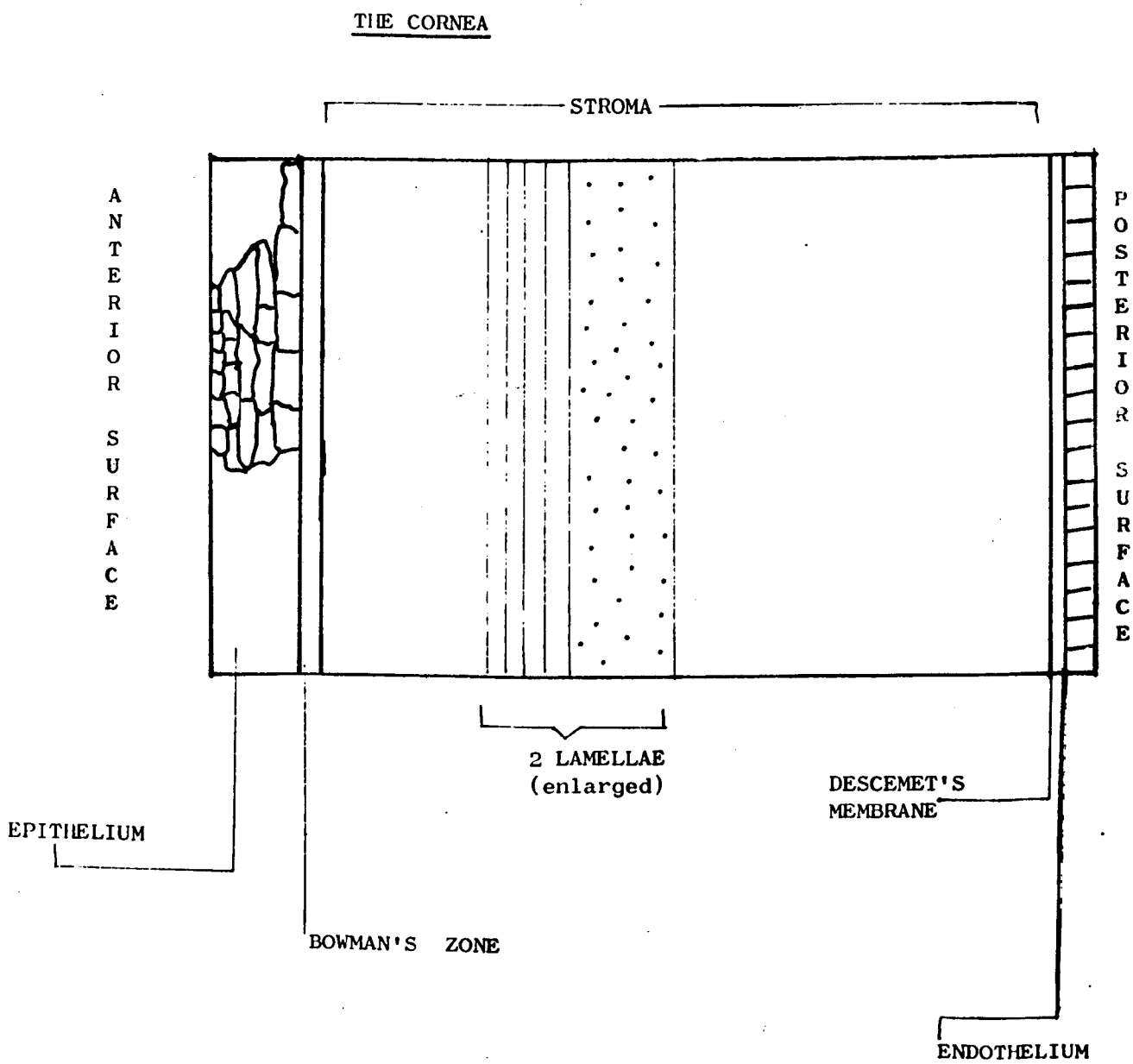

Fig. 2. Diagram of the cornea showing the different layers in the thickness direction.

Fig. 3. Electron micrograph of the corneal stroma showing the difference in orientation of the collagen fibrils in one lamella to the orientation in neighbouring lamellae.

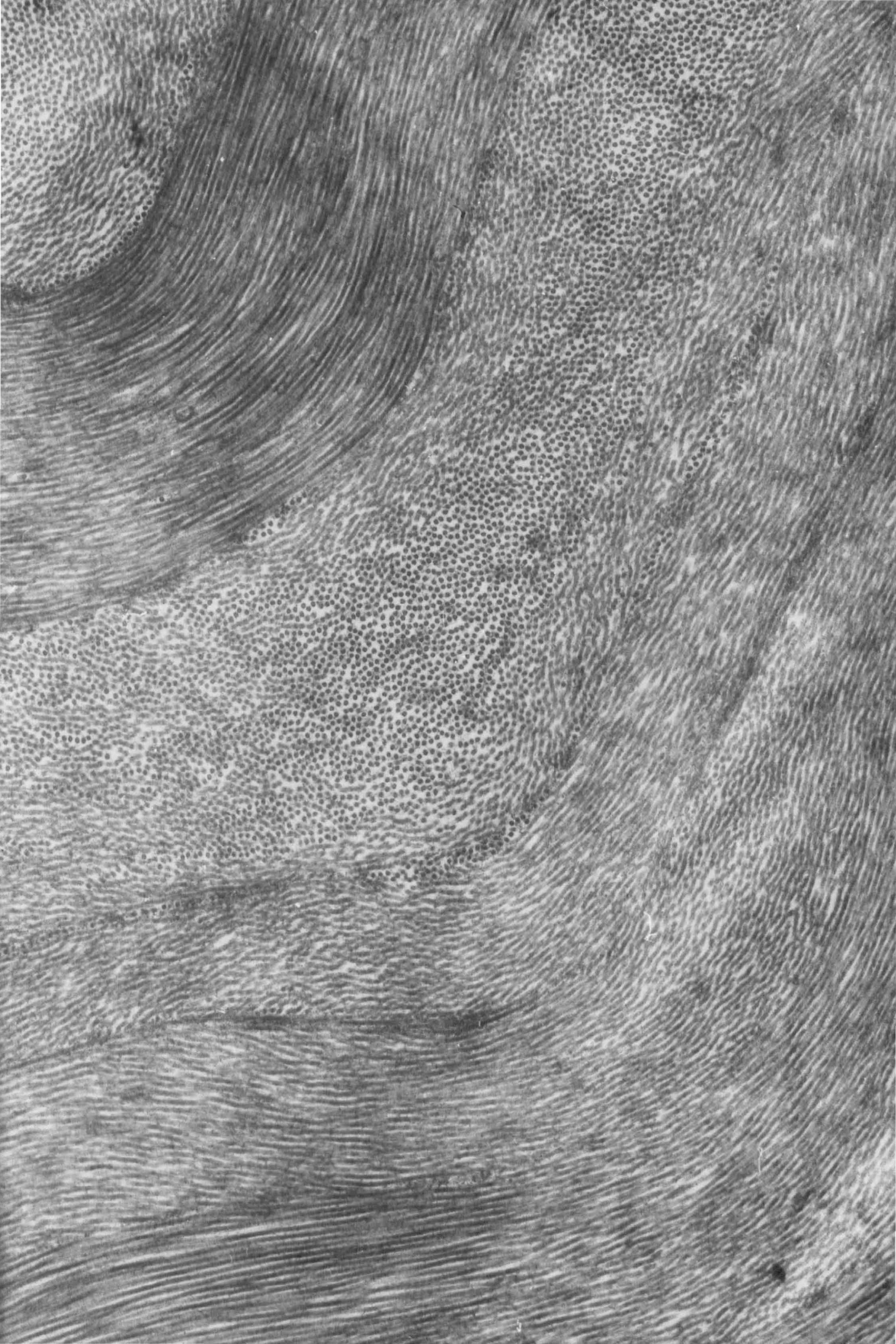

KERATAN SULPHATE

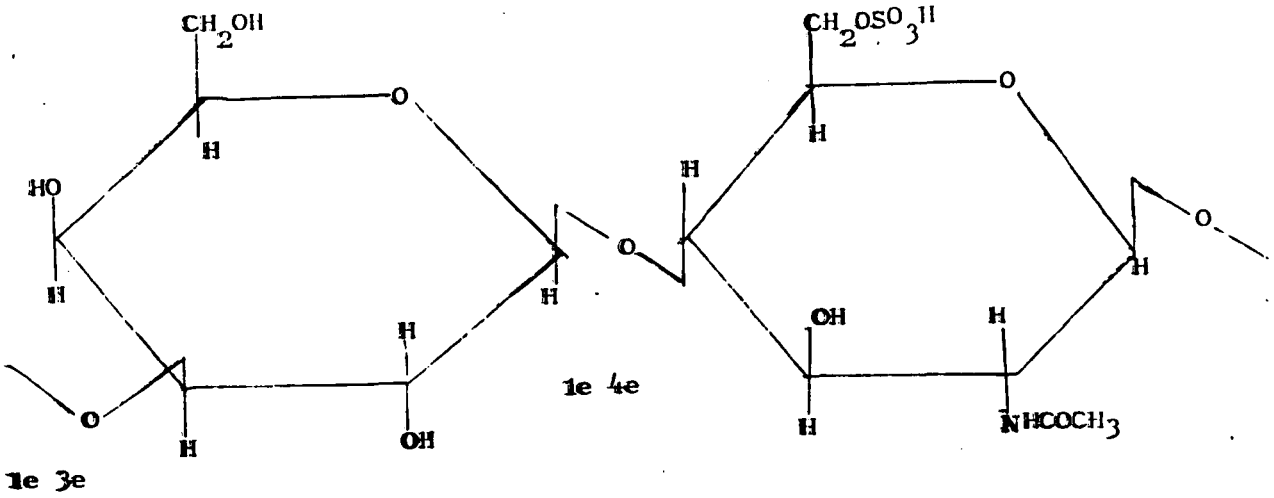

Galactose

N-acetylglucosamine-6-sulphate

CHONDROITIN SULPHATE

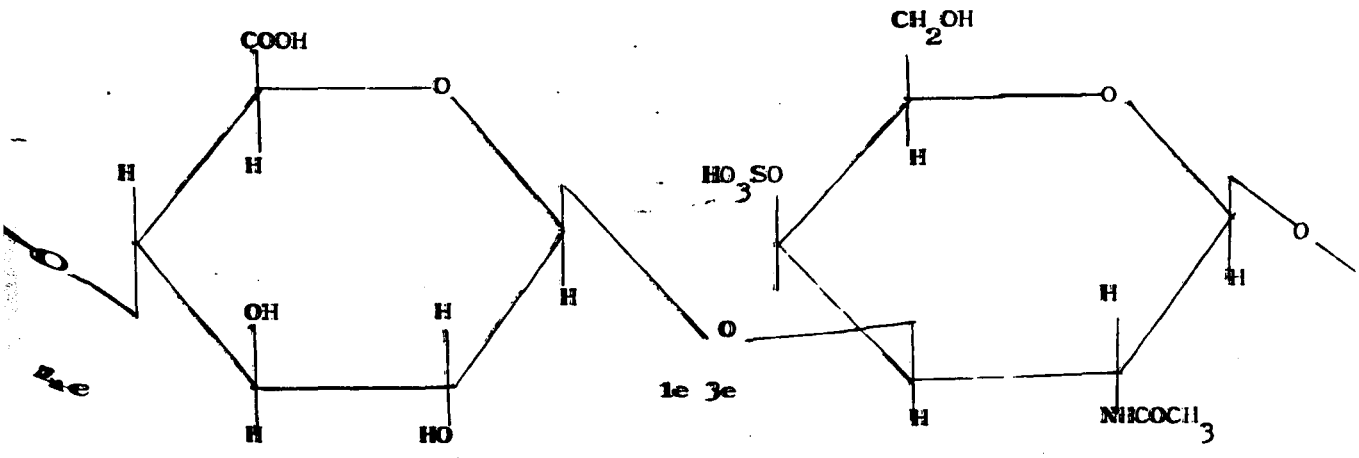

Glucuronic acid

N-acetylglucosamine-4-sulphate

Fig. 4. Diagram of the structure of the two mucopolysaccharides (glycosaminoglycans) of the corneal stroma - keratan sulphate and chondroitin sulphate.

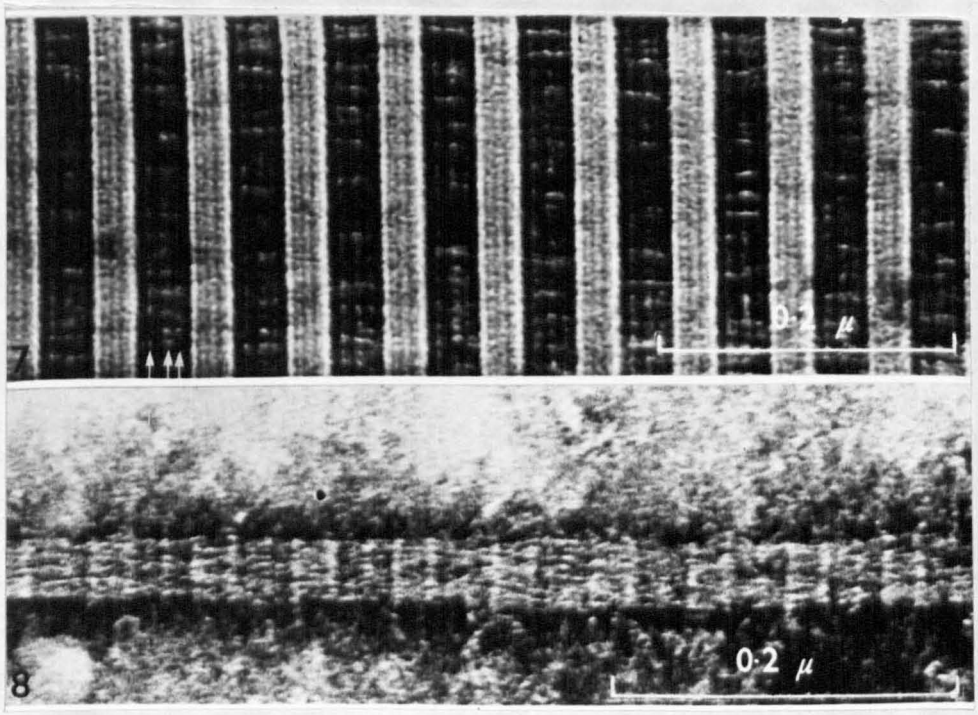

Fig. 5. 7. Fibril disintegrated tendon sprayed on grid. Arrows indicate 3 light bands in B-zone. Negative staining PTA x 215000. 8. Fibril disintegrated cornea sprayed on grid. Negative staining PTA x 250000. Both these figures are taken from Smith and Frame (1969).

Chapter 2

Swelling Properties of the Corneal Stroma

I Introduction.

(i) The Swelling Phenomenon.

Many investigators have shown that the excised corneal stroma will swell when placed in an aqueous solution. (For review see Payrau et al, 1967,). This swelling occurs in the thickness direction only (Hedbys and Mishima, 1966). In the living eye swelling of the corneal stroma occurs when the cellular layers are damaged (Maurice and Giardini, 1951) or when metabolic inhibitors are used to prevent the working of the active transport mechanisms in these cellular layers (Harris, 1957; Brown and Hedbys, 1965). The living stroma is in a state of deturgescence which means that if it is excised from the eye and placed in aqueous solution, it would be expected to swell by intake of fluid from the solution. Bito et al, (1973), using marmot cornea, have presented evidence that no 'thirst' to swell exists in vivo and that this swelling is a function of the in vitro or damaged in vivo state. However, in all experiments discussed here, it is the excised corneal stroma without living cellular layers which is of interest.

The pressure which must be exerted in order to prevent the stroma swelling is called the swelling pressure. This is known to be the order of 780-850 kg m^{-2} for fresh cornea (i.e. at physiological hydration) when placed in .9% salt solution (Dohlman and Anseth, 1957; Hedbys and Dohlman, 1963). The swelling pressure depends on the state of the tissue (i.e. water content) and also on the pH and ionic strength of the

solution in which it is placed (Kinsey and Cogan, 1942; Hedbys and Dohlman, 1963; Loeven and van Walbeek, 1954). When a saline filled cannula is inserted into the corneal stroma, the pressure with which the fluid is sucked into the tissue is called the imbibition pressure and this pressure has been found to be equal in magnitude to the swelling pressure. It has also been shown to exist in the in vivo stroma implying that the 'thirst' to swell does exist in vivo (Hedbys et al, 1963).

Corneas of some members of the elasmobranch species of fish do not swell when placed in aqueous solution (Smelser, 1962; Obenberger et al, 1971). It is thought that this is due to the presence of sutural fibres, across the thickness of the cornea, which prevent swelling mechanically (Ranvier, 1881; Payrau et al, 1965). It has also been shown that the stroma of these fish contain less glycosaminoglycan than those found in the stroma which swell in the usual manner (Payrau et al, 1967).

The purpose of the swelling experiments presented in section III is to investigate, in detail, the time dependence of swelling as a function of both the pH and the ionic strength. A theory based on the Donnan (osmotic) pressure being the main component of the swelling pressure has been derived and the results are discussed in terms of this theory.

(ii) Localisation of the Swelling.

Swelling could take place in or between any of the structural units described in Chapter 1. Maurice (1957) argues that swelling does not occur between lamellae since, if it did, the lamellae would appear irridescent because of light diffraction effects. This has not been seen. Aurell and Holmgren (1953) review the early literature on the localisation of swelling and conclude that from their own experiments on the metachromatic staining of the cornea that the collagen fibrils swell.

Hertel (1933) had supported this theory. However, swelling of collagen fibrils has not been seen in the electron microscope. Francois and Rabacy (1960) found that the diameter of the fibrils did not vary with hydration of the tissue and no significant increases in fibril diameter have been reported subsequently.

Birefringence measurements by Maurice (1957) based on the assumption that the cornea exhibits both intrinsic and textural birefringence have shown that the total birefringence decreases on drying the tissue until the value of the intrinsic component is reached. This data fits a theoretical curve calculated on the assumption that the interfibrillar distance alters and that the fibrils themselves do not increase in size with hydration.

Further evidence for this increase in spacing between the fibrils comes from the diffusion of small molecules through the stroma. For corneas at physiological hydration the largest molecule which can diffuse through the stroma has a diameter of approximately 12nm. However, on swelling to 150% of normal thickness, molecules with diameters up to approximately 15nm can diffuse through (Maurice, 1957).

Electron microscopy has also indicated that the interfibrillar distance changes with water content of the tissue (Kanai and Kaufman, 1973). More recently, areas devoid of collagen fibrils have been seen in the stroma of swollen cornea (Goldman et al, 1968). These regions have been named 'lakes' by Benedek (1971). Kanai and Kaufman (1973a) and Farrell et al (1973) have also reported seeing these lakes.

(iii) The Importance of the Glycosaminoglycans.

For many years glycosaminoglycans have been known to play an

important part in the swelling of the corneal stroma. Heringa et al (1940) showed that the extraction of the glycosaminoglycans with .02% potassium hydroxide reduced the swelling capacity of the stroma. These authors also noted that the sulphur content was reduced to 50% with this treatment. Hedbys (1961), having precipitated the glycosaminoglycans with cetylpyridimium chloride, showed a similar decrease in the amount of swelling. Digestion with the enzyme hyaluronidase, whose substrates are chondroitin-4- and -6-sulphate (Meyer et al, 1953) produces a decrease in the swelling.

Studies on the swelling of the stroma as a function of the pH of the bathing solution have shown the presence of a minimum in the swelling curve near pH 4 (Kinsey and Cogan, 1942; Loeven and van Walbeek, 1954, Smelser, 1962) whereas the minimum in the swelling curve of collagen is near pH 7 (Pirie, 1947). Loeven (1955) studied model systems of gelatin and chondroitin sulphate and showed that the pH dependence of these systems depended on the concentration of the glycosaminoglycan.

For comparison, the sclera swells about 15% of its weight in saline with a swelling pressure of 200-300 Kgm^{-2} at physiological thickness (Dohlman and Anseth, 1957; Hedbys and Dohlman, 1963). This may be because the sclera contains less glycosaminoglycan per dry weight or because the sclera has an interwoven structure. (Yamamoto et al, 1965; Francois and Rabaey, 1956).

(iv) Variation of the Swelling Pressure with External Solution.

Many workers (Kinsey and Cogan, 1942; Pau, 1954; Dohlman and Anseth, 1957; Hedbys and Dohlman, 1963) have shown that the swelling pressure

or the capacity to swell depends both on the hydration of the tissue and on the solution in which it is allowed to bathe.

Swelling in distilled water takes place at a higher rate than in salt solutions and comes to a steady value after approximately ten hours in cat cornea (Kinsey and Cogan, 1942). In 1% sodium chloride solution, the rate of swelling is slower but swelling continues for a much longer time period (over a week) and reaches higher values of hydration than in distilled water. Kinsey and Cogan (1942) also found that the pH dependence of the cat cornea showed a minimum at pH 4.3 from which the swelling increased with pH to pH 6 and then remained constant until pH 10-11. With decreasing pH, the cornea increased in hydration from pH 4.3 to 3.5 but below the latter value the hydration decreased. Loeven and Walbeek (1954) found a similar minimum in the pH hydration curve for rat and beef cornea. They showed that the valency of the anion had no effect (i.e. $Cl^{-1} = SO_4^{-2} = Fe(CN)_6^{-3}$) but that a decrease in swelling occured proportional to the valency of the cation.

Smelser (1962) found a minimum swelling of scup corneas in solutions of 0.5% sodium chloride (.08M) compared with solutions of different ionic strength. Bivalent cations decreased the hydration compared to monovalent cations, whereas bivalent anions increased the hydration of guinea pig and certain fish cornea.

Dohlman et al (1962) have shown a decreased swelling pressure at pH 4.2 and increased swelling pressure at low ionic strength (value not given) compared to that measured in physiological saline solution with beef stroma.

In solutions containing polyvinylpyrolidone (PVP) of high molecular weight with no ions present, there is little decrease in swelling compared to that in distilled water. However, in the presence of 1.23% salt solution with PVP at the same concentration and at the same pH the swelling is markedly reduced for about twelve hours because of the osmotic pressure exerted by the high molecular weight molecules. After some time, the PVP molecules themselves tend to diffuse into the stroma altering the osmotic balance (Smelser, 1962).

(v) Theories of the Origin of the Swelling Pressure of the Corneal Stroma.

The various models assumed for the distribution of material in the corneal stroma give rise to different orders of importance of the individual forces which, taken together, cause the total swelling pressure of the stroma. All authors agree that the collagen fibrils are arranged parallel to each other within each lamella and that the glycosaminoglycans are essential for the large swelling pressure recorded in fresh tissue. However, differences arise in the positions assumed for the location of the glycosaminoglycan molecules relative to the collagen fibrils. The arrangement of the chains alters the magnitude of the forces which either support or oppose swelling of the tissue. The forces which must be considered are the electrostatic forces arising from the presence of charged groups. The net fixed charge will lead to an osmotic (Donnan) swelling pressure. Secondly, the elastic forces from stretching the glycosaminoglycan chains and the mixing of these with the solvent. Thirdly, the possibility of Van der Waals forces must be considered.

Two basic models will be described. The first assumes that the

glycosaminoglycan chains extend between and fasten to the collagen fibrils (Hart et al, 1969; Farrell and Hart, 1969; Laugham et al, 1969; and Hart and Farrell, 1971). Glycoproteins are also assumed to be present but orientated parallel to the collagen fibrils with the polysaccharide chains extending orthogonally from them. This model was first suggested by Mathews (1965) for the arrangement of the macromolecular units in cartilage (and not necessarily in cornea which differs in several respects from other connective tissues -see Chapter 1, section V). The second model has been formulated by Hodson (1971) and proposes that no cross-linking exists in the stroma and that the glycosaminoglycans run parallel to the collagen fibrils. (Hodson and Meenan, 1969). The swelling pressure is considered to be totally due to the osmotic pressure within the experimental error. Further evidence in support of the first model has been presented by Friedman and Green (1971a), Green and Friedman (1971) and Friedman et al (1972).

The model proposed by Farrell and Hart (1969) is based on calculations of the radial distribution of the collagen fibrils. The radial distribution function is the ratio of the average local number density of fibrils to the average bulk number of density of the fibrils i.e. values above unity indicate regions where there is some correlation in position. A model of the structure is chosen and the radial distribution is calculated from integration of Gibbs phase function over all possible configurations. The probability of each configuration is given by the canonical distribution. The calculated radial distribution is compared with that obtained from the electron microscope examination of the tissue. Further correlation is obtained by comparing the light scattered from the corneal stroma with the amount of predicted light scattered from the calculated radial distribution (Cox et al, 1970).

The calculations start with the formation of the forces which exist in the tissue and are assumed to arise from the distribution of the glycosaminoglycan chains attaching to the collagen fibrils. The properties of the chains are inferred from general polymer theory. The only force considered in detail is that due to the stretching of the chains. Van der Waals and electrostatic forces are discounted because of the distance between the fibrils (60nm in fresh tissue). The elastic forces are divided into two parts for the calculation. The first component is the monomer-monomer interaction of a polysaccharide chain. This is assumed to be of the form $F = -kh$ where F is the force, k is the spring constant and h is the length of the chain i.e. Hook's Law is obeyed. The spring constant is assumed to be inversely proportional to the mean square end-to-end distance which is estimated from viscosity measurements on free chains from bovine cartilage (Mathews, 1967). The second component is the free energy of mixing between the monomer and the solvent.

The fibrils are divided into segments with glycosaminoglycan chains attaching to the fibrils at the ends of each segment. The chain lengths are then related to the distance between the fibrils. Different topologies are used in order to obtain the best correlation with the experimentally measured radial distribution function. A centered-hexagonal array leads to the best correlation. Other assumptions include the uniformity of the molecular weights of the glycosaminoglycans, the regularity in distance between attachment points along the collagen fibrils and that the lattice of fibrils swells only in one direction.

Hart and Farrell (1971) extend this model to account for the swelling pressure by determining the free energies associated with the

stretch of the chains, the excluded volume effect, interaction with solvent and the electrostatic charge. They concluded that at .15 M NaCl, (based on the data of Hedbys and Dohlman, 1963) that 68% of the swelling pressure is due to the electrostatic (Donnan osmotic) effect at .75 normal thickness, 72% at normal thickness and 100% at 1.5 X normal thickness respectively.

Basic criticisms can be made to some of the assumptions used in this model and to the number of unknown parameters which have to be known to give a good correlation with experimental data. The main assumption appears to be that the glycosaminoglycan chains form links between the collagen fibrils in the corneal stroma. This may well be the case in cartilage. Evidence from electron microscopy of corneal stroma is contradictory but does not appear to be consistent with the above model. Smith and Frame (1969) have found filaments thought to be protein cores of protein-polysaccharide complex, stretched between adjacent collagen fibrils i.e. orthogonal to the direction proposed by Hart and Farrell). In disintegrated corneal stroma, these chains are sometimes free and about 200nm long. After addition of bismuth ions, these filaments have a beaded appearance, the beads being 7nm in diameter. The beads are assumed to be due to a tightly coiled conformation of polysaccharide molecules. These filaments are not seen in cartilage.

Myers et al (1973) have found 3.5nm diameter filaments in rabbit cartilage using a ruthenium red stain. Again these filaments are thought to be due to aggregates of glycoprotein. However, no such interconnecting filaments are seen in the corneal stroma of rabbit. Dense granules are seen to coat the collagen fibrils in the stroma. Similarly

Hodson and Meenan (1969) found that granules coating the collagen fibrils could be seen in sections of the corneal stroma stained with silver.

If these chains of glycosaminoglycans are assumed to exist between the collagen fibrils, further criticisms can be made of the general theory. It was assumed that only elastic forces were important over distances comparable to that separating the fibrils. Van der Waals and electrostatic forces were discounted. It must be pointed out that the distance between the surfaces of the collagen fibrils is only about 30 nm in fresh tissue when the centre-to-centre distance is 60 nm. However, the attractive Van der Waals and repulsive electrostatic forces have been considered to be forces stabilising the fibril lattices in muscle (Elliott, 1968; Rome, 1968; Miller and Woodhead-Galloway, 1971). For general systems consisting of cylindrically charged molecules, Brenner and McQuarrie (1973) have considered the balance obtainable with these forces as a function of the bathing solution's pH and ionic strength. Hart and Farrell (1971) assume uniform molecular weights for the glycosaminoglycans and regularity in the spacing between attachment points of the chains along the collagen fibrils. The uniformity of the molecular weights is not supported by the facts that the corneal stroma contains two different glycosaminoglycans i.e. chondroitin-4-sulphate and keratan sulphate and that keratan sulphate is known to have a molecular weight distribution between 4,200 and 19,000 (Anseth and Laurent, 1961). Although chondroitin-4-sulphate isolated from corneal stroma has a small range of molecular weight averaging around 40,000, this weight is much greater than any found for keratan sulphate molecules. Chondroitin may also exist in the stroma as a separate species (Chapter 1, section IV, v). The regularity in attachment points of the glycosaminoglycans to the fibrils is not supported by the evidence of Smith and Frame (1969) who found

filaments (thought to be proteins, however) attaching to the collagen fibrils. They report that the distance between attachment points was not uniform but a large number of the intervals between attachment points corresponded to a distance of approximately 55nm.

Another assumption is the calculation of the elastic force and its contribution to the swelling pressure was that the lattice only distorts in one direction. The tissue is known to swell only in the thickness direction but the results presented in chapter 4 from x-ray diffraction results indicated that the distance between the fibrils changes equally in all directions on swelling although the tissue as a whole is constrained to swell in one direction.

Further problems arise in the finding of numerical values for certain parameters. Hart and Farrell (1969) admit that there is considerably uncertainty in the value of the root mean square end-to-end distance of the chains because of the existence of two different polysaccharides and their range in molecular weights. The value chosen is obtained from viscosity measurements on free polysaccharide chains from cartilage. Another parameter which is entirely unknown is the number of chains attaching to the end of each segment. The number six is chosen because this gives the best correlation with experimental data. A further assumption is that the area over which the charge is on the chains is homogenous. If the chains only occupy cylinders of fluid between the fibrils, the charge concentration is actually higher than if the chains occupied the whole free space of the stroma i.e. stroma minus collagen. The fraction of the free stroma is chosen for the normal hydration of the tissue but it is undefined for much larger hydrations.

A second model for the structure of the stroma has been proposed by Hodson (1971). Evidence is given to support the contention that no cross-linking exists in the corneal stroma between individual collagen fibrils. It is proposed that the glycosaminoglycans surround the corneal collagen fibrils (Hodson and Meenan, 1969). The physical evidence in the support of the absence of cross-linking is based on the experimental findings that the swelling pressure is always equal in magnitude to the imbibition pressure within experimental error (Hedbys et al, 1963). If P_s is the swelling pressure and P_i the imbibition pressure then

$$P_s = P_i$$

It is assumed that the osmotic pressure and the tissue pressure combine to give the total swelling pressure where the tissue pressure represents either a force opposing swelling due to the elastic forces between fibrils or a term increasing the swelling due to the electrostatic repulsion between charged groups in the stroma. The imbibition pressure is measured by sampling the fluid phase only and therefore can only be a measure of the osmotic pressure. So that

$$P_s = P + P_t$$

where P is the osmotic pressure and P_t is the tissue pressure but

$$P_i = P$$

Therefore, if $P_i = P_s$ as determined experimentally, P_t must be zero. This implies that there is no elastic force opposing swelling neither is the repulsive force between the electrostatic charges significant at normal hydration. A different relation between swelling pressure and tissue pressure is calculated by Hedbys et al (1963). However, rewriting of their equations leads to the fact that the imbibition pressure equals the external hydrostatic pressure which cannot be true (Hodson, Private Communication). Chemical evidence is provided by the electron microscopy

of Hodson and Meenan (1969). Silver staining of sections of the stroma showed that the fibrils were beaded in appearance and it was proposed that these beads represent glycosaminoglycan molecules along the fibril.

Hodson (1971) uses the theory of Donnan swelling to explain the swelling pressure of the corneal stroma. In this model, the only pressure within the experimental error is the osmotic pressure arising from the Donnan distribution of ions between the stroma and the external solution. This distribution exists because of the presence of the fixed charge concentration in the stroma due to the charged groups of the glycosaminoglucan molecules i.e. carboxyl COO^- and the sulphonic acid groups HSO_3^- and the need to maintain electroneutrality. A value for the fixed charge concentration of 48 mequivl^{-1} was estimated from the known percentage of dry weight which is due to the glycosaminoglycans. A similar value of 47.4 mequivl^{-1} was found using the Donnan exclusion techniques of Maroudas and Thomas (1970) (Hodson, 1971).

The osmotic pressure calculated from this value of the fixed charge concentrations correlates well with the values of the swelling pressure obtained experimentally by Hedbys and Dohlman (1963). When the osmotic pressure is used to calculate the rate of flow of fluid into the cornea across the endothelium, good agreement is found between this calculated value and the measured value of Trenberth and Mishima (1968).

The major assumption of this cross-link free model is that concentrations can be used instead of ionic activities. The activity

coefficient of sodium ions in .15 M sodium chloride is known to be about 0.73 but a value of unity is assumed in this theory (Robinson and Stokes, 1959). The effect of bound ions on the value of the fixed charge is considered small because the measured value of the charge concentration agreed with values previously calculated from the known content of glycosaminoglycans if all the charged groups were free. This point is discussed below in more detail. Hodson points out that this theory predicts that the electrostatic repulsive forces between the charged groups must be negligible at normal hydrations. This may be so but the theory does not take into account this repulsive force which is likely to be more important at lower hydrations when the fibrils are separated by a smaller distance. A theory for the effect of the repulsive force has been proposed by Brenner and Parsegian (1975).

Friedman et al (1972) calculate the contribution that the Donnan osmotic pressure makes to the total swelling pressure and conclude that it is only half the total pressure at near normal hydrations in physiological solutions. Their technique is based on the measurement of the total swelling pressure at the same thickness of stroma but in solutions of different ionic strength. The difference in swelling pressure at different concentrations of the external solution is due only to changes in the osmotic pressure contribution. When the osmotic pressure change is known the concentration of fixed charge can then be calculated. However, since the fixed charge concentration per dry weight was not found to be constant the Donnan contribution could not be found directly. The concentration-independent structural component had to be measured. Values of the Donnan osmotic pressure calculated by this method range from 34mm Hg to 7mm Hg when the hydration range was between 2.26 and 5.58. The mean value of the ratio of the osmotic pressure to the total swelling pressure was found to be .54. The value of the fixed charge

concentration was calculated from this value of the osmotic pressure and compared with values of the charge concentration determined in using techniques which measured the amount of bound cations in the stroma. (Friedman and Green, 1971a, and Green and Friedman, 1971). Sodium, potassium and calcium binding had been shown to exist in the cornea depending on the salt concentrations in the external solution. This binding of cations reduced the free fixed negative charge below that assumed by Hodson (1971) to a value of 12-16 mequivl^{-1}. The Donnan contribution was increased by assuming that the glycosaminoglycan chains only occupied a limited volume of the free stroma i.e. stroma-collagen. The fraction of the volume occupied by the chains and hence through which the charge concentration was assumed to be homogeneous was calculated to be about a third of the total free stroma. This leads to an increase in the osmotic pressure but this new osmotic pressure still did not account for all the swelling pressure. This factor is unknown for hydrations which are much larger than normal.

Friedman and Green's calculations depend on the accurate measurement of the bound ions in the stroma. Equilibration times were two hours although some earlier work indicated that this was long enough (Green et al., 1971). No detailed study with time of incubation was given. There are few experimental details of the solutions used. Usually only a value for the concentration of salt was given. No mention of the pH of the solutions is ever made in either of the three papers being discussed here. The pH of the external solution would be expected to have a large effect on the internal fluid and hence on the value of the charge on the glycosaminoglycan molecules.

It is concluded that there is little direct evidence to support

the contention that the glycosaminoglycan chains extend between and attach to the collagen fibrils. Electron microscopic evidence of Smith and Frame (1969) shows that the protein filaments are lying orthogonally to the direction proposed by this theory. Further work by Myers et al does not indicate the existence of any filaments between fibrils in the corneal stroma but only the presence of polysaccharides along the collagen fibrils giving support to the silver staining method used by Hodson and Meenan (1969). Finally, in the words of Friedman and Green (1971), "the importance of the Donnan contribution to the swelling pressure is seen to depend strongly on the molecular organisation of the ground substance".

II Theory:

The Prediction of the Relationship Between the Hydration of the Corneal Stroma and the Time of Swelling.

In order to compare the experimental swelling data with the theory of Donnan swelling of the corneal stroma, a relationship between the hydration of the stroma and the time of swelling was deduced on the basis of this theory. The basic assumption is that a Donnan distribution of ions exists between the stroma and the bathing solution. This distribution of small permeant ions depends on the fixed charge concentration in the stroma, which will vary with hydration of the tissue, the ionic strength and the pH of the bathing solution.

The osmotic pressure difference, P, between the stroma and the external solution, which is a result of the distribution of permeant ions can be expressed as a function of the fixed charge concentration, C_F, and the concentration of cations, C+, in the external solution

measured the flow conductivity (of Friedman, 1971, and Friedman and Green, 1971) which is defined as the rate of flow of fluid per unit area per unit time across the stroma per unit pressure gradient dP/dx

i.e. $$J = \frac{-K}{7}\frac{dP}{dx}$$

where x is the thickness across the stroma and P is the swelling pressure assumed to be totally due to an osmotic pressure. This equation can be expanded so that

$$J = \frac{-K}{7}\frac{dP}{dH}\frac{dH}{dx} \quad \ldots\ldots\ (8)$$ (Fatt and Goldstick, 1965)

where dH/dx is the constant, a, defined previously as the increase in thickness per unit increase in hydration.

If we combine equation (4) and equation (8) by eliminating J, we find that

$$-(K/7) = L_{PD}Pa/(dP/dH) \quad \ldots\ldots\ (9).$$

In order to find the value of dP/dH we can differentiate equation (3). Hence

$$\frac{dP}{dH} = -2P/H \quad \ldots\ldots\ (10)$$

so that by substituting for dP/dH from equation 10 into the expression for K/7 (equation 9), we find that

$$L_{PD} = (k/7)\ 2/aH \quad \ldots\ldots\ (11).$$

Friedman (1971) and Friedman and Green (1971) have shown that data of Hedbys and Mishima (1962) is consistent with the following relation between the flow conductivity and hydration:

$$k/7 = C_1H^3/(H + E) \quad \ldots\ldots\ (12)$$

where C_1 and E are constants and are equal in value to 31 x 10^{-9} cm^2/torr-min (46 x 10^{-9} cm^2/torr-min) and .67 (.72) for beef (rabbit) stroma respectively. This expression (equation 12) for the flow conductivity can be substituted into equation (11) so that

$$L_{PD} = 2C_1H^2/a(H + E) \quad \ldots\ldots\ (13).$$

assuming that these ions are monovalent.

$$P = RT \left[(C_F^2 + 4C_+^2)^{\frac{1}{2}} - 2C_+ \right]$$

This is equivalent to equation 10 in Hodson (1971) in which $F \times 10^{-3}$ replaces C_F and $[Na]_o \times 10^{-3}$ replaces C_+, R is the gas constant whose value is 8.314 $JK^{-1}mol^{-1}$ and T is the absolute temperature assumed to be 293K. The expression under the square root in this equation can be expanded using the Binomial theorem. A simpler relation between the osmotic pressure and the fixed charge concentration can be obtained by this procedure. (This follows a suggestion made by Dr. A. E. Woolgar). Thus

$$(1 + C_F^2/4C_+^2)^{\frac{1}{2}} = 1 + C_F^2/8C_+^2 - C_F^4/32C_+^4 \quad .....$$

(Hodgman, 1959)

Using the first two terms of this expression and substituting into the equation for the osmotic pressure leads to

$$P = RTC_F^2/4C_+ \quad ..... \quad (1)$$

This approximation is valid if $C_F < 2C_+$

The fixed charge concentration will decrease as the hydration of the tissue increases, supposing that the total fixed charge remains constant throughout the swelling process. Hence

$$C_F \times H = C \quad ..... \quad (2)$$

where C is a constant whose value depends on the pH and ionic strength of the bathing solution. By substituting for C_F from equation (2) into equation (1), it can be shown that

$$P = RT\, C^2/4C_+ \times H^2 \quad ..... \quad (3)$$

i.e. the osmotic pressure difference is inversely proportional to the square of the hydration of the stroma for a fixed bathing solution.

The flow of fluid into the stroma per unit area per unit time, J,

is proportional to the swelling pressure which is assumed to be totally due to the osmotic pressure difference (Katchalsky and Curran, 1967; Hodson, 1971). The constant of proportionality is an Onsager coefficient, L_{PD} in the notation of Katchalsky and Curran (1967). This coefficient can also be written as the product of the hydraulic conductivity, L, and the reflection coefficient, σ (Hodson, 1971)

$$J = L_{PD}P = \sigma LP \quad \ldots\ldots\ldots \quad (4)$$

When the expression for the osmotic pressure difference from equation (3) is substituted into equation (4), we obtain that

$$J = L_{PD}RTC^2/4C_+H^2 \quad \ldots\ldots\ldots \quad (5)$$

The rate of flow of fluid per unit area per unit time is proportional to the rate of hydration, dH/dt, because the stroma swells in the thickness direction while its cross-sectional area remains approximately constant (Hedbys and Mishima, 1962).

$$J = a\ dH/dt$$

where a is the increase in thickness of the stroma per unit increase in hydration. This increase can be estimated from the graph of thickness as a function of hydration presented by Hedbys and Mishima (1962) whence a = 8/35 mm. By combining equation (5) with equation (6), we have an expression for the rate of hydration

$$\frac{dH}{dt} = L_{PD}\ RTC^2/a4C_+ \times H^2 \quad \ldots\ldots\ldots \quad (7).$$

It is possible that the value of L_{PD} may alter with swelling. As the stroma swells, the distance between the fibrils will increase and so it is expected that the fluid will be able to flow through the stroma more easily. Thus, the hydraulic conductivity will be altered. No direct measurements have been made on the product, σL, for the stroma although the value of this parameter has been found for the endothelium (Mishima and Hedbys, 1967). However, Hedbys and Mishima (1962) have

Further substitution of the expression for the coefficient L_{PD} (equation 13) as a function of hydration into the equation for the rate of hydration dH/dt (equation 7) gives the full expression for the rate of hydration in terms of the hydration of the tissue. Thus,

$$dH/dt = RTC^2 2C_1/a^2 4C+(H + E).$$

By separating the variables in this expression, we have

$$\int_0^H (H + E)\, dH = \int_0^t K\, dt$$

where $K = RTC^2 C_1/a^2 2C+$ which is a constant for a fixed bathing solution. Integrating gives the final expression,

$$H^2/2 + EH = Kt + K^1$$

where K^1 is a constant of integration.

A possible source of error may occur in ignoring all but the first two terms of the expansion for $(1 + C_F^2/4C_+^2)^{\frac{1}{2}}$. The magnitude of this error can be estimated by comparing the value of the full expression to that of the approximate expression. If C_F=50 mequiv l^{-1} and C+ = 100 mequiv l^{-1}, the percentage error in ignoring all but the first two terms is .04%. If C+ = 60 mequiv l^{-1} the percentage error increases to 0.3%.

A larger source of error occurs in the assumption that $C_F > 2C_+$ for all values of hydration. If the concentration of the bathing solution, C+, is equal to 50mM l^{-1} and C_F equals 50 mequiv l^{-1} at H=3.5 (physiological hydration), then at H=1.5, C_F will equal 117 mequiv l^{-1} i.e. $C_F > 2C+$. Values of the osmotic pressure calculated using this approximation are too high compared with the correct value when $C_F > 2C_+$. It is expected that this error may give rise to non-zero values of the constant of integration K^1 i.e. the regression fit of the data will not go through the origin. If this is so, larger errors (and hence larger values of the intercept) will occur when the ionic strength

of the bathing solution is low.

It must be noted that the relation between flow conductivity and hydration (equation 12) found by Friedman (1971) has been studied within a very narrow range of hydrations ($H \leq 4$). It has been assumed that the same relation occurs at hydrations up to H=20. It might be expected that the flow conductivity would depend to a lesser extent on the hydration at higher values of hydration. The value of the integral $\int_0^H (H+E)\, dH$ would then be lower than the correct value.

III Methods.

(i) Materials.

(a) Fresh Corneal Stroma.

Beef eyes were obtained from a slaughter house. The eyes were enucleated immediately after death. The cornea were dissected from the whole eyes within two to four hours after death. Fresh rabbit eyes were removed from the animal immediately after death and the cornea obtained within five minutes. The anterior and posterior surfaces of the cornea were scraped with a scalpel to remove the epithelium and endothelium. The stroma was then cut with scissors into six evenly sized pieces. All sclera was carefully removed from the corneal edges. Fresh cornea were used as soon as possible after excision and were not stored for longer than one hour in airtight containers at $4^{o}C$.

(b) Dried Corneal Stroma.

Because of the difficulty in keeping large numbers of fresh cornea

at their normal (i.e. excision) hydration for long periods, it was decided to use dried corneal stroma for the majority of the experiments. Fresh corneal stroma was obtained as described above and were then left in Petri dishes in a dessicator over silica gel. They were allowed to dry for a minimum of one week and usually up to three weeks. Dried corneal stroma has been used in the study of the cornea by other workers (Loeven and Van Walbeek, 1954; Van Walbeek and Neumann, 1951; Hedbys, 1961). It ensures that all the stroma are in the same condition at the start of the experiment and it makes the calculation of the hydration (defined as weight of water divided by the weight of dry material) obvious. The hydration of fresh corneal pieces has to be calculated either by assuming the initial hydration is that of normal tissue i.e. 3.5 or by drying the pieces of corneal stroma after the swelling experiment until constant dry weight is achieved.

Dehydration is a method of preserving corneas which has been used in order to store cornea which may be used for grafting. The main problem involved in preserving the cornea is to keep the cells of the endothelium alive. In my experiments, the endothelium has already been scraped off so this problem is not important. Several simple techniques can be used for keeping the corneal stroma in store for many months if only the stroma is required (Payrau et al, 1967).

Urrets-Zavalia (1963) has briefly reviewed the methods available for preserving corneal stroma. The simplest method involved dessication of the tissue. King and McTigue (1962) used glycerol (95%) in the presence of sodium or calcium aluminosilicate. These substances were found to be chemically inert but had a large affinity for water. Payrau and Pouliquen (1960) have used silica gel to absorb all the water at

room temperature. However, they sterilised the cornea by placing in 95% ethanol at solid CO_2 temperatures and then stored them over silica gel. The cornea were preserved by this method for at least eleven months and it was thought by the authors that they could be kept indefinitely.

Silica gel is not the only effective drying agent which can be used in the dessicator. Others include sulphuric acid and phosphorus pentoxide (Loeven and Van Walbeek, 1954; Loeven, 1955, Hedbys, 1961). However, Payrau et al (1967) report that neither sulphuric acid nor phosphorus pentoxide can be guaranteed to preserve the structure nor do they prevent chemical reactions taking place in the tissue. In conclusion they recommend drying over silica gel as by Payrau and Pouliquen (1960). Remé et al (1972) examined fresh and room-temperature dehydrated specimens but large differences in the cells were seen. In all the experiments presented in this thesis using dried cornea the corneal stroma has been preserved by drying over silica gel. No sterilisation procedures were used before dessication.

(ii) Solutions.

All solutions used contained sodium chloride and a buffer. The type of buffer depended on the pH required (Dawson et al, 1969). Details of the buffer systems used are given in Table 1. Sodium chloride was then added to give the required ionic strength. Five values of μ, ionic strength, were used at each pH. They were $\mu = .02$, $\mu = .05$, $\mu = .1$, $\mu = .15$, and $\mu = .25$ at pH 6,7,8 and 10 and $\mu = .06$, $\mu = .1$, $\mu = .15$, $\mu = .2$ and $\mu = .3$ at pH 4 and 2. For the low ionic strength, $\mu = .02$, the buffers used at pH8 and 10 were diluted to give the required value, the buffer alone was used at pH7 and buffer and salt at pH6.

The pH of each solution was checked on a Pye Unican pH meter and corrections if necessary were made by addition of dilute solutions of hydrogen chloride or sodium hydroxide.

(iii) Swelling Measurements.

Corneal pieces were weighed on a microbalance to .1 mg to obtain the dry weight of the specimen. On average the dry weight was about 10 mg so that the dry weight could be measured to 1% accuracy. They were placed in containers containing approximately 30ml of bathing solution. Wet weights were obtained by removing the corneal stroma from solution, carefully blotting on filter paper (Whatman qualitative) to remove all excess moisture and weighing on the microbalance. They were replaced in bathing solution within one minute so that only a small loss in weight occured while they were being weighed. All containers had lids which could be used to prevent evaporation of water vapour and hence an increase in the ionic strength of the solution. The bathing solutions were replaced every 24 hours. Inaccuracies in this method occured at very high hydrations (e.g. H=20) and this is shown in the greater spread in the results at these values. It is thought that some of the differences may be because some water may be squeezed out at high hydrations on blotting the corneal tissue. At these values of hydration the tissue was blotted as gently as possible. All experiments were carried out at room temperature.

The pieces of corneal stroma could be weighed to an accuracy of .1-.2mg. The error in weighing a dried piece of corneal stroma was not more than 20%. The error in the hydration is then about 1%. It is difficult to estimate the error in the weighing of highly hydrated stroma when an unknown amount of fluid might be pressed out while drying. This quan

tity is estimated to be probably no more than 15 mg in 150 mg i.e.10% which makes a 10% error in the hydration (Topping, 1962).

IV Results.

(A) Fresh Beef Corneal Stroma.

(i) General Properties.

The free swelling of fresh corneal stroma was studied as a function of the pH and ionic strength, μ, of the external solution. The magnitude of the swelling at any time was measured in terms of the hydration of the tissue where the hydration is defined as the weight of water per unit dry weight. The hydration was recorded as a function of the time between zero and hundred hours. In general, whatever the solution, the initial swelling is fast. The exact hydration at any time depends on the bathing solution. The rate of hydration is always decreasing: only at low pH values (2 and 4) does the rate of hydration become zero within experimental error i.e. the tissue reaches a final, constant value of hydration. At higher pH values (6 and 10) the rate of swelling is always greater than zero and no final constant value of hydration was reached within the time of these experiments. The tissue behaves differently when placed in distilled water with no ions present. The rate of hydration is very fast but a final value of hydration is reached.

Because of the differences in behaviour between corneal stroma swollen at different pH values the results are divided into two sections low pH and high pH. The dependence on ionic strength is discussed within these sections. A further section on the swelling of fresh stroma in

distilled water is included.

(ii) Behaviour at Low pH.

Two low pH values were chosen namely pH2 and pH4. All the data is plotted in Fig. 1. At pH4 (μ = .15) the initial swelling is fast with a hydration of approximately 4.5 being obtained within the first hour. The final, constant value of hydration is approximately H = 5 and is obtained after five hours (Table 2). This value of hydration is maintained for at least fifty hours. When the ionic strength of the bathing solution was increased to μ = .2 , the final value of hydration was slightly larger at H = 5.5. (Table 2). This water content is maintained for at least fifty hours.

When the pH was lowered to pH2 at μ = .15, the initial rate of hydration was slightly higher. After one hour, the hydration was just over H = 5. After 20 hours, a hydration of eight had been reached (Table 2). This value stayed approximately constant for 120 hours. For a given time, the hydration of corneal stroma in a bathing solution buffered at pH2 was always larger than that of another corneal stroma maintained in a solution at pH4, at the same ionic strength (μ = .15) (Fig. 1).

(iii) Behaviour at High pH.

The bathing solutions used were buffered at pH6 and pH10 at an ionic strength μ = .15. The hydration is plotted as a function of time in Fig. 2. It can be seen that for a given time, the hydration is always greater at the higher pH (pH 10) e.g. after fifty hours, the

hydration of corneal stroma in solution buffered at pH6 is approximately 14.5 whereas the hydration of the stroma at pH10 is 17. Although the rate of swelling (proportional to the slope of the hydration versus time curve) is always decreasing it does not become zero within 120 hours.

In order to compare this data with the rate of swelling predicted by the theory presented in Section II of this chapter the function $H^2/2 + H \times E$ was calculated. This function was found to be linearly related to the time of swelling. Linear regression fits of the data were calculated and are shown plotted as the solid lines in Fig. 3. Details of the linear fits are given in Table 3. The slope of the linear regression for swelling at pH10 is $1.88 \pm .12$ and at pH6 is $1.29 \pm .11$. The intercepts (as shown in Table 3) are not zero because the tissue is swelling from an initially hydrated state. However, the value of the function $H^2/2 + H \times E$ when $H = 3.5$ is equal to 8.45 but both the intercepts are much larger than this value. A discussion on the errors which may contribute to give a higher intercept than expected is given in a later section. Both regression fits were significant as shown by f-ratios for the slopes of 228 and 135 for pH10 and pH6 respectively. (Appendix 1).

(iv) Swelling in Distilled Water.

Swelling of fresh corneal stromas takes place very quickly when they are placed in distilled water. After 1 hour, the stroma have reached a hydration of eleven and after 2 hours a hydration of approximately 18. A final value of the hydration, at $H = 31$ is reached after 20 hours of swelling in distilled water. This value was maintained for at least 40 hours (Fig. 2)

(B) Swelling of Dried Beef Corneal Stroma.

(i) General Properties.

The hydration of dried corneal stroma, allowed to swell freely in solution, showed a similar dependence on time as does the hydration of fresh pieces. An initial fast rate of intake of fluid soon decreased to a much lower value. The initial swelling was faster than with fresh corneal stroma for a given solution.

(ii) Behaviour at Low pH.

Minimum increase in water content was always found when the corneal stroma was allowed to swell in solutions at pH4 compared to swelling at either higher pH values (i.e. 6, 7, 8 and 10) or at lower value pH2. At pH4, with all ionic strengths used, a steady value of the hydration of the tissue was obtained after approximately ten hours. However, the value of this final constant hydration depended on the ionic strength of the bathing solution as shown in Table 4. In general, it was seen that an increase in the ionic strength of the bathing medium increased the hydration of the tissue. At μ = .06, μ =.1 and μ = .15 the final hydration was about 2.5-3. As the ionic strength increased to μ = .2, the final hydration altered to approximately 4 and in solutions of u = .3, the final hydration was about 4.5 (Fig. 4).

When corneal stroma was allowed to swell in solutions buffered at pH2, it was found that it took longer before a final constant value of hydration was obtained, i.e. 20 hours to reach a final constant hydration at pH2 but only 10 hours at pH4. When the ionic strength of

the solution was increased the hydration decreased in direct contrast to swelling in solutions at pH4. At μ = .06, the final value of hydration was between 10-11 while at .1 the final hydration was about 9-9.5. At μ = .15, .2 and .3 the values of the hydration after 20 hours were 8-8.5, 6-6.5 and 5.5 respectively (Fig. 5 and Table 4). For any given time, the hydration of the corneal stroma in solutions buffered at pH2 was larger than that of stroma in solution at pH4, for the same ionic strength.

(iii) Behaviour at High pH.

The bathing solutions were buffered at four different pH values - pH6,7,8 and 10. Five different ionic strengths were chosen from μ = .02 to μ = .25. At the lowest ionic strength, μ = .02, the highest values of hydration were found for a given time and given pH of the solution. In one hour, the hydration increased from zero to 2 at pH6 and zero to 6 at pH10. Values in between these were found when the pH was at 7 and 8 (Fig. 6). In general, it was found that the hydration of corneal stroma in a solution at pH10 was higher than that of stroma at lower pH values. In fact, the higher the pH of the bathing solution, the higher the water content of the tissue for a given time at u = .02.

This dependence on pH of the bathing solution was found to hold at other ionic strengths (Fig. 7,8,9,10). At μ = .05 and μ = .1 (Fig. 7,8) the more alkaline the external bathing solution, the higher the hydration of the tissue at a given time. At μ = .15, the hydrations of stroma swollen in solutions buffered at pH8 were slightly larger than those buffered at pH10 (Fig. 9). However, the swelling rates were found to be equal at pH8 and at pH10 (Fig. 10). The latter pH

values always followed the general findings that the more alkaline the bathing solution, the greater the water content of the stroma. The swelling curves in Figs. 6,7,8,9, and 10 have been plotted by eye through the experimental data points. In some cases, there is a large spread in the data points. This cannot be attributed to the error in the weighing measurements which was found to be approximately 2% (see chapter 2, section III). The spread in results must be an indication of the differences in the tissue.

(iv) Analysis of Results in Terms of Donnan Theory.

In the theory section, II, of this chapter, it was shown that assuming all the swelling pressure was due to an osmotic (Donnan) pressure then a linear relationship was predicted between the time of swelling and the function G(H) equal to $H^2/2 + H \times E$ where H is the hydration and E is a constant. The data obtained from the swelling of corneal stroma at pH 6,7,8 and 10 and μ = .02, .05, .1, .15 and .25 was analysed in terms of this function G(H). The values for each G(H) are shown in Figs. 11(a-d), 12(a-d), 13(a-d), 14(a-d) and 15(a-d) as a function of the time in the bathing solution. Linear regression fits were calculated for each of the 20 solutions used in the experiment. The slope $\pm$ standard error, intercept and f-ratio (significance of the slope) are given in Table 5.

The rate of hydration is directly proportional to the slope of the linear regression fit i.e. the larger the slope, the larger the rate of swelling. The relationship between the rate of hydration, the ionic strength and the pH of the bathing solution can be seen by comparing the values given in Table 5 for each solution or by studying

Figs. 11-15. The fastest rates of hydration are found at μ = .02 where the relation $H_6 < H_7 \lesssim H_8 < H_{10}$ seems to hold. (H_j stands for the rate of hydration at pH = j). The rates of hydration at pH7 and 8 are the same within both the errors. At μ = .05, $H_6 < H_7 < H_8 \lesssim H_{10}$ where the rate of hydration at pH8 is equal to that at pH10 within the error. The values of swelling rate at each pH are less than at the corresponding pH for μ = .02 by a factor of approximately 2.5. By increasing the ionic strength of the bathing solution to μ =.1, lower values of the rate of hydration are found except at pH6 where the rate of hydration at μ = .05 is the same as that at μ = .1 within the error. The rates of hydration, at μ = .10, at different pH are nearer in value with $H_6 \lesssim H_7 < H_8 \lesssim H_{10}$. An anomalous rise in rates of hydration occurs at μ = .15 with each rate of hydration being a factor of 1.6 (on average) less than the rate at μ = .02. The relation $H_6 \lesssim H_7 < H_8 = H_{10}$ is seen to occur with the rate of hydration at pH8 being the same as that at pH10 within the error of each reading.

At μ = .25, the swelling rate at pH6 is larger than at the other pH values. However, the rate of hydration at pH7,8, and 10 follow the relation $H_7 < H_8 < H_{10}$. Each of these rates of swelling is lower than at the corresponding pH at ionic strength, μ = .1. In Fig. 16, the rate of hydration for one solution has been plotted as a function of hydration. In Fig. 17 the rate of hydration (at H = 3) has been plotted as a function of the pH of the bathing solution.

The dependence of the hydration on ionic strength was more complicated than that of pH of the bathing solution. It can be seen by comparing values of hydration in the Figs. 6-10 that, for a given pH, the swelling is largest at the lowest ionic strength μ = .02. The

smallest values of hydration are found for stroma swollen at μ = .25 the highest ionic strength used. The swelling in solutions of ionic strength μ = .05 is lower than at μ = .02 and slightly higher than at μ = .1. However, at μ = .15, the values of the hydration appear to increase above those found, for the same time and pH, at μ = .1 or μ = .25. Thus, although a general decrease in swelling is found as the ionic strength is increased, it appears that swelling at μ=.15 does not correspond to this general trend. Ionic strength dependence will be discussed in more detail in the section V of this chapter.

(v) Swelling in Distilled Water.

Corneal stroma swelling in distilled water (Fig. 18) exhibited different rates of hydration compared to swelling in solutions containing small ions (mainly sodium and chloride ions). The hydration of the corneal pieces increase very rapidly for about 6 hours. In the first hour, the hydration has increased from zero to 8 or 9. After this very rapid initial swelling, the rate of hydration becomes practically constant at a hydration of 3000% i.e. H = 30 as shown in Fig. 18. This is unlike swelling in sodium chloride solution where the initial swelling is slower but the swelling continues for a longer time. A curve of hydration as a function of time for one salt solution is shown in comparison.

(C) Swelling Properties of Dried Rabbit Corneal Stroma.

Rabbit cornea were used in a few swelling experiments in order to compare with the swelling relationships found for dried beef corneal stroma.

(i) Behaviour at Low pH.

Swelling at pH4 reached a final, constant hydration whose value depended on the ionic strength of the bathing solution. At μ = .1, the final value of the hydration was between H = 2.5 and 2.75. Increasing the ionic strength, increased the value of the final hydration to approximately 9.5 (Fig. 19).

At pH2, the maximum value of the hydration was about 7 at μ = .1 and 6 at μ = .3 i.e. increasing the ionic strength decreased the swelling (Fig. 19).

(ii) Behaviour at High pH.

Only two pH values, at two ionic strengths were used (i.e. four solutions). Swelling was greater at pH10 compared to swelling at pH7 at both μ = .05 and at μ = .25. The swelling at μ = .05 was greater than at μ = .25 (Fig. 20).

The data was analysed in terms of a linear fit between the function $G(H) = H^2/2 + H \times E$ and time of swelling. The data points and the regression fit (solid line) are shown in Fig.21 , for swelling in all four solutions. The details of the regression fits are given in Table 6.

(D) Estimates of the Fixed Charge Concentrations.

It was shown, in section II, that the rate of hydration dH/dt was equal to a constant for a given solution divided by the term (H + E). The constant, K, was a function of the fixed charge concentration C_f

such that

$$K = RT\ C^2 C_1 / a^2 2C+$$

where $C = C_f \times H$.

Thus $C_f \times H = (2Ka^2C+/RTC_1)^{\frac{1}{2}}$.

The values of these parameters are known. RT is 2436 $Jmol^{-1}$ at 20°C, a is approximately 8/35mm (Hedbys and Mishima, 1962), C_1 is 22 x 10^{-14} cm^4/dyne-sec (Friedman and Green, 1971b) which is 22 x 10^{-17} m^4/N-sec. C+ is known for each solution, K is found from Table 3, for each solution. In Table 7, a list of the predicted values of $C_f \times H$, for each solution, are presented as well as the value of C_f at H = 3.5 (i.e. physiological hydration).

V Discussion.

(i) Comparison of Fresh and Dried Tissue.

All swelling curves presented in this chapter show a similar dependence on the rate of hydration with the time of swelling. Initially, the swelling rate is fast but it gradually decreases. For some bathing solutions at low pH values, the rate of hydrations becomes zero whereas at high pH values 6,7,8, and 10, the hydration continually increased. Swelling of dried tissue appeared to be similar to the swelling of fresh tissue as found by Payrau et al (1967, chapter 5). The initial swelling is faster with dried tissue but it eventually becomes similar to that of fresh tissue. At pH2, the final value of the hydration was found to be approximately H = 8 for dried tissue at μ = 1.5 and the same value is found for fresh tissue (Fig. 1). However, some differences occur when the stroma is swollen at pH4. With dried tissue, the final, constant value of hydration is approximately 3(μ = .15) and 4.25 (μ = .2).

The former value is below the hydration of fresh tissue. It was found that with fresh tissue the final hydrations were H = 5 (μ = .15) and H = 5.5 (μ = .20). The differences may be due to the differences in the internal environment of the stroma, between fresh tissue and dried tissue. When the final hydration value is near to that of fresh tissue, the time taken for the distribution of ions to take place may be longer with fresh tissue and hence allows time for more swelling.

At higher pH values, pH6 and 10, at μ = .15, it can be seen that there is agreement between the linear regression fits obtained from fresh and dried tissue. With dried tissue, at pH6, the slope of the regression fit is 1.55 $\pm$.06, whereas the fresh tissue gives a value of 1.46 $\pm$.11. At pH10, the slope of the regression curve is 1.99 $\pm$ .14 for dried tissue and 1.88 $\pm$ .12 for fresh tissue.

The swelling data for fresh and dried tissue in distilled water is also similar. The final value of hydration is approximately 30 for dried tissue and 31 for fresh tissue. This agreement is reasonable considering the variation in water content found with one type of tissue at these high hydrations.

(ii) Comparison of the Swelling Properties of Dried Beef and Dried Rabbit Corneal Stroma.

It is known that different mammalian cornea swell by different amounts when placed in the same bathing solution (Ehlers, 1966). Thus differences in the magnitude of the hydration between beef and rabbit cornea were expected and were seen. The dried rabbit cornea in solutions at low pH would swell to a constant, final hydration and would remain

at this water content for up to 70 hours. At pH4, the final hydration was 2.5 at μ = .1 but 9.5 at μ = .3. Similarly to beef cornea, an increase in ionic strength at pH4 increased the amount of swelling. However, the increase in swelling was greater with rabbit cornea compared with beef cornea at μ = .3 (compare Fig. 20 with Fig. 4). Rabbit cornea swollen at pH2 showed the opposite behaviour with increasing ionic strength compared with swelling at pH4. The final value of hydration at pH2, μ = .1, was about 6.5 and at μ = .3 was only 6.

At higher pH values, the swelling was found to be faster the more alkaline the bathing solution as found for beef corneas. The swelling rate was higher in solutions of μ = .05 than in solutions of μ = .25 at the same pH. This is the same qualitative dependence on ionic strength as seen with the swelling of beef corneal stroma.

(iii) General Characteristics of the Swelling of the Corneal Stroma.

It can be seen from the results section that the swelling of the corneal stroma depends to a large extent on the bathing solution. The minimum amount of swelling occurs at or near pH4 in beef cornea (Loeven and Van Walbeck, 1955). The cornea swells to a fixed value of hydration at pH4 but the magnitude of the swelling depends on the ionic strength. Increasing the ionic strength increases the final hydration. At pH2, a final value of hydration is also found but it depends inversely on the ionic strength i.e. decreasing the ionic strength increases the amount of swelling. Swelling at higher pH values does not become zero within the time limit of the experiment. After an initial fast rate of swelling, the increase in water content becomes slower and slower. In general, the more alkaline the bathing solution the higher the swelling

rate. Increasing the ionic strength tends to decrease the rate of hydration except that an increase in the rate of swelling occurs at $\mu = .15$ above that at $\mu = .1$ or $\mu = .25$.

(iv) Donnan (Osmotic) Theory of Swelling.

The analysis of the swelling data presented in the results section IV, (B)(iv) showed that good linear fits could be obtained between the time of swelling and the function G(H) where $G(H) = H^2/2 + H \times E$. This relationship was predicted by assuming that the swelling pressure was wholly osmotic in origin. The osmotic pressure was due to the distribution of permeant ions between the stroma and the external solution. The distribution of ions was different in these phases because of the presence of fixed charged groups in the stroma. Donnan theory of swelling would predict that an increase in ionic strength should decrease the osmotic pressure according to the approximate formula

$$P = RT \frac{C_F^2}{4C_+}$$

where C_+ is the external ion concentration. Altering the pH of the external solution will alter the pH of the internal solution and thus alter the number of ionised charged groups on the glycosaminoglycans and the distribution of small ions between the corneal phase and the external solution. Increasing the pH above the isoelectric point will cause the polymer to be negatively charged. Conversely, lowering the pH below the isoelectric point will cause the polymer to be positively charged.

The osmotic pressure will cause the stroma to swell by intake of bathing solution. If there is no force acting against the expansive

swelling pressure the stroma will swell indefinitely. At low pH, the swelling continues for the order of 10 hours and then constant hydration is maintained. There must be a balance of forces at this point. It may be that all the charge on the glycosaminoglycans is neutralised after bathing in solution at pH4 (the approximate isoelectric point of the stroma). If this occurs there will be no Donnan distribution of ions between the two phases and therefore no swelling pressure i.e. there is no need for an opposing force to balance the osmotic pressure.

The swelling rate also becomes zero at pH2. The molecules would be expected to be positively charged at this pH, and thus a definite osmotic pressure will exist. It may be that at this low pH, some sort of attractive forces (probably Van der Waal's forces) can exist which counteract the osmotic force causing the tissue to swell.

At higher pH values, it appears that the swelling pressure is totally osmotic and that there is no (or very small) force opposing the swelling of the tissue. Hence, the tissue will go on swelling.

An interesting point is the fact that the swelling ceases at a high value of hydration (H = 30) when the stroma is swollen in distilled water. Although this value of hydration was not obtained with salt in the bathing solution in these experiments, Kinsey and Cogan (1942) report that cat cornea go on increasing in water content above this value if left in salt solution for over one week. In distilled water, initially the osmotic pressure difference between the stroma and the bathing solution is going to be large because of the absence of ions in the outside solution. Swelling will be fast because of this large osmotic pressure difference. However, it is thought that the ions in

the stroma will try to distribute themselves according to the Donnan theory until there are very few ions in the stroma. At this time, there will be no large osmotic pressure difference and therefore the swelling will cease.

It must be admitted that the Donnan theory is being used in a situation when no equilibrium exists i.e. the osmotic forces are not being balanced by elastic forces of the tissue. Overbeek (1956) states that Donnan systems should be in equilibrium. However, Helfferich (1962) states that although the Donnan potential is an equilibrium phenomenon the equations used for its derivation can also be used in nonequilibrium systems in which fluxes across the interfaces occur, provided that the interfaces offer no resistance to diffusion. In the cornea, it is thought that the resistance to diffusion is due to the glycosaminoglycan excluded volume effect and to the collagen fibrils (Hedbys and Mishima, 1962). These effects will certainly be low at high hydrations when the interface itself will not offer much resistance to solvent or solutes. (Cogan and Kinsey, 1942; Donn, 1962).

It must also be noted at this time that no membrane exists between the stroma and bathing solution in these experiments because the endothelium has been removed. The presence of a membrane has been found not to be necessary for Donnan theory. The presence of two different phases is required e.g. one phase with fixed negative charge and one without (Overbeek, 1956).

The straight line fits obtained by the method of least squares have non-zero intercept values on the ordinate axis. It would be expected that the regression fit should pass through the origin because the tissue is initially dried ($H = 0$) at $t = 0$. The reason for this

may be due to the fact that the collagen fibres themselves become hydrated in the corneal stroma (see chapter 1, section IV, II) and this mechanism of swelling is not included in the theory. Another assumption, used in the theory, is that the fixed charge concentration should always be less than twice the concentration of sodium ions in the external solution. This is expected to hold at most hydrations but may not be true for $H < 3$ especially when the ionic strength of the bathing solution is small. If this were the cause of non-zero intercept values, a larger error would be expected at low ionic strengths. This is seen in Table 5 where the intercept values at $\mu = .02$ are larger than at other ionic strength. The approximation used leads to larger values of osmotic pressure compared with the full expression when the fixed charge concentration is larger than or equal to twice the external sodium ion concentration. It was also shown that the relation used between flow conductivity and hydration might lead to values of the function G(H) which were too low at high hydrations. These two effects i.e. too high values at low hydration and too low values at high hydration would lead to the slope being lowered and possibly a larger value of the intercept.

(v) Polyelectrolyte Gel Theory.

The swelling behaviour of the corneal stroma can be explained to some extent in terms of the theory of polyelectrolyte gels (Katchalsky, 1954). Katchalsky (1954) in his introduction mentions an important group of biogels which result from the interaction of collagen and chondroitin sulphate in connective tissues. However, in the cornea it does not seem likely that polysaccharide chains mechanically cross-link the collagen fibrils. (Chapter 2, Section I(v)). The other forces

which can cross-link a gel are Van der Waals attractive forces and electrostatic forces. It is the latter forces which are strongly influenced by the pH and ionic strength of the external solution (Rome, 1968).

Katchalsky (1954) states that the classical example of electrovalent bonding in gels occurs at their isoelectric points. At this point, the molecule has an equal number of positive and negative charges. In concentrated solutions, these charges will favour the formation of intermolecular attractive forces. This type of bonding will be strongest in ordered structures such as collagen fibrils.

(vi) Polyelectrolytes in the Cornea.

The cornea can be regarded as a mixed polyelectrolyte as it contains both collagen and glycosaminoglycans. At pH7, the corneal collagen probably has equal numbers of positive and negative groups. Therefore, it does not swell much (Pirie, 1947; Bowes and Kenten, 1950). However, at pH7 the glycosaminoglycans are negatively charged and will behave as polyanions (chapter 4). On lowering the pH, the net charge on the glycosaminoglycans will become less until their isoelectric point is reached. Further lowering of the pH will result in the glycosaminoglycan being positively charged. At the same time, the change in pH will affect the collagen fibrils unless the effect of the charged groups is masked by their coating of ground substances (Francois et al, 1954, Garzino, 1955). The ground substance may be the structural glycosaminoglycan isolated by Robert (chapter 1, section IV,(vi)). However, if the charged groups of the collagen fibrils are exposed then the lowering of the pH below pH7 will result in the collagen fibrils being positively charged in contrast to the glycosaminoglycans which

are negatively charged. Increasing the pH above 7 will make the collagen molecules negatively charged i.e. the same sign as the glycosaminoglycans. Bungenberg de Jong (1949) has described such complex colloid systems. Loeven and Van Walbeck (1954) conclude that it is highly probably that connective tissue complexes are similar to the complex colloid systems described by Bungenberg de Jong (1949).

(vii) Behaviour at the Isoelectric Point.

As stated previously, the polyelectrolyte theory of Katchalsky (1954) maintains that there are electrovalent attractive forces between the equal numbers of positive and negative charges (zwitterion pairs) which must exist at the isoelectric point of an ordered system. Addition of salt to a polyelectrolyte system at the isoelectric point is known to produce specific effects. The main effect of the salt is to produce Debye atmospheres around the fixed charged groups. This reduces the force between the charged groups. At the isoelectric point, reduction in the attractive forces results in the system becoming looser and allows the gel to swell by a greater amount. This is the exact behaviour seen on swelling the beef corneal stroma at pH4 when the salt concentration was increased (chapter 2, section IV, B(ii)). It was also seen with rabbit cornea (chapter 2, section IV, C(i)).

(viii) Behaviour Away From Isoelectric Point.

Altering the pH of the external solution away from the isoelectric point will reduce the number of zwitterion pairs and produce a net charge on the polysaccharide. This will allow increased swelling in two ways. First the addition of alkali or acidic ions will result in

more counterions in the gel to neutralise the net fixed charge on the polyelectrolyte. This accumulation of small permeant ions will increase the osmotic pressure and hence the amount of swelling. Secondly, the reduction in the attractive zwitterion pairs causes the number of electrovalent bonds to be reduced and thus generally loosens the system. This again allows for increased hydrations. This behaviour is seen in the cornea. Swelling at pH2 is always larger than at pH4 for a given ionic strength. Swelling at pH6 is also larger than at pH4. Increasing the pH above the isoelectric point from pH6 to pH10 produced a notable increase in the rate and amount of swelling.(Fig. 6-10).

When the pH of the external solution is altered away from the isoelectric point, the addition of salt has the opposite effect to the swelling than at the isoelectric point (Katchalsky, 1954). This is due to formation of Debye atmospheres around the charged groups. This reduces the repulsive forces between, say, the negatively charged groups at pH values greater than pH4. Thus the swelling capacity is reduced as seen for the swelling of the corneal stroma at pH2 and, in general, at higher pH values.

However, an increase in the ionic strength of the bathing solution does not linearly decrease the swelling. In fact, after an initial decrease in swelling as the ionic strength is increased from μ = .02 to μ = .10, an increase is noted at μ = .15 with a further decrease as μ is increased to .25. A minimum in the swelling curve, at .5% sodium chloride, has been noted previously by Smelser (1962) and non-linear behaviour by Kinsey and Cogan (1942).

It is thought that this minimum in the swelling curve as a function of ionic strength may be due, in part, to the fact that the pH inside and outside the corneal stroma will not be the same. At a given external ionic strength, the hydrogen ion concentration inside, H^i, is related to the hydrogen concentration inside, H^o, by

$$H^i Cl^i = H^o Cl^o$$

i.e. a Donnan distribution of ions. This becomes, on taking the logarithm of each side

$$pH^o = pH^i + \log (Cl^o/Cl^i)$$

According to Katchalsky (1954) the concentration of the chloride ions can be used because the polyelectrolyte slightly increases the activity of the coions but they are practically equal to unity. If the concentration of chloride ions outside is greater than the concentration of chloride ions inside, then pH^o will be greater than pH^i i.e. the internal pH is less than the external pH. The chloride ion concentrations will become equal only when the external concentration becomes very high.

It is thought that a combination of the decrease in magnitude of swelling with an increase in the ionic strength, expected from polyelectrolyte gel theory, and the effect of the difference in internal and external pH increasing with decreasing ionic strength (i.e acting to reduce swelling as the ionic strength is increased in opposition to the expected ionic strength dependence) may possibly explain the non-linear decrease in swelling with ionic strength.

(ix) Effect of Buffer Ions.

It must be noted that although sodium and chloride ions were the most common ions in the bathing solutions, some divalent ions were present in the buffer at pH6,7 and 8. Only divalent anions have been used. Loeven and Van Walbeek (1954) found that although the

valency of the cation effected the swelling of beef cornea, the valency of the anion did not effect the swelling behaviour. Smelser (1962) presents swelling data showing that bivalent anions increase the swelling rate but this experiment was carried out with scup corneas.

(x) Possible Elution of Polysaccharides.

Errors will occur in the calculation of the swelling rate if polysaccharides are eluted from the corneal stroma by the external solution. Differences in the staining of the acid mucopolysaccharide has been noted on the hydration of the cornea (Cejkova and Brettschneider, 1969, Cejkova and Bolkova, 1970, Bolkova and Cejkova, 1971). However, a quantitative analysis of the acid mucopolysaccharide content has shown that no polysaccharide is eluted from the rabbit corneas when they were swollen in distilled water (Čejková and Brettschneider, 1969). Woodin (1952) has shown that either 10% calcium chloride or high concentrations of hydrochloric acid (3.5N) are needed to remove large amounts of polysaccharide from the cornea. Moreover not only were these high acid or salt concentrations required but the tissue itself had to be swollen in distilled water to approximately a hydration of 3200% in order to give good yields. Sodium chloride, the main salt used in these experiments, was found to be less efficient than calcium chloride.

Loeven (1955) presents measurement of the glucosamine content of cornea after different pH treatments to show that rinsing out of the glycosaminoglycans does not occur. Further studies by Hedbys and Dohlman (1963) showed that no macromolecules diffused out of the stroma during their measurements of swelling pressure versus hydration. It was also noted that the bathing solutions did not appear cloudy even

after the corneal stroma had been left for 24 hours. Polysaccharides in solution have a cloudy appearance.

Thus, it is concluded that although some polysaccharide may be eluted by the higher salt concentration it is a small fraction of the total content.

Table 1.

pH	Buffer	μ
2	25ml 0.2M KCl + 6.5ml 0.2M HCl in 100ml	.06
4	18ml 0.2M NaOAC + 82ml 0.2M HOAC in 1000ml	.02
6	12.3ml 0.1 Na_2HPO_4 + 87.7ml 0.1 NaH_2PO_4 in 1000ml	.01
7	61ml 0.1 Na_2HPO_4 + 39ml 0.1 NaH_2PO_4 in 1000ml	.02
8	94.7ml 0.1 Na_2HPO_4 + 5.3ml 0.1 NaH_2PO_4 in 1000ml	.03
10	50ml .05M $NaHCO_3$ + 10.7ml .1M NaOH in 100ml	.035

Table 2.

Fresh Tissue

Solution	Final Hydration
pH4 .15	5
pH4 .20	5.5
pH2 .15	8

Table 3.

Details of Linear Regression Fit for Swelling of Fresh Tissue.

pH	μ	Slope ± SE	Intercept	F-ratio*
6	.15	1.46 ± .11	3.16	165
10	.15	1.88 ± .12	45.6	228

Table 4.

Dried Tissue Swelling at Low pH.

Ionic Strength of Solution.	Final Hydration in Solutions at pH4.	Final Hydration in Solutions at pH2.
.06	2.75-3.00	10.00
.1	2.75-3.00	10.00
.15	2.75-3.00	8.00
.20	4.25	6-6.5
.3	4.50	6-6.5

* see Appendix 1 for explanation of f-ratio.

Table 5.

Details of Linear Regression Fits for Swelling of Dried Corneal Stroma

Solution Ionic Strength	pH	Slope	Intercept	N[1]	F-Ratio *
	6	2.58 ± .3	39	56	76
	7	3.60 ± .23	33	63	241
.02	8	3.92 ± .19	33	67	436
	10	4.94 ± .39	65	69	163
	6	1.01 ± .05	15	45	381
	7	1.27 ± .05	17	45	643
.05	8	1.86 ± .15	14.6	35	147
	10	2.1 ± .13	36	66	254
	6	1.02 ± .04	10.9	30	555
	7	1.06 ± .04	16.8	35	533
.1	8	1.28 ± .11	8.7	54	125
	10	1.41 ± .10	16.1	26	181
	6	1.55 ± .06	15.5	83	729
	7	1.68 ± .08	18.9	93	402
.15	8	2.08 ± .2	27	93	106
	10	1.99 ± .14	28	90	195
	6	1.62 ± .13	8.8	32	153
	7	.76 ± .06	12.1	35	142
.25	8	1.1 ± .11	12.8	35	108
	10	1.48 ± .26	32.0	76	45

* See Appendix 1 for definition of f-ratio

1 number of data points used to compute slope

Table 6.

Details of Linear Regression Fit for Swelling of Rabbit Stroma.

Solution pH	ionic strength	slope ± SE	intercept	F-ratio *
7	.05	3.52 ± .2	31	326
10	.05	3.41 ± .3	43	105
7	.25	0.70 ± .08	13.7	65
10	.25	3.19 ± .14	26	546

* see Appendix 1 for explanation of f-ratio.

Table 7.

Solution Ionic Strength	pH	$(Kx3600)S^{-1}$	$C_f \times H$ Mm^{-3}	C_f at H=3.5 mM^{-1}
μ = .02	6	2.58	53.1	15
	7	3.6	62.5	18
	8	3.92	65.2	19
	10	4.94	73.2	21
μ = .05	6	1.01	52.3	15
	7	1.27	58.65	17
	8	1.86	70.98	20
	10	2.1	75.4	22
μ = .1	6	1.02	74.3	21
	7	1.06	75.8	22
	8	1.28	83.3	24
	10	1.41	87.4	25
μ = .15	6	1.55	112.2	32
	7	1.68	116.8	33
	8	2.08	130	37
	10	1.99	127	36
μ = .25	6	1.62	148	42
	7	0.76	101	29
	8	1.1	122	35
	10	1.48	142	41

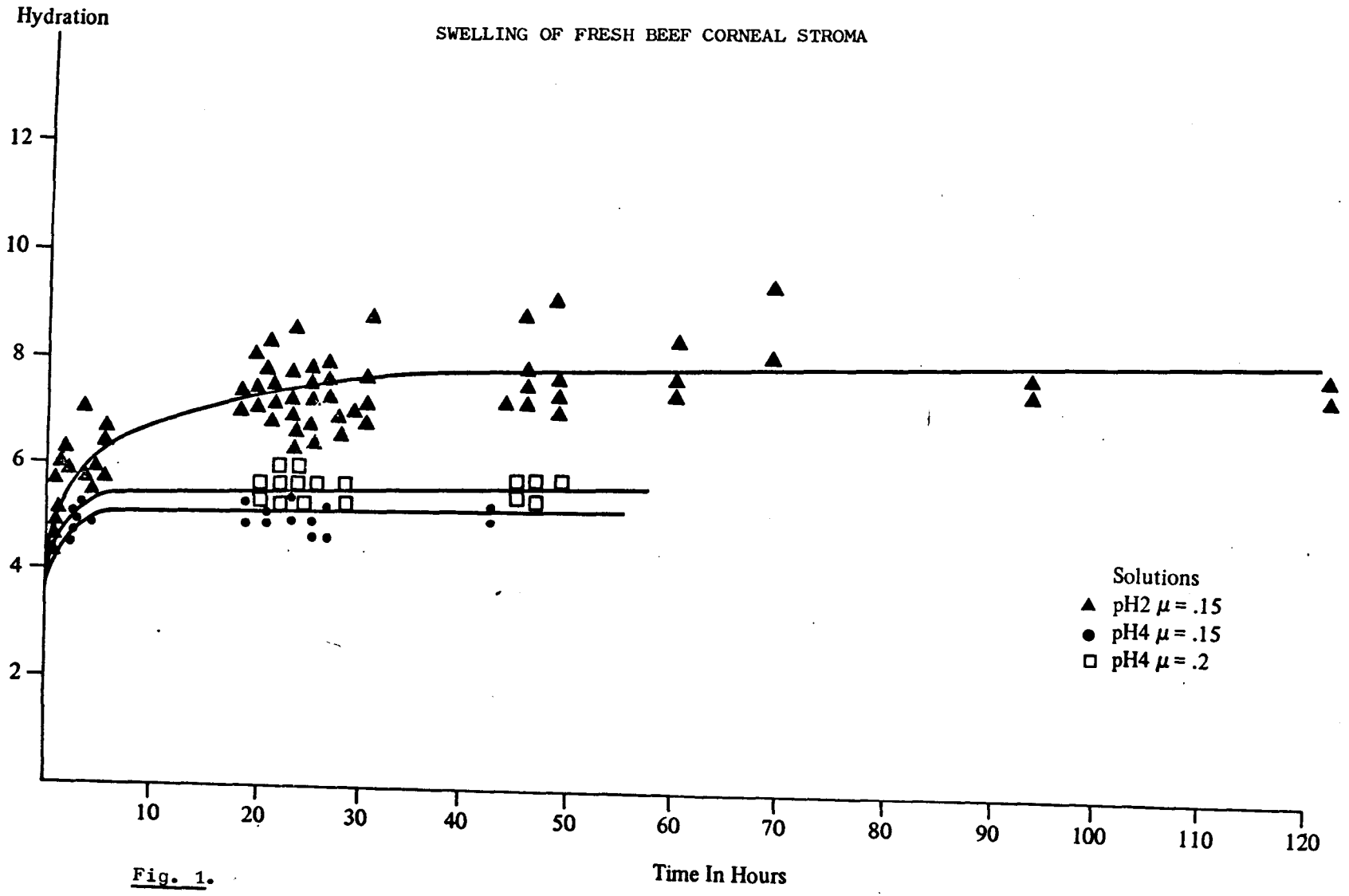
SWELLING OF FRESH BEEF CORNEAL STROMA
Hydration
12
10
8
6
4
2
10
20
30
40
50
60
70
80
90
100
110
120
Time In Hours
Solutions
pH2 μ = .15
pH4 μ = .15
pH4 μ = .2

Fig. 1.

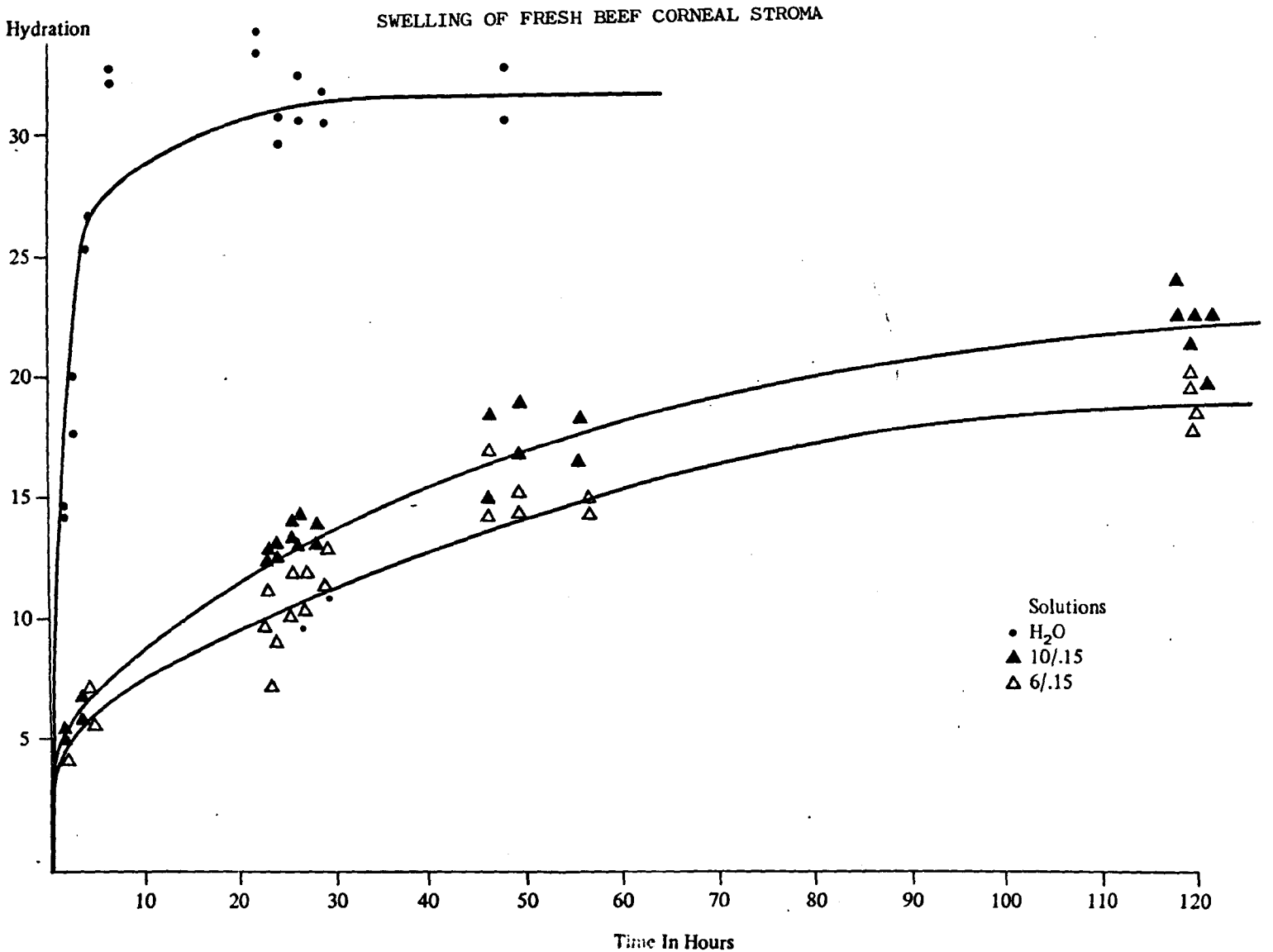
SWELLING OF FRESH BEEF CORNEAL STROMA
Hydration
30
25
20
15
10
5
10
20
30
40
50
60
70
80
90
100
110
120
Time In Hours
Solutions
• H_2O
▲ 10/.15
△ 6/.15

Fig. 2.

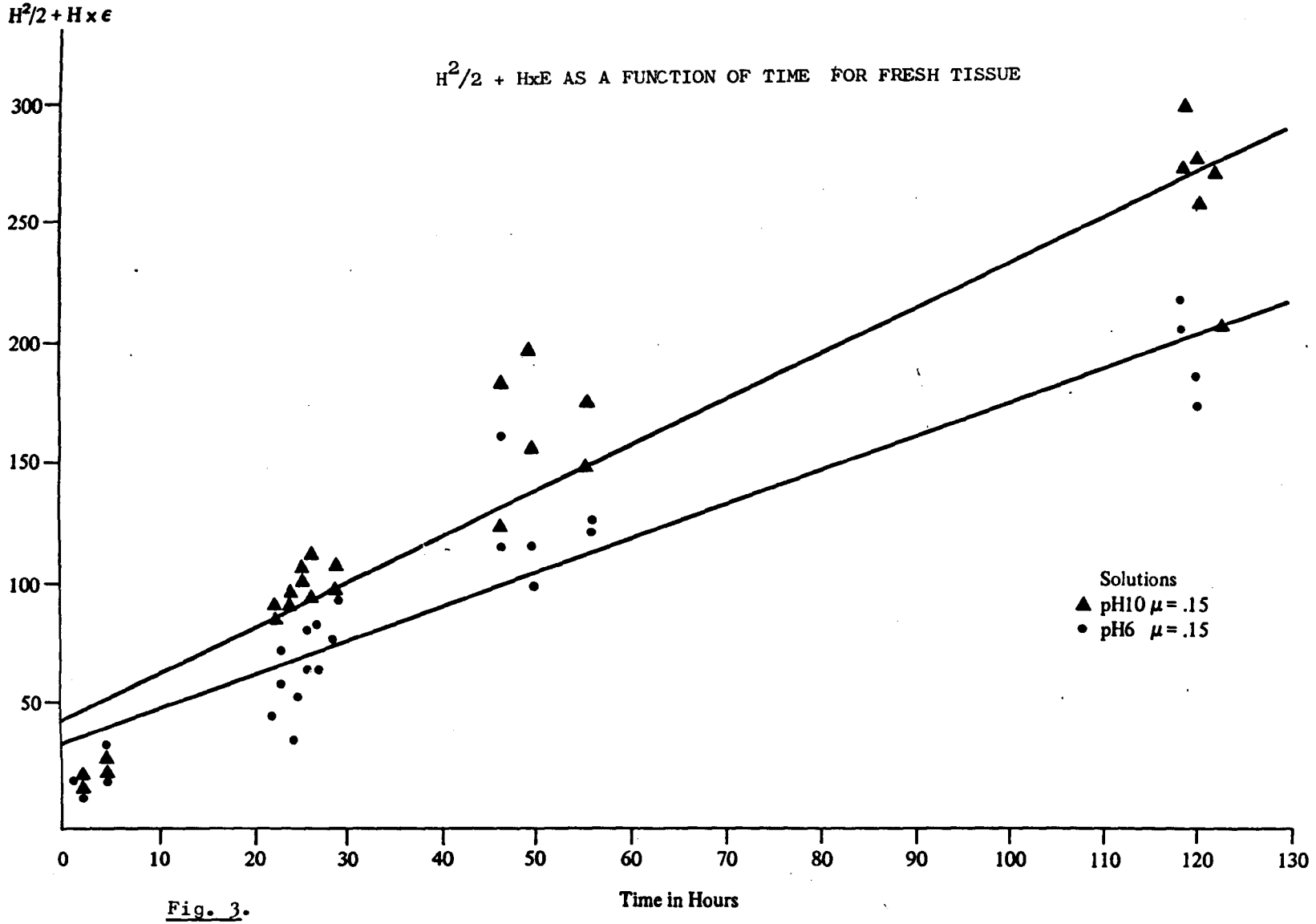
$H^2/2 + H \times \epsilon$
$H^2/2$ + HxE AS A FUNCTION OF TIME FOR FRESH TISSUE
300
250
200
150
100
50
0
10
20
30
40
50
60
70
80
90
100
110
120
130
Time in Hours
Solutions
▲ pH10 μ = .15
● pH6 μ = .15

Fig. 3.

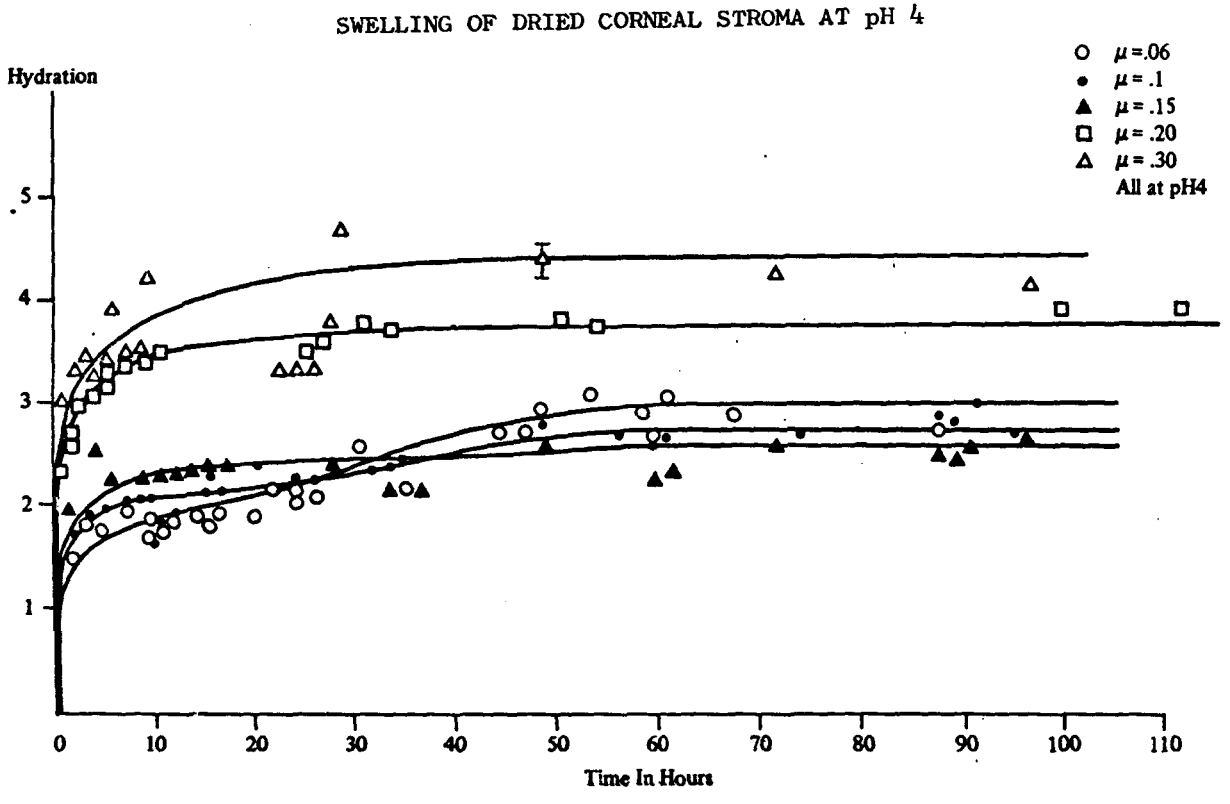
SWELLING OF DRIED CORNEAL STROMA AT pH 4
Hydration
5
4
3
2
1
0
10
20
30
40
50
60
70
80
90
100
110
Time In Hours
μ=.06
μ=.1
μ=.15
μ=.20
μ=.30
All at pH4

Fig. 4.

SWELLING OF DRIED CORNEAL STROMA AT pH 2

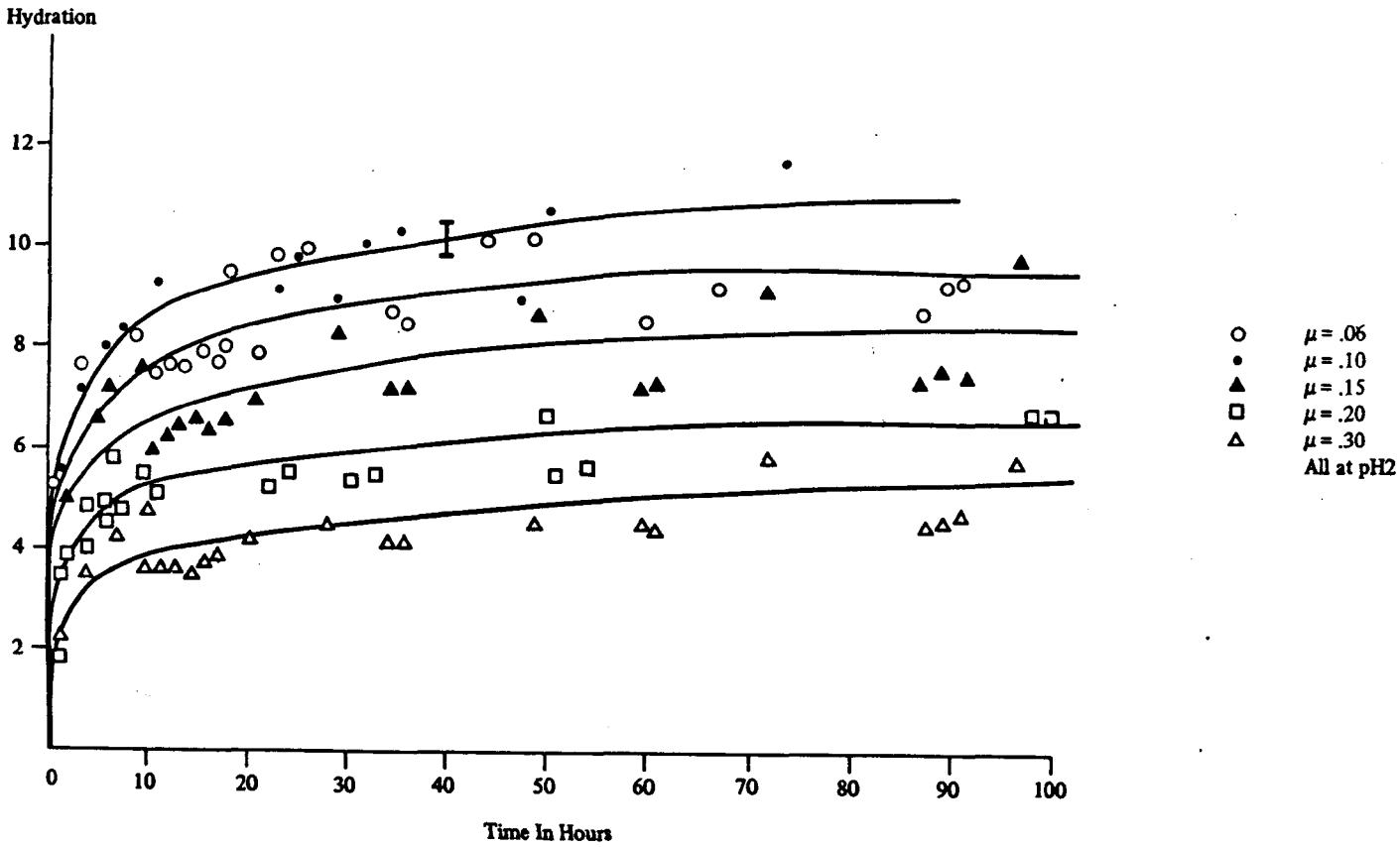

Fig. 5.

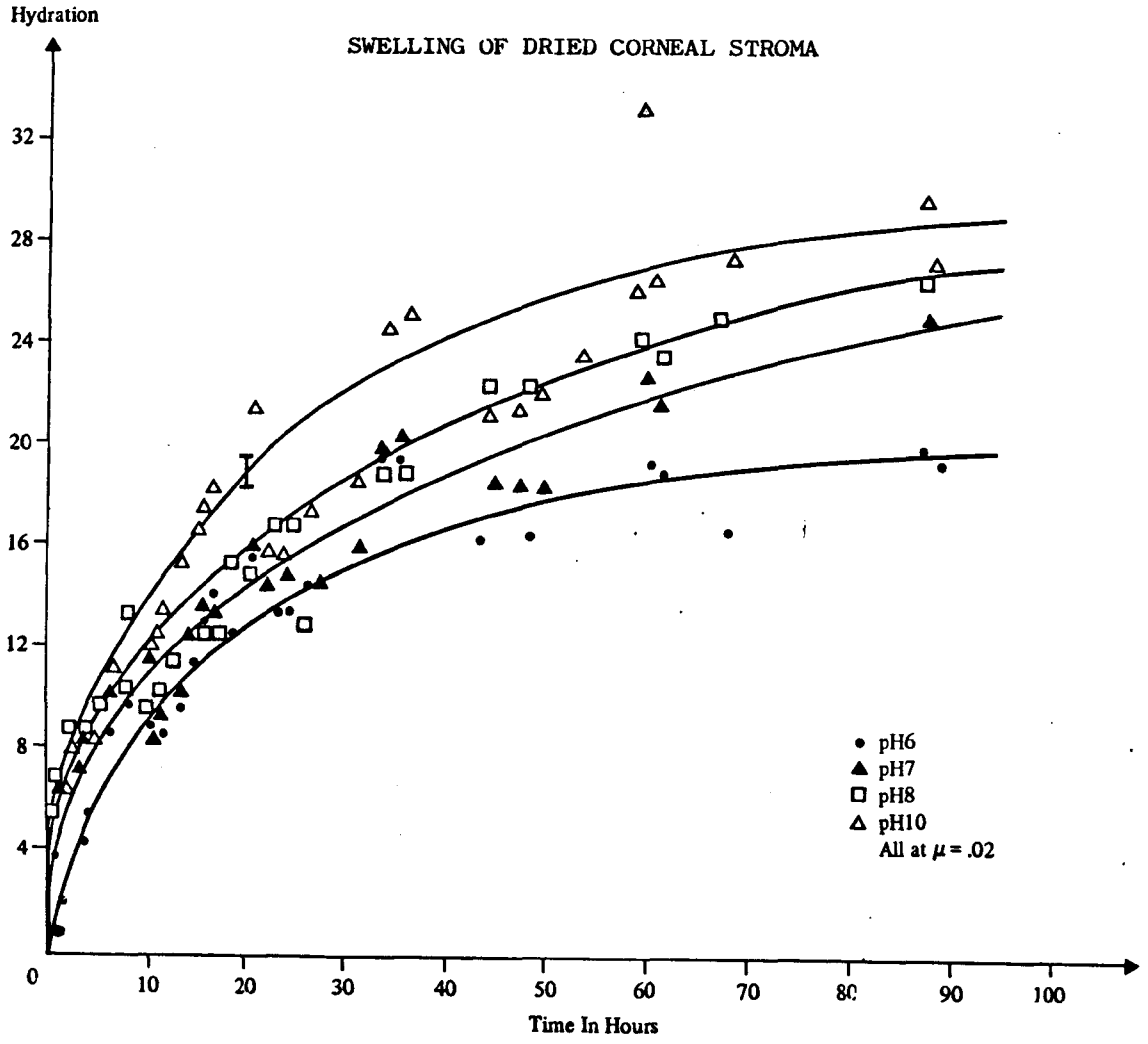
Hydration
SWELLING OF DRIED CORNEAL STROMA
32
28
24
20
16
12
8
4
0
10
20
30
40
50
60
70
80
90
100
Time In Hours
pH6
pH7
pH8
pH10
All at μ = .02

Fig. 6.

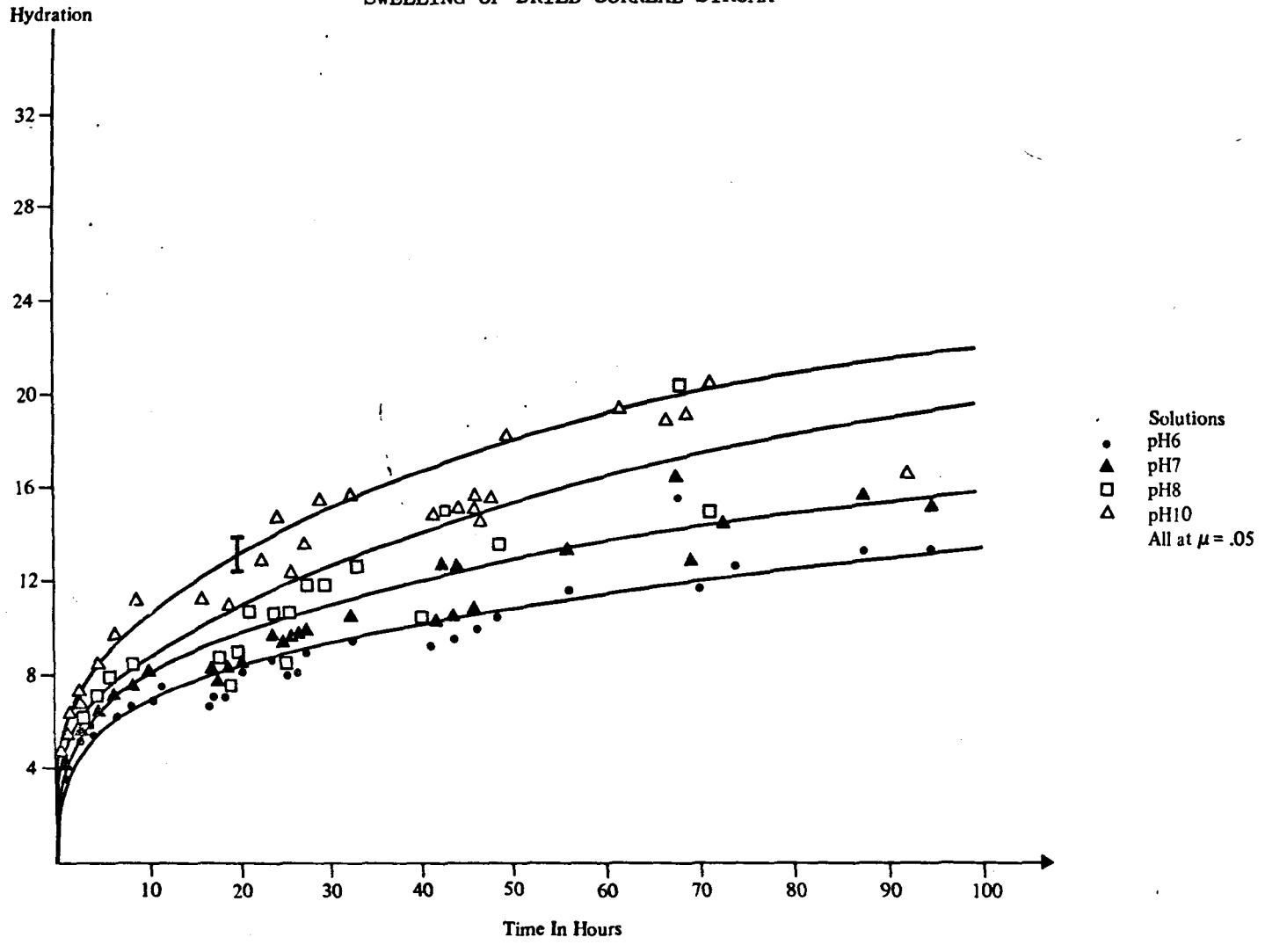
SWELLING OF DRIED CORNEAL STROMA
Hydration
32
28
24
20
16
12
8
4
10
20
30
40
50
60
70
80
90
100
Time In Hours
Solutions
pH6
pH7
pH8
pH10
All at μ = .05

Fig. 7.

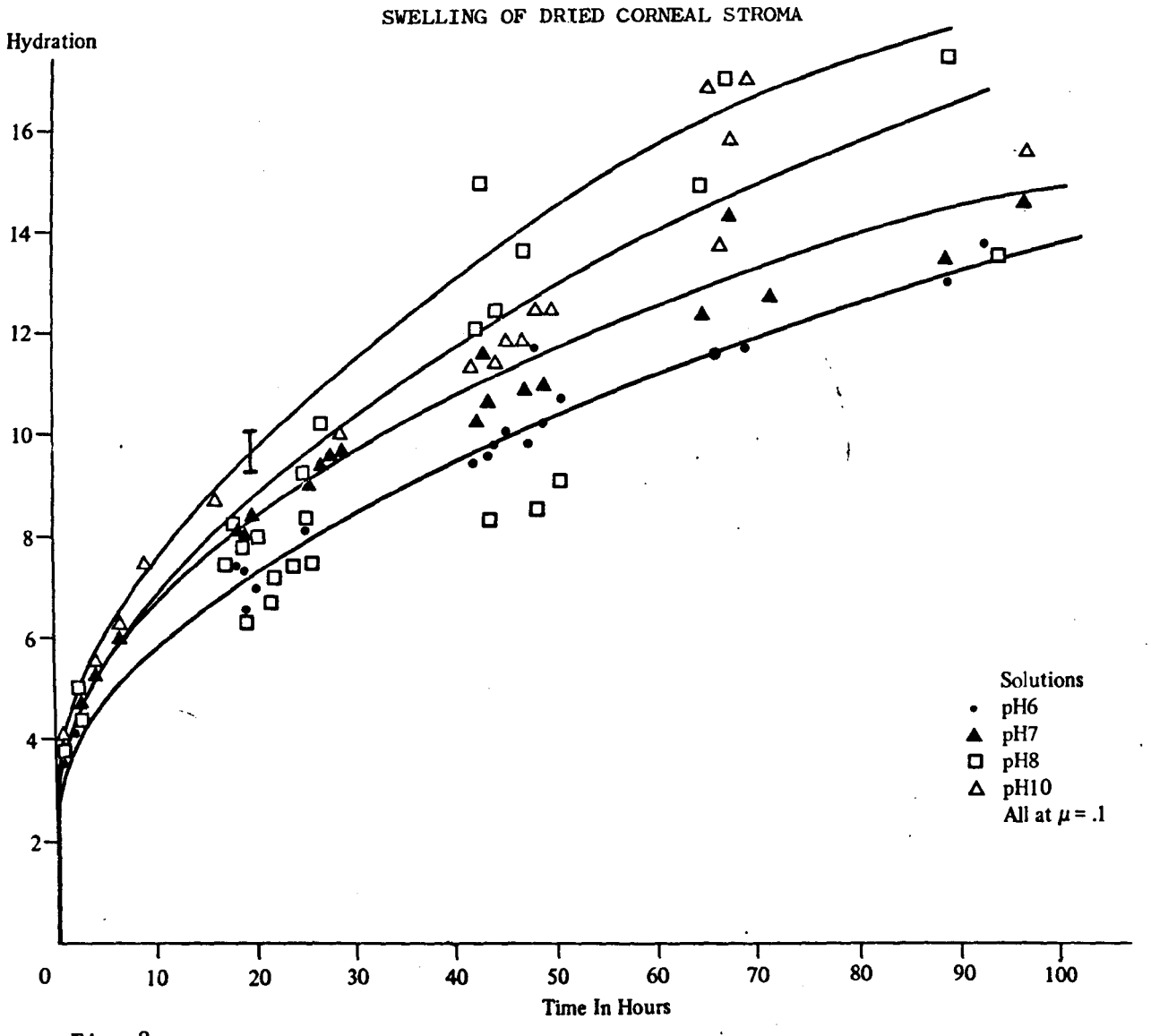
SWELLING OF DRIED CORNEAL STROMA
Hydration
16
14
12
10
8
6
4
2
0
10
20
30
40
50
60
70
80
90
100
Time In Hours
Solutions
pH6
pH7
pH8
pH10
All at μ = .1

Fig. 8.

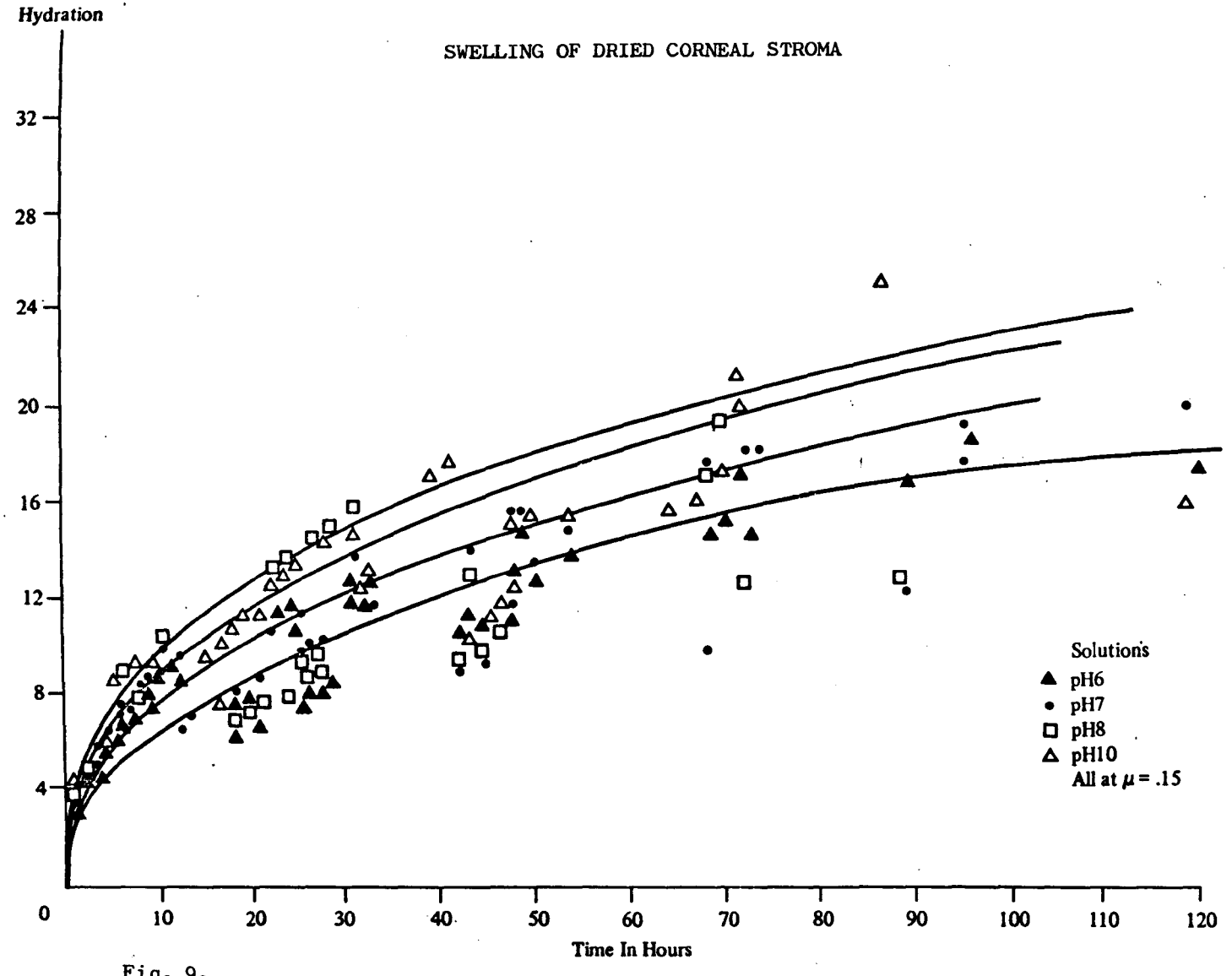
SWELLING OF DRIED CORNEAL STROMA
Hydration
32
28
24
20
16
12
8
4
0
10
20
30
40
50
60
70
80
90
100
110
120
Time In Hours
Solutions
pH6
pH7
pH8
pH10
All at μ = .15

Fig. 9.

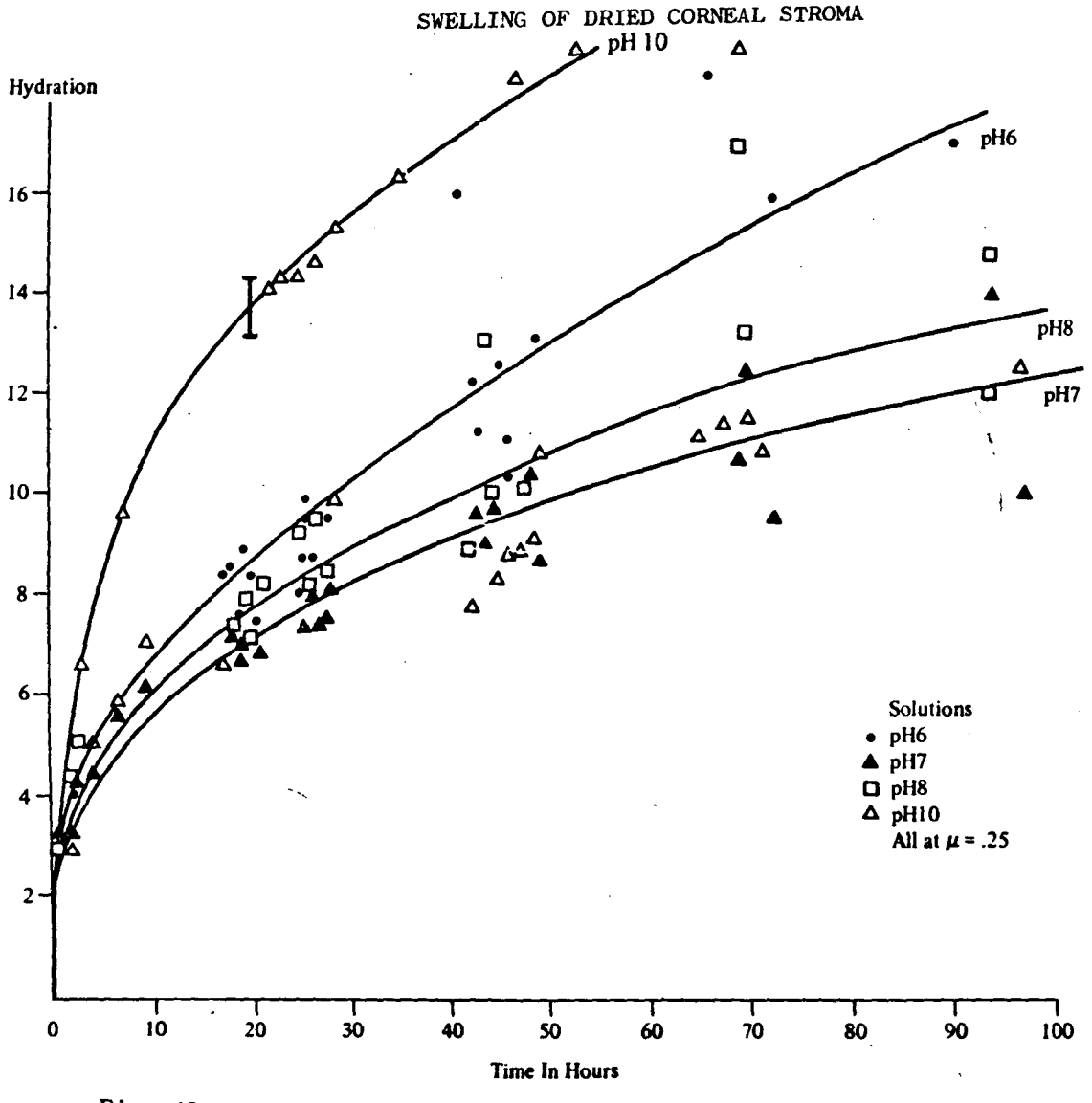
SWELLING OF DRIED CORNEAL STROMA
pH 10
pH6
pH8
pH7
Hydration
16
14
12
10
8
6
4
2
0
10
20
30
40
50
60
70
80
90
100
Time In Hours
Solutions
pH6
pH7
pH8
pH10
All at μ = .25

Fig. 10.

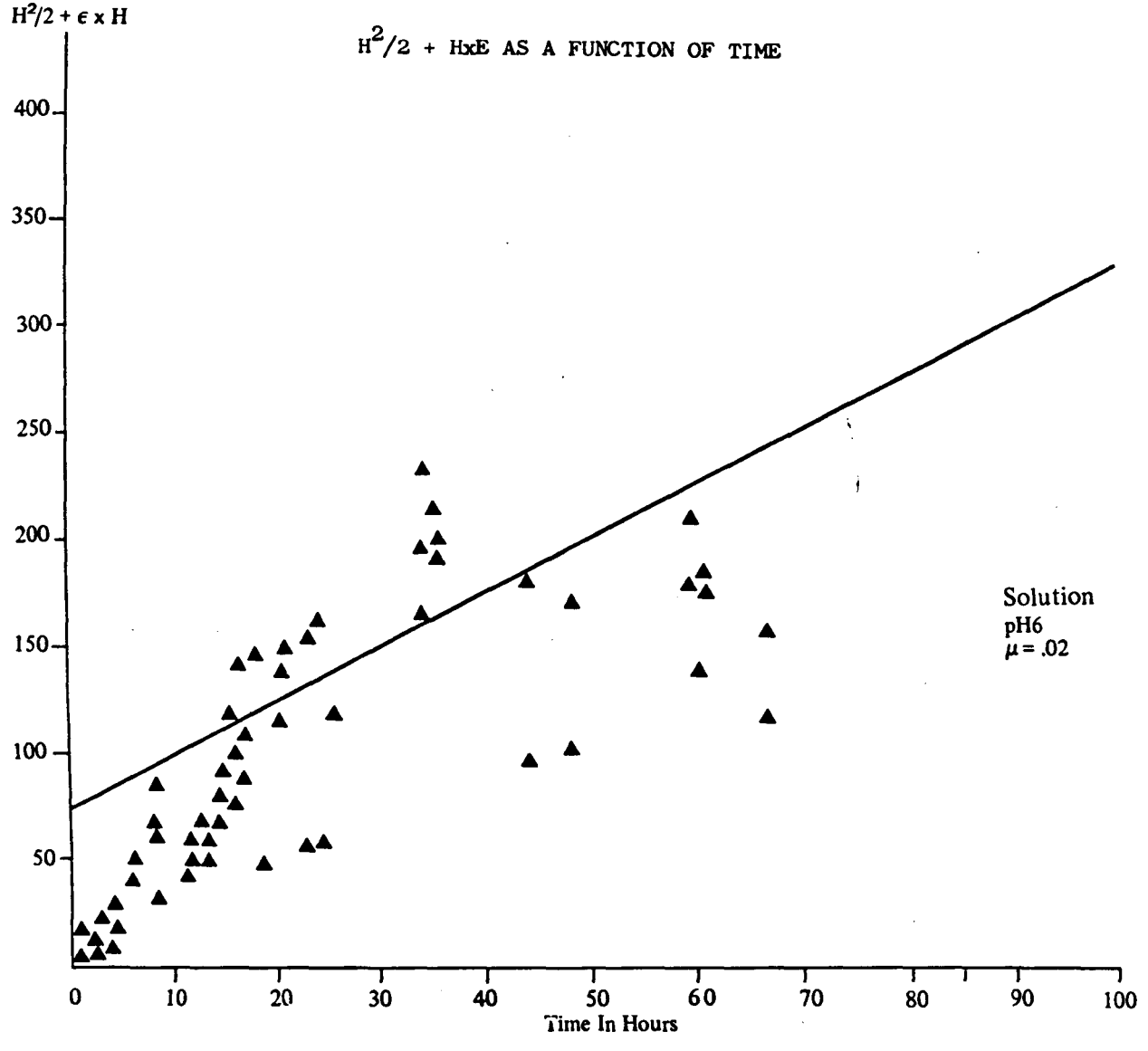
$H^2/2 + \epsilon \times H$
$H^2/2$ + HxE AS A FUNCTION OF TIME
400
350
300
250
200
150
100
50
0
10
20
30
40
50
60
70
80
90
100
Time In Hours
Solution
pH6
$\mu = .02$

Fig. 11a.

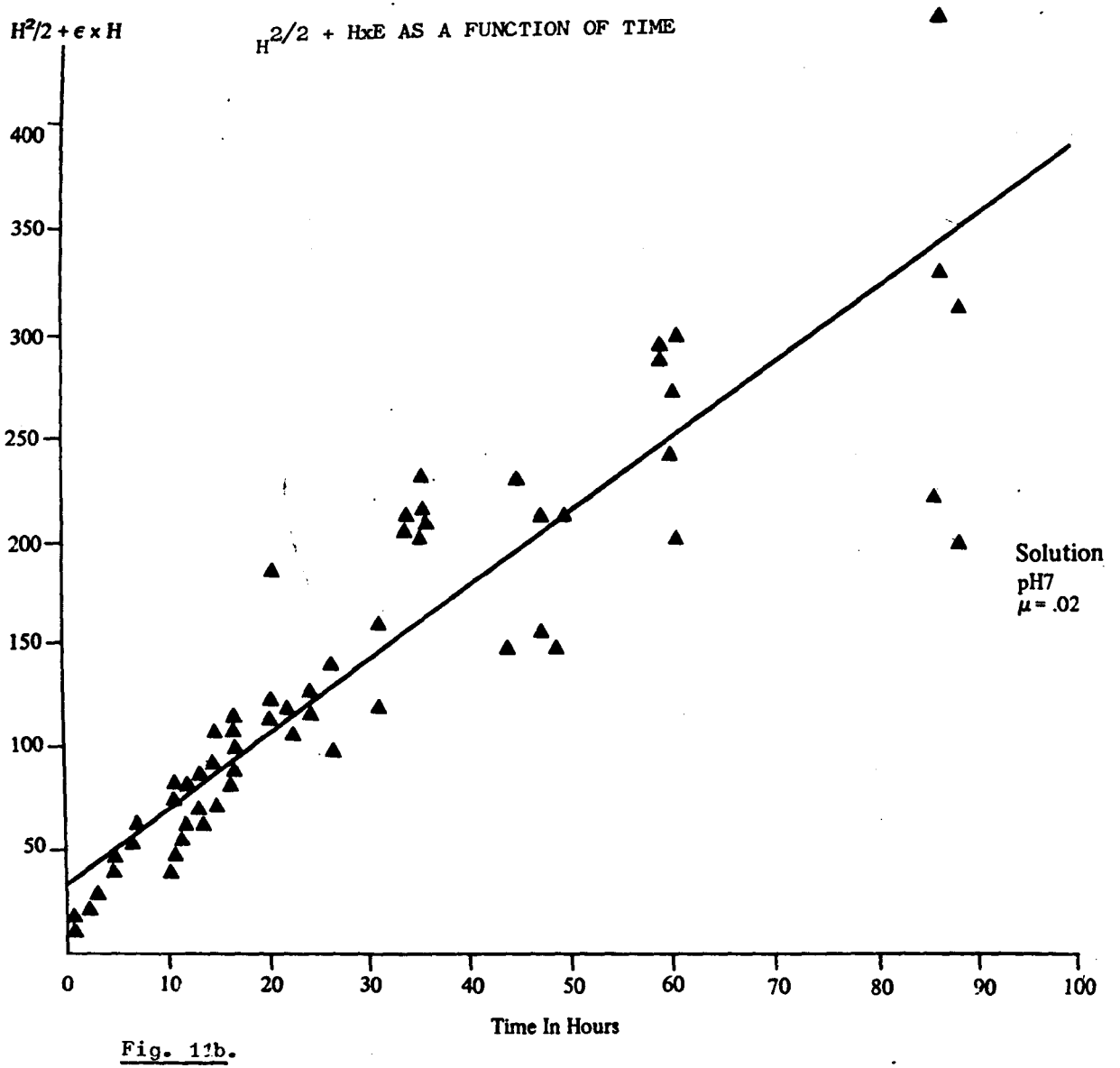
$H^2/2 + \epsilon \times H$
$H^2/2 + HxE$ AS A FUNCTION OF TIME
400
350
300
250
200
150
100
50
0
10
20
30
40
50
60
70
80
90
100
Time In Hours
Solution
pH7
$\mu = .02$

Fig. 12b.

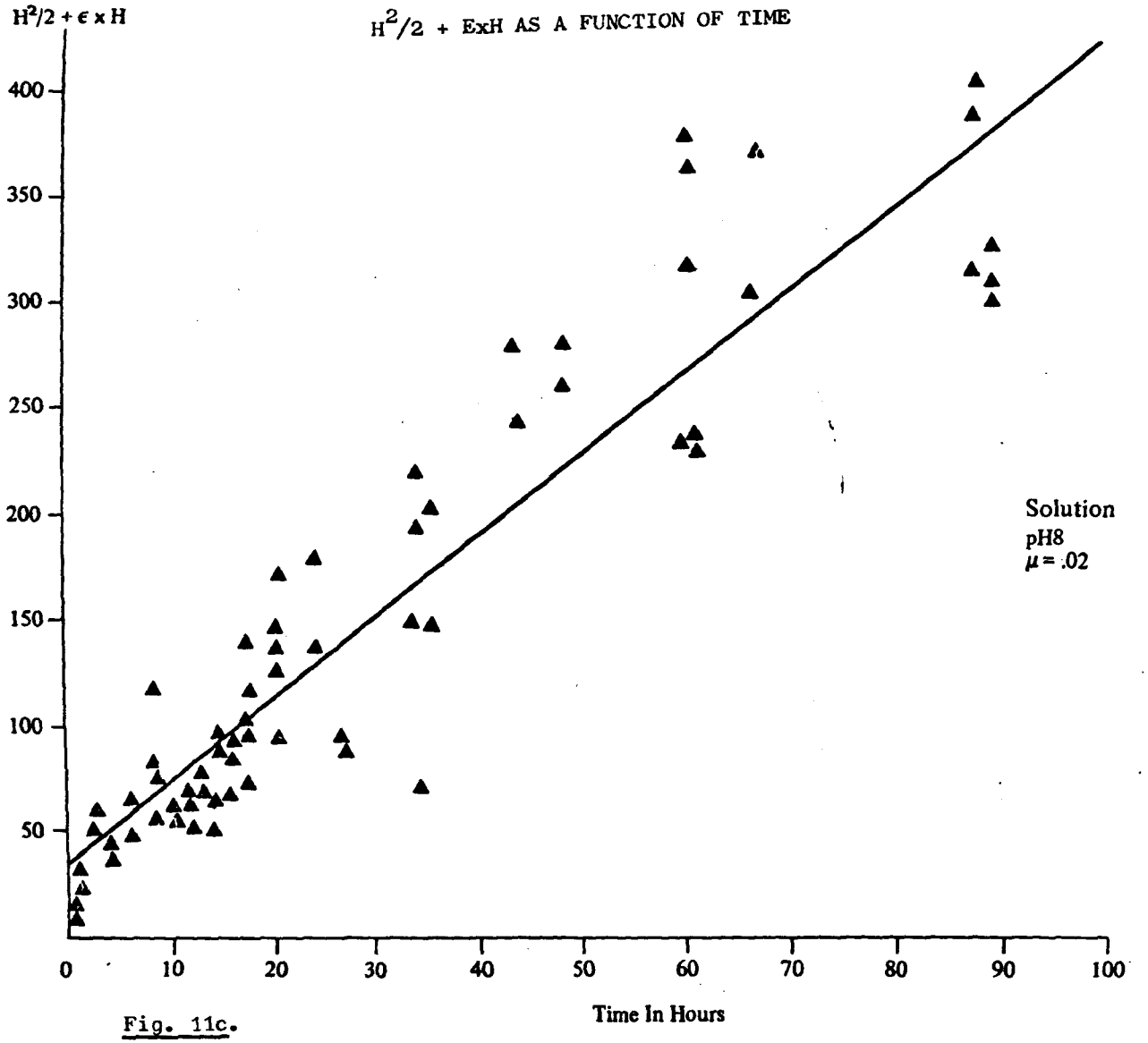
$H^2/2 + \epsilon \times H$
$H^2/2$ + ExH AS A FUNCTION OF TIME
400
350
300
250
200
150
100
50
0
10
20
30
40
50
60
70
80
90
100
Time In Hours
Solution
pH8
μ = .02

Fig. 11c.

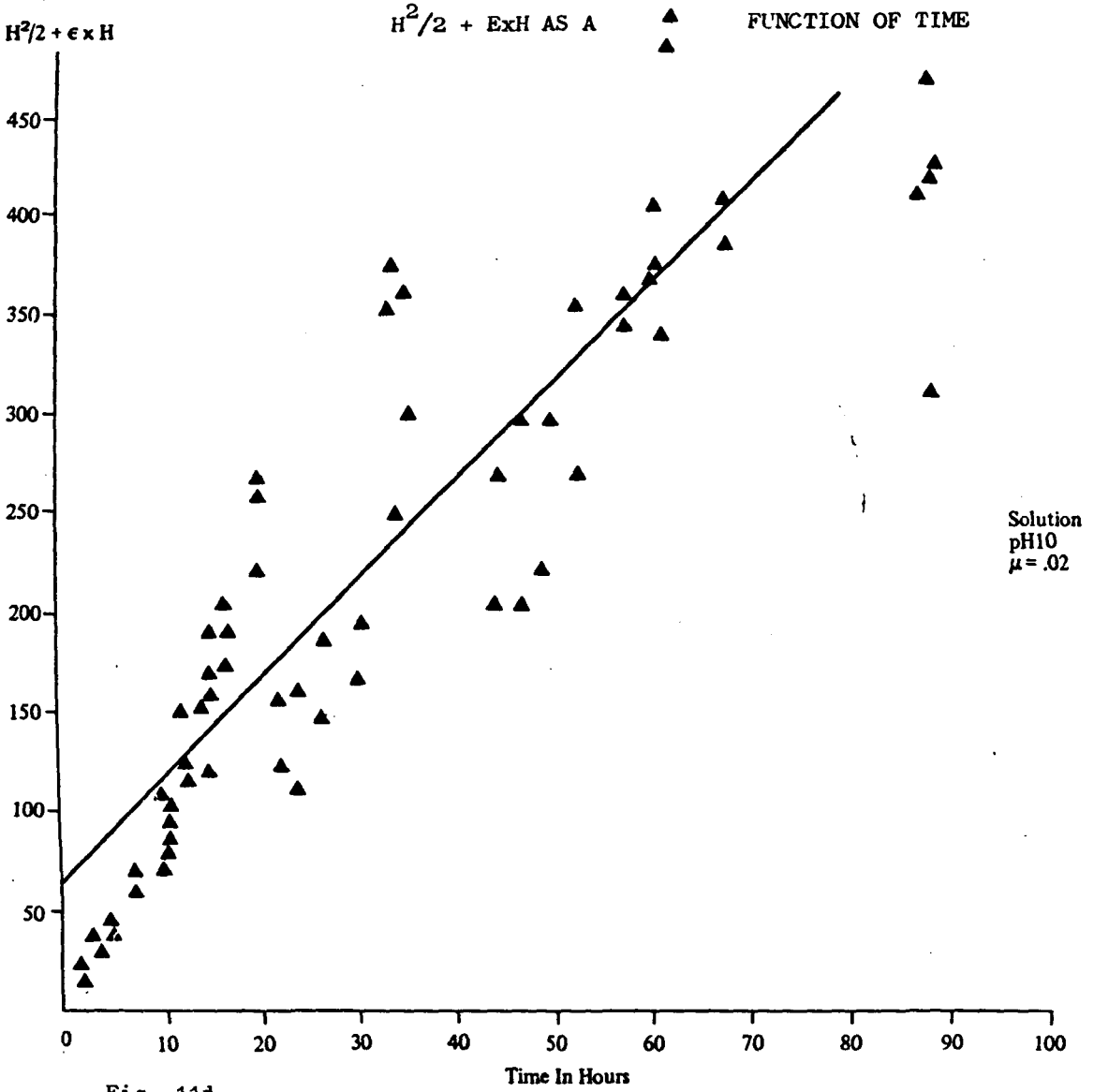
$H^2/2 + \epsilon \times H$
$H^2/2$ + ExH AS A FUNCTION OF TIME
450
400
350
300
250
200
150
100
50
0
10
20
30
40
50
60
70
80
90
100
Time In Hours
Solution
pH10
μ = .02

Fig. 11d.

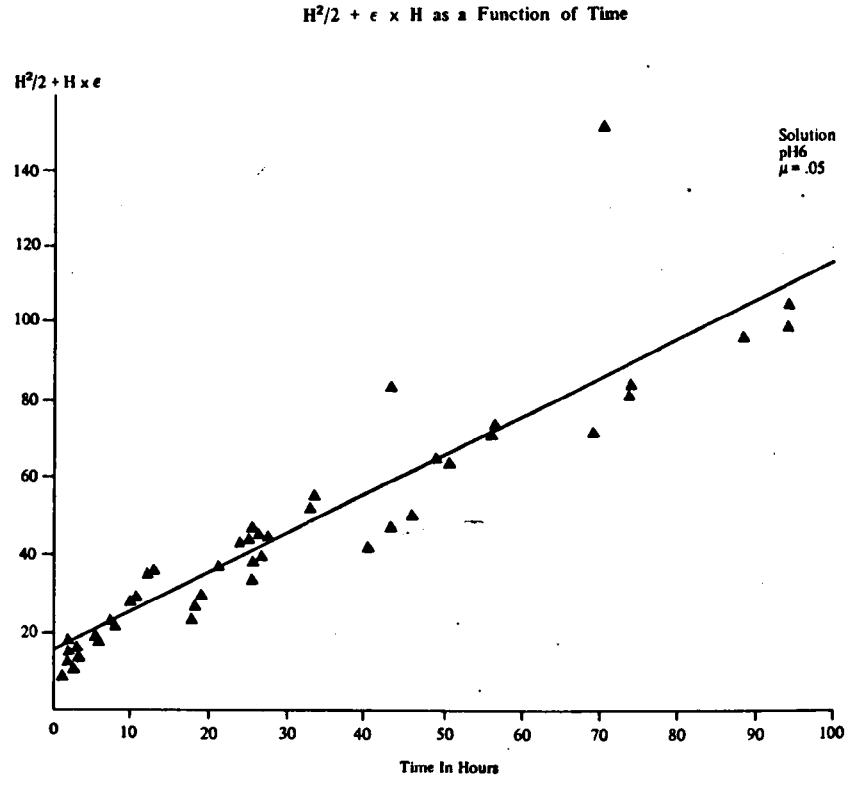

Fig. 12a.

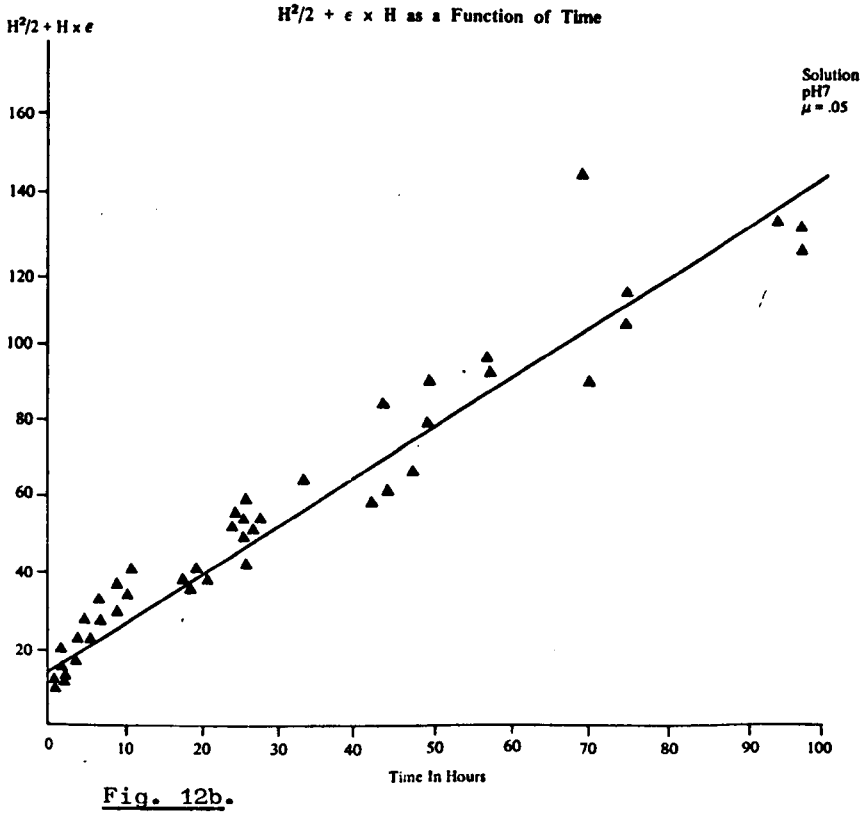

Fig. 12b.

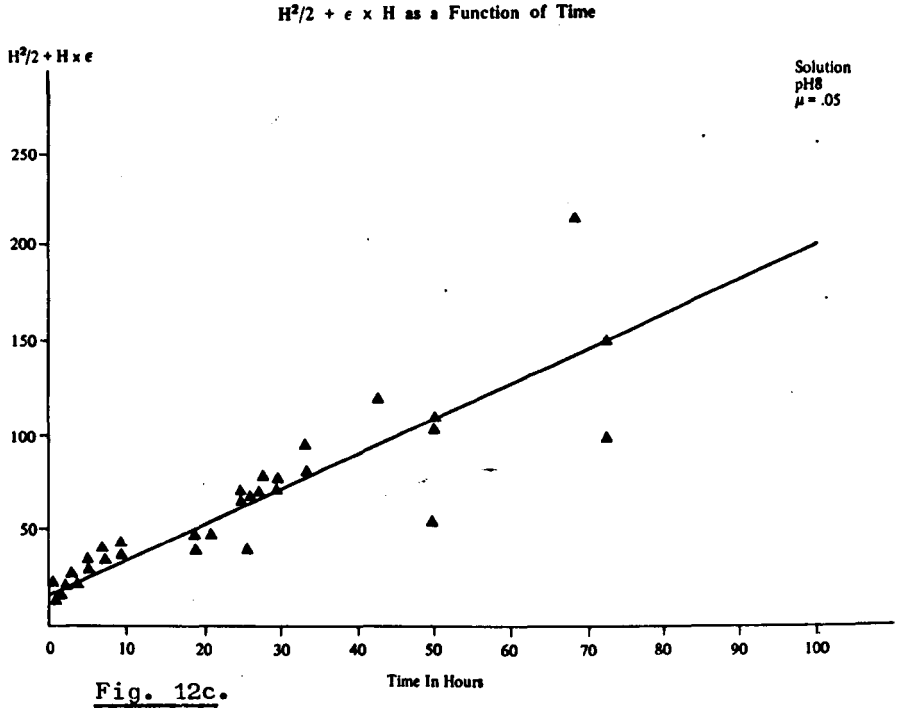

Fig. 12c.

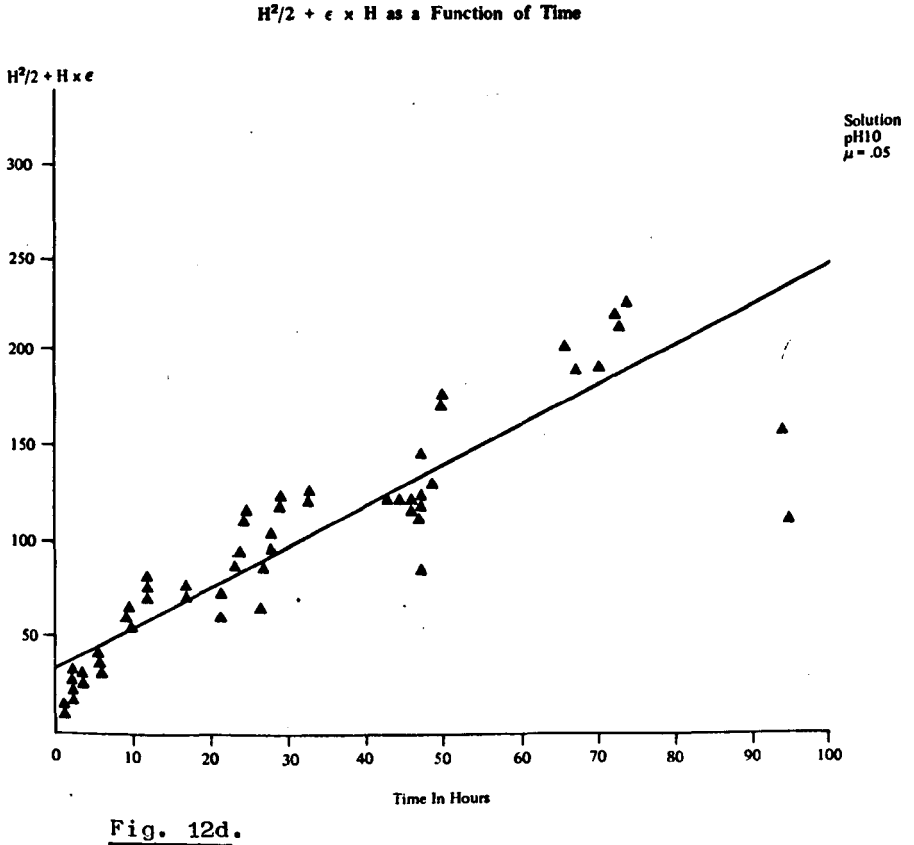

Fig. 12d.

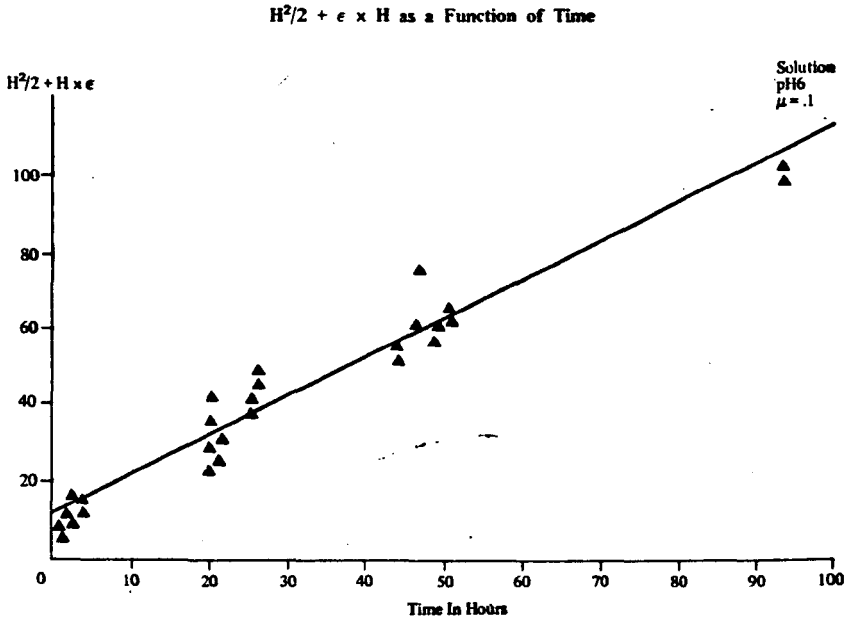

Fig. 13a.

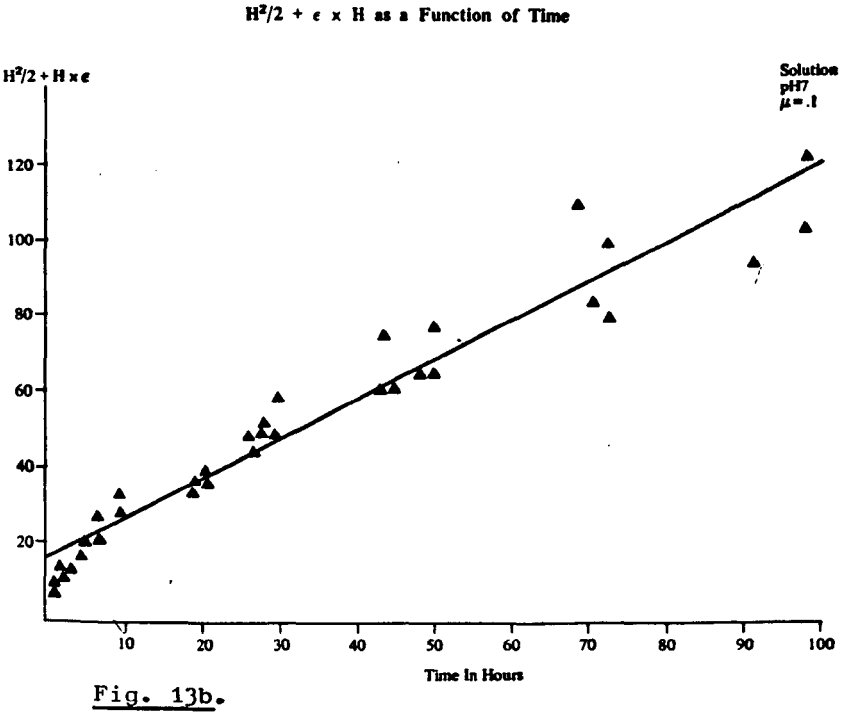

Fig. 13b.

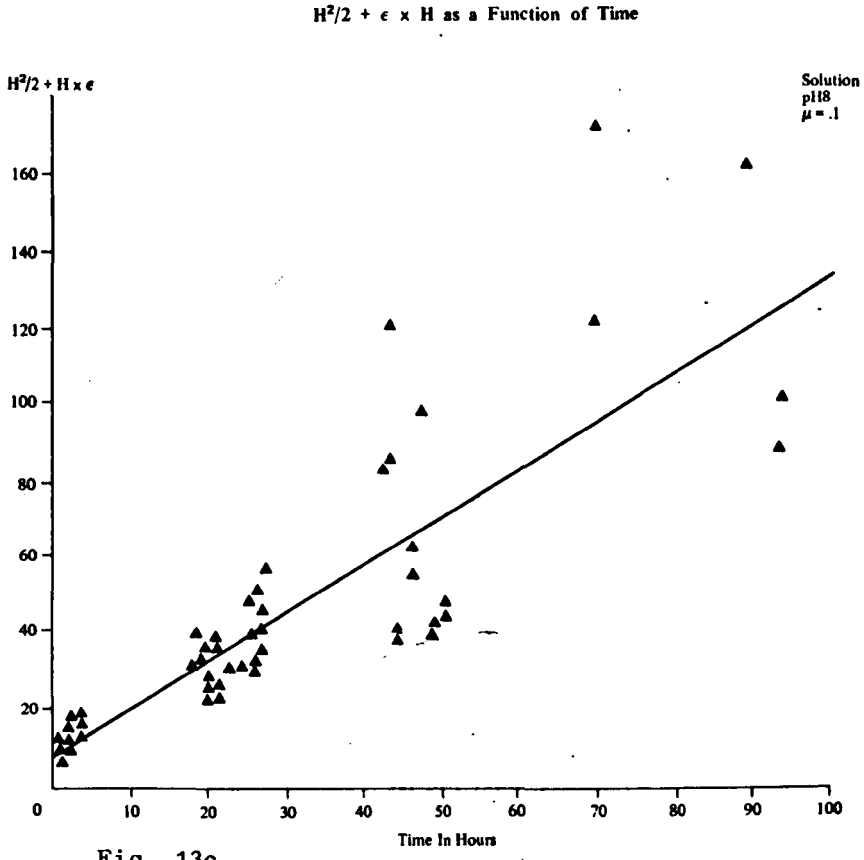

Fig. 13c.

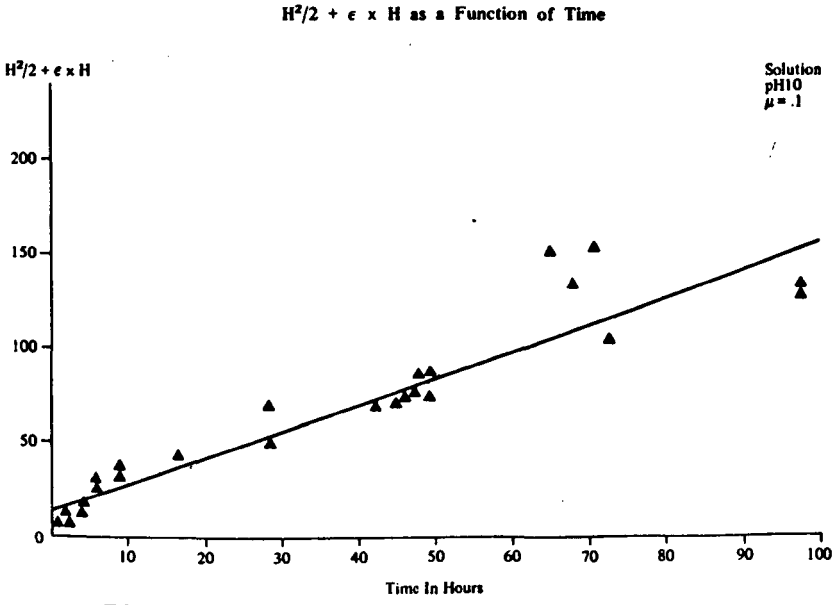

Fig. 13d.

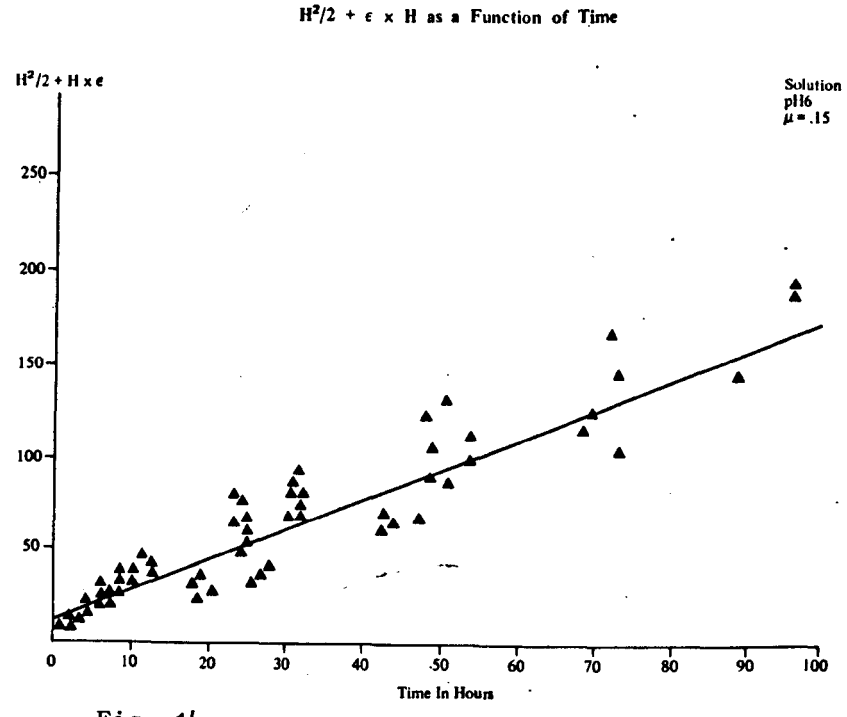

Fig. 14a.

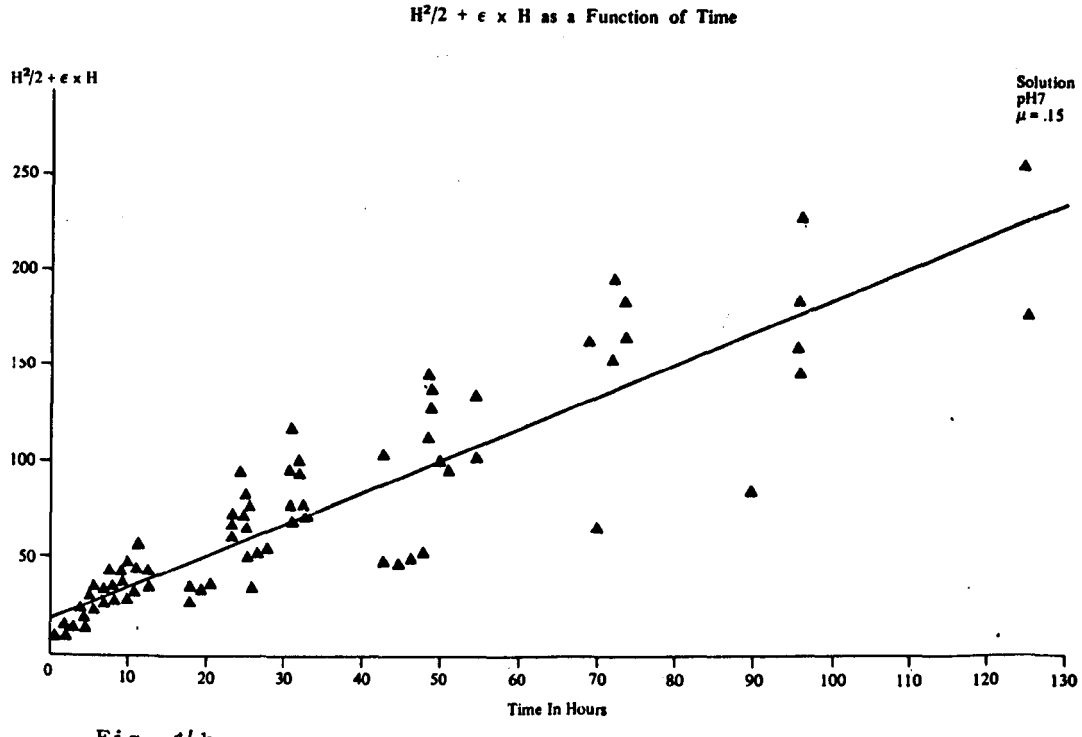

Fig. 14b.

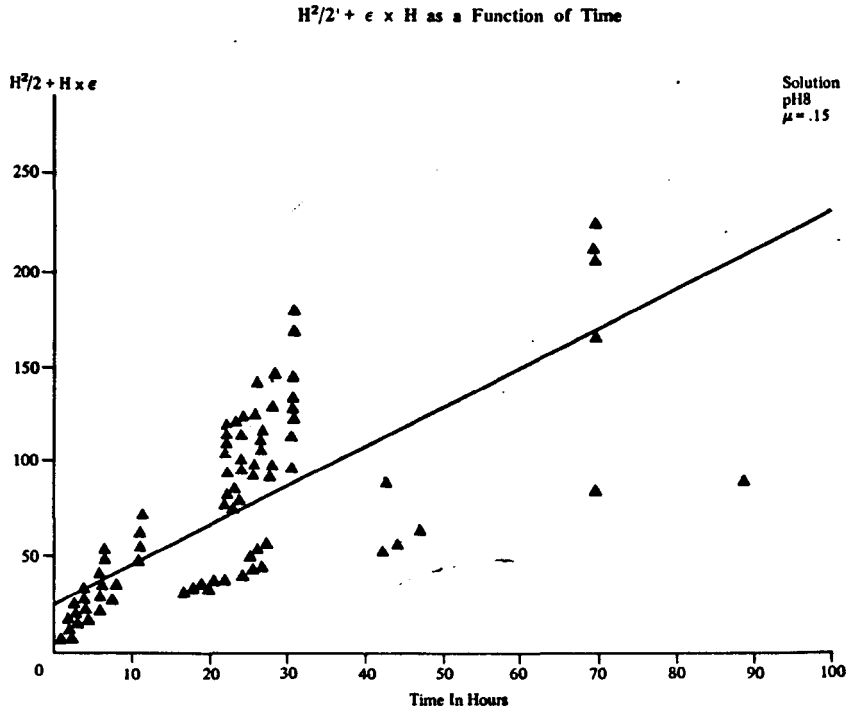

Fig. 14c.

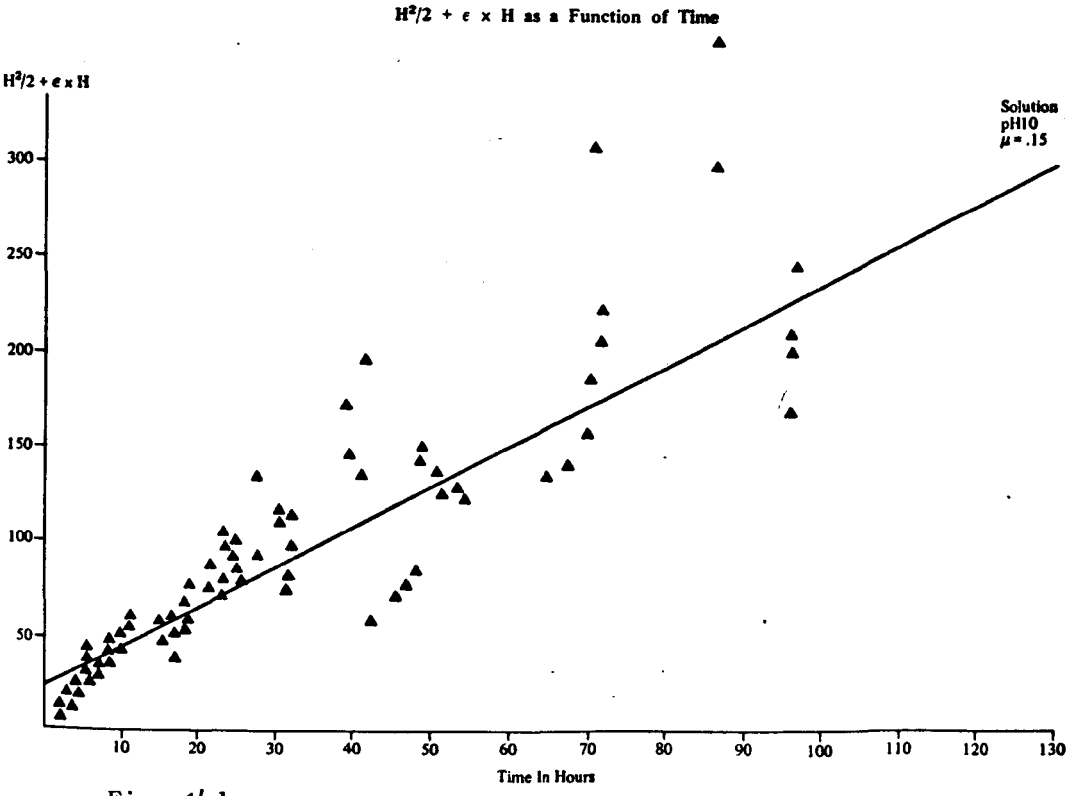

Fig. 14d.

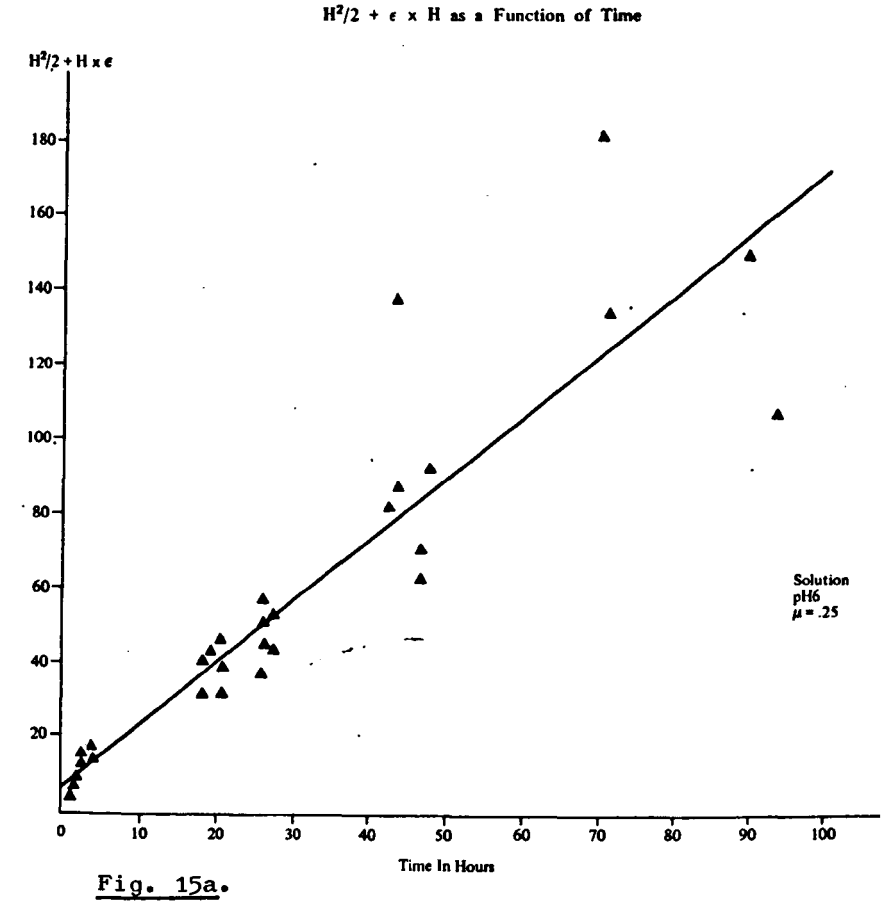

Fig. 15a.

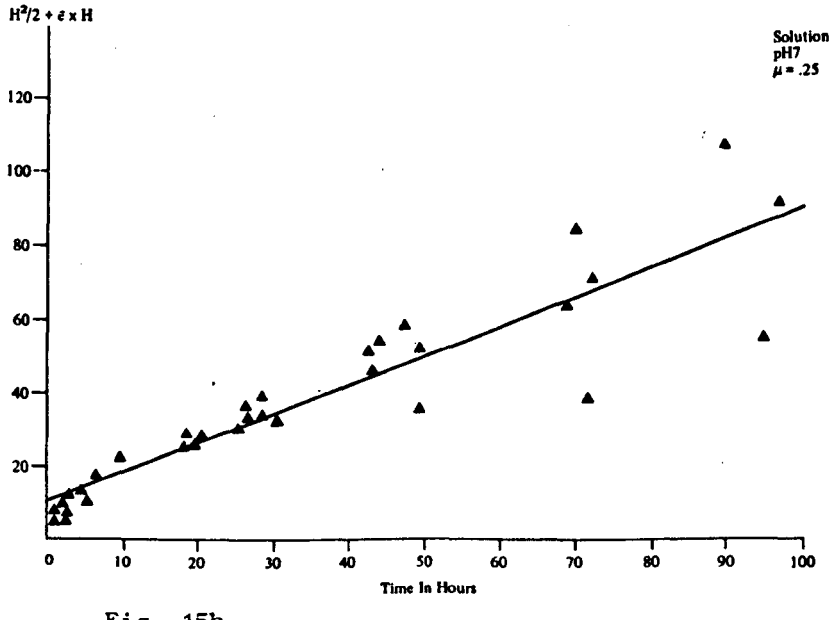

Fig. 15b.

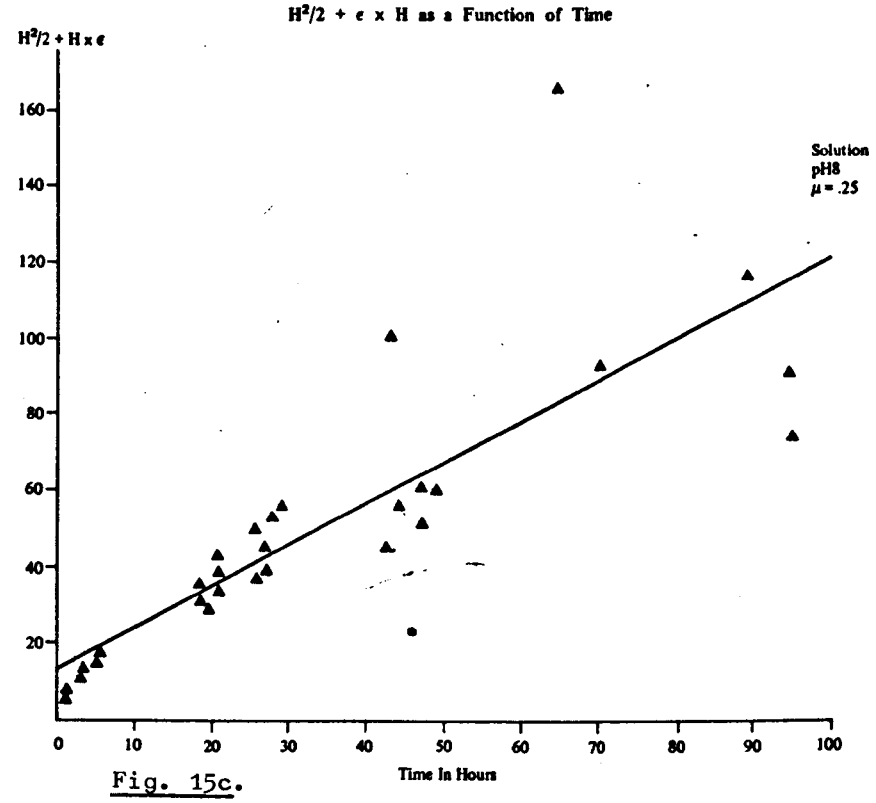

Fig. 15c.

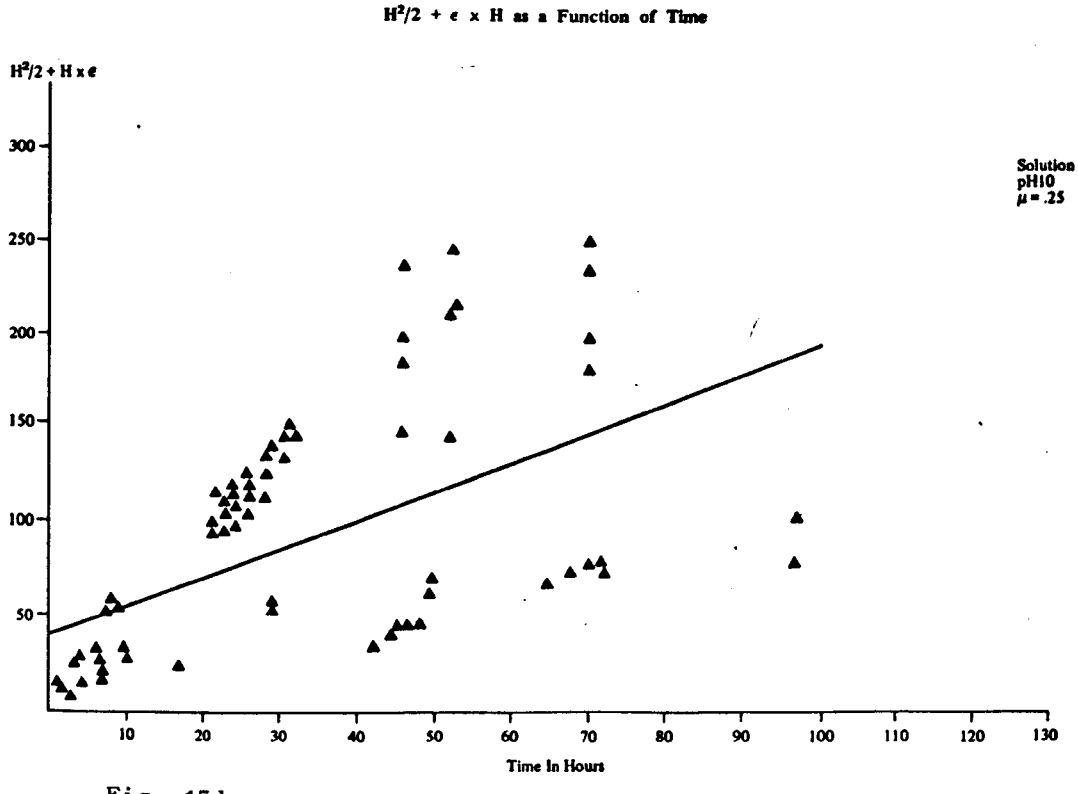

Fig. 15d.

RATE OF HYDRATION AS A FUNCTION OF HYDRATION

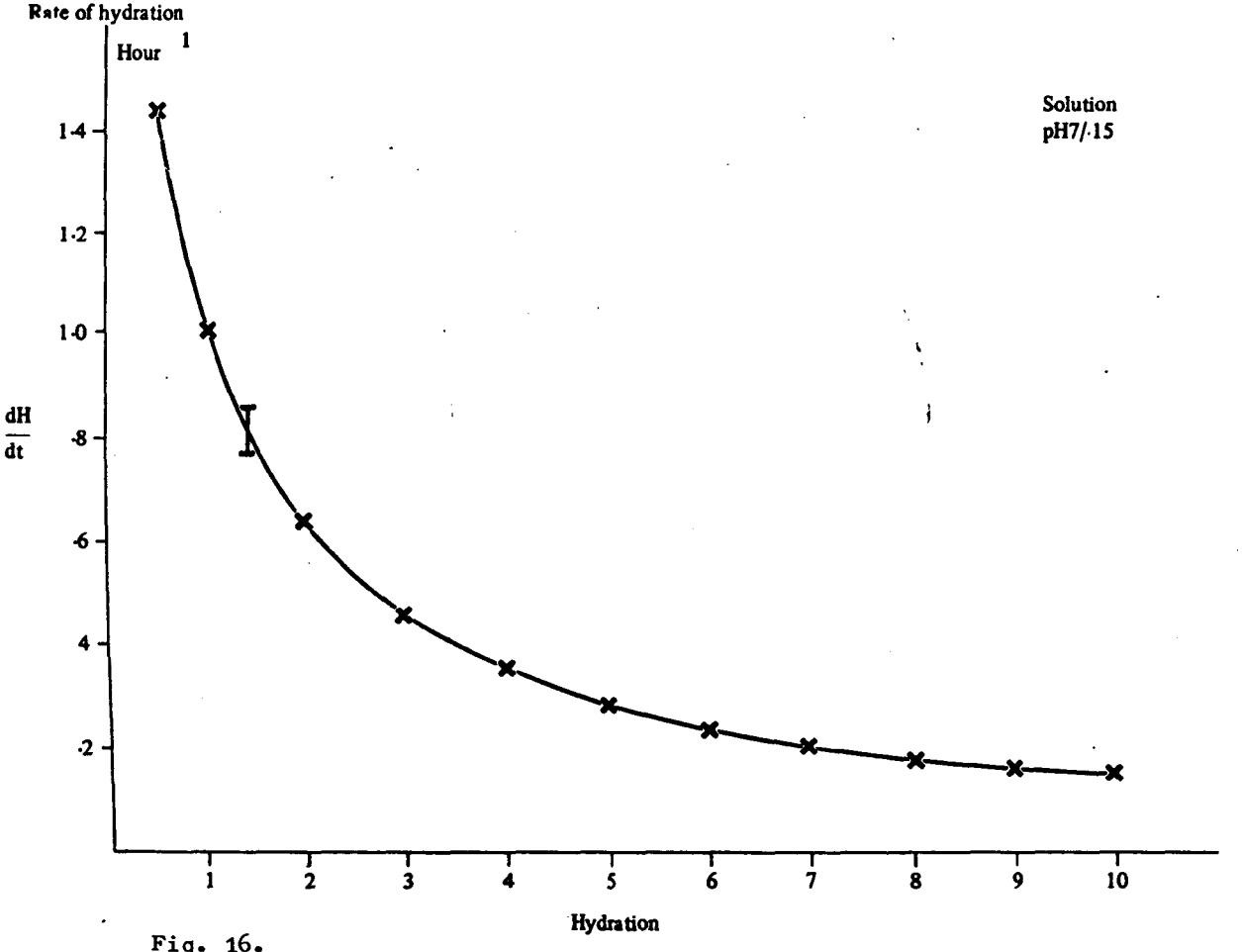

Fig. 16.

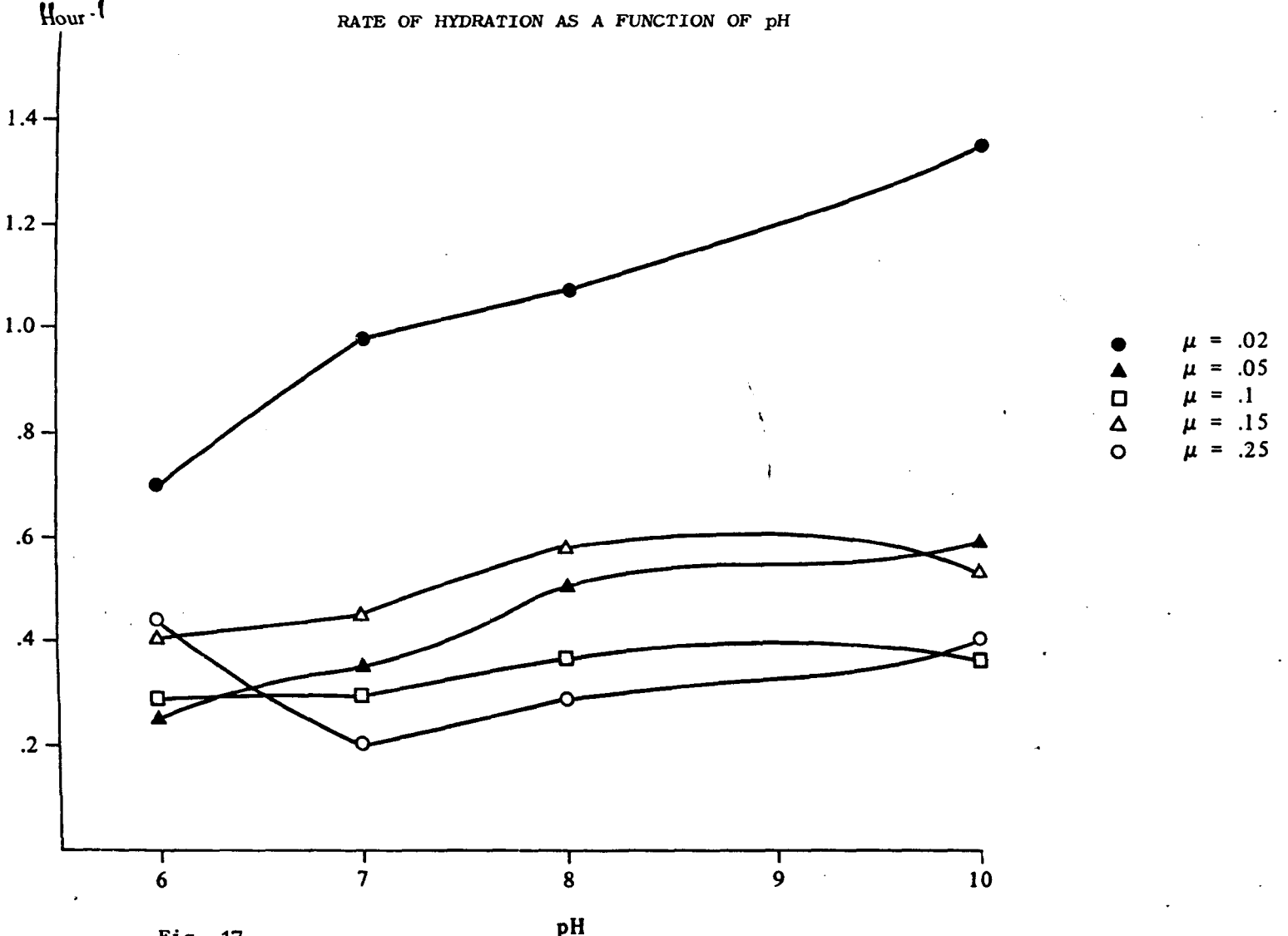
RATE OF HYDRATION AS A FUNCTION OF pH
Hour-1
1.4
1.2
1.0
.8
.6
.4
.2
6
7
8
9
10
pH
μ = .02
μ = .05
μ = .1
μ = .15
μ = .25

Fig. 17.

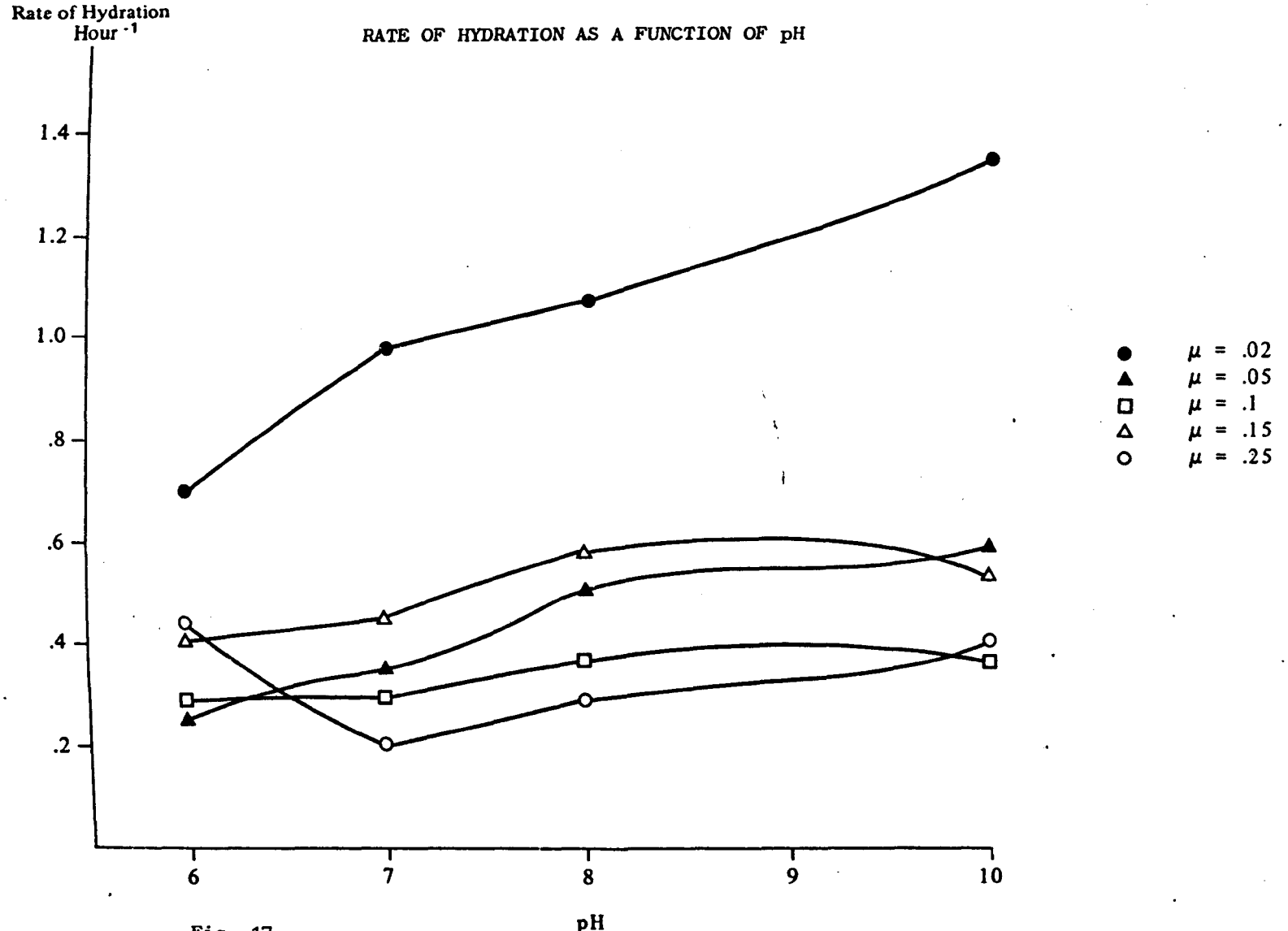
RATE OF HYDRATION AS A FUNCTION OF pH
Rate of Hydration
Hour -1
1.4
1.2
1.0
.8
.6
.4
.2
6
7
8
9
10
pH
μ = .02
μ = .05
μ = .1
μ = .15
μ = .25

Fig. 17.

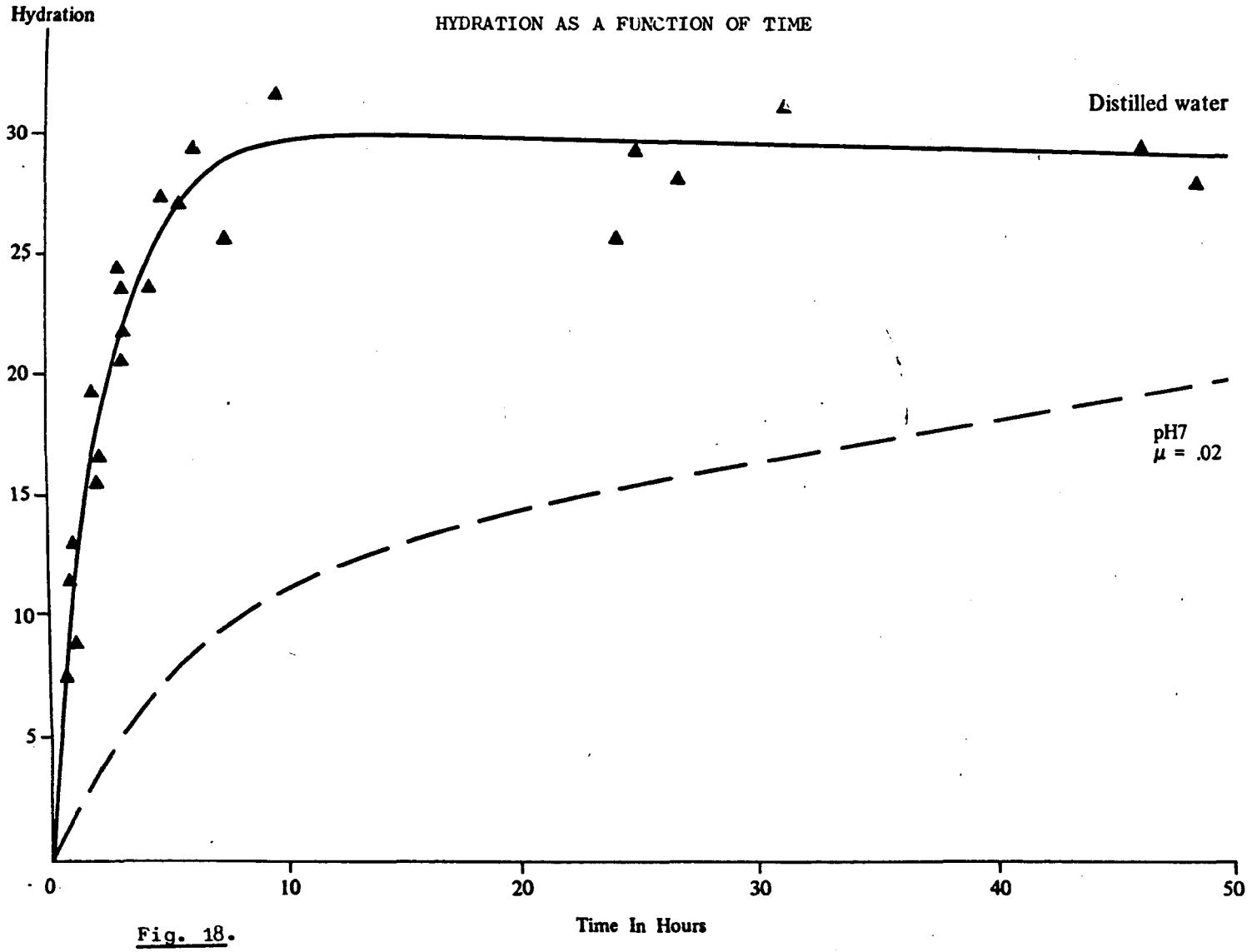
HYDRATION AS A FUNCTION OF TIME
Hydration
Distilled water
pH7
μ = .02
30
25
20
15
10
5
0
10
20
30
40
50
Time In Hours

Fig. 18.

Hydration as a Function of Time for Rabbit Corneal Stroma at low pH

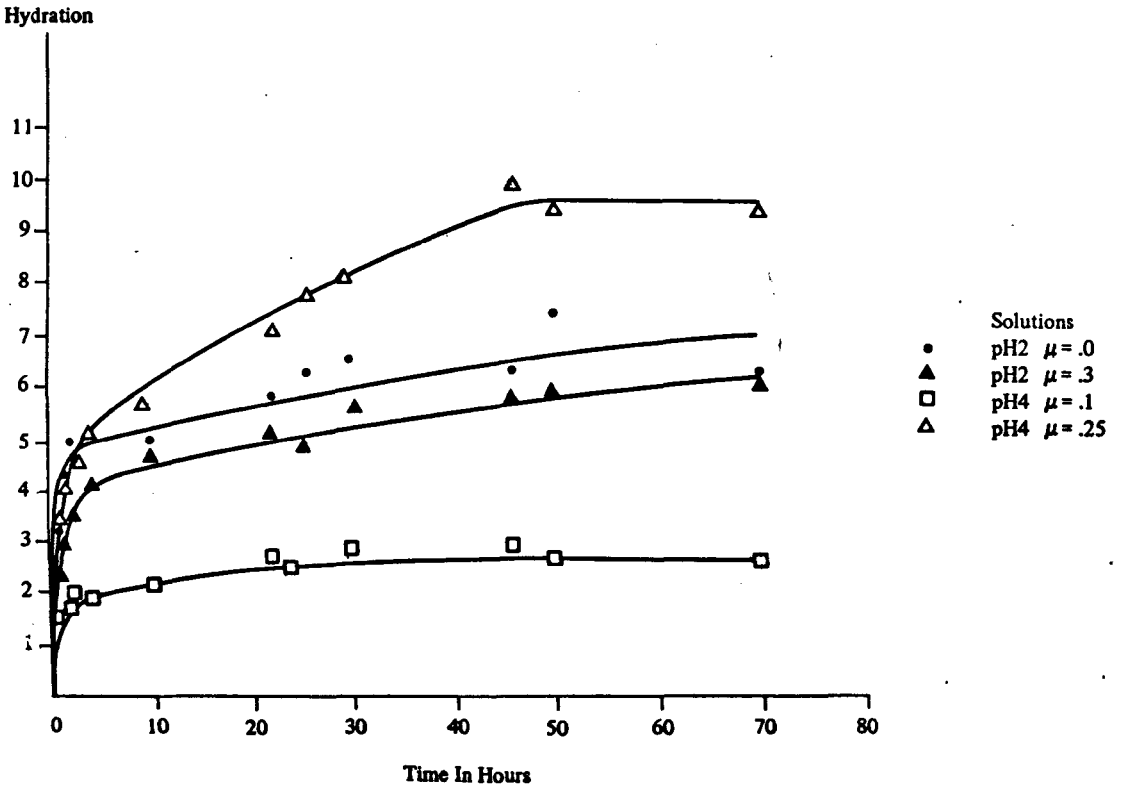

Fig. 19.

Hydration as a Function of Time for Rabbit Corneal Stroma

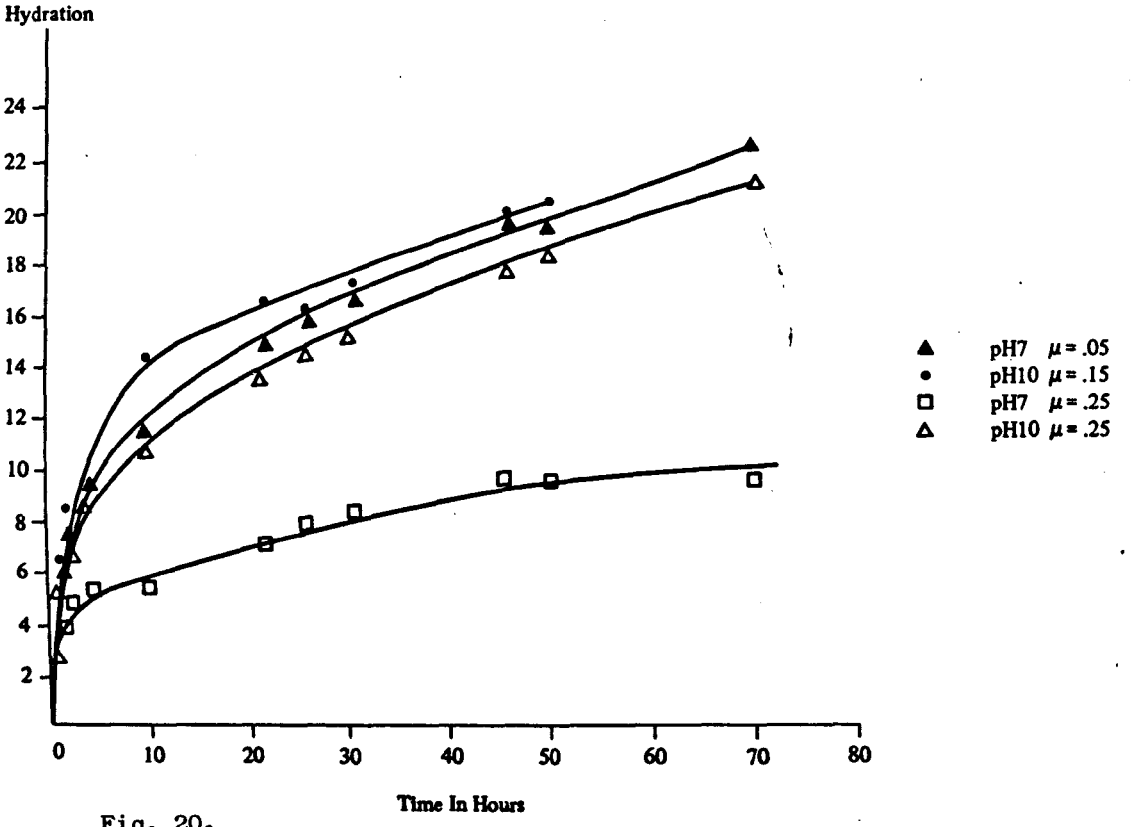

Fig. 20.

$H^2/2 + H \times e$ as a Function of Time for Rabbit Corneal Stroma

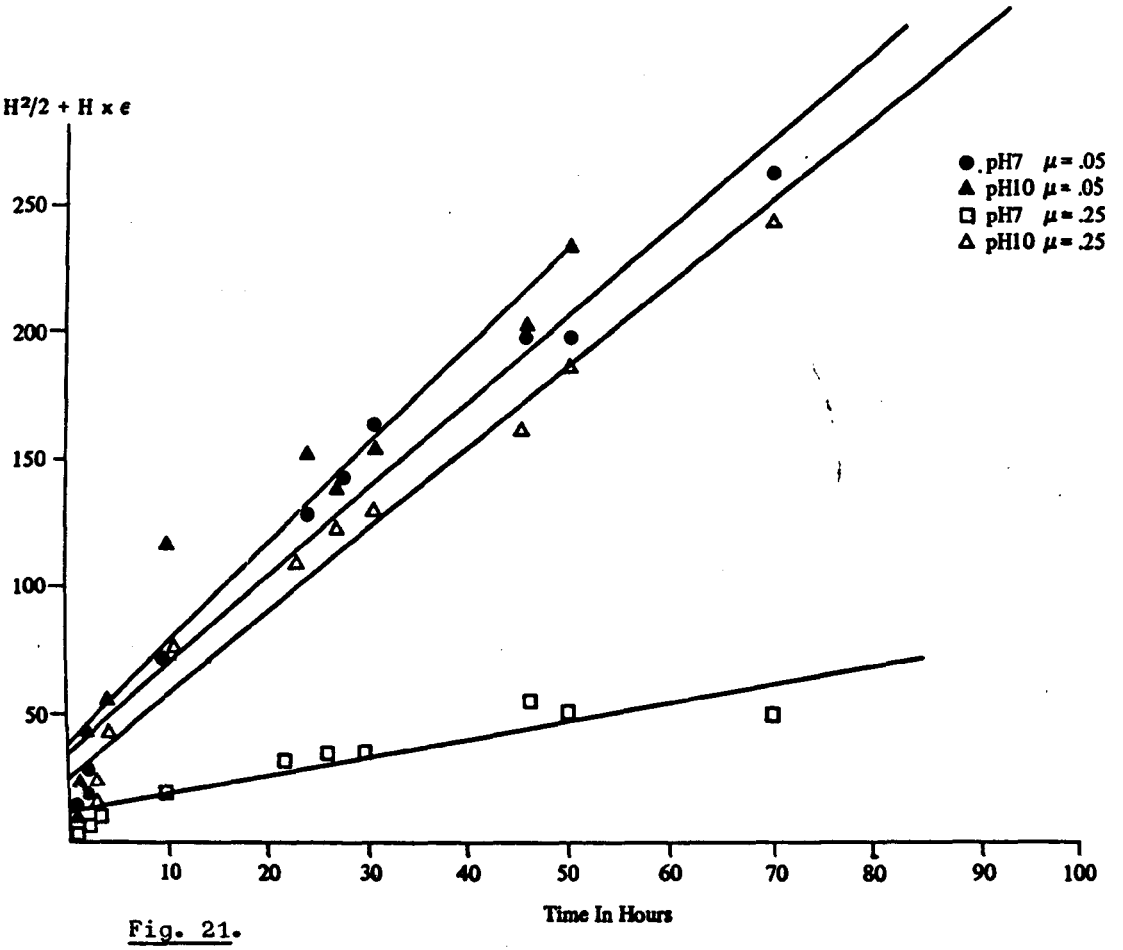

Fig. 21.

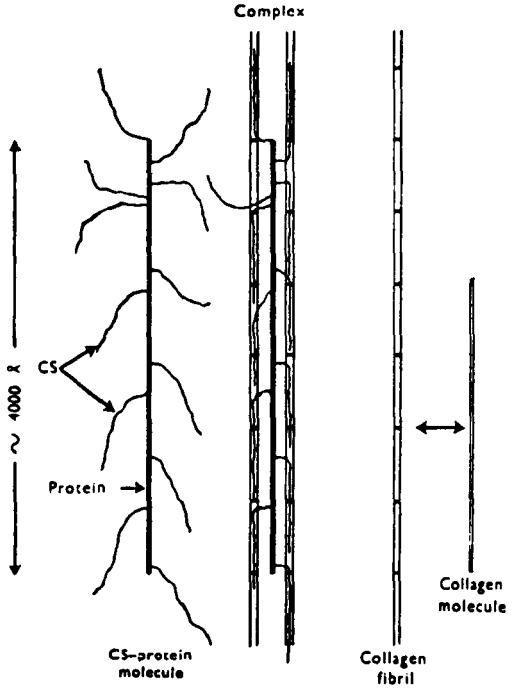

Fig. 22. Schematic representation of the interaction between collagen and the basic unit of chondroitin sulphate-protein macromolecules from bovine cartilage. This diagram is taken from Mathews (1965).

Chapter 3

Low-Angle X-ray Diffraction of the Corneal Stroma

I Introduction

(i) The Low-Angle X-ray Diffraction Pattern from the Cornea.

X-ray diffraction techniques have not been used extensively on the corneal stroma even though the possibility of a crystalline lattice structure was suggested by Maurice (1957) in order to explain the transparency of the tissue. The main reason for the scarcity of x-ray data is the size of the diffracting regions. If a regular arrangement of the collagen fibrils gave rise to a diffraction pattern the spacing would be the same order as the centre-to-centre distance between the fibrils i.e. 60nm. The x-rays from a copper target have a wavelength of 1.54Å. Hence any reflection would be at very low angles and thus requires a well focused x-ray beam.

Maurice (1957) took one low-angle x-ray diffraction pattern which showed the presence of two diffraction rings corresponding to spacings of 20.5 and 13.5nm. Rings of diffracted intensity were expected because of the superposition of lamellae (remembering that in each lamella the fibrils are parallel to each other but are not parallel to those in neighbouring lamellae). Although these spacings were too small to represent the first order, they might have been higher orders of the interfibrillar distance. Maurice (1957) suggests a possible first order of 41nm so that the reflections he found would correspond to the second and third orders.

(ii) The High-Angle X-ray Diffraction Pattern from the Cornea.

The other x-ray diffraction studies on the cornea by Hertel (1933), Adler et al (1949) and Agarwal et al (1972) have shown that a high-angle x-ray diffraction pattern exists. Hertel (1933) found reflections corresponding to 2.8, 4.4, 7.1. 10.9, 12 and 22 Å in dried cornea. Fresh cornea gave rise to similar spacings but the rings were diffuse showing very blurred maxima. The high-angle x-ray diffraction pattern of the sclera was similar to that of the cornea, but on dehydrating both tissues slightly the diffraction rings from the sclera were sharper than those from the cornea.

Adler et al (1949) confirmed Hertel's results for fresh cornea. Aging of the cornea at saturated relative humidity at 2-5°C leads to indications of small changes in the low-angle scattering region. On stretching the samples, the fibre period was found to be 11.2 Å compared with Hertel's 9.7 Å and the most intense spacing at 2.85 Å (cf Hertel's 4.4 Å). Agarwal et al (1972), using lyophilized corneas, could find no significant differences between normal cornea and opaque cornea (with the opacity caused by either a heat burn or an alkali burn). In all cases, they found an innermost strong broad ring at about 11.5 Å. Next there was a wide diffuse band at 5.0-3.6 Å, followed by a strong broad ring at approximately 2.9 Å and finally an outermost ring at 2.0 Å.

(iii) Comparison of the High-Angle X-ray Diffraction Pattern of Cornea with that from Collagen.

Agarwal et al (1972) found that the high-angle diffraction pattern of the cornea was very similar to that of collagen (Ramachandran,

1962). There is one exception in that the reflection from the cornea at 2.0 Å does not seem to fit the known collagen pattern. (Table 1) Ramachandran (1962) gives the x-ray reflections for collagen as an equatorial spacing at 11 Å and diffuse reflections at 4.5 Å, with a meridional reflection at 2.9 Å and layer lines at 10 Å and 4 Å.

(iv) The Low-Angle X-ray Diffraction Pattern from Collagen.

A low-angle x-ray diffraction can be obtained from collagen fibrils based on a 66nm repeat distance (Bear, 1942). A similar sized banding pattern can be seen in suitably stained specimens in the electron microscope (Schmitt et al, 1942). The low-angle x-ray diffraction pattern and the pattern seen in the electron microscope are interrelated (Burge and Randall, 1955). Both patterns depend on the structure of the collagen fibrils, which is now thought to be a staggered array of tropocollagen molecules (chapter 1, section IV, (iv)). François et al (1954) found that bands every 21nm occurred along stained corneal collagen with every third band being more intense which lead to an approximate 66nm repeat. 13nm bands were also noted by these authors.

It is expected that the cornea will give rise to a low-angle x-ray pattern due to this 66nm banding along the axes of the fibrils. However, the intensity of the reflections may be weak because, in stained and fixed fresh tissue, in the electron microscope, the fibrils are coated with ground substance and the banding is obscured (François et al, 1954; Garzino, 1955). Bear (1944) has shown that the exact value of the collagen spacing depends upon the source of the fibres and on the degree of hydration.

II Methods.

(i) X-ray Techniques.

All the x-ray diffraction patterns were obtained with an Elliott GX6 rotating anode x-ray generator. This produces a focal spot approximately 100 μ square when viewed at 6^{o} with the generator running at about 35kv and 25 mA. In order to record the low-angle diffraction patterns a well collimated beam was obtained using either a Franks' camera or a mirror monochromator camera (Franks, 1955; Witz, 1969, review). The Franks' camera consists of two glass mirrors (one horizontal and one vertical). The x-ray beam is reflected from the surface of the mirrors at a glancing angle and is focused by bending the mirrors. The mirror monochromator has one Franks' mirror and a quartz crystal which is specially cut in order that the x-ray beam which is Bragg reflected from a given set of planes in the crystal can be focused by bending the crystal. The mirror monochromator used in these experiments was designed and constructed by Dr. A. E. Woolgar. (Fig. 1a, 1b).

All x-ray patterns were recorded on Kodak x-ray film. The distance between the specimen and the film was varied between 45-65cm depending on the expected, approximate value of the spacing required. This distance could be measured with a metre rule. The exposure times depended on the camera. When the Frank's camera was used, the exposure times were two hours in order to see the reflection due to the interfilament spacing. However, the exposure had to be longer (up to six hours) to obtain both the third and fifth order of the collagen pattern. When using the mirror monochromator camera, exposure times were twice

those used on the Franks' camera.

(ii) Material.

The dried corneal stroma was swollen as described in chapter 2. At a given hydration, it was removed from its bathing solution, blotted and weighed. It was then placed in the centre of a small airtight cell. The lid to this cell was screwed tightly to the main part of the cell and a rubber "O" ring was used to make the seal airtight. The x-rays passed through two mylar windows.

Fresh sclera was used in some experiments. This was cut from areas adjacent to the cornea. All fatty tissues were cut away from it as was the iris which attaches to it. Sclera was used as soon as possible after dissection from the eye.

(iii) Measurement of X-ray Reflections.

The reflections obtained on photographic film were measured using either a travelling microscope (accurate to .01mm) or an eye glass with mm scale (accurate to .1 mm). The latter had to be used with reflections of weak intensity which could not be distinguished in the travelling microscope.

The relative intensities of the reflections were measured on a double beam recording densitometer made by Joyce, Lobel & Co. Ltd. This instrument was made available through the courtesy of the Molecular Biophysics Group of Oxford University.

III Results.

(i) Low-Angle X-ray Diffraction Pattern from Fresh Cornea.

The x-ray diffraction pattern from fresh beef cornea (i.e. at physiological hydration) shows three diffraction rings (Figs. 2a, 2b). The inner ring corresponds to a spacing of 57.9 $\pm$ .55nm (mean $\pm$ S.E.). This average was taken from the data of 28 specimens. The second reflection, which is less intense than the inner reflection, is due to a spacing at 22.4 $\pm$ 1.3nm (9 specimens). The third reflection, corresponding to a spacing of 13.8 $\pm$ 1.0nm (3 specimens) was the least intense. Similar patterns have been obtained from the cornea of other species of animals. Fresh rabbit cornea gave rise to reflections at 58nm, 23nm and 13.8nm while the x-ray pattern from guinea pig cornea showed rings of diffracted intensity at 60nm, 23nm and 14nm.

(ii) Low-Angle X-ray Diffraction Patterns from Swollen Beef Corneal Stroma.

The largest spacing of 58nm, recorded with fresh tissue, increased in size with increasing water content of the corneal stroma (Fig. 2c d and e). This spacing was ascribed to the interfilament packing. Fig. 6 shows the dependence of the square of the interfilament spacing on the water content of the tissue. Values of hydration below that of fresh tissue were obtained by allowing the corneal stroma to dry slightly in air, at room temperature.

The reflections at 22.4nm and 13.8nm did not change in value within their experimental error. Table 2 gives the values obtained

from fresh, swollen and dried tissue. For dried tissue the spacing was 22.4 $\pm$ .6nm (8 specimens) and from swollen tissue 22.4 $\pm$ .4 (11 specimens). The smallest spacing had the value 13.8 $\pm$ 1.0nm from fresh tissue, 14.1 from swollen and 13.1 from dried tissue. These spacings are most likely the third and fifth orders of the 66nm collagen repeat.

(iii) The X-ray Diffraction Pattern at Different Orientations.

Most x-ray diffraction patterns were obtained by allowing the x-ray beam to pass through the cornea from the anterior to posterior surface (fig. 4a). Thus, information about the interfilament spacings in planes parallel to the surface was obtained. However, when the specimen was rotated by 90^{o} so that the x-rays travelled at right angles to the surface of the stroma (fig. 4b), information about the spacings in the planes orthogonal to the surface was obtained. It was found that the same interfilament spacing for a given hydration was recorded whatever the direction of the incident x-ray beam relative to the surface. Fig. 3 shows the interfilament spacing measured with the x-ray beam travelling at right angles to the surface and the spacing measured with the x-ray beam parallel to the surface. The line through the data is approximately the bissector of the angle between the ordinate and abscissa axes. This implies that although the tissue as a whole swells only in one direction, the interfilament distance increases in size equally in all directions. Fig 5 shows a hypothetical regular lattice of collagen fibrils (in cross-section). The two possible ways of swelling are shown in which the system as a whole swells only in one direction but the lattice of fibrils swells either only in the direction of swelling of the lattice or equally in all directions.

(iv) The Interfilament Spacing as a Function of the pH and ionic strength of the Solution.

X-ray diffraction patterns were obtained from dried corneal stroma hydrated by swelling in a series of solution of differing pH and ionic strength. Four pH values were chosen - pH6,7,8 and 10. At each pH, four different ionic strengths were used, between μ = .02 and μ = .25. The interfilament spacing was recorded as a function of hydration for each of the sixteen solutions. A minimum of two specimens and eight hydrations were used for each solution. The data is presented in Figs. 6-11. Fig. 6 shows the data from fresh tissue while Figs.7-10 are from rehydrated beef stroma. Fig. 11 shows the change in the interfilament spacing on swelling in distilled water.

It can be seen that the square of interfilament distance is linearly related to the hydration of the tissue. This is to be expected if the fibrils are moving apart equally in two directions (although the tissue is swelling unidirectionally). The length of the fibrils is assumed to remain constant. The solid lines represent the linear regression fits through the data points. Details of these fits are given in Table 3.

The error in the value of the interfilament spacing is dependent on the measurements of the specimen to film distance and the size of the reflection on the film. The specimen to film distance can be measured to an accuracy of .005m in .5m i.e. 1%. The measurement of the diameter of the diffraction ring is not so accurate. The average size of the diameter on the film is 3mm. The scale on the magnifying glass is accurate to .1mm. Thus the percentage error is about 3%.

This leads to an error of 2% in the value of $\sin\theta$, where

$$2d \sin\theta = n\lambda$$

is the usual Bragg equation (Topping, 1962). Larger errors will occur in the measurement of spacings at large hydrations because the diameter of the reflections decreases to around 2mm. The percentage error is then 5%. Moreover, the reflections may become more diffuse at higher hydrations making the measurement of the diameter even less accurate. The error in the square of the interfilament spacing is approximately twice the percentage error of the spacing (Topping, 1962).

When trying to correlate changes in the interfilament spacing with changes in pH, it is perhaps easiest to study the slopes of the regression fits given in Table 3. At each ionic strength, the lowest slope occurs at pH6 except at μ = .05 when the slopes at pH6 and at pH10 are equal within the error. Increasing the pH to pH7 increases the slope of the data (plotted as interfilament distance squared versus hydration). Thus a larger spacing is recorded when the tissue has been swollen with the external solution buffered at pH7 compared with pH6 for the same water content of the tissue. At pH8, the slope is larger than at pH7 at two ionic strengths (μ = .05 and μ = .15) but is lower at the low ionic strength (μ = .02) and at the high ionic strength (μ = .25). With a further increase in the alkalinity of the solution to pH10 the slope either remains the same as that at pH8 (μ = .02, .15 and .25) within the error or decreases compared to the slope at pH8 at μ = .05.

The dependence of the slope on the ionic strength is not obvious. It is noted that a larger spread in slopes with pH occurs at μ = .02

and $\mu = .25$ compared with $\mu = .05$ and $\mu = .15$.

It can also be seen from Table 3 that two of the intercepts are negative. This is not expected when the square of the spacing is plotted on the ordinate axis. However, these negative intercepts are small compared with the value of the product of the slope and the hydration. Moreover, extrapolation of the data to zero hydration is not expected to be useful because at low hydrations it is necessary to consider the water associated with the collagen fibrils (Chapter 1, section IV, ii).

(v) Theoretical Calculation of the Swelling of the Lattice.

If a hexagonal lattice of fibrils is assumed to exist throughout one lamella, the corneal stroma can be divided into NN' unit cells where N is the number of unit cells in the direction of swelling and N' is the number at right angles to the direction of swelling and to the length of the fibrils. The area of a unit cell is $d_{10}^2\ 2/3^{\frac{1}{2}}$ (see Fig. 12) where d_{10} is the interfilament spacing. The volume of one unit cell is then $l \times d_{10}^2\ 2/3^{\frac{1}{2}}$ where l is the length of a collagen fibril. The total volume of the tissue, V, is given by

$$V = NN' d_{10}^2 2/3^{\frac{1}{2}}.$$

The hydration of the tissue at this volume, H_1, is equal to the ratio of the weight of water to the dry weight of the tissue so that

$$H_1 = \frac{(\text{volume of lattice - volume of fibrils})}{\text{volume of fibrils} \times \rho_c} \rho_w$$

where ρ_w (ρ_c) is the density of water (collagen). The water content associated with the collagen fibrils was thought to be approximately 1g per g dry weight so that

$$H_1 = 1 + \frac{\rho w(\text{volume of lattice - volume occupied by fibrils})}{\text{volume occupied by fibrils}}$$

$$= 1 + \frac{10^3(d_{10}^2 N_1 N_1^1 \, 1 \, 2/\sqrt{3} - \pi R^2 N N_1^1 1)}{\pi R^2 N N_1 1 \rho c}$$

where $\rho w = 10^3$ kg/m^3. The value of $\rho c = 1.42 \times 10^3$ kg/m^3. (Maurice, personal communication).

$$H_1 = \frac{d_{10}^2 \, 2/\sqrt{3} + \pi R^2(1.42 - 1)}{\pi R^2 \, 1.42}$$

The value of the radius of the collagen fibrils, R, is not known accurately but can be estimated by normalising the experimental data with the theoretically calculated interfilament distance at a given hydration.

This procedure has been carried out for all the solutions used. The theoretical and experimental curves were normalised at H = 2. The value of the radius of the fibrils, R, was chosen to make this agreement for each solution in turn. This value of R could then be used to calculate the theoretical value of the interfilament distance at any hydration. Reasons for choosing to normalise the experimental and theoretical curves at H = 2 will be given in the next section.

(vi) The Percentage of "Lakes" in the Corneal Stroma.

It can be seen from any of the graphs in Figs. 6-11 or from the data of the regression fits that different spacings are found at the same hydration depending on the pH and ionic strength of the external solution. This means that for a given water content (i.e. hydration) the collagen fibrils are a different average distance apart. If this is so, it implies that in those solutions which give rise to a small

interfilament spacing for a given hydration, that not all the fluid can be going into the lattice of fibrils and increasing their distance apart. The water not in the lattice of fibrils may be forming "lakes" as proposed by Benedek (1971). These "lakes", or areas devoid of collagen fibrils, have been seen in electron micrographs of swollen cornea by Goldman et al (1968), Cox et al (1970), Farrell et al (1972) and Kanai and Kaufman (1973a). The percentage of the volume of the corneal stroma occupied by these "lakes" can be calculated from comparison of the experimental data with the theoretical calculation (last section) in which all the fluid was assumed to go into the lattice.

If H_1 is the theoretical hydration at a spacing d_{10} and H_2 is the experimental hydration at the same value of d_{10} the amount of water not in the lattice is H_2-H_1. If this water is in "lakes", the percentage of the volume of the stroma occupied by "lakes" compared to the total volume of stromal fluid is given by

$$(H_2-H_1) \times 100/H_2.$$

In Fig. 13 the percentage of "lakes" in the stroma is shown as a function of the pH of the external solution for one hydration, H=3.

The main difficulty arises in choosing where to normalise the theoretical calculation with the experimental results. If the normalising procedure is carried out at H = 3.5 (i.e. physiological hydration) a negative volume of lakes is found to occur for certain solutions i.e. the experimental curves show that more water is in the lattice than the theory, which assumes all the water is the lattice of fibrils. As the theory is not applicable at low hydrations, because of the different mechanism of hydration (i.e. intra-fibril swelling

instead of interfibril swelling), normalisation was carried out at a hydration above H = 1. A hydration of two was chosen for convenience being as low as possible but not in the intra-fibril swelling region.

The reason for the fibril diameter varying with each solution may be due to the fact that collagen fibrils are known to swell by varying amounts in different solutions (Pirie, 1947, Bowes and Kenten, 1950). Both these papers report that the minimum swelling of collagen occurs at around pH7. The radius, found by equating the theoretical spacing with the experimental spacing, will be a minimum when d_{10} (experimental) is a minimum. Small values of d_{10} will occur when the slope and the intercept of the linear regression fits are low. From Table 3, it can be seen that the radius varies slightly with the solution from 17.5-21.8nm. It is a minimum, at pH7, when μ = .02 and μ = .15. It is slightly larger at pH7 than at other pHs for μ = .05. This solution also gives a high percentage of "lakes" and it is approximately the same at pH7 as at other pHs when the ionic strength equals .25.

The error in the percentage of "lakes" in the stroma depends on the error in the least square fits of the data. If the percentage of "lakes" is required, at a tissue hydration of 3, the calculation involves finding the experimental interfilament spacing from the regression data and using this value of the spacing to calculate the theoretical value of the hydration. Therefore, the percentage "lakes" depends on the function (3a + b) where a and b are the values of the slope and the intercept, respectively, of the regression fit. However, the radius of the collagen fibrils is also required for the calculation of the number of "lakes". The radius was found by equating the theoretical and experimental values of the interfilament spacing at

H = 2 and so it depends on the function (2a + b). The percentage 'lakes' depends on the quotient (3a + b)/(2a + b). From Topping (1962), the fractional error, f, of a quotient, $Y = Y_1/Y_2$, is given by

$$f^2 = f_1^2 + f_2^2$$

where f_1 and f_2 are the fractional errors in Y_1 and Y_2 respectively. f_1 and f_2 can be expressed in terms of the standard error in a, α_a, and the error in b, α_b, according to the general formula

$$Y_i^2 f_i^2 = (dY_i/da)^2 \alpha_a^2 + (dY_i/db)^2 \alpha_b^2.$$

Using this formula, it can be shown that

$$f^2 = \alpha_a^2 \frac{(72a^2 + 60ab + 13b^2)}{(3a + b)^2(2a + b)^2} + \alpha_b^2 \frac{(13a^2 + 10ab + 2b^2)}{(3a + b)^2(2a + b)^2}$$

If α_a and α_b are assumed to be approximately the same size then the second term can be neglected as being much smaller than the term in α_a^2. Thus the percentage error in Y can be written as a function of a, b and α_a and can be calculated (Fig. 13).

(vii) Theoretical Intensities from a Lattice of Cylinders.

The intensity of the scattering of electromagnetic radiation from a system of cylinders is dependent on the first order Bessel function J(x). For an isolated solid rod, the scattered amplitude, F, is given by

$$F = \frac{2J_1(KR)}{KR} \quad \text{..... (Oster and Riley, 1952)}$$

with $K = (4\pi/\lambda) \sin \theta$

R is the radius of the cylinder, λ is the wavelength of radiation and 2θ is the scattering angle.

For a hexagonal lattice of cylinders

$$d_{hk} = (3/(h^2 + hk + k^2))^{\frac{1}{2}} (a/2)$$

where a is the centre-to-centre distance of nearest neighbours and where h and k are Miller indices.

$$KR = 2\pi R/d_{hk} = 4\pi R(h^2 + hk + k^2)^{\frac{1}{2}}/\sqrt{3}a$$

Fig. 14 shows a graph of the intensity of scattering, I, equal to F^2, for an isolated cylinder against KR. The values of the Bessel function $J_1(x)$ were taken from Abramowitz and Stegun (1970). The reflection measured experimentally d_{10} (57.9nm for fresh tissue) corresponds to KR equal to 1.86. If a hexagonal lattice existed the d_{11} spacing would be expected to occur at $d_{10}/\sqrt{3}$ i.e. 33.4nm. As the intensity distribution of the reflections is given by the overall shape of the intensity curve, it can be calculated that the ratio of the intensities of the measured d_{10} reflection to the theoretically calculated d_{11} reflection is 0.112:0.008 from Fig. 14 i.e. 14:1. Higher orders, eg d_{20} will correspond to larger values of KR which can be seen from Fig. 14 to give even higher ratio of intensities.

If a cubic lattice is assumed, the intensity of the d_{11} reflection is higher. In this case, d_{11} = 40.8nm if d_{10} is still 57.9nm. (For a cubic lattice $d_{hk} = a/(h^2 + k^2)^{\frac{1}{2}}$). The value of KR for d_{11} = 40.8nm is 2.62. The ratio of the intensities of d_{10}/d_{11} is then .112:.037 i.e. 3:1. Thus the large difference in intensities of the d_{11} reflection to the d_{10} reflection of a hexagonal lattice may account for the absence of the d_{11} reflection.

However, on swelling, the d_{10} has been shown to increase up to 90nm i.e. the maximum spacing that can be measured with the apparatus

used. In this case, KR for the d_{10} reflection would equal 1.18 and KR for a theoretical d_{11} reflection from a hexagonal lattice would be 2.05. This would give a ratio of the intensities of the d_{10} to d_{11} reflection is 1.78:.08 i.e. 2:1. However, the d_{11} reflection has not been seen in any x-ray patterns of highly hydrated material. Possible reasons for this are given in the discussion section V, (iv).

(viii) X-ray Diffraction Pattern from Fresh Sclera.

Fresh sclera gives rise to a strong reflection corresponding to a spacing of 66nm. Further reflections are seen at 23.2, 17.4, 13.5, 11.1, 9.0nm corresponding to the third, fourth, fifth, sixth and seventh orders respectively (Fig. 15). It appears that this was entirely due to the repeat along the axis of the collagen fibrils (Bear, 1942, 1944). No interfilament spacing is expected because there is very little order in the arrangement of the fibrils in the sclera (François et al, 1954).

(ix) The Patterson Functions of the Cornea and Sclera.

The Patterson function is a useful method for obtaining information about the distribution of electron density in a periodic structure without knowing the phase of each reflection since the intensity is the only information needed for the calculation (James, 1962, Azaroff, 1968). The Patterson function, P(x), is defined as

$$P(x) = (1/D) \int_{-D/2}^{D/2} \rho(y) \; \rho(x+y) \; dy$$

where D is the periodic spacing, x is a fraction of this periodic spacing and $\rho(y)$ and $\rho(x+y)$ are the electron densities at fractions y

and (x+y) of D along the repeat distance. By substitution of $\rho(x)$ in terms of the structure factors, Fn

$$\text{i.e. } \rho(x) = \frac{1}{D} \sum_{n=-\infty}^{\infty} F_n e^{-2\pi i n x/D}$$

the Patterson function reduces to

$$P(x) = \frac{1}{D^2} \sum_{n} F_n^2 \cos(2\pi n x/D).$$

For this calculation only the structure factors are required. For the case of low-angle reflections under the conditions which were used here the square of the structure is proportional to the intensity of the reflection (James, 1962, Tomlin and Worthington, 1956, Elliott, 1960). Maxima in the Patterson function correspond to vectors between regions of high electron density. No information on the order of these vectors is obtained.

Microdensitometer traces of the reflections from the corneal diffraction pattern show that the 22nm reflection (third order of the usual collagen spacing) is approximately $1\frac{1}{2}$x more intense than the 13.0nm reflection (fifth order of the collagen spacing)(Fig. 16). The average values of the intensity (from either side of the backstop) are given in Table 4. We are interested,in this section, only in the reflections from the repeats in electron density along the axes of the collagen fibrils and not in the reflection due to the packing of the fibrils (the interfilament spacing).

Using an arbitrary intensity scale, the Patterson function was calculated for positions differing by .05D from x = 0 to x = D/2. Fig. 17 shows the result of plotting P(x) against x. An obvious peak occurs at x = 0.38. However on extending the tail of this peak and subtracting from the total curve, it can be seen that an overlap of

another peak, at approximately x = .24, occurs with the tail of the maximum at x = .38. This second maximum, at x = .24, is not so distinct as that at x = .38.

In order to compare the collagen reflections from the cornea with those from the sclera which appeared to be similar to other collagens, the Patterson function for sclera was calculated from a microdensitometer trace of the x-ray diffraction pattern (fig. 18). The relative intensities of the reflections from the sclera are given in Table 4. Each value is the average of two readings from either side of the backstop. The intensity of the first order was so strong that it merged into the scattering around the backstop on the long exposure required to see the higher order reflections. For this reason, a value of ten times the intensity of the third order reflection was assumed. This is compatible with measured intensities from kangaroo tail tendon (Ericson and Tomlin, 1959). Using these values, the Patterson function was plotted as a function of x (Fig. 19). P(x) decreases from x = 0 to x = D/2 showing no distinct maxima in contrast to that of the cornea.

Tomlin and Worthington (1956) have interpreted the Patterson function from kangaroo tail tendon (which is similar to that of the sclera) in terms of a band and interband model. The band has either a larger diameter or a larger electron density or possibly both. The band width has been estimated at .46 x D. This has been confirmed by staining the fibrils (Erikson and Tomlin, 1959). However, Kaesberg and Shurman (1953) interpreted the Patterson function from beef tendon as a single high density band. Improved profiles of electron density distribution along the collagen fibrils have been obtained by Chandross

and Bear (1973).

(x) Laser Diffraction of Electron Micrographs.

(a) Further evidence on the order or disorder of the fibril arrangement in the cornea has been obtained using laser diffraction of electron micrographs of corneal fibrils in cross section. This technique was undertaken in collaboration with Dr. P. Cooke. The preparation of the corneal specimens is described in Appendix at the end of this chapter.

Electron micrographs of thin sections of fresh corneal stroma were taken with the fibrils in cross section so that their packing arrangement could be studied (Fig. 21). The electron micrograph was placed in a diffractometer(which was made available by the courtesy of the Molecular Biophysics Laboratory, Oxford University). The light diffraction pattern from the arrangement of fibrils was recorded on film (Fig.22). Three diffraction rings can be seen. The ratio of the spacings is 1:.47:.28 (Fig. 22). The ratio $d_{10}:d_{20}:d_{22}$ for a hexagonal lattice would be 1:.5:.29 which is very similar to that found experimentally for the cornea. The d_{11} and the d_{21} reflections are missing.

(b) The absence of the first order of the collagen repeat has been confirmed using the technique of laser diffraction of electron micrographs. Fig. 24 shows the light diffraction patterns from an electron micrograph of a group of longitudinal arranged corneal collagen fibrils (Fig. 23). No first order is seen although second, third and sixth order is visible.

IV Discussion.

(i) General Properties of the X-ray Diffraction Pattern from the Corneal Stroma.

It was seen, in the last section, that the corneal stroma gives rise to three low-angle x-ray diffraction rings. These reflections can be divided into two groups because of the difference in their behaviour on swelling the stroma. The inner reflection, corresponding to the largest spacing, increased in size with increasing water content of the tissue (Fig. 6). Its magnitude in fresh tissue was the same order as expected, from electron micrographs of the cornea, it was thought to be the interfilament spacing due to the packing arrangement of the collagen fibrils.

The other two reflections behaved differently on swelling the tissue. Although Maurice (1957) thought that they were the second and third order of the interfilament spacing of 41nm, it was decided that these reflections were more likely to be due to the collagen 66nm repeat along the fibrils. They appear to be the third and fifth orders of such a repeat. This assignment is based on the experimental evidence that the size of the spacings did not alter, within the experimental error, on either swelling or drying the tissue (Table 2).

All further experimental work was divided into studies on the interfilament spacing and studies on the reflections from the repeat along the collagen fibrils.

(ii) The X-ray Diffraction Pattern at Different Orientations.

It was shown in the results section (iii) that the interfilament distance does not change with orientation of the tissue. From electron microscope studies, the arrangement of the fibrils is assumed to be such that the fibrils are approximately equally spaced in fresh tissue. However, because the stroma as a whole swells unidirectionally (Hedbys and Mishima, 1962) then the lattice of fibrils was expected to do likewise e.g. the calculations of Hart and Farrell (1971) are based on this premise. The experimental data from x-ray diffraction patterns of swollen tissue shows that the interfilament distance is the same whether the specimen is orientated with the corneal surface parallel or perpendicular to the x-ray beam (Fig. 4). Therefore, it is assumed that the lattice of fibrils must swell equally in all directions although the tissue as a whole swells in only one direction. Fig. 5. shows a hypothetical arrangement of the collagen fibrils which are shown to be in a cubic lattice for convenience only. This diagram is intended to illustrate a point and not to be a representation of the structure of the cornea. The first arrangement in this figure shows the hypothetical packing in fresh tissue. The second arrangement shows how the lattice could swell in only one direction so that the tissue does the same. Finally, this figure indicates how the lattice of fibrils could be rearranged in order that the fibrils are equally spaced but the tissue is still swelling in one direction. It can be noted that the number of unit cells remains the same in each case . It is possible that during the rearrangement of the fibrils, which is necessary on swelling, 'lakes' may occur in the structure as proposed by Benedek (1971).

At least part of the reason for the tissue as a whole swelling in only one direction can be seen from studying Fig. 20. In this figure, two lamellae are drawn with the axes of the fibrils at right angles to each other. The fibrils all lie parallel to the surface of the cornea. (Maurice, 1969). Diagram (a) shows part of a lamella in which the fibrils are orientated along the X-direction. Swelling of the tissue occurs perpendicular to the surface along the Z-direction. However, the lattice of fibrils can swell in both the Z- and Y-directions but not in the X-direction i.e. along the axes of the fibrils. In diagram (b) the axes of the fibrils lie in the Y-direction. The tissue must still swell only in the Z-direction but the lattice of fibrils can swell in both the Z- and X-directions but not in the Y-direction. The other possible orientations of the fibrils must lie between those in (a) and (b) such that the direction in which the lamellae does not swell (i.e. the direction of the axes of the fibrils) is always in the X Y plane. In every lamella, swelling can occur in the thickness direction but swelling will not be able to occur in one direction in the X Y plane. The method by which the lamellae communicate the constraint to swell in one direction to the neighbouring lamellae, which cannot swell in another direction, is not known. It may be due to attractive forces, such as the van der Waals forces, between neighbouring elements in each lamella.

(iii) Swelling of the Lattice as a Function of the pH and the Ionic Strength of the Bathing Solution.

It can be seen that the interfilament distance depends mainly on the hydration of the tissue (Figs. 6-11). In the results section (iv), it was noted that the slope of the linear regression fit of the data (as d_{10}^2 versus hydration) was found to depend slightly on the pH of the

bathing solution. In general, the slope appeared to be larger at pH7 and pH8 and to decrease in value if the pH was lowered to pH6 or raised to pH10. More information can be obtained by comparing the percentage 'lakes' (at H=3) as a function of the pH of the external solution (Fig. 13). From Fig. 13 it is seen that the percentage 'lakes' decreases to a minimum at pH7 when the ionic strength equals .02, 1.5 and .25. This means that the maximum amount of fluid is in the lattice of collagen fibrils at pH7. This does not occur at an ionic strength of .05. When the pH is altered away from pH7, the percentage 'lakes' increases, i.e. the amount of water in the lattice decreases.

The dependence of the amount of 'lakes' on the ionic strength is not so clear. At pH8 and pH10, the minimum number of lakes occurs at an ionic strength equal to .15, and the highest number at an ionic strength of .25. The amount of 'lakes' at ionic strength .05 and .02 lie in between these values. The amount of water in the lattice of fibrils at pH7 is approximately the same for all the ionic strengths except at ionic strength .05 which is particularly low. The percentage 'lakes' at pH6 is high, about 20-25% for ionic strengths of .02, .15 and .25 but at ionic strength of .05 the percentage is low at approximately 10%.

(iv) How Ordered is the Arrangement of the Collagen Fibrils?

The arrangement of the collagen fibrils in the corneal stroma gives rise to one reflection, the interfilament spacing, from which it is not possible to say whether the arrangement of fibrils is like that of an ordered crystalline lattice or what type of lattice this may be. Calculations on the intensities of the higher order reflections, e.g. d_{11}, from a hypothetical hexagonal lattice were found to be very weak compared

with the intensity of the d_{10} reflection. (1:14). This implies that even if a hexagonal lattice existed it would be difficult to see the d_{11} reflection. This large decrease in intensity of the d_{11} reflection occurs because of the overall shape of the transform of a cylindrical fibril of 17nm radius and the fact that the diameter of the fibrils is the same order of magnitude as the spacing between the fibrils (i.e. centre-to-centre distance between the fibrils is 58nm in fresh tissue).

However, it was noted that swelling the lattice of fibrils until d_{10}= 90nm, would increase the relative intensity of the d_{11} spacing to the d_{10} to a ratio of 1:2. The d_{11} spacing has not been seen even at these high hydrations. On swelling the corneal stroma, more fluid is imbibed so that the x-ray beam has to pass through a larger amount of fluid by which it is absorbed. Therefore the d_{10} intensity at 90nm is weakened relative to that at 60nm. Moreover, cutting a thinner section of the cornea does not improve the intensity greatly because, although the absorption is less, there is a decrease in the density of the fibrils at high hydrations. There is also the possibility that at high hydrations, the lattice of fibrils becomes more disordered so that the reflection due to their packing arrangement is more diffuse. This, again, reduces the intensity of the reflections. Thus it must be concluded that x-ray diffraction techniques cannot yield definite evidence for or against the possibility of an ordered crystalline lattice of collagen fibrils existing in the corneal stroma.

The laser diffraction pattern from the electron micrograph of stroma with the fibrils in cross-section shows three diffraction rings. The ratio of the size of these spacings is 1:.47:.28. The presence of these rings indicates that some order must exist even in stroma which have been

stained and fixed for electron microscopy. The ratio of these spacings was shown to be very near that of the $d_{10}:d_{20}:d_{22}$ spacings from a hexagonal lattice. However, the reason for the missing d_{11} and d_{21} reflections is not known. This technique may provide more evidence for the existence of an ordered lattice but more data is needed from stroma hydrated under different conditions.

(v) The Lack of the First Order of the Collagen Spacing from Cornea.

When comparing the Patterson functions from corneal collagen (Fig. 17) with that of scleral collagen (Fig. 19), it can be seen that the distances between regions of high electron density along the collagen fibrils are very different to each other in these different tissues. The Patterson function from sclera is dominated by the first order reflection which is very intense. This reflection is absent from the x-ray diffraction pattern of corneal collagen. The main features of the Patterson function from cornea are two peaks at X = .38 and X = .24 where X is a fraction of the repeat distance D. The maximum at X = .38 is stronger suggesting that more material is separated by a vector of .38 x D along the collagen fibril rather than by the distance .24 x D. Interpretation of this function is aided by noting that one repeat distance, D, can be made up of two distances of .38 x D and one distance of .24 x D. Thus it is suggested that, in corneal collagen, distances between regions of high electron density occur twice at .38 x D and once at .24 x D within one repeat period. The order of these vector distances is immaterial because distances of 2 x .38 x D and 1 x .24 x D can only be arranged in one unique way, except at the ends of the fibrils.

The reason for this difference in electron density along the corneal

collagen fibril compared to other collagens is not known. It may be due to the attachment of the glycosaminoglycans (possibly keratan sulphate which is not present in the sclera) at specific sites within one repeat period. It may also be connected with the thirding of the more usual repeat period seen by Francois et al (1954) and Garzino (1955) by electron microscopy of stained sections. Francois et al (1954) also noted the presence of bands every 13nm which would correspond to a fifth of the repeat period.

V Appendix.

The corneal stroma used in the electron microscopy was rehydrated to a known hydration in a bathing solution of known pH and ionic strength. The tissue was fixed in 3% glutaraldehyde made up in the buffered bathing solution used to swell the corneal stroma initially. The fixed tissue was stained with 2% osmium tetroxide and 2% uranyl acetate. Progressively more concentrated alcohol solutions were used in order to dehydrate the specimen. The specimen was then set in hard-setting resin. Thin sections, whose thickness was approximately 80-90nm, were cut on a microtome. They were placed on copper grids and stained with uranyl acetate and lead citrate.

The specimens were viewed on a Philips 301 electron microscope and recorded on Ilford E-M4 photographic plates. These plates were developed and placed in the diffractometer in order to record the light diffraction pattern.

Table 1

Comparison of the High-Angle X-ray Diffraction Patterns from Cornea and Collagen.

Cornea Hertel (1933) Å	Cornea Agarwal et al (1972) Å	Collagen Ramachandran (1962) Å
10.9	11.5	11
7.1	-	-
4.4	3.6-5.0	4.5
2.8	2.9	2.9
-	2.0	-

Table 2

Comparison of the Spacings from the Repeat Along the Collagen Fibril on Swelling and Drying.

	Fresh	Swollen	Dried
(a)	23.0	22.4	22.1
	22.0	22.8	22.8
	24.0	21.9	21.6
	21.0	21.9	23.3
	22.0	22.8	23.0
	24.0	22.7	22.7
	22.8	22.0	22.7
	20.0	21.9	21.6
	23.0	22.0	
		21.9	
		21.9	
Average ± s.e (no. of data points)			
	22.4 ± 1.3(9)	22.2 ± .4(11)	22.4 ± .6(8)
(b)	14.8	13.8	13.1
	13.8	14.4	
	12.9		
Average ± s.e (no. of data points)			
	13.8 ± .95(3)	14.1 ± .4(2)	13.1 (1)

All Spacings in nm

Table 3

Data of Linear Regression Fits for d_{10}^2 Versus Hydration.

Solution pH	Ionic Strength	$nm^2 \times 10^4$ a (slope) ± S.E.	$nm^2 \times 10^4$ b(intercept)	Radius(nm) **	F-ratio *
6	.02	5.38 ± .7	14	19.4	59
7		11.67 ± .78	-1.7	18.1	22.5
8		9.03 ± 1.5	5.4	18.8	346
10		7.89 ± .72	4.9	17.7	119
6	.05	8.56 ± .54	3.5	18.0	269
7		9.39 ± .76	7.9	20.1	152
8		10.27 ± .69	3.5	19.1	222
10		8.33 ± .46	5.4	18.3	236
6	.15	7.23 ± .6	16.9	21.8	146
7		10.24 ± 1.5	-0.35	17.5	44
8		10.7 ± 1.09	1.74	18.7	97
10		10.2 ± 2.7	3.1	18.8	53
6	.25	3.81 ± .88	16.4	19.1	19
7		12.26 ± 1.6	0.71	19.6	57
8		6.11 ± .89	12.37	19.3	47
10		5.02 ± .95	15.12	19.5	28
Distilled water		5.96 ± .74	9.59	18.1	64
Fresh tissue	.15	5.54 ± .69	15.8	20.2	64

* defined in Appendix 1.

** Radius of collagen fibrils as calculated from regression fits

Table 4

Relative Intensities of Reflections from Cornea and Sclera.

Order	Cornea	Sclera
	Intensity - arbitrary units	
1	-	110
2	-	-
3	11	11
4	-	5.6
5	6.13	5.7
6	-	3.85
7	-	3.05

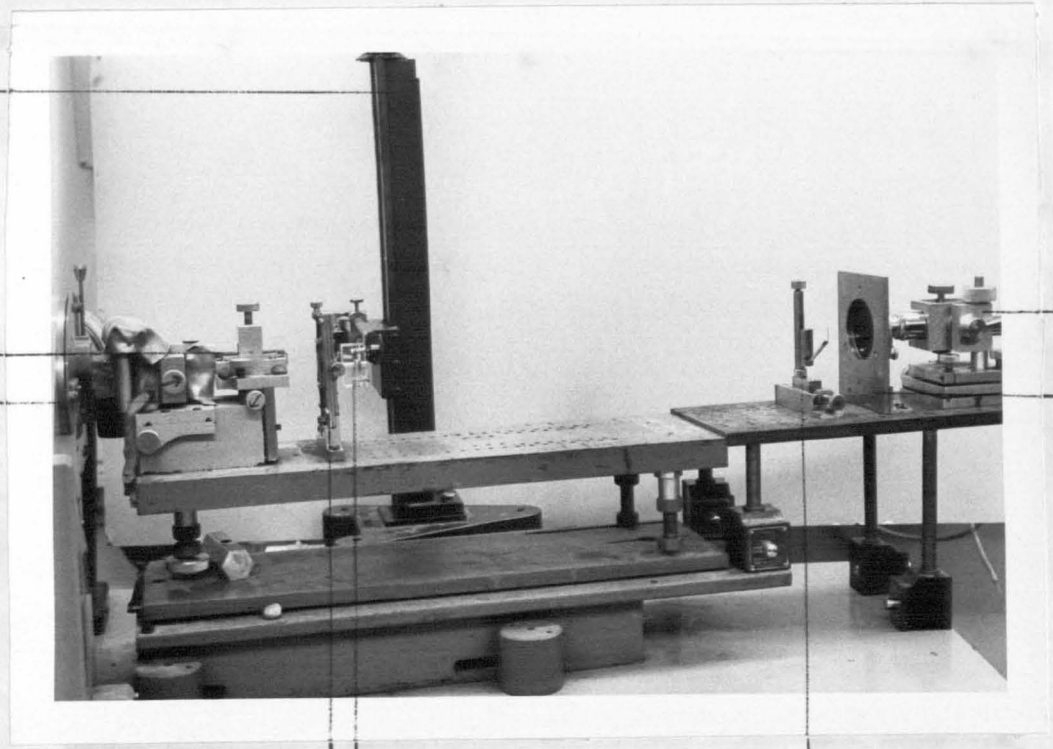

Fig. 1a. A Franks' x-ray camera

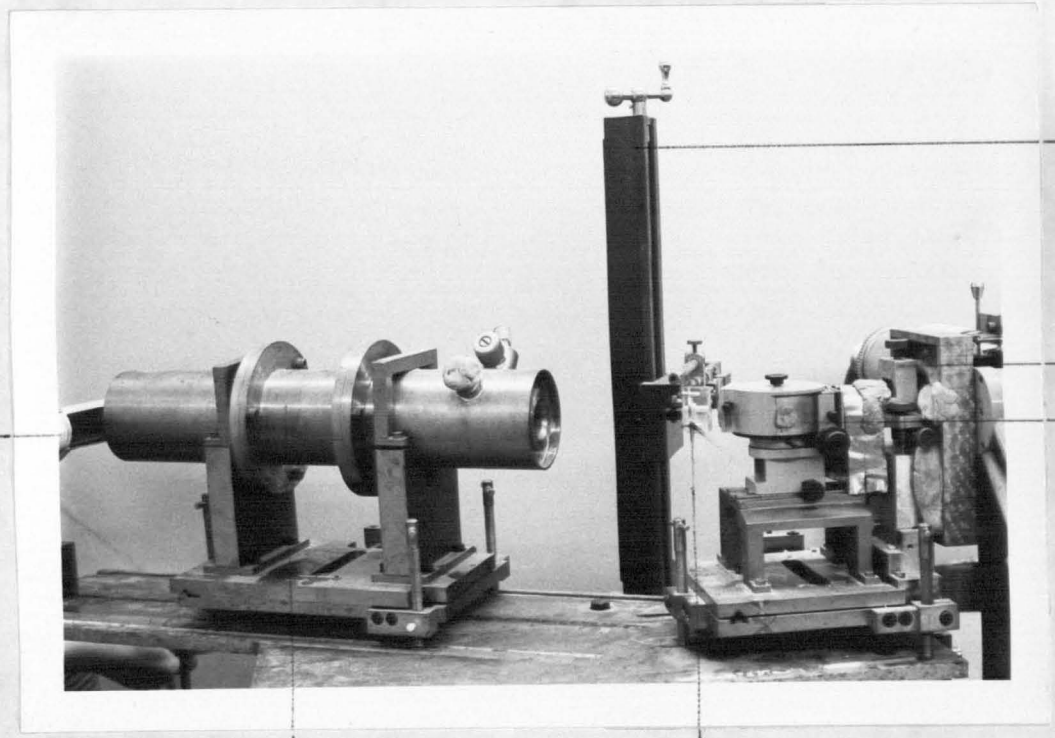

Fig. 1b. A crystal monochromator x-ray camera

Fig. 2a. X-ray diffraction pattern from fresh beef stroma.

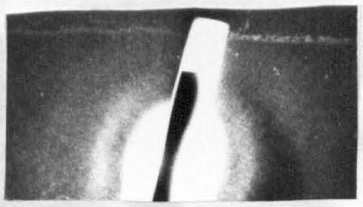

In this x-ray diffraction pattern from fresh beef stroma, the third and fifth orders of the collagen repeat of 66nm are visible. The interfilament spacing is hidden within the scatter from around the backstop because of the long exposure needed for the third and fifth orders to be visible.

Fig. 2b. X-ray diffraction pattern from fresh beef stroma.

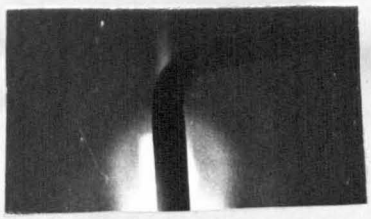

In this x-ray diffraction pattern the reflection corresponding to the interfilament spacing is clearly visible although the exposure is not long enough to bring up the third and fifth orders of the collagen pattern.

Fig. 2. c-e. X-ray diffraction patterns from swollen cornea.

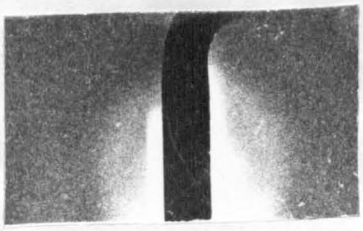

(c) Hydration = 1.6 ; Interfilament spacing = 46.2 $\pm$ 1.9 nm

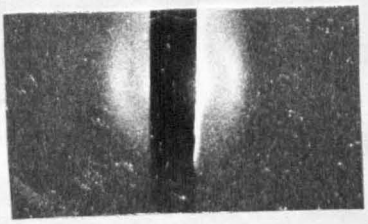

(d) Hydration = 3.02 ; Interfilament spacing = 49.1 $\pm$ 2 nm

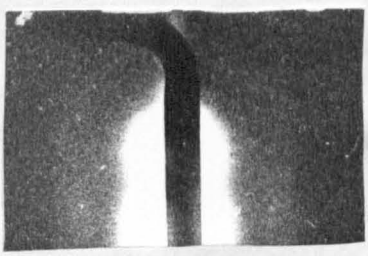

(e) Hydration = 6.15 ; Interfilament spacing = 64.1 $\pm$ 2.6 nm

COMPARISON OF INTERFILAMENT SPACINGS WITH DIFFERENT SPECIMEN ORIENTATIONS.

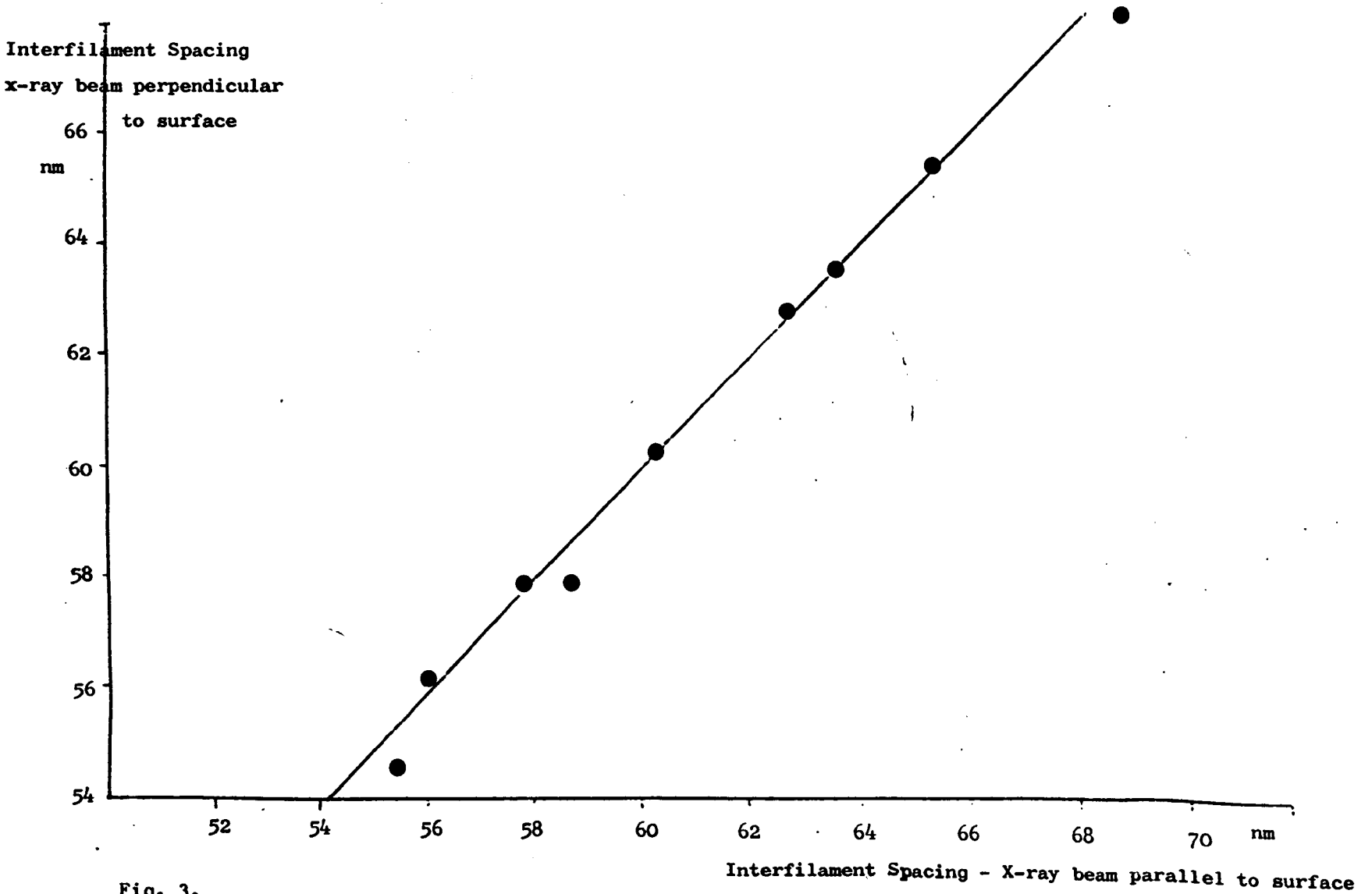

Fig. 3.

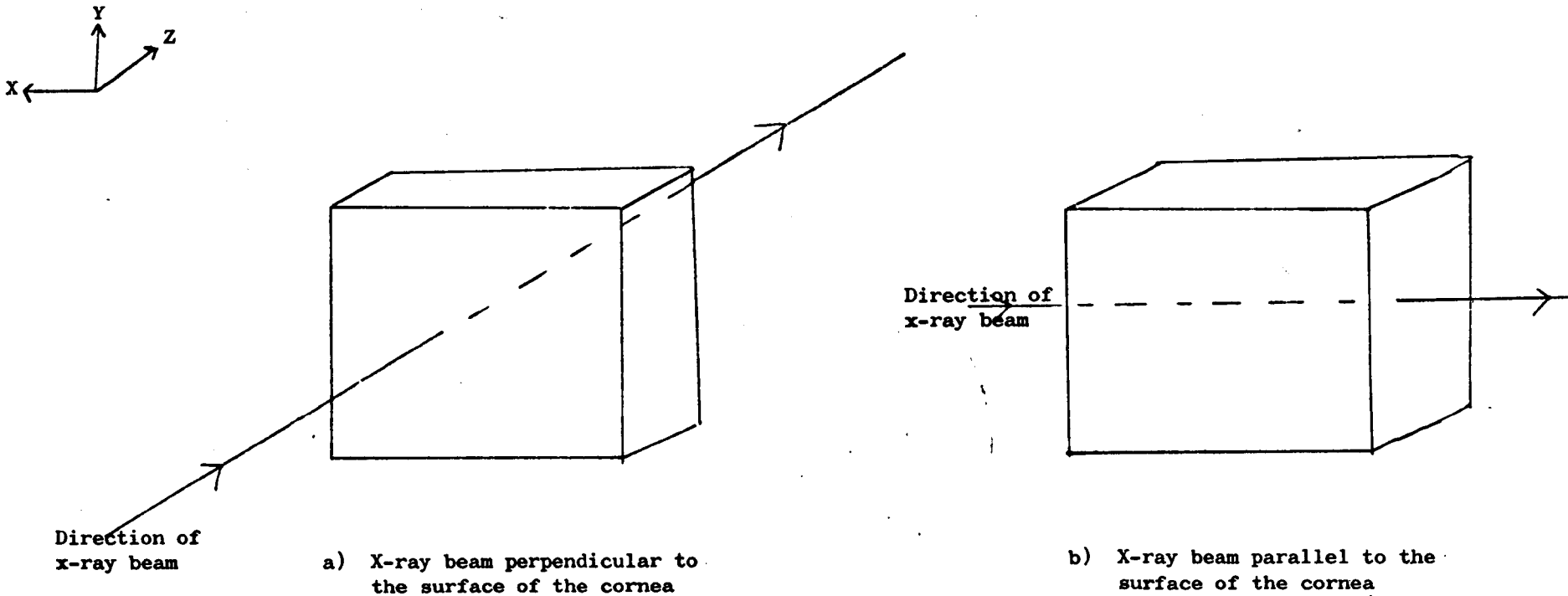

Fig. 4. Diagram of the cornea showing direction of x-ray beam relative to the orientation of the cornea.

The surface of the cornea is in the X-Y plane and the swelling direction is in the Z-direction.

Fig. 5. Diagram of hypothetical cubic lattices of collagen fibrils in which the tissue swells only in one direction but the lattice can swell either only in the direction of the tissue or equally in all directions.

DIAGRAM OF HYPOTHETICAL ARRANGEMENTS OF FIBRES IN NORMAL AND SWOLLEN STROMA

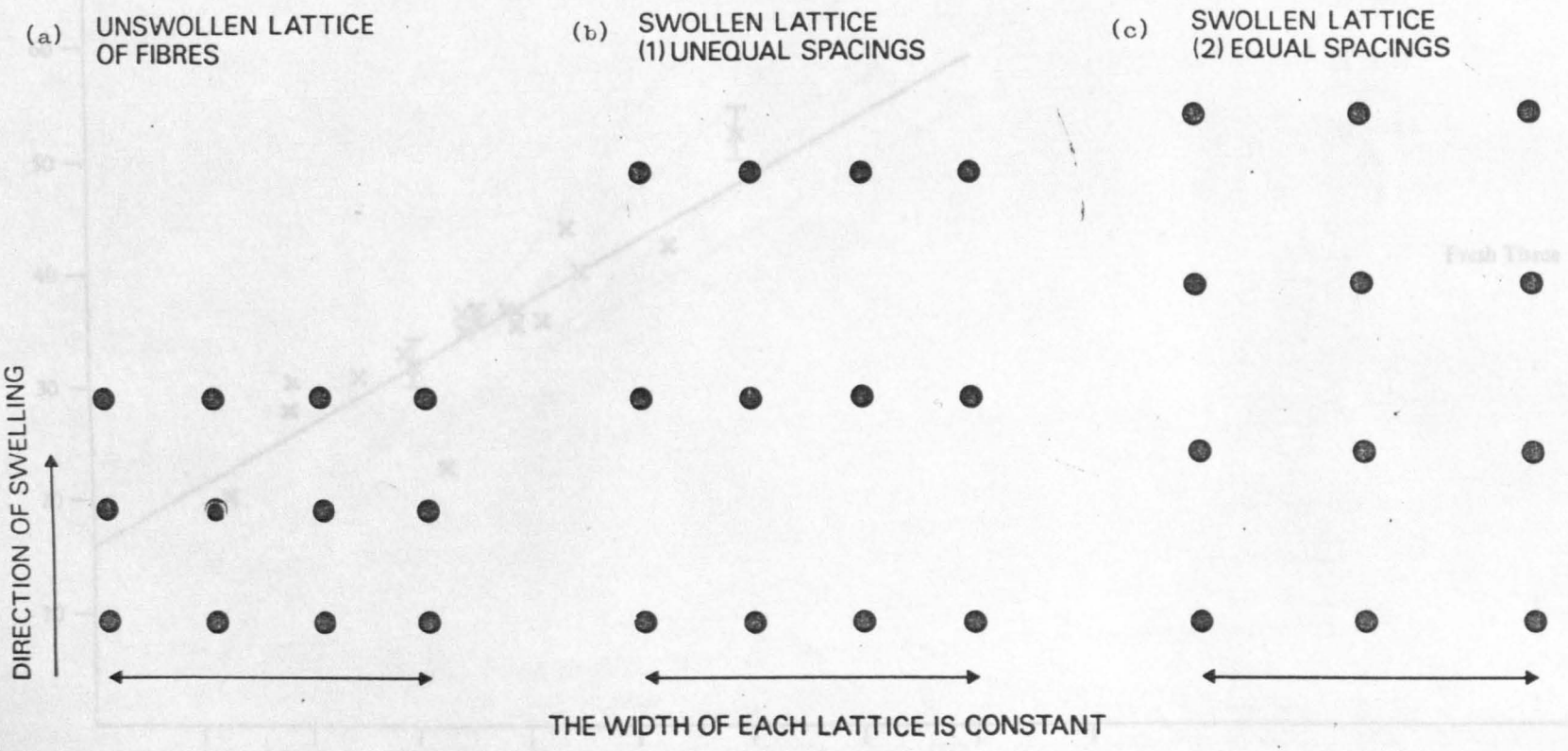

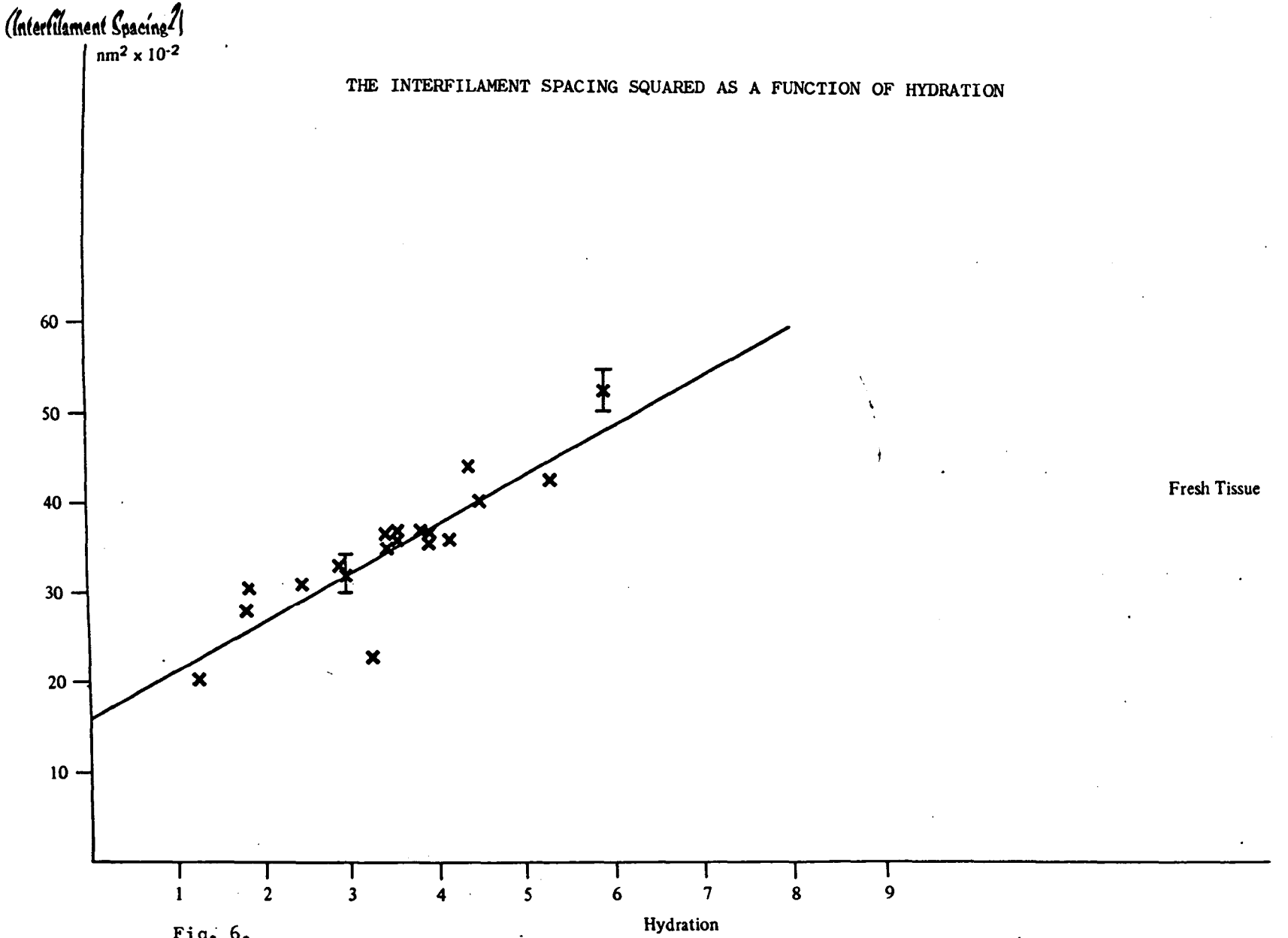
(Interfilament Spacing²)
nm² x 10⁻²
THE INTERFILAMENT SPACING SQUARED AS A FUNCTION OF HYDRATION
60
50
40
30
20
10
1
2
3
4
5
6
7
8
9
Hydration
Fresh Tissue

Fig. 6.

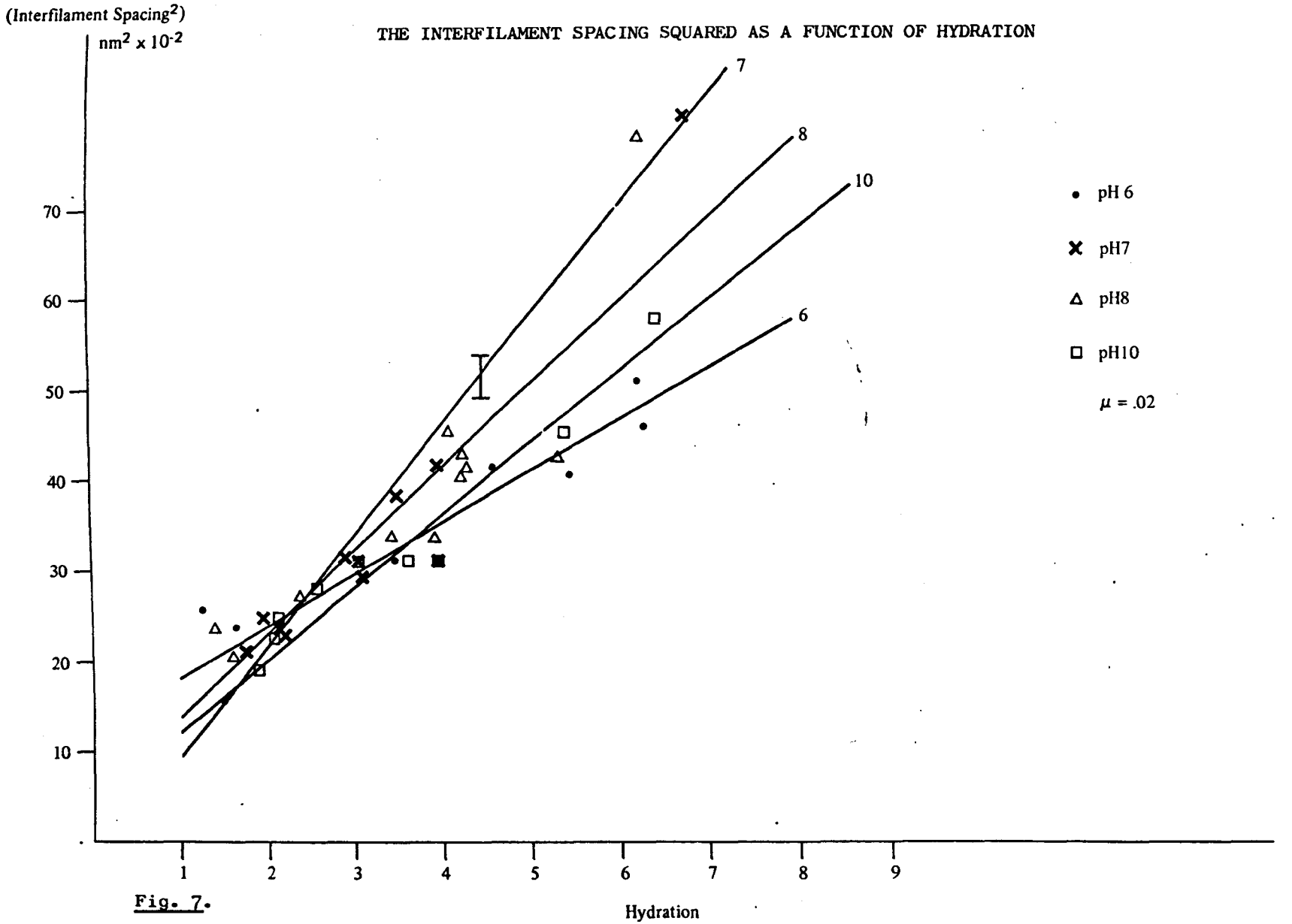
(Interfilament Spacing²)
nm² x 10⁻²
THE INTERFILAMENT SPACING SQUARED AS A FUNCTION OF HYDRATION
7
8
10
6
pH 6
pH7
pH8
pH10
μ = .02
70
60
50
40
30
20
10
1
2
3
4
5
6
7
8
9
Hydration

Fig. 7.

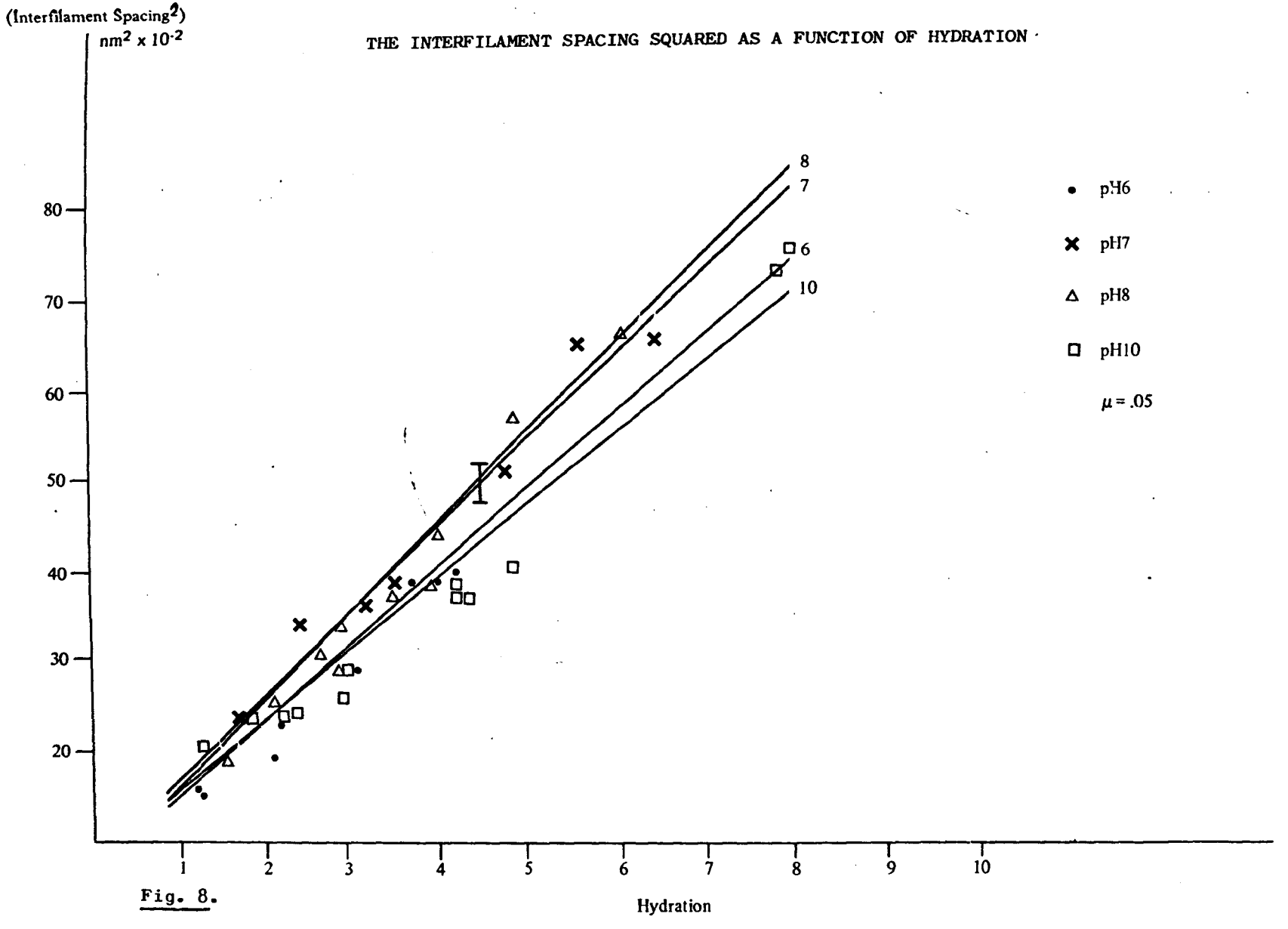
(Interfilament Spacing^2)
nm^2 x 10^{-2}
THE INTERFILAMENT SPACING SQUARED AS A FUNCTION OF HYDRATION
80
70
60
50
40
30
20
1
2
3
4
5
6
7
8
9
10
Hydration
8
7
6
10
pH6
pH7
pH8
pH10
μ = .05

Fig. 8.

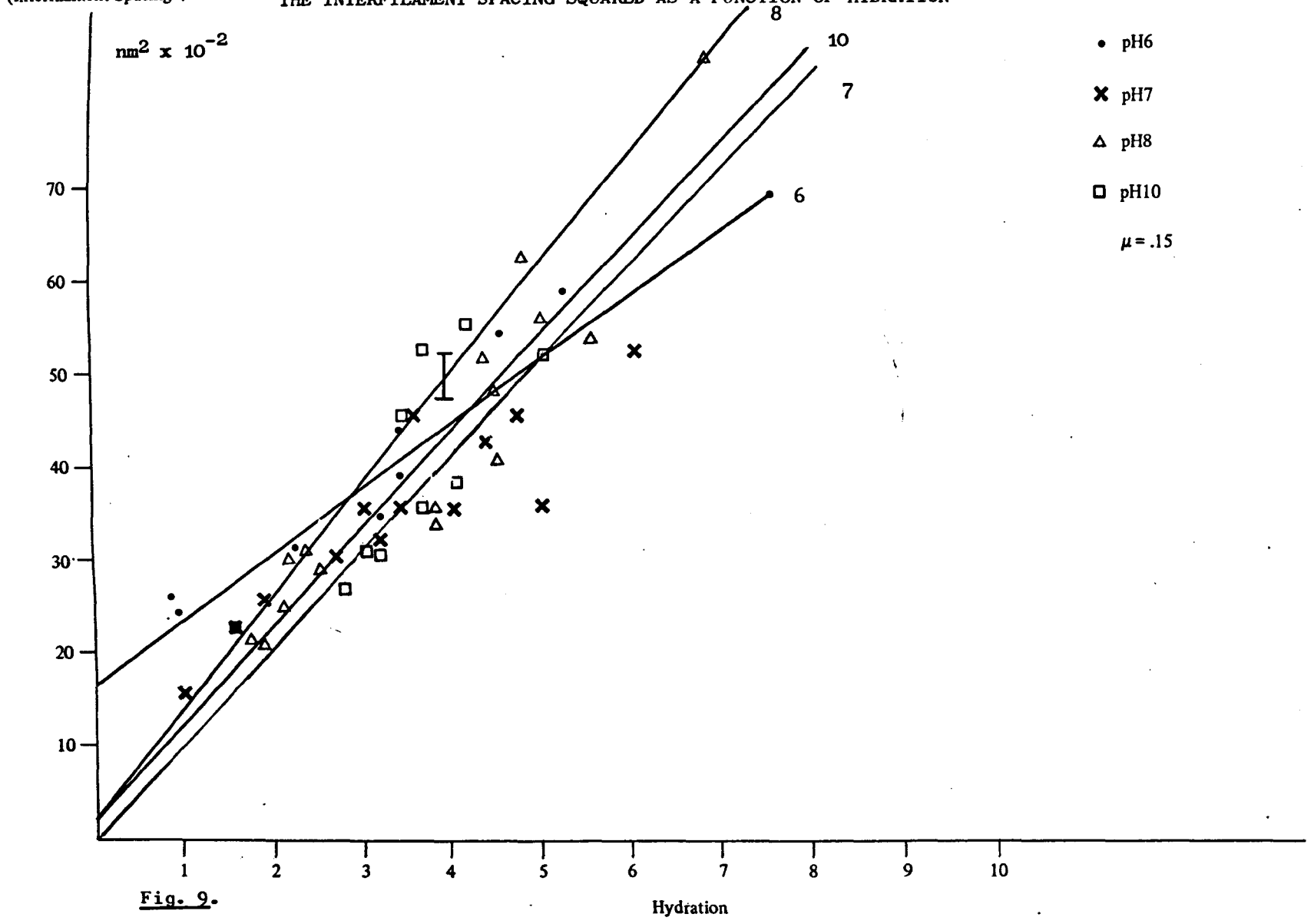
(Interfilament Spacing²)
THE INTERFILAMENT SPACING SQUARED AS A FUNCTION OF HYDRATION
nm² x 10⁻²
8
10
7
6
pH6
pH7
pH8
pH10
μ = .15
70
60
50
40
30
20
10
1
2
3
4
5
6
7
8
9
10
Hydration

Fig. 9.

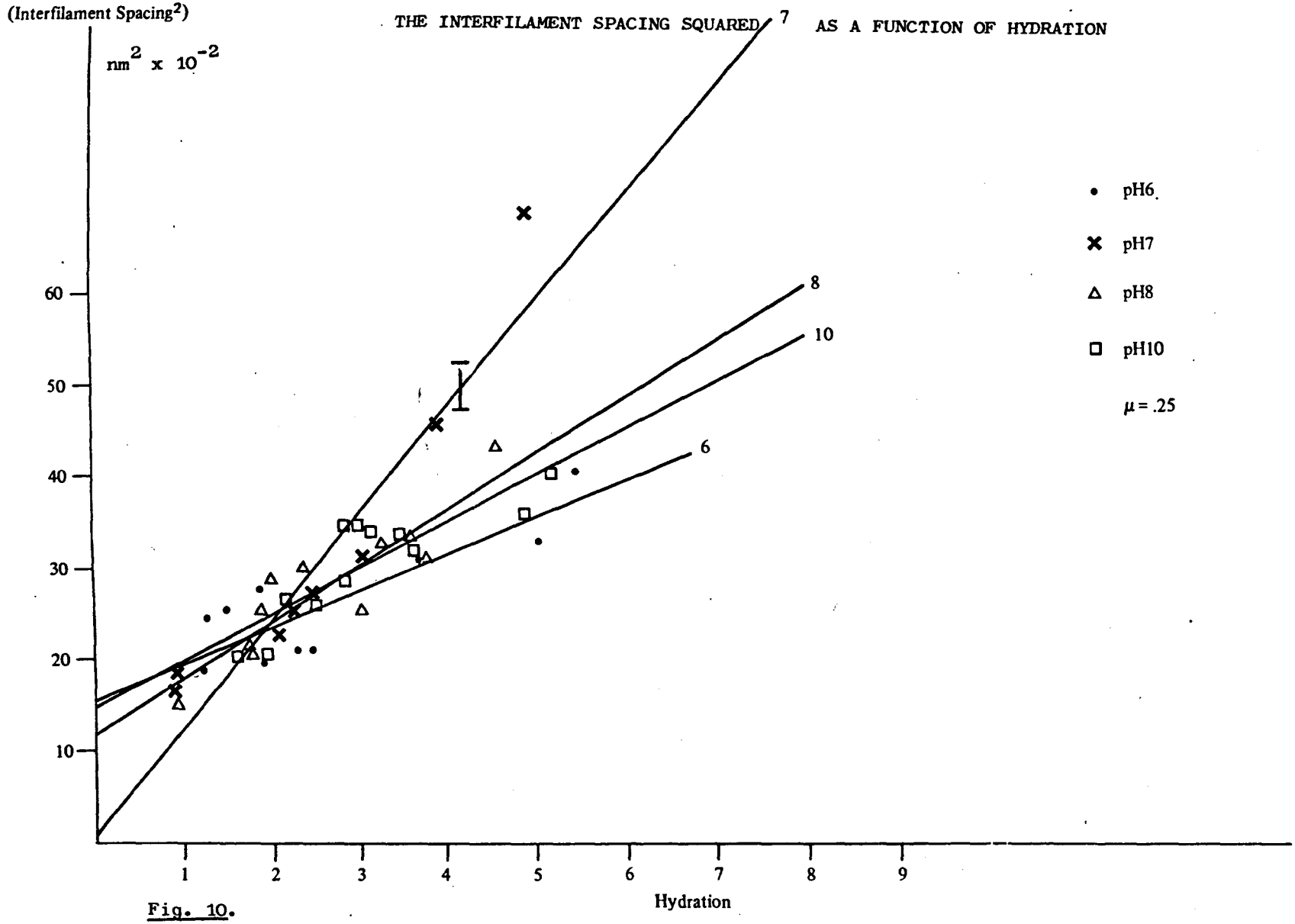
(Interfilament Spacing²)
nm² x 10⁻²
THE INTERFILAMENT SPACING SQUARED AS A FUNCTION OF HYDRATION
7
8
10
6
pH6
pH7
pH8
pH10
μ = .25
60
50
40
30
20
10
1
2
3
4
5
6
7
8
9
Hydration

Fig. 10.

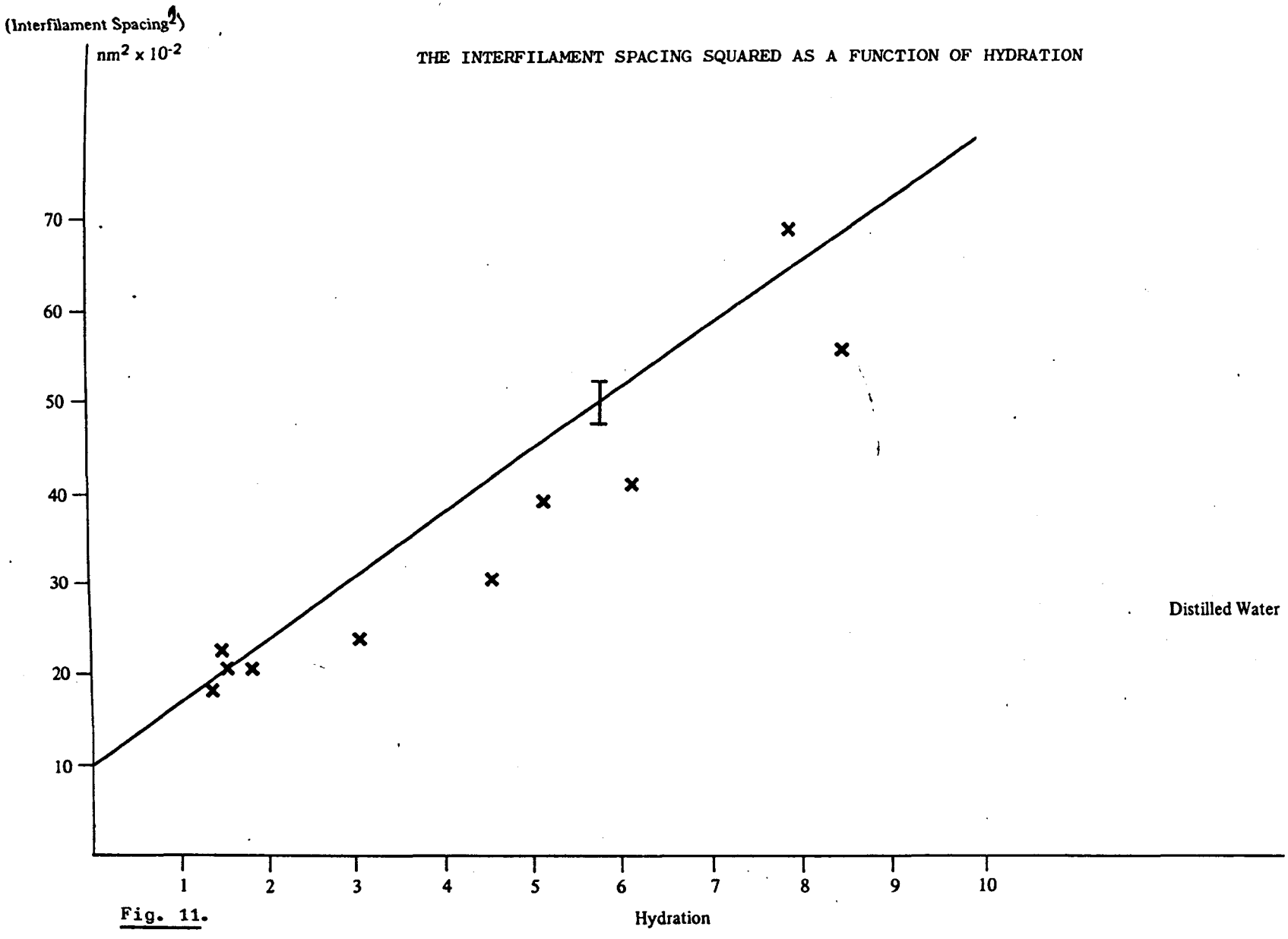
(Interfilament Spacing²)
nm² x 10⁻²
THE INTERFILAMENT SPACING SQUARED AS A FUNCTION OF HYDRATION
70
60
50
40
30
20
10
1
2
3
4
5
6
7
8
9
10
Hydration
Distilled Water

Fig. 11.

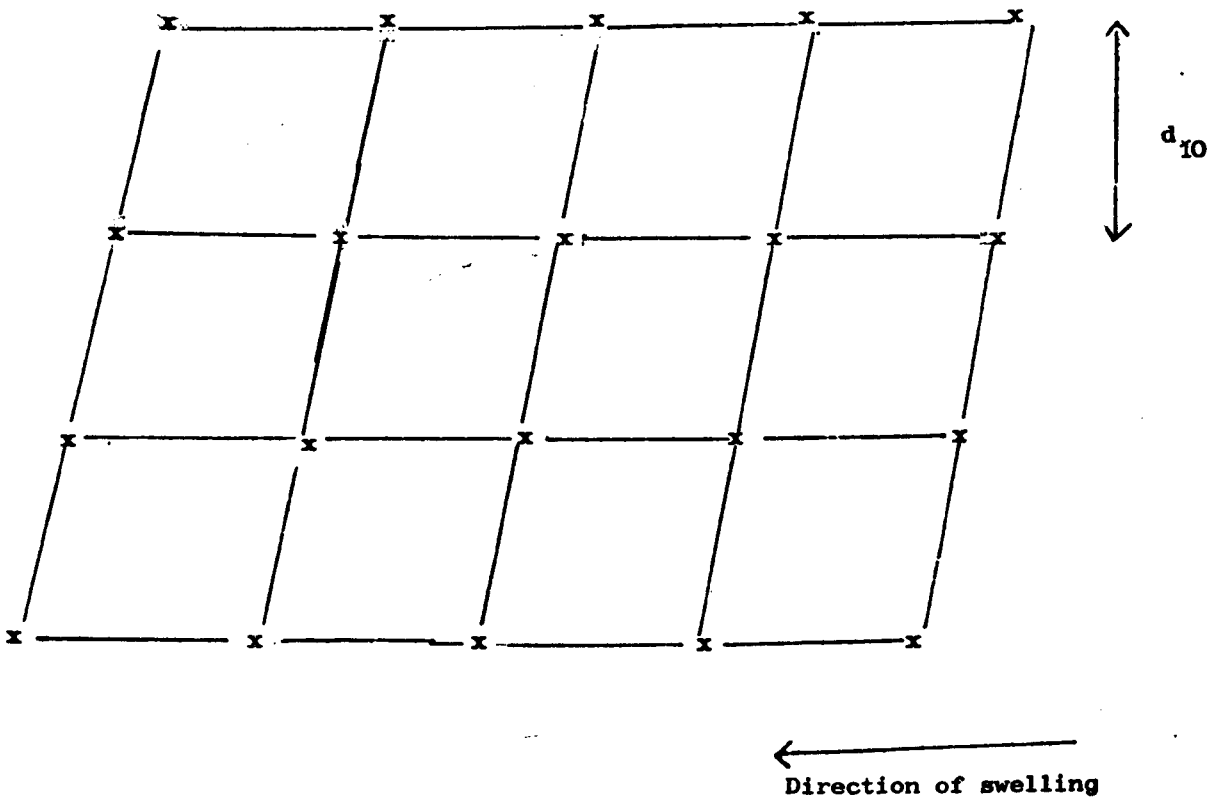

Fig. 12. A diagram of a hypothetical hexagonal lattice showing 12 unit cells and the positions of the d_{10} spacing. x indicates that the fibril axis is into the paper.

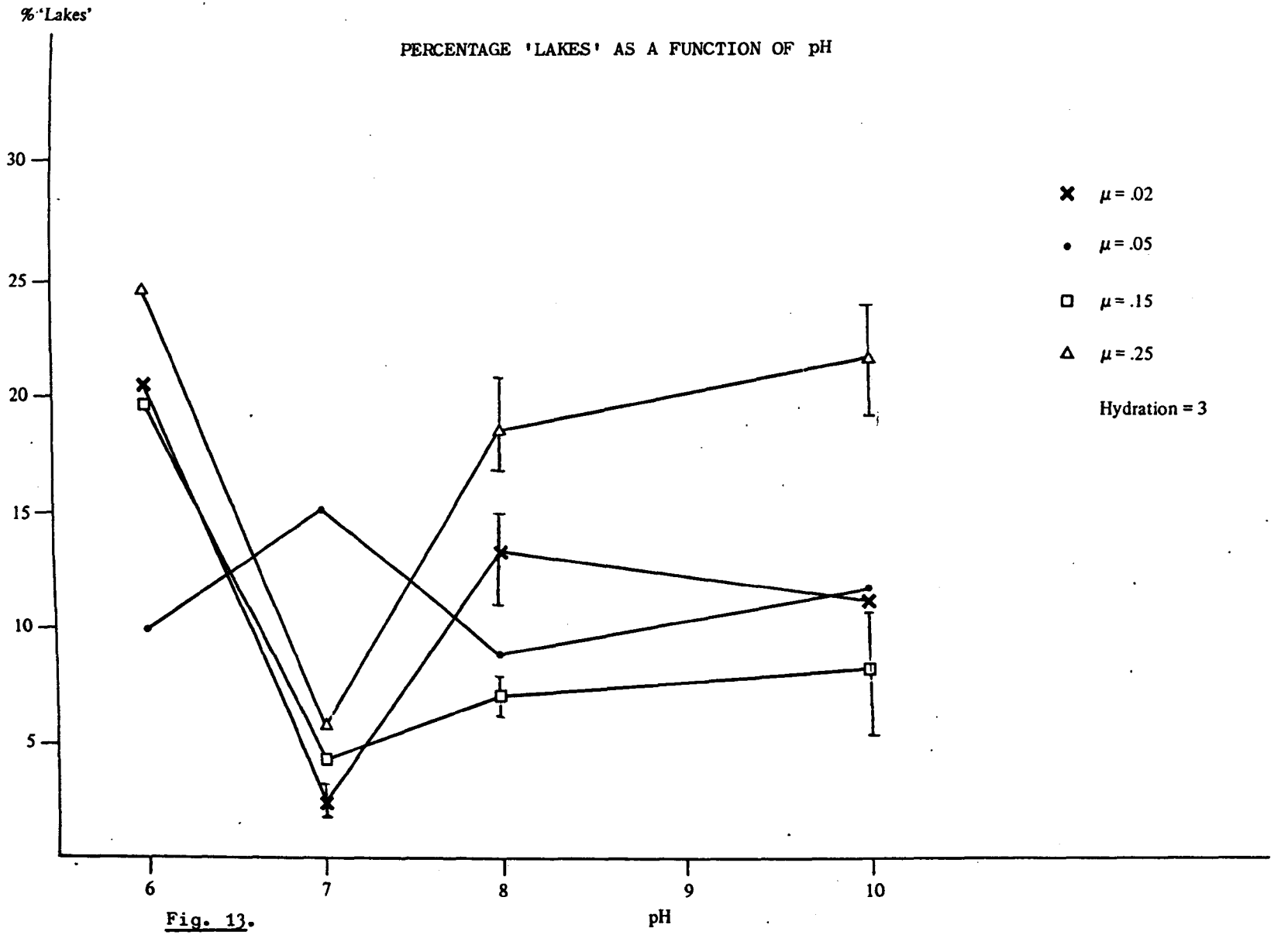
% 'Lakes'
PERCENTAGE 'LAKES' AS A FUNCTION OF pH
30
25
20
15
10
5
6
7
8
9
10
pH
μ = .02
μ = .05
μ = .15
μ = .25
Hydration = 3

Fig. 13.

Fig. 14. Diagram showing the expected ratio in intensity of the experimentally measured interfilament spacing to the intensity of a hypothetical d_{11} spacing from a given lattice. Data for two different interfilament spacings and two different types of lattice are indicated.

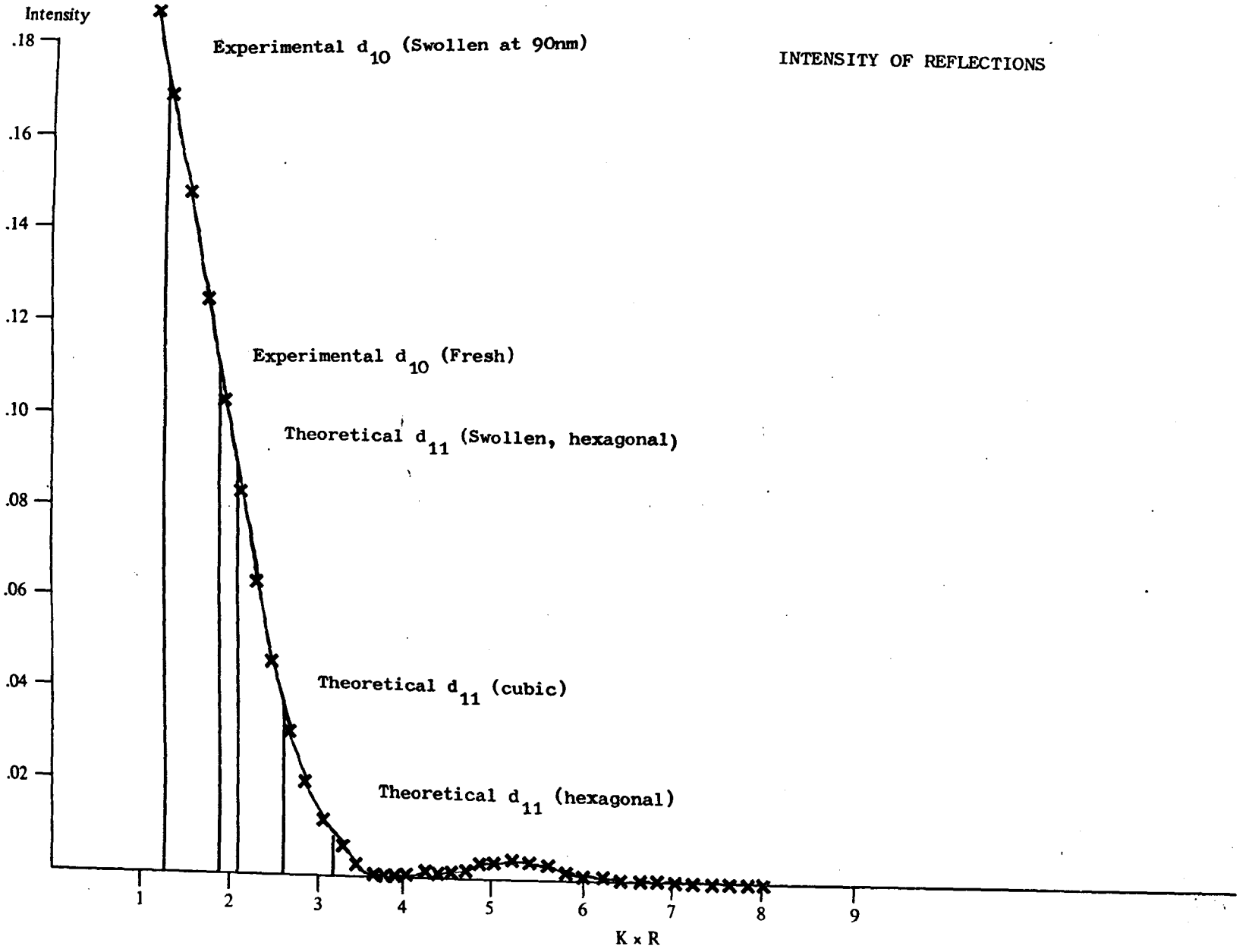
Intensity
.18
.16
.14
.12
.10
.08
.06
.04
.02
Experimental d_{10} (Swollen at 90nm)
INTENSITY OF REFLECTIONS
Experimental d_{10} (Fresh)
Theoretical d_{11} (Swollen, hexagonal)
Theoretical d_{11} (cubic)
Theoretical d_{11} (hexagonal)
1
2
3
4
5
6
7
8
9
K x R

Fig. 15. X-ray diffraction patterns from fresh sclera.

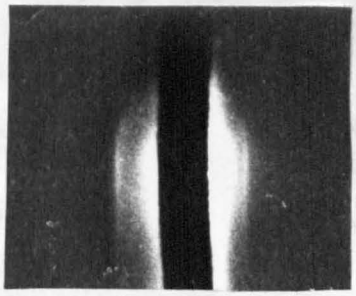

(a) First order

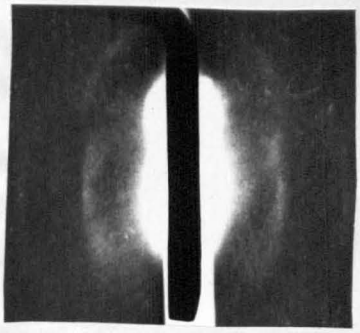

(b) Third and fifth orders are visible but the first order is hidden in the scatter around the backstop.

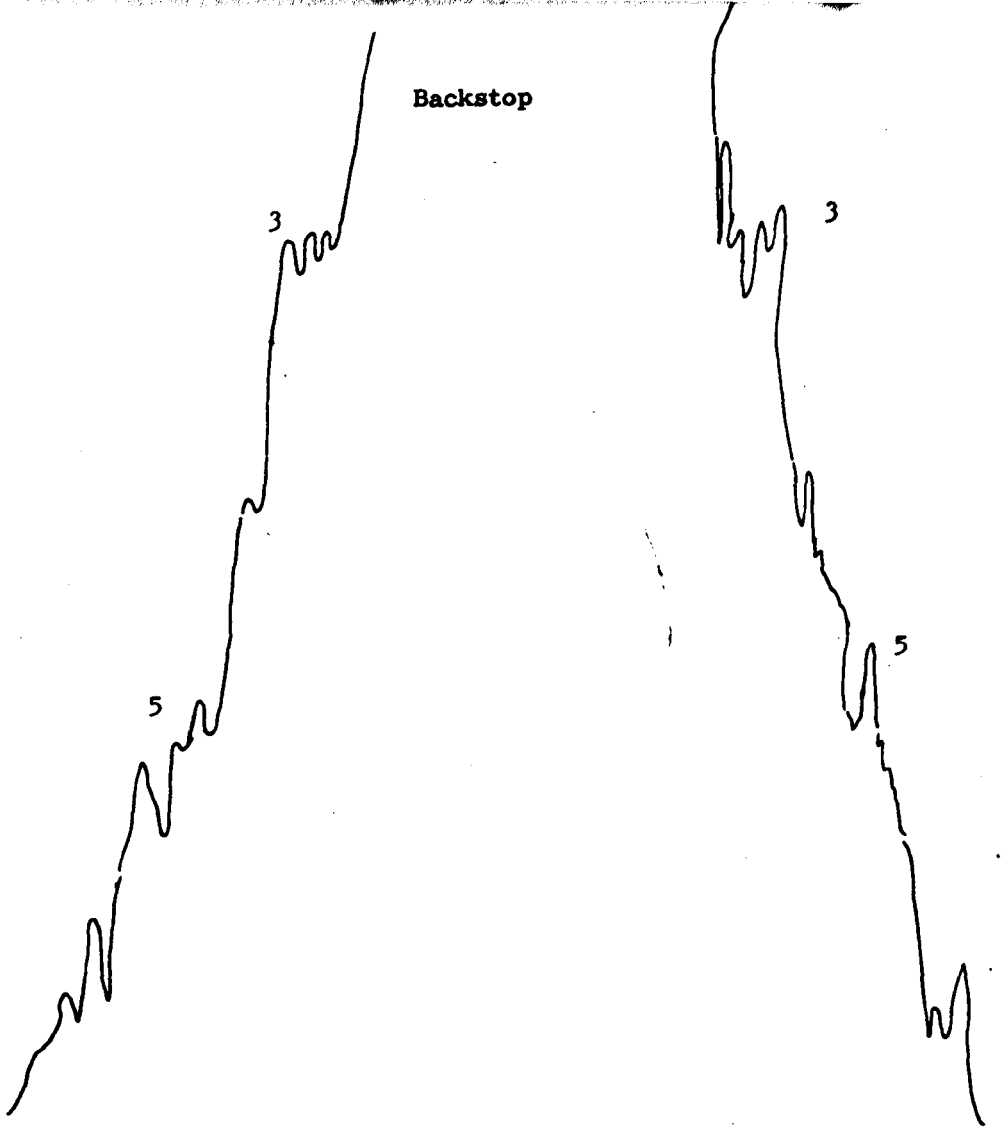

Fig.16. A microdensitometer trace of an x-ray diffraction pattern from fresh corneal stroma showing the position of the third and fifth orders of the collagen repeat.

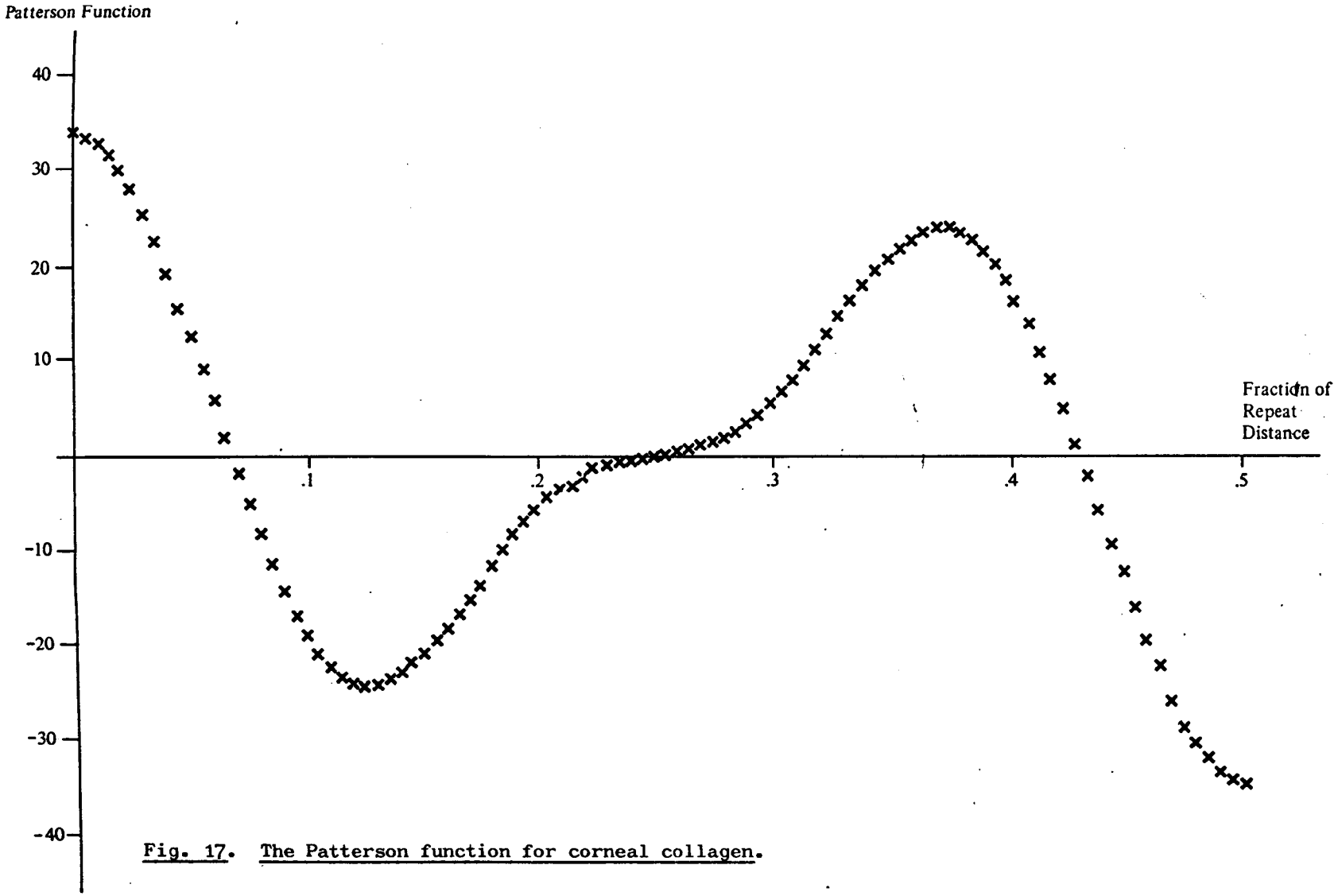

Fig. 17. The Patterson function for corneal collagen.

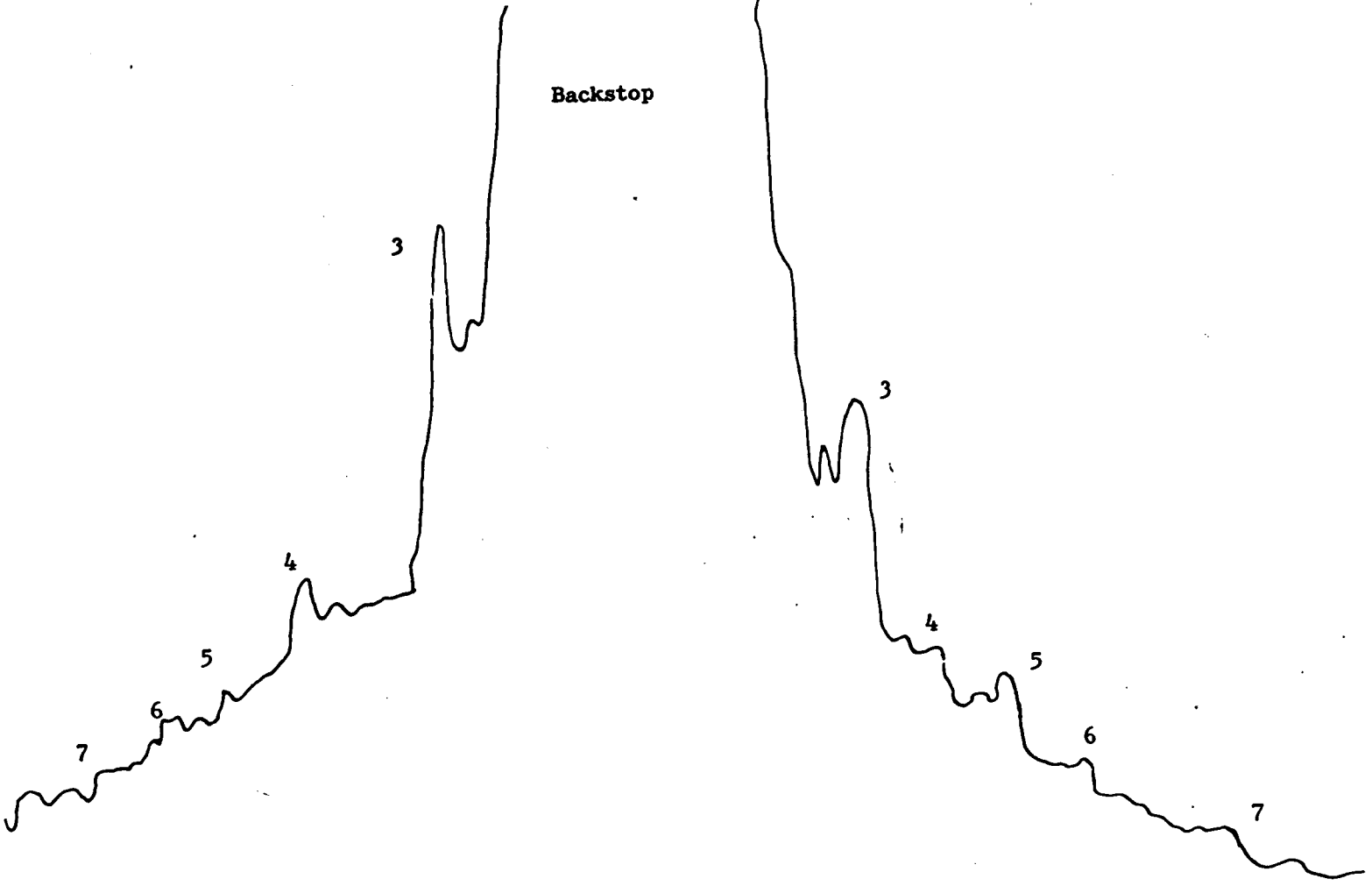

Fig.18. A microdensitometer trace of an x-ray diffraction pattern from fresh sclera showing the positions of the reflections corresponding to the 3rd, 4th etc. order of the collagen repeat. It can be seen that the first order is within the scatter from the backstop because of its size and also because of its high intensity relative to the other reflections.

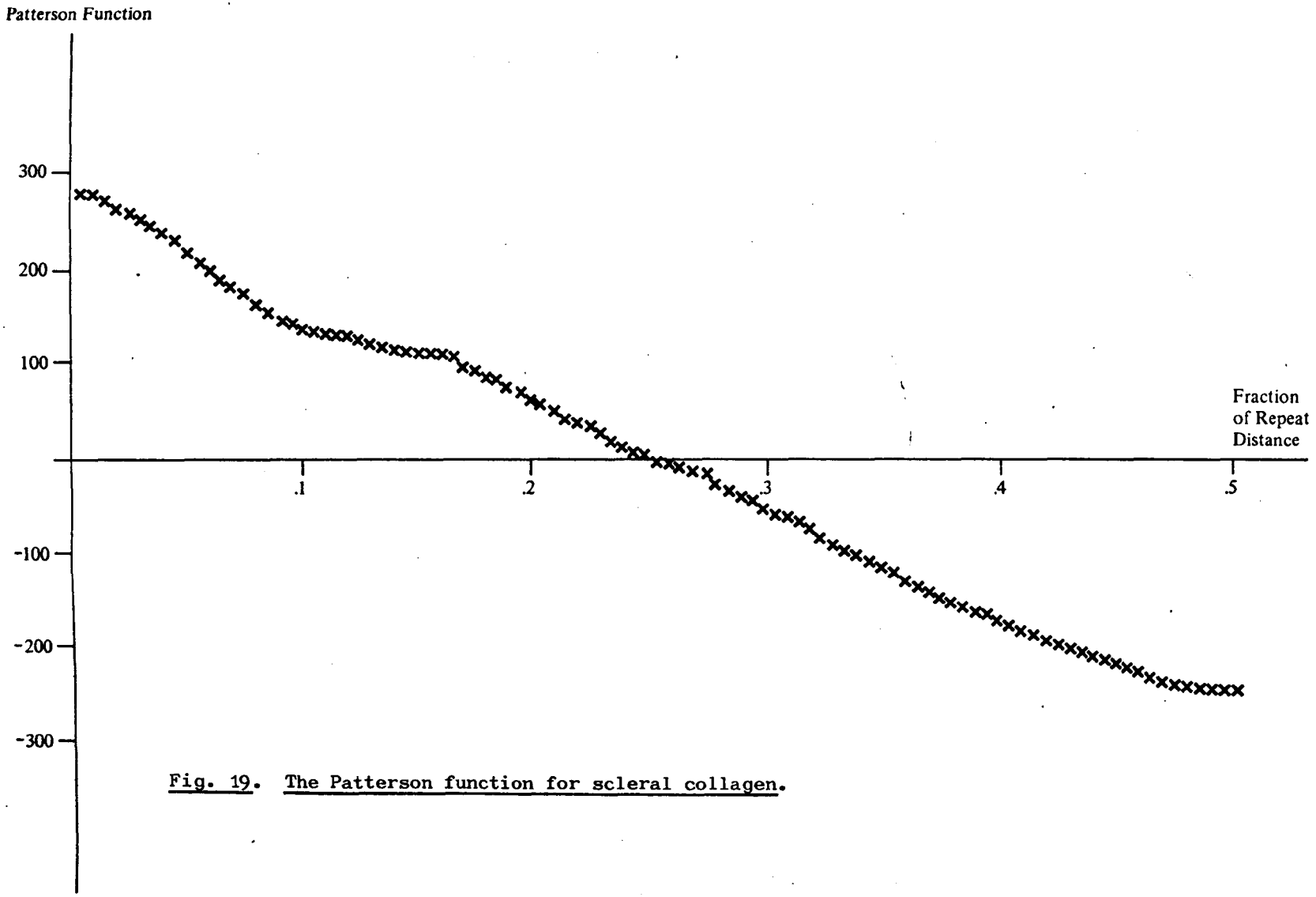

Fig. 19. The Patterson function for scleral collagen.

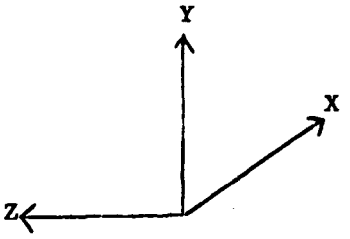

a) Part of one lamellae with fibrils in X-direction.

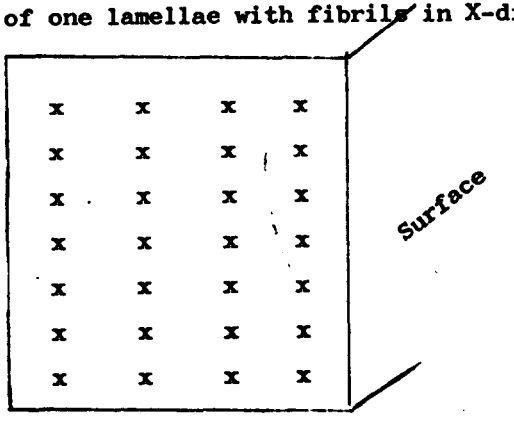

b) Part of one lamellae with fibrils in Y direction

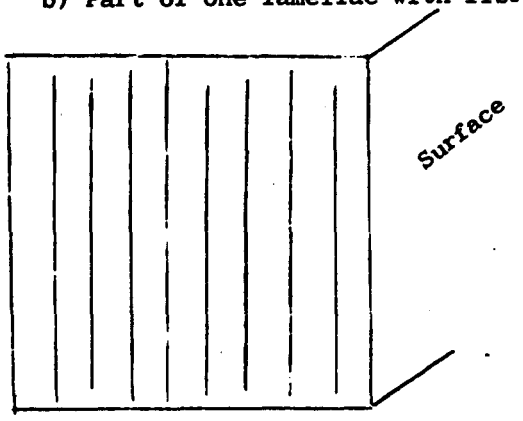

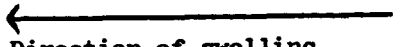

Fig. 20. Diagram of parts of two lamellae with the fibrils orientated in different di rections but perpendicular to the swelling direction. The surface of the cornea is in the X-Y plane. x indicates that the orientation of the axes of the fibrils is into the paper.

Fig. 21. An electron micrograph of corneal stroma showing collagen fibrils in cross-section.

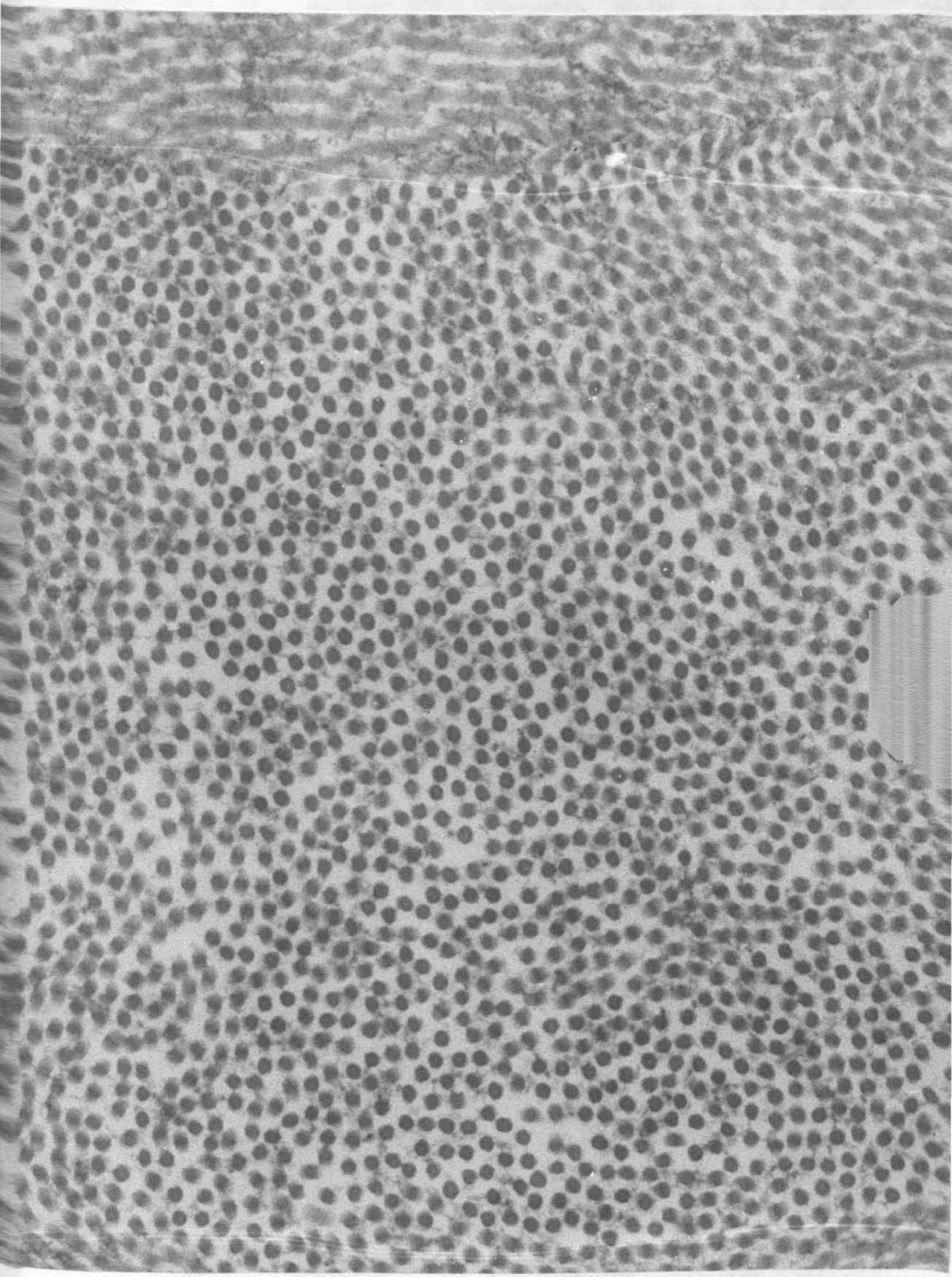

Fig. 22. A laser light diffraction pattern from an electron micrograph of corneal stroma with the fibrils in cross-section. Three diffraction rings can be seen due to the packing of the fibrils.

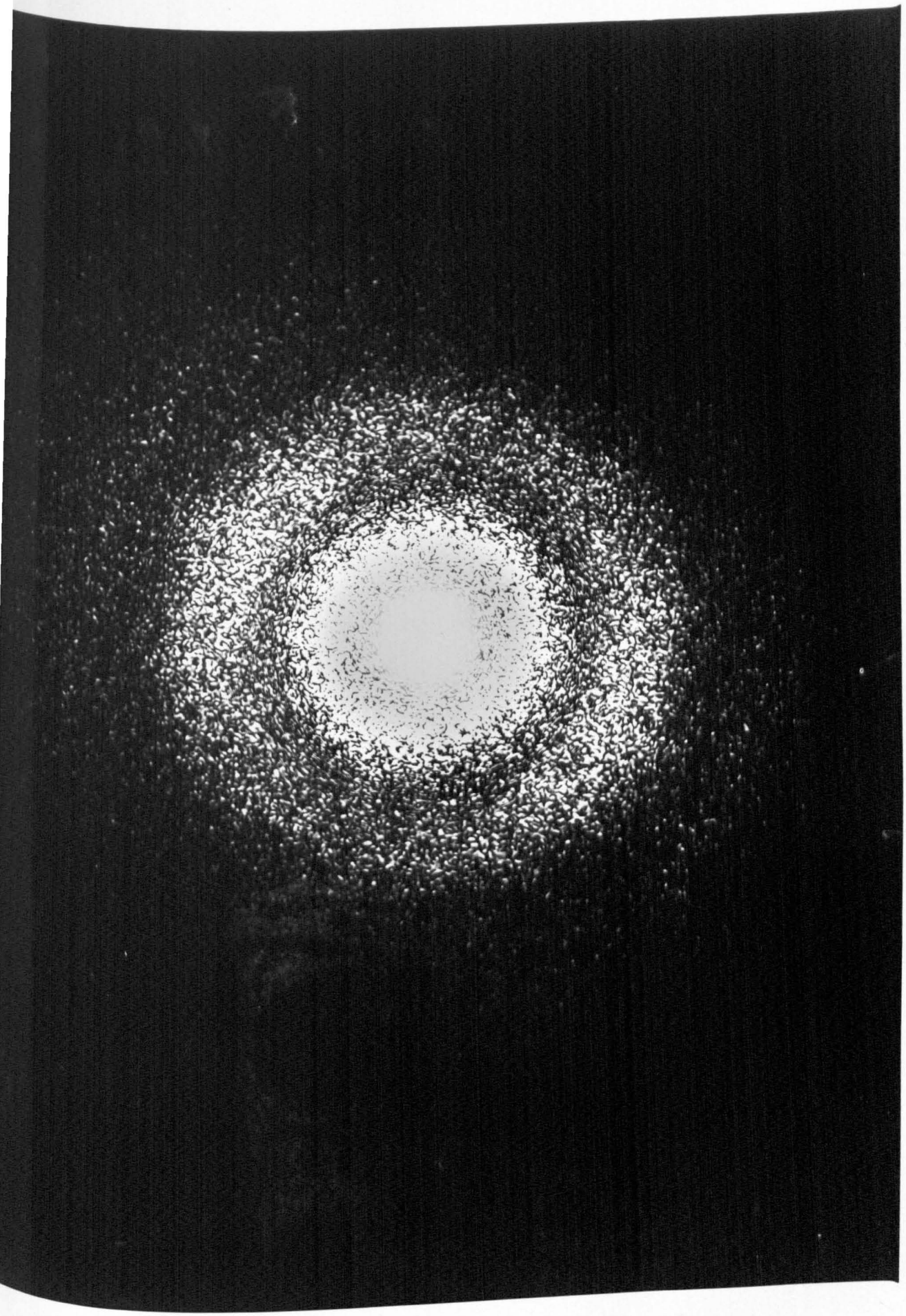

Fig. 23. An electron micrograph of swollen corneal stroma showing longitudinally orientated collagen fibrils with banding along the fibrils.

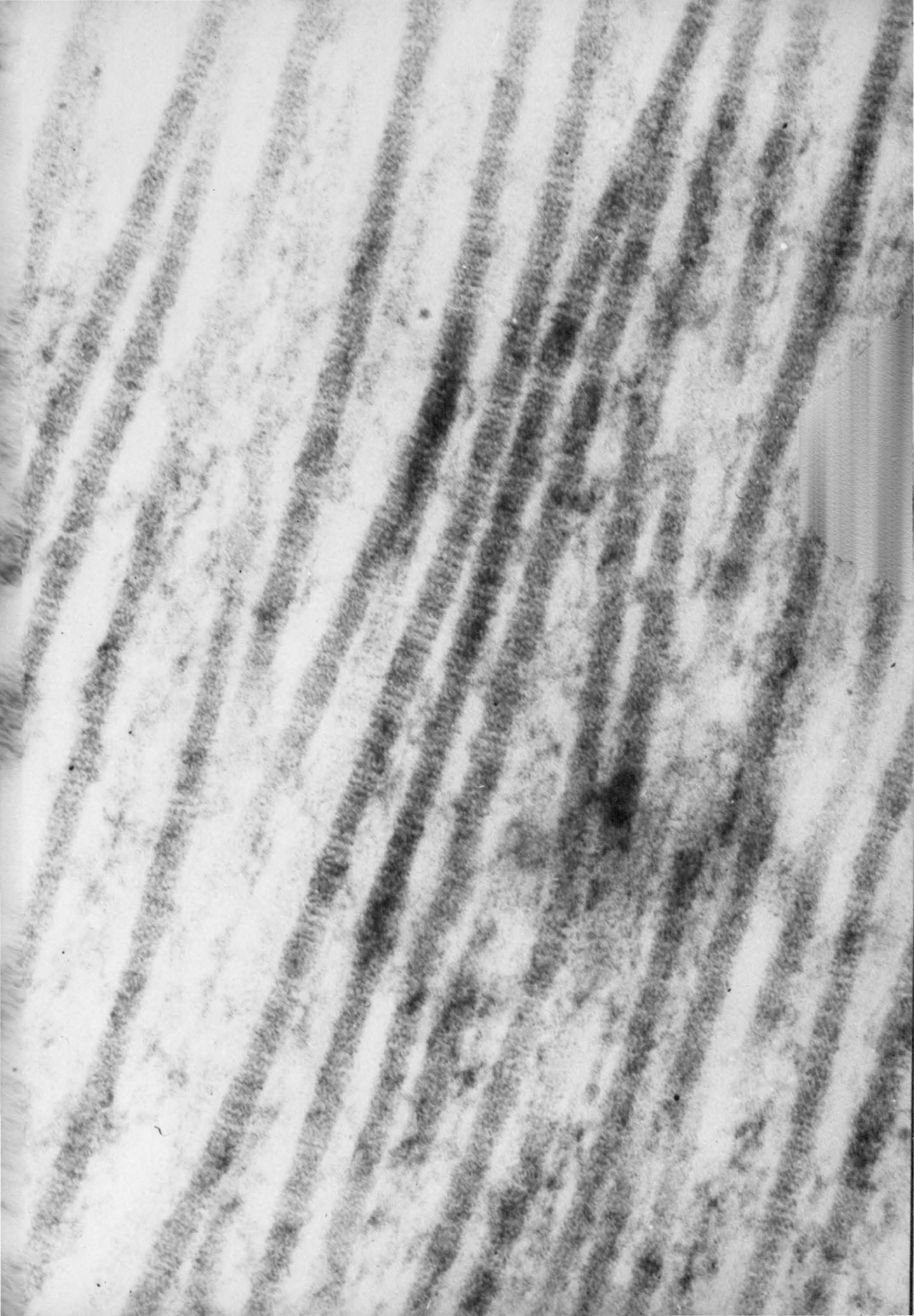

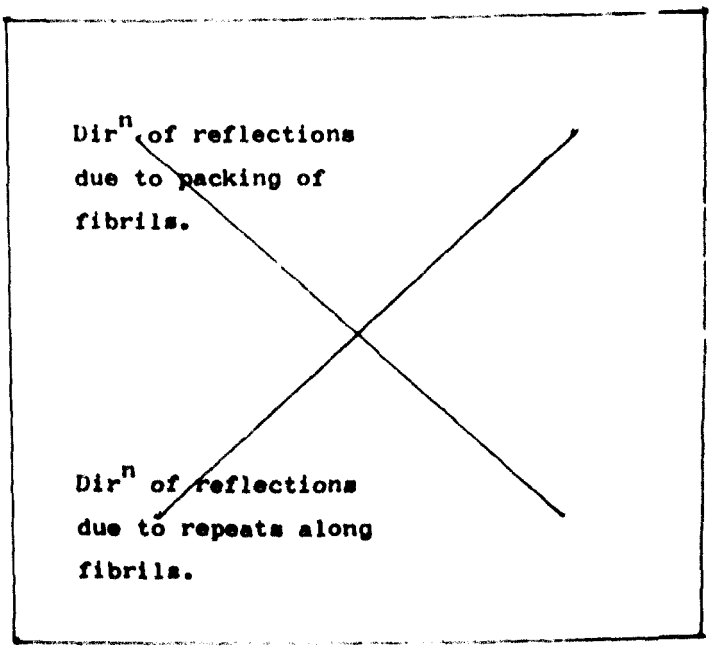

Fig. 24. A laser light diffraction pattern from an electron micrograph of swollen corneal stroma with the fibrils longitudinally orientated showing the diffraction rings due to the banding along the fibrils and the packing of the fibrils.

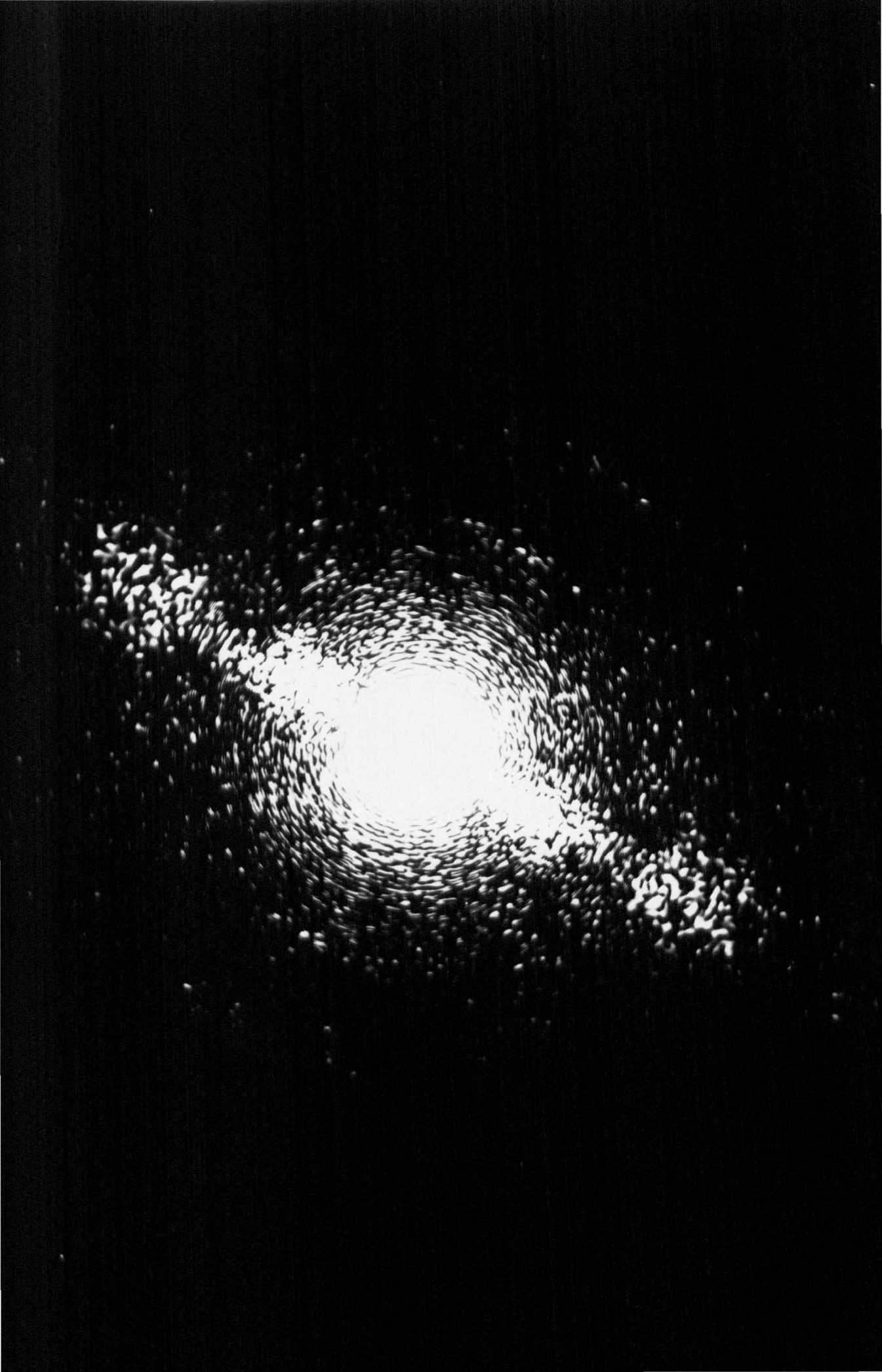

Chapter 4.

Microelectrode Studies on the Corneal Stroma.

I Introduction.

(i) The Origin of the Potential Difference Between the Corneal Stroma and the Bathing Solution.

The importance of the glycosaminoglycans in the swelling of the corneal stroma has been described in Chapter 2. All hypotheses for the origin of the swelling pressure take account of the Donnan (osmotic) pressure arising from the presence of the fixed charge on the glycosaminogycans (Chapter 2, Section I, v). These theories differ in the proportion of the swelling pressure which is due to the osmotic pressure. In order to calculate the osmotic pressure directly it is necessary to measure the fixed charge concentration in the stroma for a known external solution. This can be done by measuring the potential difference which arises between the stroma and the bathing solution due to the presence of the fixed charge concentration.

The fixed charge on the glycosaminoglycans is due to the presence of the carboxyl (COO^-) groups and sulphonic acid (HSO_3^-) groups on chondroitin-4-sulphate and keratan sulphate (Fig 4, Chapter 1). At pH 7, it is not expected that the collagen will carry a net charge because it is near to its point of minimum swelling (Pirie, 1947; Bowes and Kenten, 1950; Katchalsky, 1954). However, when the pH is changed from 7, it is possible that a net charge will appear on the collagen. This will affect the total charge concentration. It may be that the charge

on the collagen molecules is screened by the ground substance which is known to coat the fibrils (François et al, 1954; Garzino, 1955) or by the glycosaminoglycans which may attach to the collagen fibril (Hodson and Meenan, 1969; Myers et al, 1973). However, the possibility that the collagen is charged must be considered at pH values away from pH7.

Otori (1967) has estimated the fixed charge concentration, at normal hydration, to be 35.7 mequivl^{-1} from the data of Laurent and Anseth (1961). However, Hodson (1971) has obtained values of 47.4 $\pm$ 2.6 mequivl^{-1} using Donnan exclusion techniques described by Maroudas and Thomas (1970). This value is in agreement with Otori's data if the charge due to the carboxyl groups is not neglected as it was in Otori's calculation. Friedman and Green (1971,a) found that the magnitude of the free fixed charge concentration was only between 12-16 mequiv.l^{-1} because of sodium ion binding.

Microelectrode techniques are usually used to measure potential differences across membranes. Potts and Modrell (1957), Modrell and Potts (1959), Friedman and Kupfer (1960), Kikkawa (1964, 1966), Davis et al, (1970), Klyce (1972), Ehlers (1973) and Klyce (1973) measured a potential difference across the outer cellular membranes of the cornea. However, in this experiment the membranes were removed and it is the potential difference between the fluid in the stroma and the external solution which is to be measured when there is no membrane present. The existence of a membrane is normally assumed in the calculation of the Donnan equilibrium but, in fact, it is only necessary to have two distinct phases with fixed, impermeable, charged groups in one phase only (Overbeek, 1956).

Relatively few experiments have measured fixed charge on non-cellular tissue using microelectrodes. Glycerinated muscle (i.e. muscle which has been soaked in glycerol to make the membrane permeable to small ions) has been studied by this technique (Naylor and Merrillees, 1964; Weiss et al, 1967; Collins and Edwards, 1971; Pemrick and Edwards, 1974). The presence of a Donnan potential was indicated if (1) the sign of the potential difference can be changed by changing the pH to a value below the isoelectric point of the tissue. This implies that the potential difference will be zero or near zero at the isoelectric point. (2) The potential difference decreases with increase in the ionic strength of the bathing solution as the atmosphere of counter-ions (the Debye atmosphere) around the charged groups increases (Collins and Edwards, 1971).

A further correlation is possible for the corneal stroma as the fixed charge concentration from the microelectrode studies can be compared with that estimated in chapter 2. This correlation will be discussed in chapter 6 of this thesis.

Davis et al (1970) report that frog stroma was 22.6 $\pm$ 6 mV negative to a microelectrode in the aqueous humour when the electrode was filled with three molar potassium chloride but was zero when the electrode was filled with Ringer. They conclude that microelectrodes filled with 3M KCl give rise to an artefactual potential of -23mV. The reason for the zero potential difference when the electrodes were filled with Ringer is not known but might possibly be due to the input impedance of the amplifier not being large enough compared with the resistance of the microelectrode when filled with Ringer (this chapter, section III, (iv)). The resistance of the electrode depends on the solution with which it is

filled (Kennard, 1958). The value of the tip resistance is only given for electrodes filled with 3M KCl and is not given for electrodes filled with Ringer. The composition of the aqueous fluid is not given so that the fixed charge concentration cannot be calculated. The hydration of the cornea is not discussed even though $0.36cm^2$ of surface was exposed to solution and would be expected to swell. However, the value of -23mV is the same order of magnitude as the potential which gives rise to the fixed charge concentrations presented in figs. 3-14 of this chapter.

(ii) Use of Microelectrodes.

Many biological tissues give rise to potential differences between the inside of the tissue and the external medium, often a Ringer solution. This potential can be measured by inserting an electrode into the tissue. If the tissue is damaged, the potential recorded will not necessarily correspond to the true value i.e. that from undamaged tissue. When 60μm diameter electrodes were inserted into the giant nerve fibre of the squid (Curtis and Cole, 1942; Hodgkin and Huxley, 1952) they were inserted through a cut end for a distance of 2-3cm so that potential from undamaged tissue could be studied. Smaller electrodes can now be made which have a very fine tip, less than 1μm. Ling and Gerrard (1949) were the first to use such small electrodes successfully in order to record the potential from frog striated muscle. The tip diameters were the order of 0.5μm. Although metal electrodes are the simplest way of recording potential differences, difficulties arise if steady values rather than changes in value are required. Glass electrodes can be used as a bridge between a metal electrode and the tissue so that changes in tissue fluid do not result in changes in the potential between the metal electrode and the liquid junction.

The glass electrode has to be filled with potassium chloride solution in order to reduce its resistance and to make good electrical contact with the tissue fluid. Potassium ions are used because they have approximately the same mobility as the chloride ions. Sodium ions do not have the same mobility as chloride ions which tend to diffuse faster than the sodium ions causing a potential difference between solutions of different concentrations of the same ions. There is only a small potential difference ,0.4mV, between potassium chloride solutions with a concentration ratio of 1:10 (Kennard, 1958). The metal electrode is usually a silver wire coated electrolytically with chloride. It is then placed in the potassium chloride filled electrode so that a KCl/AgCl/Ag junction is formed. The silver wire is then connected to copper leads. Three molar KCl is used in preference to lower ionic strengths so that the resistance of the electrode is reduced as much as possible. However, potassium chloride can diffuse through the tip. Nastuk and Hodgkin (1950) have calculated that a 0.4μm outside diameter tip would allow the diffusion of 6×10^{-14} moles^{-1}.

Further experimental details of the microelectrode technique including the problems of the high resistance and the tip potential are given in section III of this chapter.

II Theory.

(i) The Calculation of the Donnan Potential.

A potential difference, the Donnan Potential, exists between two phases when the concentration of permeant ions is different in each

phase due to the presence of a fixed charge concentration in one of the phases. It is not necessary to have a membrane separating the phases but often the presence of this membrane is assumed. Overbeek (1956) states that "as a rule the restriction is caused by a membrane, permeable to the solvent and to small ions, but impermeable to ions of colloidal size, and therefore these equilibria are often called Donnan membrane equilibria. The presence of this membrane is, however, not essential".

The basic premise is that the electrochemical potentials, η, of all permeant components are equal in both phases. The superscript i is used to represent properties of the ions inside the stroma whereas o is used for ions outside the stroma i.e. in the bathing solution.

Hence, for all permeant ionic species

$$\eta^1 - \eta^o = p^i v^i - p^o v^o + RT \ln \frac{c^i}{c^o} + ZF(\psi^i - \psi^e) = 0 \quad \ldots\ldots\ldots (1)$$

where p is the pressure

v is the partial molar volume

ψ is the potential difference

F is the Faraday

R is the gas constant

T is the temperature

Z is the valency and

c is the concentration and $p^i v^i - p^o v^o$ is negligible.

The external solution consists mainly of sodium chloride at all but the lowest ionic strength (μ = .02). The ions of the buffer are assumed to be present in small concentrations. All the cations in the buffers

are monovalent and the concentration of these ions is added to the concentration of sodium ions from sodium chloride to give the total cation concentration. The monovalent anion concentration is assumed to be equal to the total monovalent cation concentration. The presence of small amounts of divalent anion is neglected (Table 1, chapter 2). At μ = .02, the concentrations of all the ionic species are considered separately.

For all ionic strengths other than μ = .02, the following derivation applies. To ensure electrical neutrality,

$$C_+^o = C_-^o \quad \ldots\ldots\ (2)$$

for the external solution and

$$C_+^i - C_-^i - C_F = 0 \quad \ldots\ldots\ (3)$$

for the stroma where C_F is the concentration of fixed charge. When the electrochemical potential of each ionic species is considered, we obtain the following equations:

$$RT \ln \frac{C_-^i}{C_+^o} + F\psi = 0 \quad \ldots\ldots\ (4)$$

$$RT \ln \frac{C_-^i}{C_-^o} - F\psi = 0 \quad \ldots\ldots\ (5)$$

By rearranging equations 4 and 5, we find that

$$C_+^i = C_+^o e^{-F\psi/RT} \quad \ldots\ldots\ (6a)$$

$$C_-^i = C_-^o e^{+F\cdot\psi/RT} \quad \ldots\ldots\ (6b)$$

Substituting these expressions for C_+^i and C_-^i into equation 3,

$$C_F = 2 C_+^o \sinh (F\psi/RT) \quad \ldots\ldots\ (7)$$

This equation for the fixed charge concentration is used to evaluate

C_F from each potential measurement, ψ , for each solution. At μ=.02, it is necessary to take account of the monovalent anion, dihydrogen phosphate and the divalent anion, hydrogen phosphate. If the external concentration of $H_2PO_4^-$ is denoted by C^o_{-1} and HPO_4^{--} by C^o_{-2} then

$$C^o_+ - C^o_- - C^o_{-1} - 2C^o_{-2} = 0 \quad \ldots\ldots\ (8)$$

$$C_F = C^i_+ - C^i_- - C^i_{-1} - 2C^i_{-2} \quad \ldots\ldots\ (9)$$

By equating the electrochemical potentials of each ionic species, we find that

$$\begin{aligned} C^i_+ &= C^o_+ e^{-F\psi/RT} \\ C^i_- &= C^o_- e^{+F\psi/RT} \\ C^i_{-1} &= C^o_{-1} e^{+F\psi/RT} \\ C^i_{-2} &= C^o_{-2} e^{+2F\psi/RT} \end{aligned} \quad \ldots\ldots\ (10)$$

By substitution of equations 10 into equation 9,

$$C_F = C^o_+ e^{-F\psi/RT} - C^o_- e^{+F\psi/RT} - C^o_{-1} e^{F\psi/RT} - 2C^o_{-2} e^{2F\psi/RT} \quad \ldots\ldots\ (11)$$

This equation has to be used in full at low ionic strength in the presence of phosphate buffer. A similar equation can be written for solutions at pH10 with carbonate/hydroxide buffer when all the ions are univalent.

The fixed charge concentration varies with hydration such that

$$C_F \times H = C \quad \ldots\ldots\ (12)$$

where C is a constant (Hodson, 1971).

(ii) <u>The Calculation of the Osmotic Pressure.</u>

The osmotic pressure, P, can be calculated from the value of

C_f according to the formula

$$P = RT((C_f^2 + 4C_+^2)^{\frac{1}{2}} - 2C_+)$$

where C_+ is the external sodium ion concentration. This can be reduced to

$$P = RTC_f^2/4C_+ \qquad \text{(chapter 2, section II)}$$

when $C_f < 2C_+$. Using equation (12) (from the last section)

$$P = RTC^2/4C_+H^2$$

where the average value of C can be used. At low ionic strength, the concentration of the $H_2PO_3^-$ and HPO_3^{--} buffer ions are significant so the osmotic pressure has to be calculated by substitution of equations 10 (last section) into the full expression for P i.e.

$$P = RT(C_+^i + C_-^i + C_{-1}^i + C_{-2}^i - C_+^o - C_-^o - C_{-1}^o - C_{-2}^o).$$

Thus the osmotic pressure, at low ionic strengths, can be written in terms of the potential difference, ψ, and the external ions concentrations all of which are known. The value of P at physiolical hydration is shown in Table 3.

III Methods.

(i) Production of Glass Electrodes.

Microelectrodes were made from borosilicate glass tubing with an external diameter of 1-1.25mm. The tubing was cleaned in acetone and then cut into lengths about .08m long. These lengths were placed and clamped in an electrode puller (Fig. 1a). The puller consisted of a platinum heating coil through which the tubes were centrally placed. On heating, the glass melted and was pulled to a narrow tip by a constant force applied to one end of the tubing. By alteration of the magnitude of the force and the temperature of the heating coil, microelectrodes of the required tip diameter and taper could be produced. Glass wool was inserted into the tubing before the electrode was made. This ensures that when the electrodes are

filled with potassium chloride solution, the solution penetrates to the tip by capillarity (Tasaki and Singer, 1968). This is an easier method for filling a small number of electrodes than those described by Kennard (1958). Three molar potassium chloride was carefully inserted into the glass electrode with a syringe so that no air bubbles were trapped.

(ii) Chloriding of the Silver Wire.

A silver wire about .03m long was placed in an electrolytic bath of 0.1M hydrochloric acid. A current of around 4μA was applied for approximately fifteen minutes in order that a layer of chloride ions deposited on the surface of the wire. The wire should look 'plum' in colour after chloride has been deposited. A clean surface is required if the layer is to remain for any length of time. The cleaning procedure involved washing in acetone to remove grease, 30% nitric acid and, finally, distilled water.

(iii) The Circuit for Potential Measurements.

The microelectrode, made by inserting the silver/silver chloride wire in the potassium chloride filled glass electrode, is placed in a micromanipulator (made by W. R. Prior). This allows small mensurable movement of the electrode to be controlled in three perpendicular directions. The microelectrode was connected via a gold male/female junction to copper leads which connect it with the rest of the circuit.

A variable resistance box is added to the circuit in order to measure the resistance of the microelectrode. The signal from the electrode passes through the resistance box to a preamplifier and thence to a cathode ray oscilloscope. The preamplifier increases the potential difference by a factor of ten. This voltage is then displayed on a calibrated screen. The reference electrode, a calomel electrode containing saturated potassium chloride solution, is earthed. The whole circuit (except for the cathode ray oscilloscope) is contained in a Faraday cage to avoid spurious potentials from stray electromagnetic fields. The cage is earthed. The resistance box, preamplifier casing, the cathode ray oscilloscope and micromanipulator must be either connected to the Faraday cage, or earthed separately. Figs. 1b and 1c show photographs of the apparatus.

(iv) Resistance of the Microelectrode.

The high resistance of the glass microelectrode is lowered by using three molar potassium chloride instead of Ringer solution. Nastuk and Hodgkin (1950) found that the resistance of the electrodes filled with isotonic potassium chloride was 5-7 times greater than those filled with three molar potassium chloride. Even when this concentrated solution of potassium chloride is used, the electrodes have a resistance between 5 MΩ and 100 MΩ. The input resistance of the preamplifier has to be many times larger than that of the microelectrode in order that the true potential is recorded. The input resistance of the preamplifier is large because of the presence of an operational amplifier (Brophy, 1966).

(v) Tip Potential.

The tip of the glass microelectrode is the source of a potential difference (Nastuk, 1953; del Castillo and Katz, 1955; Adrian, 1956) which is often larger than the expected diffusion potential, between 3M KCl and .1 M KCl, of 0.6 mV (Schanne et al, 1968). This potential difference is known as the tip potential and is a complicated function of the tip diameter, ionic strength, pH and nature of the ions of the internal and external solutions. (Adrian, 1956; Lavallée, 1964; Fatt, 1961). On breaking the tip of the electrode, the tip potential becomes equal to the diffusion potential expected between the internal and external solutions (Schanne et al, 1968).

The tip potential is due to a layer of negative charge, on the internal surface of the electrode, from the dissociation of the silicic groups (Schanne et al, 1968). The charge can be reduced by the use of borosilicate glass i.e. glass containing B_2O_3. When the electrode is filled with potassium chloride solution, the positive potassium ions form an electrical double layer with the negative ions on the glass surface. The chloride ions, in the potassium chloride solution, are then more mobile than the potassium ions attracted to the glass surface. A further reduction in the charge can be obtained by decreasing the pH of the solution filling the electrode. However, if the internal solution diffuses into the tissue, more changes will occur in the tissue if the internal solution is at low pH than at physiological pH.

The tip potential becomes nearly constant as the ionic strength is increased. For this reason, the electrodes are used if the potential

difference between them and the solution is the same in 10mM as in 100mM sodium chloride solution. This ensures that the tip potential is constant in value when the microelectrode is placed in the external solution and then placed in the stroma. Zeroing of the potential when the electrode is in the bathing solution takes account of this non-zero but constant tip potential.

(IV) Results

(i) The Fixed Charge Concentration as a Function of Hydration.

The fixed charge concentration was calculated according to equation 7, derived in the theory section of this chapter, except at low ionic strengths when equation 11 had to be used in order to take account of the significant concentration of divalent ions in the buffer. In order to test the reliability of the data, the fixed charge concentration was plotted against the reciprocal of the hydration of the tissue. It is expected that this will produce a linear plot, if the total fixed charge is remaining constant during the experiment. The data for several solutions is presented in Figs. 2 - 14.

In all cases , the fixed charge concentration increased as the reciprocal of the hydration increased leading to linear fits. The solid lines on Figs 2 - 14 represent the best fit through the data obtained by calculating the mean of the product $C_f \times H$. If the mean is represented by $\overline{C_f \times H}$, then the equation for the straight line is

$$C_f = \overline{C_f \times H} \times H^{-1}$$

The error bars, in Figs. 2 -14 represent the error in the fixed charge concentration assuming that it is equal to the percentage error in $\bar{C}_f \bar{x} \bar{H}$, the error in the hydration being negligible. The average values of the product C_f x H and the standard error are given in Table 1 for all solutions. The fixed charge concentrations plotted in these figures are taken from the average of between five to eight potential readings. The percentage error in the potential measurements was found to range from 8% to 20% due to the spread in readings at a given hydration.

(ii) The Fixed Charge Concentration as a Function of pH

The fixed charge concentration is seen to vary with the pH of the bathing solution. At high values of pH i.e. pH 6,7, 8 and 10 an increase in alkilinity of the bathing solution increases the average value of the product C_f x H. This increase in fixed charge concentration with pH occurs at both ionic strength .15 and .02 except at pH 6 and 7 when the values of $\bar{C}_f \bar{x} \bar{H}$ for these solutions are equal. (Table 1). However, the standard error of these products are large. At low ionic strength, .02, the value of $\bar{C}_f \bar{x} \bar{H}$, at pH 6, was less than at pH 10, within the error. Likewise, $\bar{C}_f \bar{x} \bar{H}$ at pH 7 was significantly less than at pH 10 although that at pH 8 was not significantly different from either that at pH 7 nor at pH 10. (Table 1.). At μ = .15, the value of $\bar{C}_f \bar{x} \bar{H}$ was the same at all pH values within the error although the mean value increased with pH.

Decreasing the pH to 4 reduces the potential difference which is measured. The values of the potential difference varied between 4 mv positive and negative. It was not possible to plot a fixed charge concentration as a function of hydration because the

potential readings were so small and variable. It is found that the stroma becomes very tough at pH 4 so that the tips of the microelectrodes often break when penetrating the surface.

A further decrease in the pH to pH 2 produces potential differences which are positive relative to earth. The potential readings at high pH are all negative. The tissue could swell sufficiently at pH 2 to allow the measurement of the fixed charge concentration as a function of the hydration of the stroma. This is shown in Figures 13 and 14. Two ionic strengths were used at this low pH. Again it is found, subjectively, that the tissue was tougher at pH 2 than when allowed to swell at pH 6 but it was not as tough as at pH 4.

(iii) The Fixed Charge Concentration as a function of Ionic Strength.

The dependence of the fixed charge concentration on the ionic strength of the bathing solution is more complex than the dependence on pH. At pH 2, the readings at $\mu = .06$ and $\mu = .15$ are just equal within the experimental error although the average value of the fixed charge concentration occurs at the lowest ionic strength i.e. $\bar{C}_f^{---}\bar{x}\bar{H}$ at $\mu = .06$ may be greater than that at $\mu = .15$ (Table 1).

Four values of the ionic strength are used at pH 7. The lowest value of $\bar{C}_f^{---}\bar{x}\bar{H}$ is found at $\mu = .02$. Increasing the ionic strength to $\mu = .05$ and thence to $\mu = .15$ increases the fixed charge concentration for a given hydration. A further increase in the ionic strength to $\mu = .25$ results in a decrease in the fixed charge

concentration. Two ionic strengths are used at pH 6, 8 and 10. These readings are consistent with the dependence on ionic strength found at pH 7 in that the value of $\bar{C}_f\bar{x}\bar{H}$ was higher at $\mu = .15$ than at $\mu = .02$.

(iv) The Dependence of the Potential on Ionic Strength.

As the dependence of the fixed charge concentration on ionic strength was complex, it was decided to look at the dependence of the potential difference on this parameter. From equation 7,

$$C_f = 2C_+ \sinh(\psi F/RT).$$

By multiplying each side by H, averaging and dividing by the constant C_+, we find that

$$(\bar{C}_f\bar{x}\bar{H})/C_+ = \bar{2}\bar{H}\bar{\sinh}(\bar{\psi}\bar{F}/\bar{R}\bar{T}).$$

At H = 3.5,

$$\psi = (RT/F)\sinh^{-1}(C_f xH)7/C_+$$

Thus ψ can be found from the average value of $C_f xH$, for a given hydration and a given solution. At low ionic strength, equation 11 apllies so that

$$C_f = C_+e^{-.04\psi} - C_-e^{+.04\psi} - C_{-1}e^{+.04\psi} - 2C_{-2}e^{+.08\psi}$$

Multiplying each side by H and averaging, we find that

$$\overline{(C_f xH)}/3.5 = C_+e^{-.04\psi} - C_-e^{+.04\psi} - C_{-1}e^{+.04\psi} - C_{-2}e^{+.08\psi}$$

at physiological hydration, from which the value of ψ can be found numerically.

The values of the potential difference, calculated in this manner from the average value of the fixed charge, are shown in Table 2, for each solution. By considering the results from the solutions buf-

fered at pH 7, it is seen that thepotential difference decreases as the ionic strength is increased from -27.5 mv at μ = .02 to -5.8 mv at μ = .25. At pH 2, thepotential at μ = .06 is +17.5mv compared with +5mv at μ = .15. The values of the potential difference in solutions buffered at pH 6,8 and 10 are all highest at μ = .02, being 25.5, 37 and 37.5 mv respectively, compared with 11, 12 and 13 mv at μ = .15.

(v) Calculation of the Osmotic Pressure

The Donnan, osmotic, pressure,P, can be calculated from the measurements of the fixed charge concentration. Using the full expression for the osmotic pressure i.e. $P = RT((C_f^2 + 4C_+^2)^{\frac{1}{2}} - 2C_+)$, the pressure P is calculated for each solution at a given hydration (H = 3.5). The values thus calculated are given in Table 3. It is seen that the osmotic pressure, at a given ionic strength, increases as the pH of the solution is increased e.g at μ = .02, the osmotic pressure at pH 6 is 53x 10^3 Nm^{-2} while at pH 10 the pressure has more than doubled to 131 x 10^3 Nm^{-2}. Likewise at μ = .15, the osmotic pressure at pH 7 is 70 x 10^3 Nm^{-2} and at pH 10 it is 88 x 10^3 Nm^{-2}. The pressure is not significantly different at pH 6 and at pH 7 at ionic strength, μ, =.15 but it increases when the pH is altered to pH 8 so that this value lies between that at pH 7and that at pH 10.

The dependence of the osmotic pressure on the ionic strength can be seen by comparing the values of osmotic pressure when the bathing solution is buffered at pH 7. At μ = .02, the osmotic pressure is 59 x 10^3 Nm^{-2}. Increasing the ionic strength to μ = .05 decreases the osmotic pressure to 42.3 x 10^3 Nm^{-2} while a further increase in ionic strength to μ = .15 results in a

large increase in the pressure to 70 x 10^3 Nm^{-2}. Finally, the highest ionic strength used, μ = .25, gives the lowest osmotic pressure, 31.2 x 10^3 Nm^{-2}. At pH 8 and pH 10, the osmotic pressure at μ = .02 is larger than at μ = .15 but at pH 6, the opposite relation is found. i.e. the pressure at μ = .15 is higher than at μ = .02. At the lowest pH, 2, the osmotic pressure is larger at μ = .06 than at μ = .15 by a factor of five.

The error in the values of the osmotic pressure can be estimated from the function

$$P = RTC_f^2/4C_+$$

from which it can be seen that the percentage error in P will be twice the percentage error in C_f assuming the error in C_+ is negligible. When P cannot be calculated from this formula then the fractional error in P is equalto $C_f \Delta C_f/(C_f^2 + 4C_+^2)^{\frac{1}{2}}((C_f^2 + 4C_+^2)^{\frac{1}{2}} - 2C_+)$ assuming the fractional error in C_+ to be negligible.

(vi) Potential Measurements from Fresh Tissue.

Thirty four readings were taken with three pieces of fresh corneal stroma (i.e. H = 3.5) in a bathing solution buffered at pH7 and with an ionic strength of .15. The potential was found to be 10.9 $\pm$ 4.2 mv (mean $\pm$ standard error) leading to a fixed charge concentration of 133 $\pm$ 50 $mequivl^{-1}$.

(V) DISCUSSION

(i) The Donnan Potential.

The potential difference, measured by microelectrodes,

between the corneal stroma and the bathing solution has been assumed to arise from a Donnan distribution of ions between these two phases and it has been used to calculate the fixed charge concentration in the stroma due to the presence of polyelectrolytes. This potential cannot arise from the cellular layers because the preparation of the tissue involves both the scraping of the surface, with a scalpel, and dehydration of the tissue. These processes will remove or kill the cells.

The microelectrodes were carefully selected so that spurious potentials e.g. tip potentials should not occur. The tip of the electrodes are small, the order of 0.5μm, to avoid damaging the tissue and thus giving rise to an incorrect reading. Their resistance was chosen to be between 5 and 80 MΩ so that the tips of the electrodes are neither broken nor blocked. (Adrian, 1956; Schanne et al, 1968). The tip potential of each electrode is measured in 10 mM and 100 mM sodium chloride. If the potential is the same at both concentrations the tip potential should be the same in the stroma as in the bathing solution. (Schanne et al, 1968).

Thus it is concluded that the potential difference, measured using microelectrodes, is most likely due to the distribution of ions in the stroma relative to the bathing solution and not due to the cellular layers nor to tip potentials.

(ii) Dependence of the Fixed Charge Concentration on the Hydration.

The potential difference was used to calculate the fixed

charge concentration in the stroma using equations derived in section II from Overbeek (1956). The concentration of the internal ions can be expressed as exponentials depending on the valency of each ion and the potential difference between the stroma and the bathing solution. The fixed charge concentration is equal to the difference between cation and anion concentrations in the stroma.

It is expected that the total fixed charge should remain constant on swelling so that the product of the fixed charge concentration and the hydration is a constant (Hodson, 1971). Thus, for each bathing solution, the fixed charge concentration should be linearly related to the reciprocal of the hydration. If corneal glycosaminoglycans were eluted from the tissue during the swelling process then some of the total fixed charge might be lost. Thus the fixed charge concentrations would be smaller than expected. The possibility of elution of the glycosaminoglycans was discussed in Chapter 2, section V, x where it was thought that it was unlikely that glycosaminoglycans were lost under ou experimental conditions though it was possible.

From the results presented in Figs. 3 - 14 of this chapter, it appears likely that there is a linear relation between the fixed charge concentration and the reciprocal of the hydration and thus the fixed charge appears to remain constant.

(iii) The Dependence of the Fixed Charge Concentration on pH

The variation of the fixed charge concentration as a function of pH is consistent with that expected from a polyelectrolyte system.

Increasing the pH above pH7 will increase the concentration of the fixed charge in the stroma as more acidic groups and less basic groups become ionised along the glycosaminoglycan molecules. It is also possible that the collagen molecules may acquire a net negative charge at pH values above pH7 (Bowes and Kenten, 1950; Katchalsky, 1954). Decreasing the pH of the bathing solution, below pH7, would decrease the net fixed charge concentration of the glycosaminoglycans. However, below pH7, the collagen molecule may acquire a net positive charge. This would also reduce the net value of the total fixed charge concentration. After decreasing the pH to low enough values the charge should become zero and then, with a further decrease, become positive as the isoelectric point of the stroma is passed (Katchalsky, 1954). This type of behaviour is seen with the corneal stroma. Potential measurements at pH 2 (Figs 13 and 14) are positive indicating that the net fixed charge is also positive. Readings at pH 4 were found to vary a few millivolts either side of zero. This dependence is consistent with the theory of polyelectrolyte gels (Katchalsky, 1954) discussed in Chapter 2, section V.

(iv) Dependence of the Potential on Ionic Strength.

The dependence of the fixed charge concentration on the ionic strength of the bathing solution cannot easily be seen. For this reason, the potential, ψ, at physiological hydration was calculated using the average value of the product $C_f xH$ for each solution. From this calculation it was seen that increasing the ionic strength decreased the potential difference at all pH values.

One reason for this decrease in potential, ψ, with increasing ionic strength is given, in detail, by Brenner and McQuarrie (1973). Their argument is as follows. The ionic strength of the bathing medium affects the density of the counterions which screen the fixed charge groups. The effectiveness of this screening is given by the Debye length which is a measure of how quickly the potential decreases as one moves away from the surface of the charged molecules and is inversely related to the square root of the ionic strength. Thus, at low ionic strength, there is a small density of ions in solution so that a thick layer of these counterions must be built up in order to balance the fixed charge. Because the counterion atmospheres are diffuse they do not balance the surface charge completely leading to a net negative charge and hence a net surface potential so that there is a non-zero average electrostatic potential. A thick atomosphere has a smaller balancing effect than a thin atmosphere because the charge of the thick atmosphere is, on average, farther from the surface of the polyelectrolytes i.e. the potential does not decrease so rapidly as one moves away from the fixed charge with a thick atmosphere compared with a thin atmosphere. There is also another effect which increases the degree of dissociation which increases with increasing ionic strength and hence increases the surface potential. This effect is counteracted by the large decrease in surface potential as the Debye length decreases (Brenner and McQuarrie, 1973).

(v) Comparison with Glycerinated Striated Muscle.

Glycerinated striated muscle is another system without membranes from which Donnan potentials have been measured using microelectrodes. A small negative potential difference is found between glycerinated striated muscle and the bathing solution (Collins and Edwards, 1971). The magnitude of the potential increases if the ion concentration is lowered. The potential difference becomes positive when the pH is lowered but the size of the potential still increases as the ionic strength is decreases at this low pH. Collins and Edwards (1971) calculate that the fixed charge density at pH 7.5 was about 40 mequiv. l^{-1}. From this behaviour, they conclude that a Donnan equilibrium is likely to be present in striated muscle due to the fixed charge on the contractile protèins.

It is seen that the behaviour of the fixed charge concentration from contractile proteins in muscle is similar to that of the polyelectrolytes in the stroma. The fixed charge concentration increases with increasing pH of the bathing solution and changes sign when the pH is lowered through the point of minimum swelling of the tissue. The potential is reduced by increasing the ionic strength.

Brenner and McQuarrie (1973) have proposed a general theory applicable to cylindrical polyions in which the response of the potential, due to the fixed charge groups on the polyion, to the ionic strength and pH is discussed and compared with experiemental observations. It is concluded that the corneal stroma may well belong to such a system because of the behaviour of the fixed charge groups in response to changes in the external solution.

(vi) Comparison with other Experimental Techniques for measuring the Fixed Charge Concentration.

The fixed charge concentration of the corneal stroma has been measured by other techniques and also extimated from the calculation of the glycosaminoglycan content of the stroma.

Calculations by Otori (1967) indicated that 36 mequivl^{-1} of charge , at physiological hydration, were available from the known glycosaminoglycan content. Keratan sulphate provides one charge per disaccharide unit while chondroitin sulphate provides two charges per disaccharide unit (Chapter 1, Fig. 4). Hodson (1971) found that, if both the charged groups from the chondroitin sulphate were used in the calculation, then 48 mequivl^{-1} of charge existed at H = 3.5. This means that the average value of $C_f xH$ will be approximately 168 mequivl^{-1}. However, values higher than this were found using microelectrodes to measure the potential (Table 1).

Freidman and Green (1971a) found that the total concentration of negative charge was about 70 mequivl^{-1} at normal hydration in .9% NaCl. However, they supposed that sodium ions were bound by this negative charge and calculated that the free charge density of rabbit stroma was 12 - 16 mequivl^{-1} on this basis. Unfortunately, Friedman and Green make no mention of the pH of the bathing solution. It has been seen in section IV of this chapter that this parameter can alter the magnitude and sign of the fixed charge concentraion.

Hodson (1971), using ion exclusion techniques of Maroudas and Thomas (1970), reports a concentration of 47.4 ± 2.6 mequivl^{-1} for the fixed charge concentration in the corneal stroma. This value appears to be consistent with the fixed charge concentration found at low ionic strength, $\mu = .02$, using microelectrodes which is 47 ± 6 mequivl^{-1} at pH 7.

The value of the fixed charge concentration found by microelectrode techniques at ionic strengths above $\mu = .02$ appears to be higher than that reported by other authors. Friedman and Green's (1971) results of 70 mequivl^{-1} of total negative charge is the nearest in value to those reported in this chapter. However, the value of the fixed charge concentration at $\mu = .15$ (Table 2) is approximately twice Friedman and Green's value.

Several effects may increase the theoretical value of the fixed charge concentration above that obtained from consideration of one sulphate group disaccharide unit on keratan sulphate and one carboxyl and one sulphate group on chondroitin sulphate. At pH values above 7, it may be necessary to take account of the fixed charge on the collagen molecules and this would be expected to be negative and so increase the net negative charge in the stroma. However, at values of pH below 7, the collagen molecules would be expected to be positively charged and therefore the net negative charge would be lowered compared with that of the glycosaminoglycans alone (Katchalsky, 1954). The calculation of 48 mequivl^{-1} (Hodson, 1971) does not appear to take account of the extra sulphate

reported to be attached to the keratan sulphate molecules by Bhavandan and Meyer (1966, 1967). This extra sulphate would be expected to increase the net negative charge in the corneal stroma.

(vii) Effect of Activity Coefficients.

A more rigorous derivation of the fixed charge concentration in terms of the external cation and anion concentrations would involve the use of activities instead of concentrations. By re-arrangement of equation 3, section III, it can be shown that

$$C_f = C_+^i - C_-^i$$

In equations 4 and 5 the concentrations should be replaced by the activities so that

$$RT \ln (C_+^i a_+^i / C_+^o a_+^o) + F \psi = 0$$

and

$$RT \ln (C_-^i a_-^i / C_-^o a_-^o) - F \psi = 0$$

where a_+^i, a_+^o, a_-^i and a_-^o are the activity coefficients of C_+^i, C_+^o, C_-^i and C_-^o respectively. By rearrangement we find that

$$C_+^i = (a_+^o/a_+^i) C_+^o e^{-F\psi/RT}$$

$$C^i = (a_-^o/a_-^o) C_-^o e^{+F\psi/RT}$$

so that $$C_f = C^o((a_+^o/a_+^i) e^{-F\psi/RT} - (a_-^o/a_-^i) e^{+F\psi/RT})$$

because C_+^o must equal C_-^o.

The activity coefficients of the counterions in the presence of polyelectrolytes is known to decrease markedly from unity (Katchalsky, 1954) so that (a_+^o/a_+^i) is greater than unity. The activity coefficient of the coion stays essentially the same

(Katchalsky, 1954) so that the ratio a_-^o/a_-^i can be regarded as unity. This means that the first term in the expression for C_f (i.e. (a_+^o/a_+^i) $e^{-F\psi/RT}$ increases in value from $e^{-F\psi/RT}$ whereas the second term remains the same. Thus the value of the fixed charge concentration is reduced when the activity coefficients of the counterions are included.

Unfortunately, no measurements of the activity coefficients of the counterions in the stroma have been undertaken so the size of this effect cannot be calculated. Thus, the high values of the fixed charge concentration found by microelectrodes compared with other estimates may be partly due to the possible charge on the collagen molecules and partly to the neglect of the activity coefficients of the permeant ions.

The osmotic pressures calculated from the fixed charge measurements (Table 3) are higher by a factor of ten from values of the total swelling pressure reported in the literature. (See Maurice, 1969, for a review of such measurements). The reason may be due to the lack of activity coefficients in the calculations. The activity coefficient of the counterions, C_+^i, is thought to be less than that of the external sodium ions, C_+^o, (Katchalsky, 1954) so that the overall effect will be to reduce the osmotic pressure.

(viii) Comparison of Fixed Charge Concentration from fresh and rehydrated tissue.

In section IV, vi, of this chapter, it is shown that the fixed charge concentration from fresh tissue is equal to -133 ± 50 mequivl^{-1} in a bathing solution buffered at pH 7 and at $\mu = .15$. For a similar

bathing solution, the fixed charge concentration from dried stroma, rehydrated to physiological hydration, is found to be -134 ± 28 mequivl^{-1}(Table 2). Thus the fixed charge concentrations from fresh and from rehydrated tissue are in close agreement.

Table 1.

The Average Value of the Fixed Charge Concentration times the Hydration.

Solution pH	Solution μ	n'	N	$\overline{C_f \times H}$ ± s.e.
6	.15	2	39	-470 ± 132
7	.15	4	28	-470 ± 99
8	.15	3	37	-515 ± 121
10	.15	2	26	-529 ± 151
6	.02	4	14	-163 ± 38
7	.02	4	20	-164 ± 20
8	.02	5	23	-240 ± 134
10	.02	6	16	-299 ± 44
7	.05	2	34	-215 ± 55
7	.25	2	34	-398 ± 88
2	.06	3	10	+329 ± 49
2	.15	2	8	+209 ± 75

where n' is the number of specimens and

N is the number of different hydration used to calculated the average value of $C_f \times H$.

Table 2.

The Value of the Fixed Charge Concentration and Potential at H = 3.5

Solution pH	Solution μ	$C_f \pm$ s.e. at H =3.5	ψ at H = 3.5
6	.15	-134 ± 38	11
7	.15	-134 ± 28	11
8	.15	-147 ± 35	12
10	.15	-151 ± 43	13
6	.02	-47 ± 11	25.5
7	.02	-47 ± 6	27.5
8	.02	-69 ± 38	37
10	.02	-85 ± 13	37.5
7	.05	-61 ± 16	15
7	.25	-114 ± 25	5.8
2	.06	$+94 \pm 14$	17.5
2	.15	$+60 \pm 21$	5

Table 3.

Calculation of the Osmotic Pressure at H =3.5

Solution pH	Solution μ	Osmotic Pressure at H =3.5 in $Nm^{-2} \times 10^{-3}$
6	.15	69.6
7	.15	69.6
8	.15	82.9
10	.15	87.6
6	.02	53.3
7	.02	59.2
8	.02	111.6
10	.02	131.1
7	.05	42.3
7	.25	31.2
2	.06	79
2	.15	14.5

Fig. 1a. The Microelectrode Puller.

A - clamp for glass tubing

B - heating filament

C - clamp for glass tubing

D - solenoid

Fig. 1b. Microelectrode in Specimen.

A - gold junction for connecting silver wire to copper wires

B - silver/silver chloride wire

C - glass microelectrode containing 3M KCl

D - cornea specimen

E - bathing solution

F -reference electrode

(a)

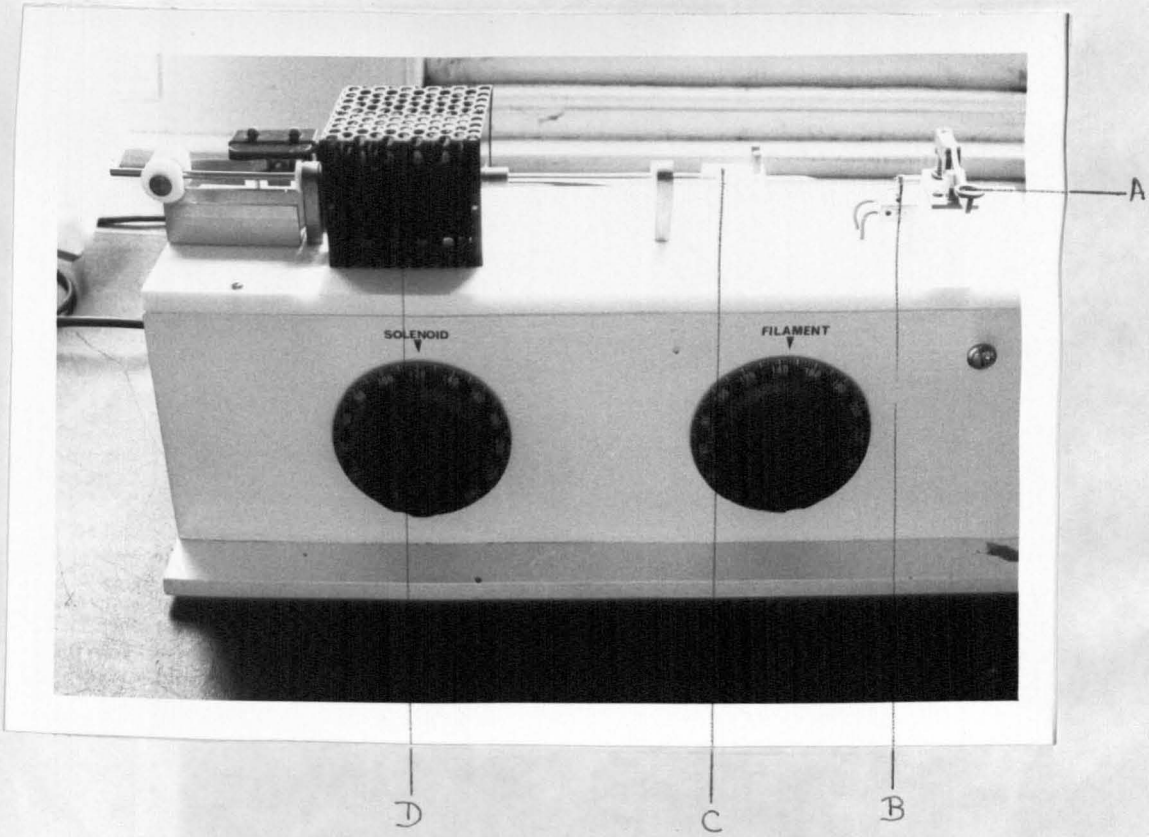

(b)

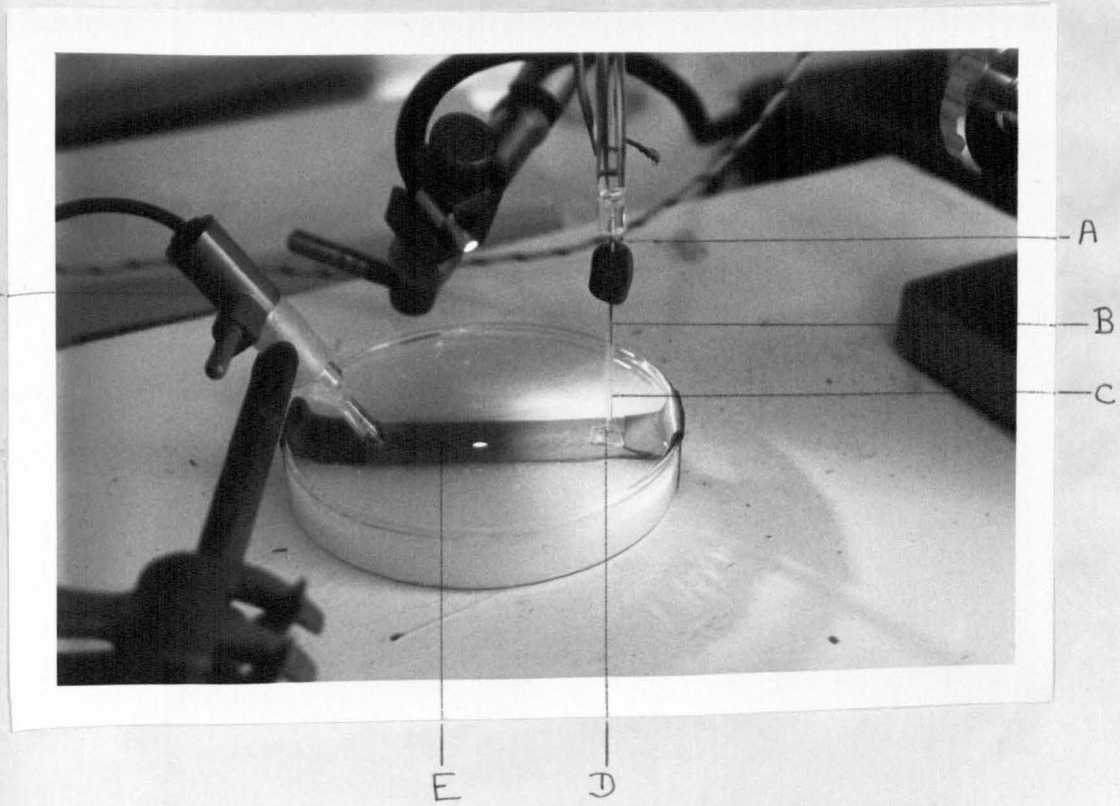

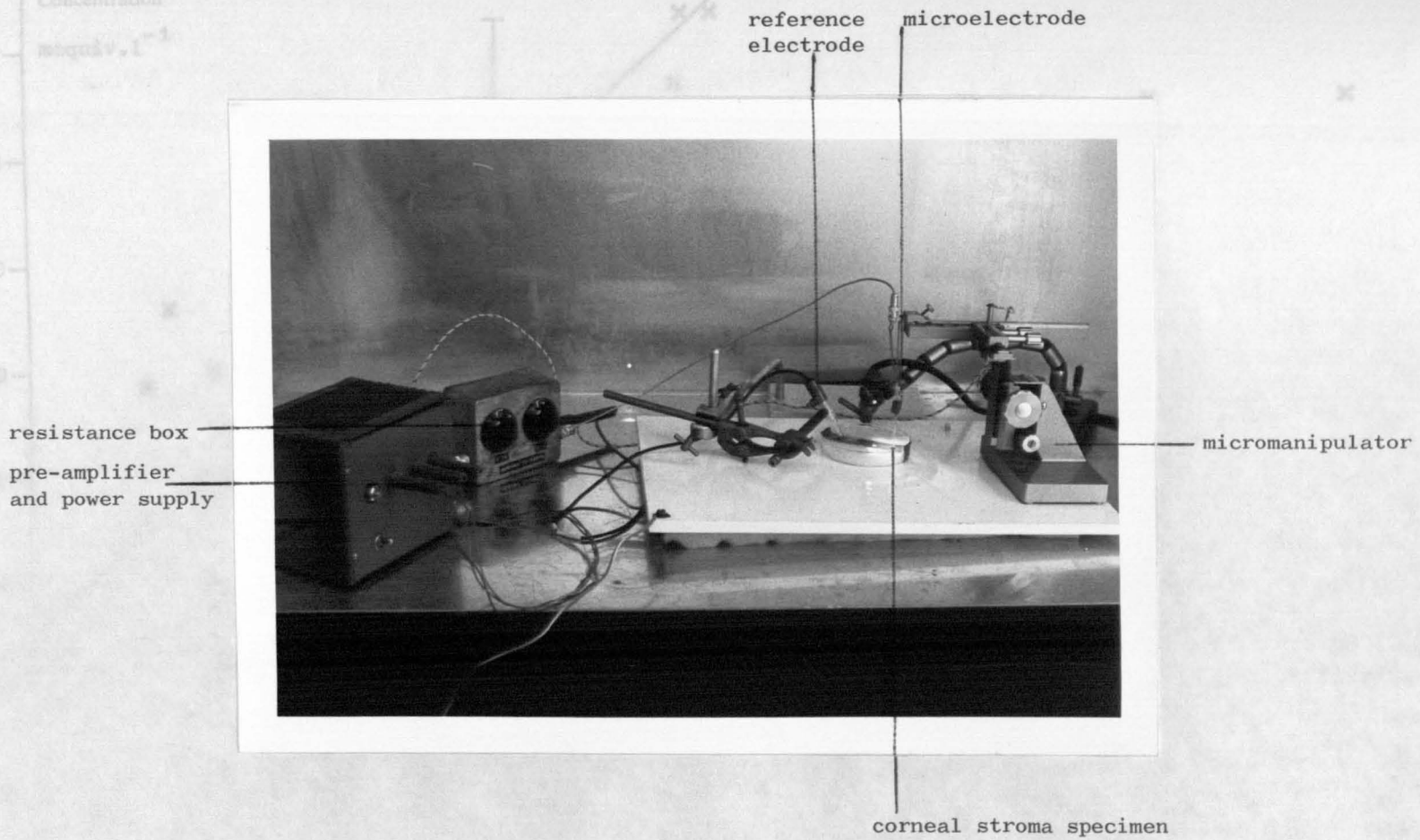

Fig. 1c. Circuit for measuring potentials.

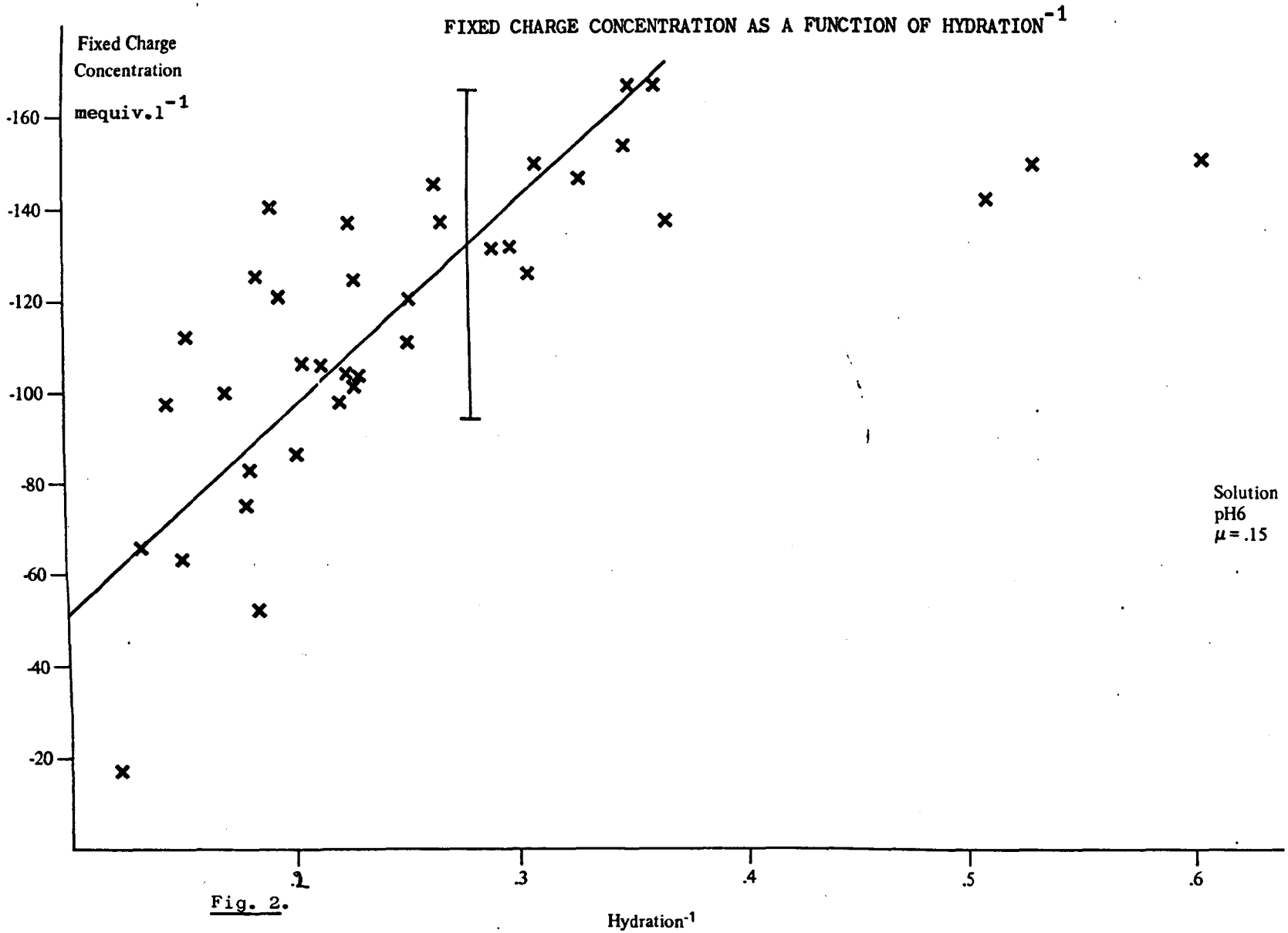
FIXED CHARGE CONCENTRATION AS A FUNCTION OF HYDRATION^{-1}
Fixed Charge Concentration
mequiv.l^{-1}
-160
-140
-120
-100
-80
-60
-40
-20
.2
.3
.4
.5
.6
Hydration^{-1}
Solution
pH6
μ = .15

Fig. 2.

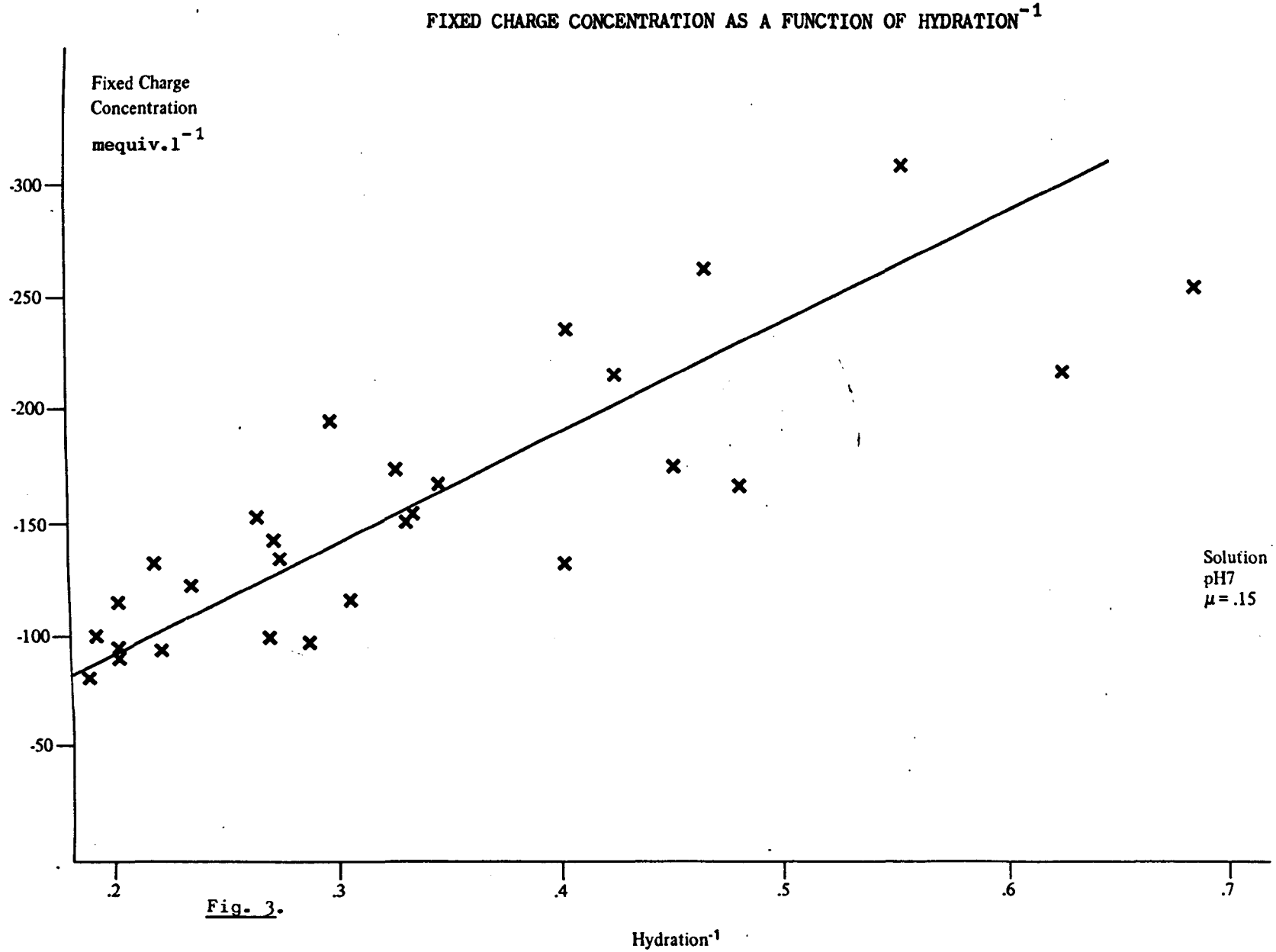
FIXED CHARGE CONCENTRATION AS A FUNCTION OF HYDRATION^{-1}
Fixed Charge Concentration
mequiv.l^{-1}
-300
-250
-200
-150
-100
-50
.2
.3
.4
.5
.6
.7
Hydration^{-1}
Solution
pH7
μ = .15

Fig. 3.

FIXED CHARGE CONCENTRATION AS A FUNCTION OF HYDRATION^{-1}

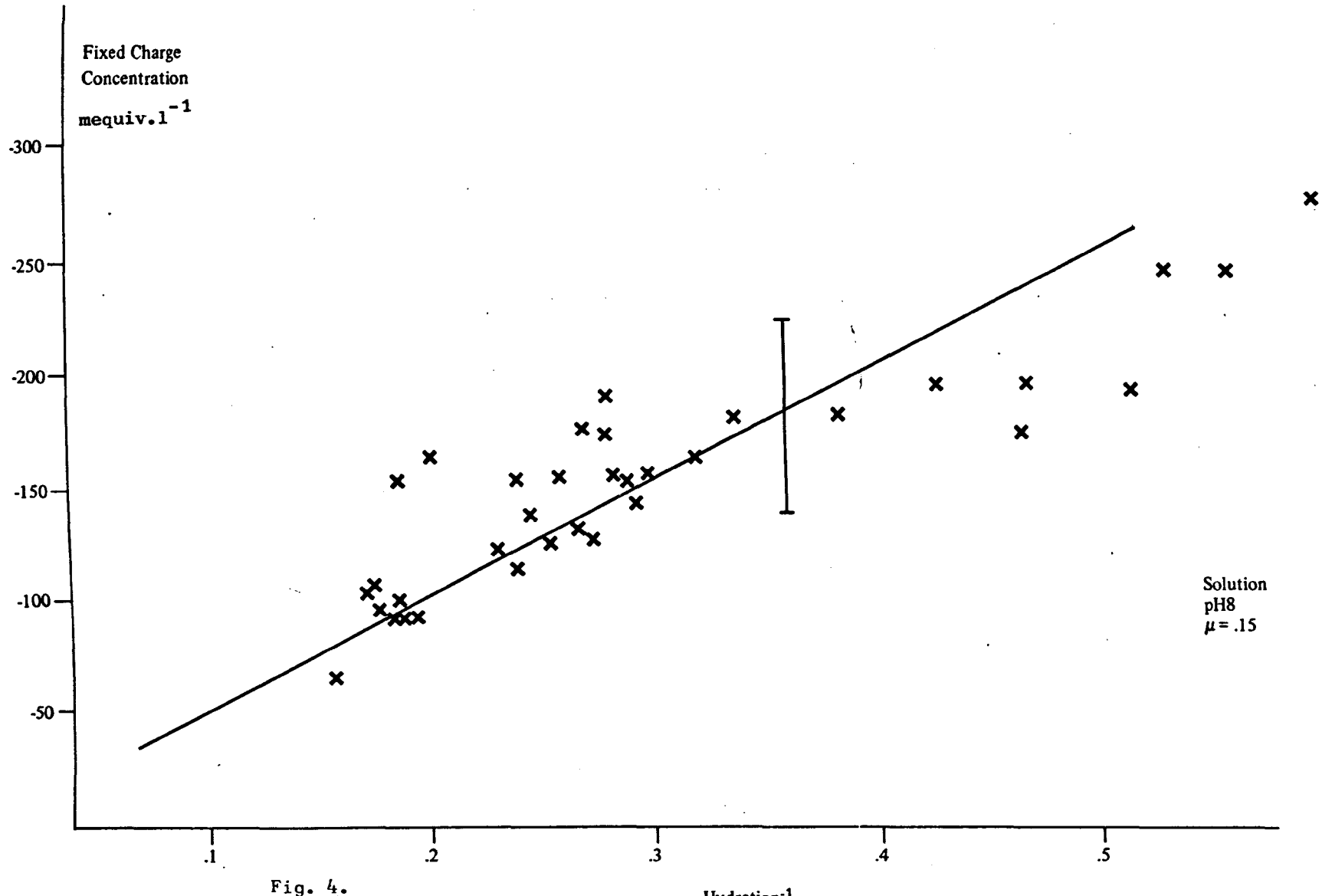

Fig. 4.

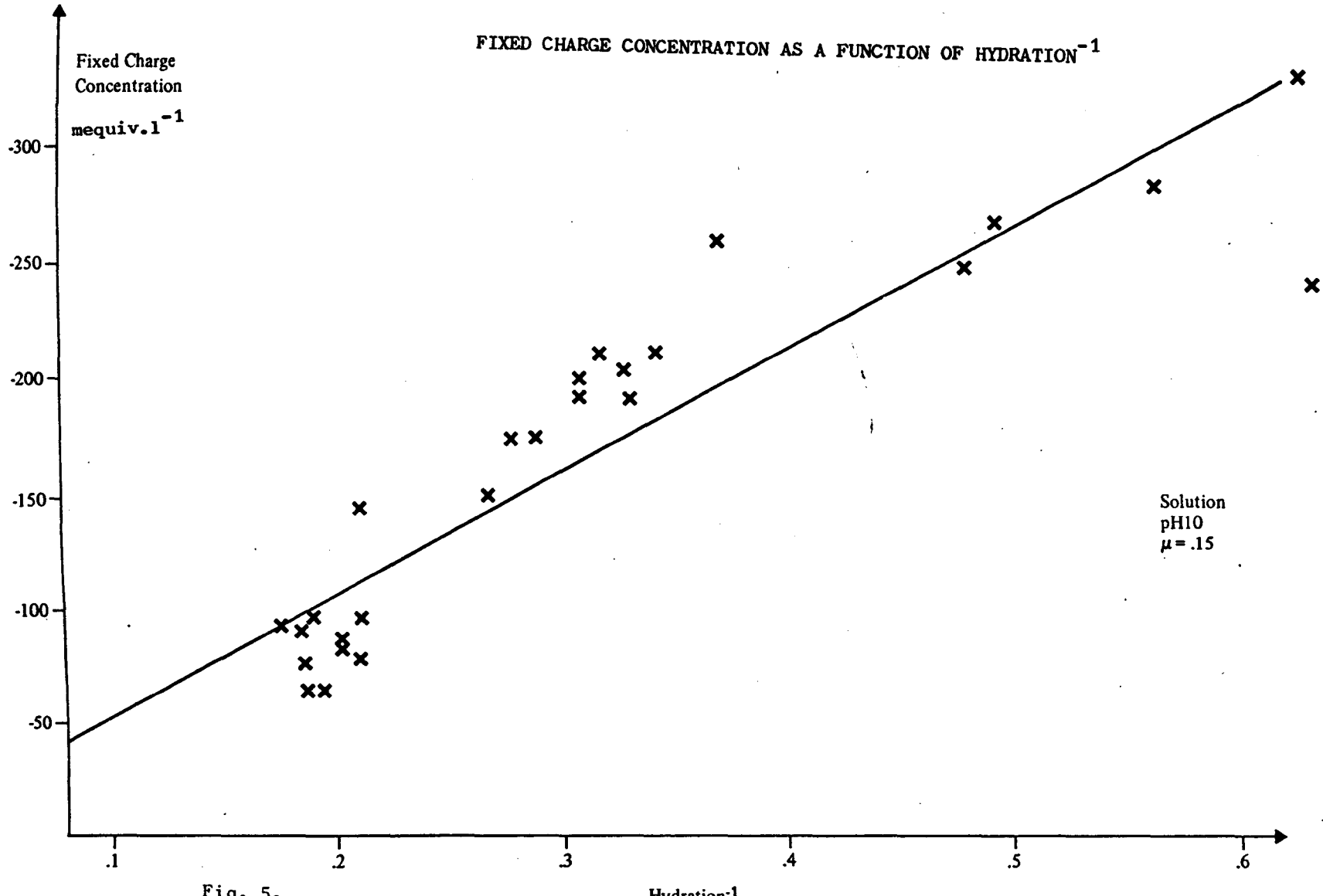
FIXED CHARGE CONCENTRATION AS A FUNCTION OF HYDRATION^{-1}
Fixed Charge Concentration
mequiv.l^{-1}
-300
-250
-200
-150
-100
-50
.1
.2
.3
.4
.5
.6
Hydration^{-1}
Solution
pH10
μ = .15

Fig. 5.

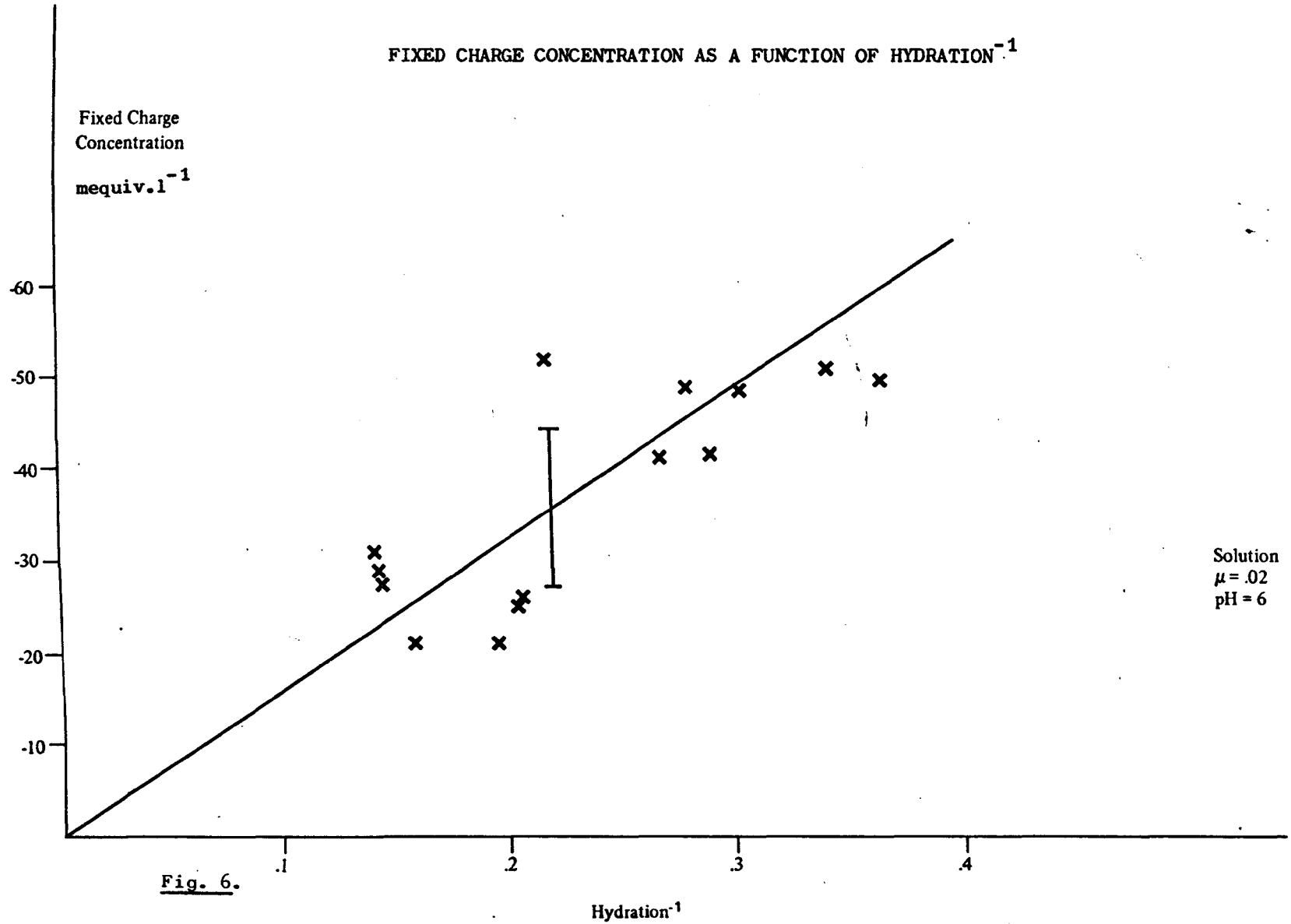
FIXED CHARGE CONCENTRATION AS A FUNCTION OF HYDRATION^{-1}
Fixed Charge Concentration
mequiv.l^{-1}
-60
-50
-40
-30
-20
-10
.1
.2
.3
.4
Hydration^{-1}
Solution
μ = .02
pH = 6

Fig. 6.

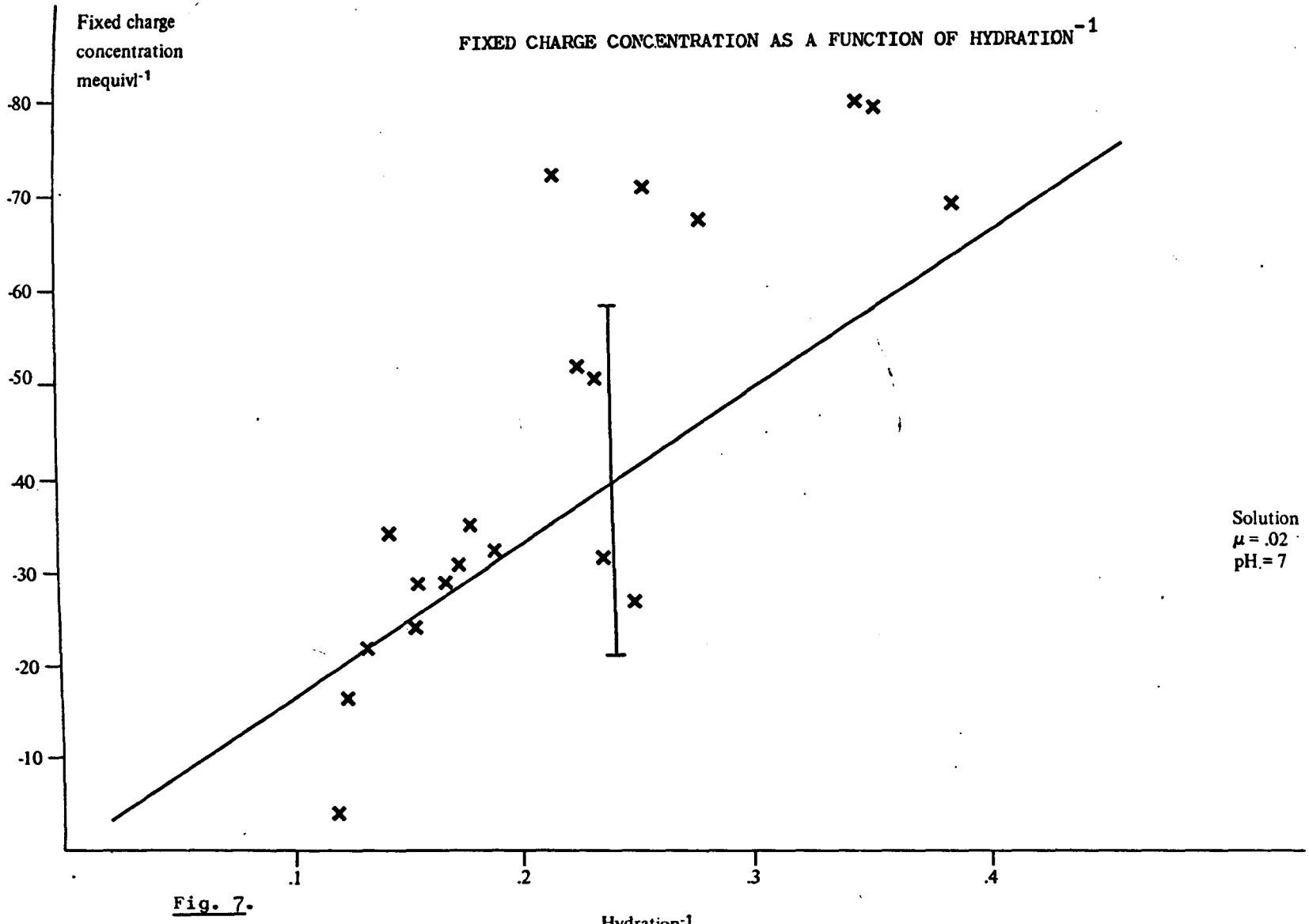
FIXED CHARGE CONCENTRATION AS A FUNCTION OF HYDRATION^{-1}
Fixed charge concentration mequivl^{-1}
-80
-70
-60
-50
-40
-30
-20
-10
.1
.2
.3
.4
Hydration^{-1}
Solution
μ = .02
pH = 7

Fig. 7.

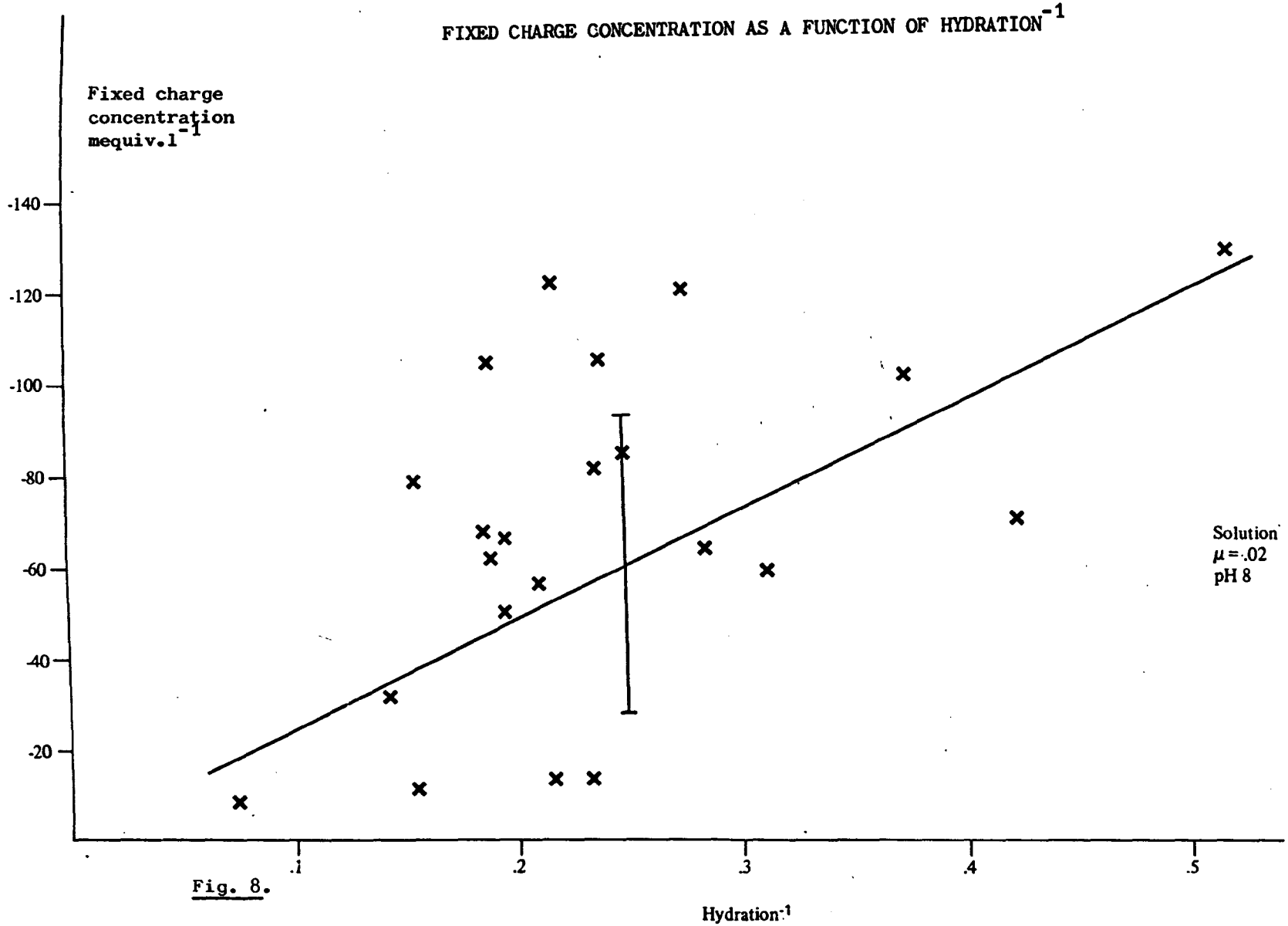
FIXED CHARGE CONCENTRATION AS A FUNCTION OF HYDRATION^{-1}
Fixed charge concentration mequiv.l^{-1}
-140
-120
-100
-80
-60
-40
-20
.1
.2
.3
.4
.5
Hydration^{-1}
Solution
μ=.02
pH 8

Fig. 8.

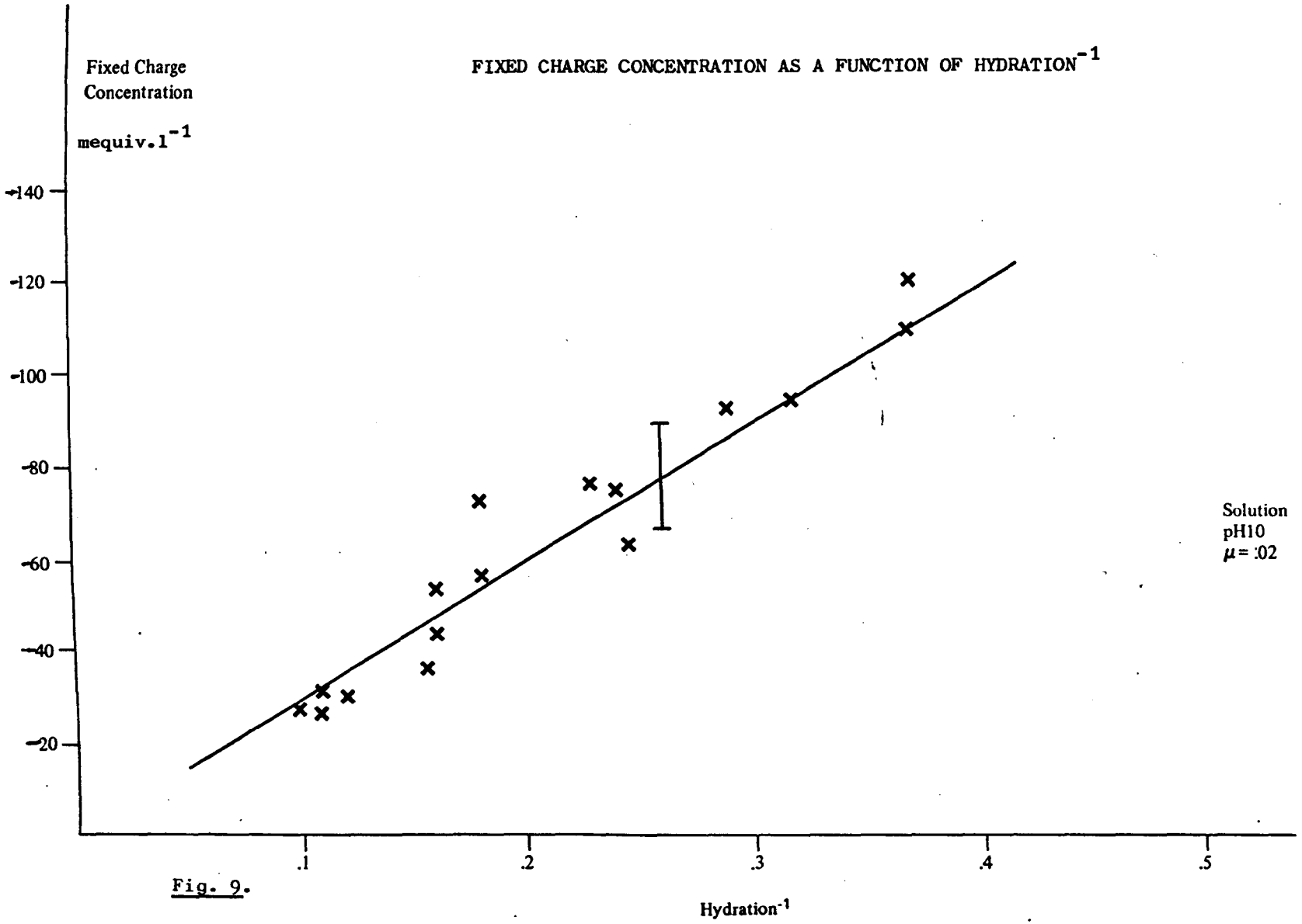
FIXED CHARGE CONCENTRATION AS A FUNCTION OF HYDRATION^{-1}
Fixed Charge Concentration
mequiv.l^{-1}
140
120
100
80
60
40
20
.1
.2
.3
.4
.5
Hydration^{-1}
Solution
pH10
μ = .02

Fig. 9.

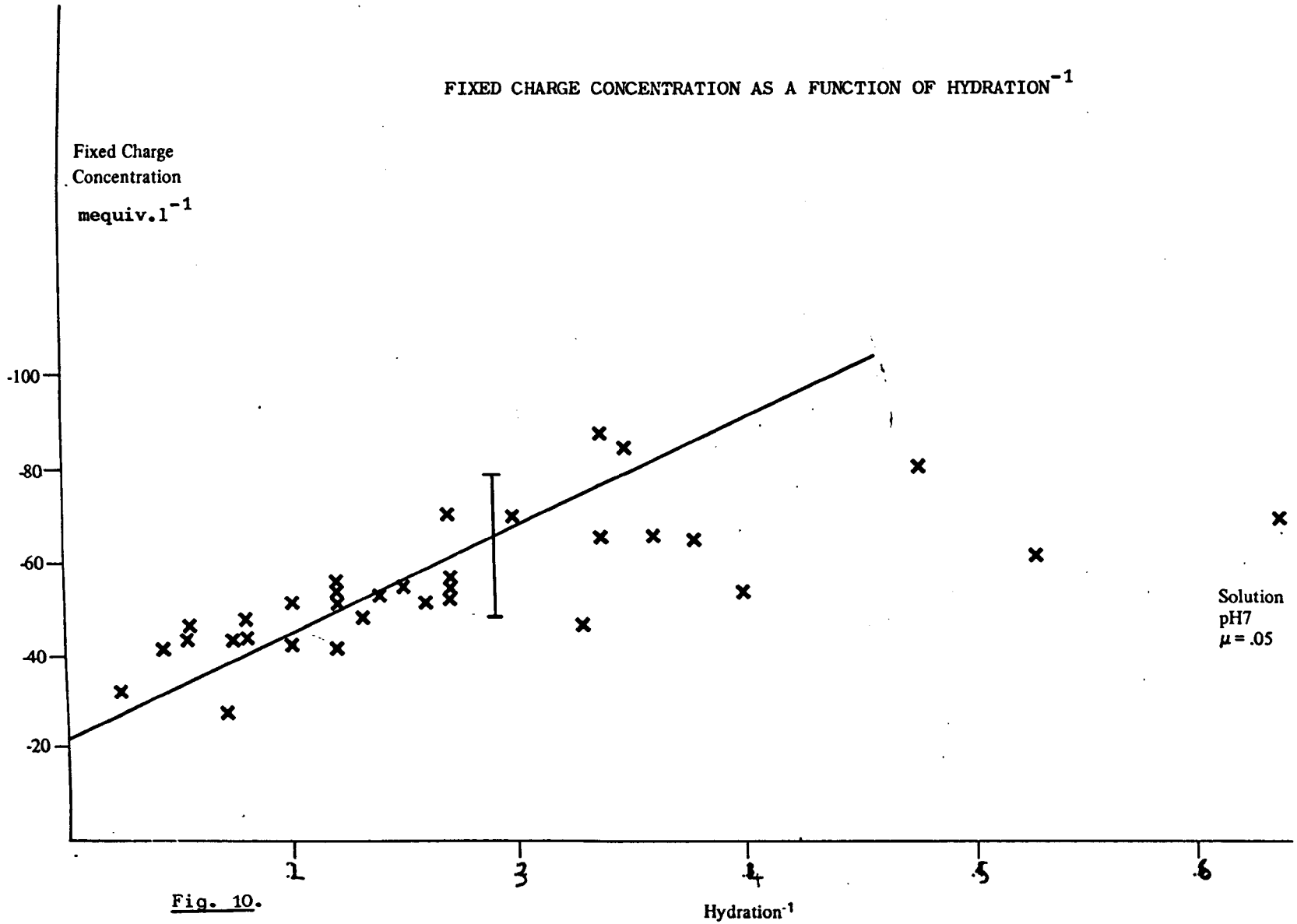
FIXED CHARGE CONCENTRATION AS A FUNCTION OF HYDRATION^{-1}
Fixed Charge Concentration
mequiv.l^{-1}
-100
-80
-60
-40
-20
.2
.3
.4
.5
.6
Hydration^{-1}
Solution
pH7
μ = .05

Fig. 10.

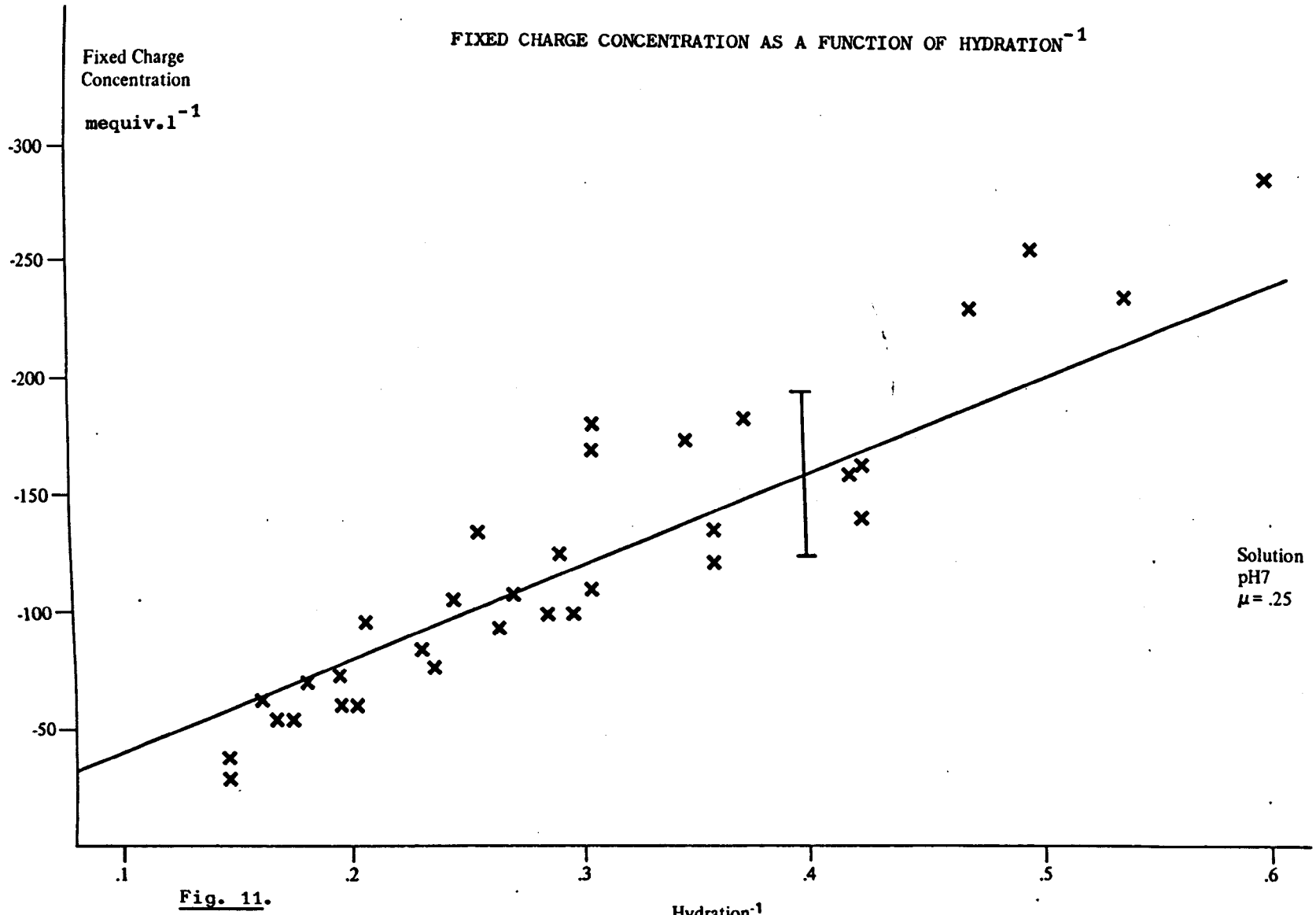
FIXED CHARGE CONCENTRATION AS A FUNCTION OF HYDRATION^{-1}
Fixed Charge Concentration
mequiv.l^{-1}
-300
-250
-200
-150
-100
-50
.1
.2
.3
.4
.5
.6
Hydration^{-1}
Solution
pH7
μ = .25

Fig. 11.

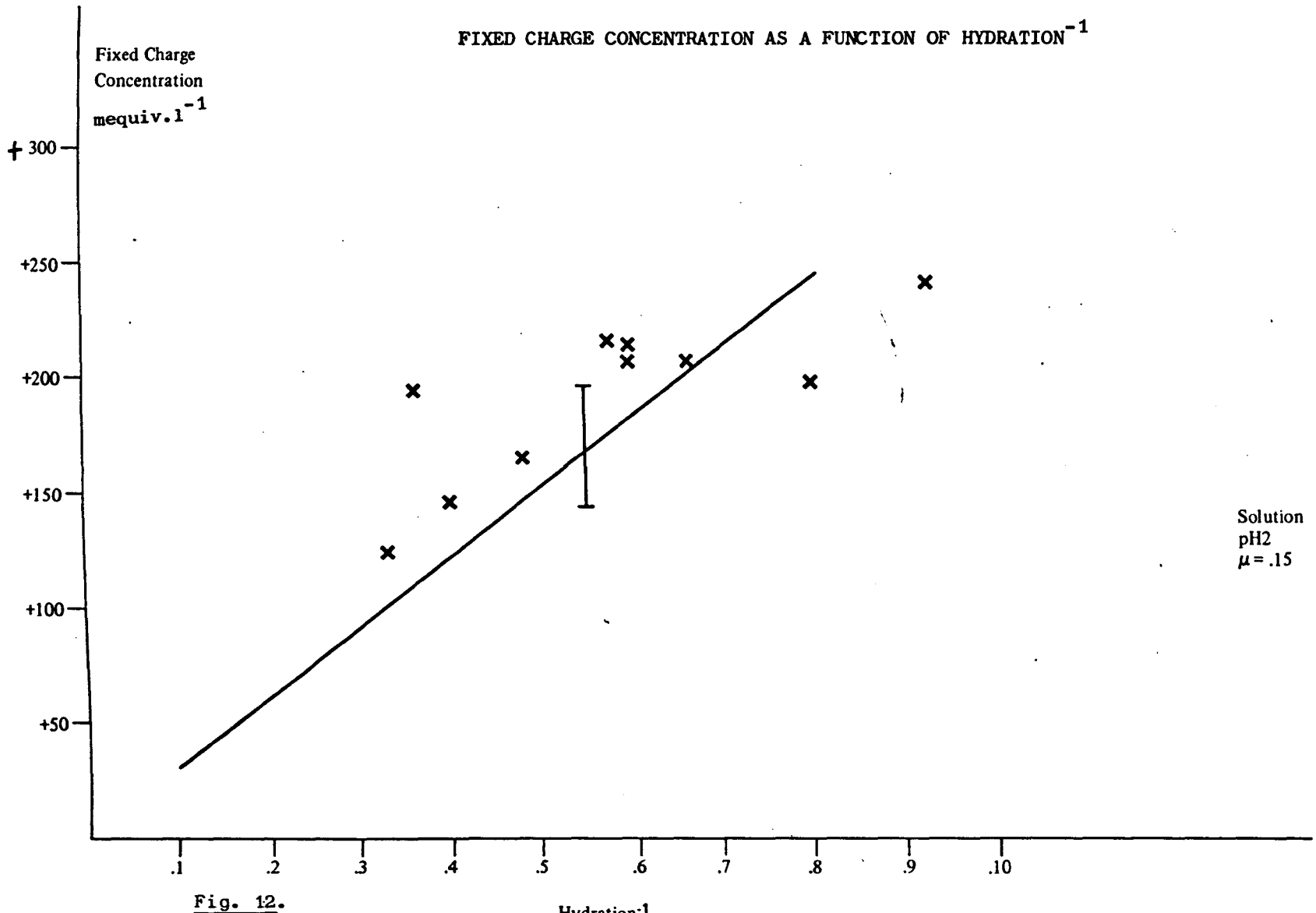
FIXED CHARGE CONCENTRATION AS A FUNCTION OF HYDRATION^{-1}
Fixed Charge Concentration
mequiv.l^{-1}
+300
+250
+200
+150
+100
+50
.1
.2
.3
.4
.5
.6
.7
.8
.9
.10
Hydration^{-1}
Solution
pH2
μ = .15

Fig. 12.

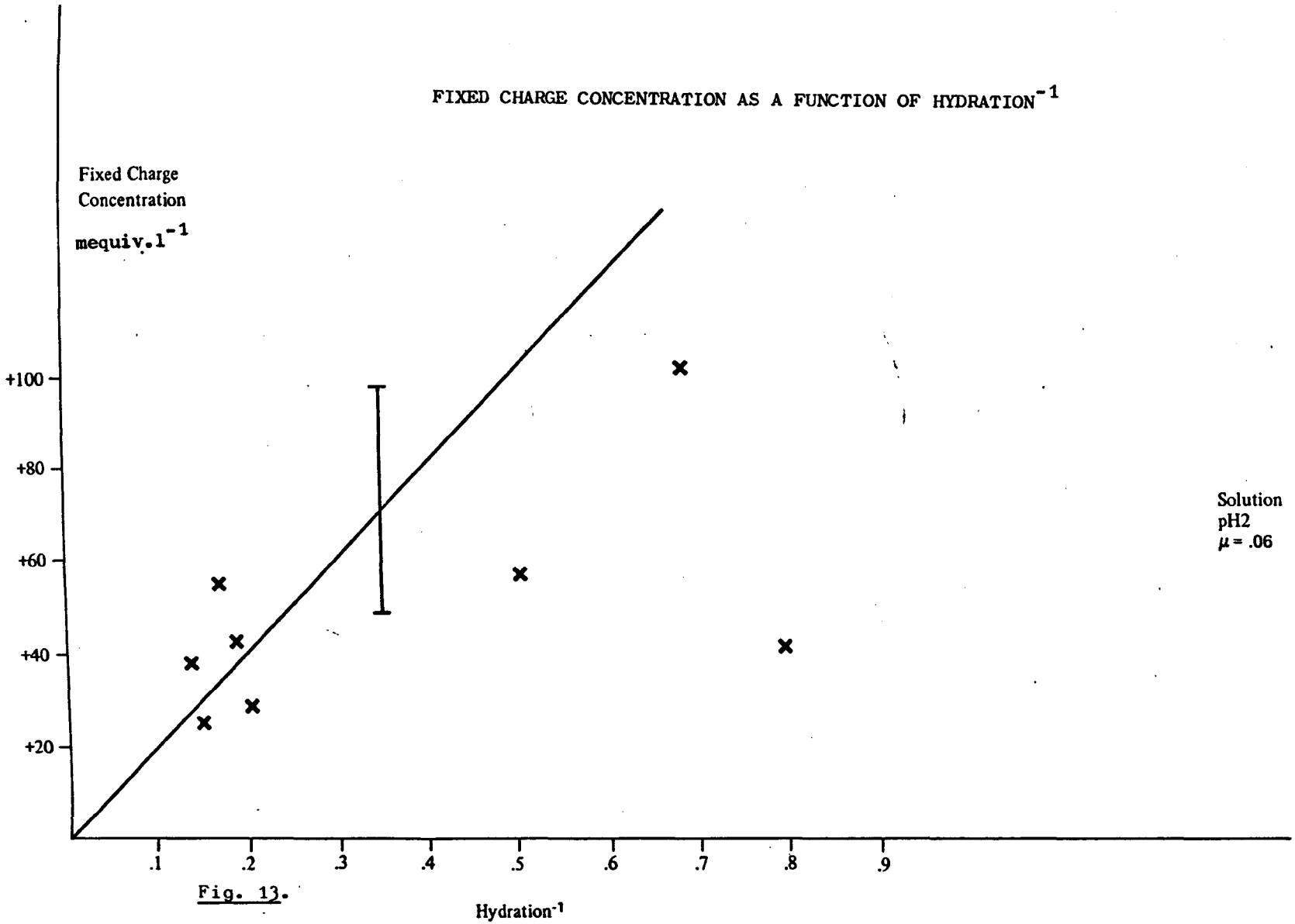
FIXED CHARGE CONCENTRATION AS A FUNCTION OF HYDRATION^{-1}
Fixed Charge Concentration
mequiv.l^{-1}
+100
+80
+60
+40
+20
.1
.2
.3
.4
.5
.6
.7
.8
.9
Hydration^{-1}
Solution pH2
μ = .06

Fig. 13.

Chapter 5.

Absorbance of Visible Light by the Corneal Stroma.

I Introduction.

(i) Transparency and its Relation to Hydration.

The corneal stroma is unusal ammong connective tissues in that it is transparent to visible light at physiological hydration. Changes in the water content of both the *in vivo* and *in vitro* cornea can easily lead to changes in the transparency (Payrau *et al*, 1967 for review). These changes are due both to the clouding of the epithelium and to clouding of the stroma (Payrau *et al*, 1967). The decrease in transparency with hydration varies with the wavelength of the incident radiation (Boettner and Wolter, 1962).

Several workers have studied the amount of light transmitted through the cornea (Adler *et al*, 1949; Van Walbeek and Neumann, 1951; Loeven and Van Walbeek, 1954; Coulombre and Coulombre, 1958; Potts and Friedman, 1959). Adler *et al*,(1949)found that the 'aging' of corneas in a moist chamber lead to a considerable decrease in their transparency compared to that of corneas preserved in mineral oil. Van Walbeek and Neumann (1951) and Loeven and Van Walbeek (1954) found that dried corneas allowed to swell to physiological hydration showed differences in their transparency depending on the bathing solution. Minimum absorbance occured at approximately pH 4, the point of minimum swelling. The transparency of corneas bathed in solutions of higher pH increased until the pH reached 5 and then remained constant up to pH 7.

Differences in transparency with ionic strength of the bathing solution were also noted. Maximum transmission of light through the corneas bathed in potassium chloride occured at log concentration of .7. Coulombre and Coulombre (1958) and Potts and Freidman (1959) noted that the initial clouding of the cornea on swelling was due to a decrease in the transparency of the epithelium and not due to changes in the stroma. Payrau et al (1967) present data showing that clouding of the corneal epithelium is important for the first thirty minutes of swelling in distilled water but it then remains constant for the next 4.5 hours. During this time the corneal stroma is gradually decreasing in transparency. Potts and Freidman (1959) found that varying the ionic strength of the medium bathing the epithelium and endothelium altered the transparency of the tissue. Substitution of potassium ions for sodium ions caused less clouding for the same time of swelling. No correlation was found between the optical density (absorbance) and hydration of the tissue by Potts and Freidman (1959).

(ii) Transparency as a Function of Wavelength of the Incident Light.

The transmission of the human cornea has been studied as a function of the wavelength of the incident light by Boettner and Wolter (1962). The maximum wavelength which can be transmitted through the cornea is 2500 nm in the infra-red. Eighty percent transmission occurs at 380 nm and this increases to 90% transmission at 500nm. This level of transmission remains constant until around 1300nm when absorption bands due to the water in the tissue occur in the infra-red region. Kinsey (1948) has shown that the limit of transmission of rabbit cornea is approximately 280 nm and is due to the nucleoprotein in the epithelium which is thought to absorb strongly in the ultra-violet region. The

cornea probably acts acts as a protective layer preventing possible damage to the lens and other tissues by the ultra-violet radiation. Kinsey (1948) reports that the transmission through rabbit cornea is 94% at 400 nm compared with the 80 -90 % for human cornea (Boettner and Wolter, 1962). A detailed review of transmission at all wavelengths through a variety of species of cornea is given by Payrau et al (1967).

When the corneal stroma is hydrated the dependence of the transmission on the wavelength is altered (Payrau et al, 1967). As the water content of the tissue increases there is a greater decrease in the transparency at low wavelengths than at high wavelengths within the visible region. This decrease in transparency of the stroma is due to scattering of the light and to some absorption of the light (Maurice, 1957,1962; Kikkawa, 1960; Kinoshita et al, 1965; Feuk, 1971 ; Feuk and McQueen, 1971). Most of the scattering occurs within 5^{o} of the main beam but the angle increases with increasing hydration (Kikkawa, 1960).

(iii) Diffraction and low-angle scattering.

Kikkawa (1958) has shown that some light is diffracted by the cornea. The spacing of the diffracting regions is approximately 13 μm. This distance increases on swelling but changes only slightly on drying the tissue. Low angle scattering patterns (of light) have been observed by Bettelheim and Vinciguerra (1969) corresponding to a distribution of superstructures of the size 1 - 20 μm. The origin of these dif-

fraction patterns is not known because the size of the diffracting regions is much larger than the size of a fibril. The author and colleagues did not succeed in obtaining any recognisable diffraction patterns using laser light with either fresh or dried cornea.

(iv) Physical Theories of the Transparency.

A review of the early theories of the transparency of the cornea is given by Payrau et al (1967). All modern theories (since 1950) depend on the structure of the stroma as seen in the electron microscope. However, the arrangement of the collagen fibrils which is seen in the electron micrograph is always open to the criticism that the fixing and staining procedures, necessary to produce an electron dense specimen, may alter the structure.

The corneal stroma is known to consist of the collagen fibrils embedded in a ground substance (Schmitt et al, 1942). Aurell and Holmgren (1953) measured the refractive index of the fluid extruded from the cornea by squeezing and found that it was different from that of collagen. Maurice (1957) calculated that the refractive index of the ground substance was different from that of corneal collagen and used these calculations to determine the birefringence of the cornea. Good correlation is found between this calculated value and the measured values of the birefringence.

If this refractive index is assumed to exist, then light will be scattered by the fibrils according to standard electromagnetic theory (Schaefer, 1909). According to Maurice (1957), 95% of the incident light will be absorbed if the fibrils are randomly arranged in the ground substance. He, therefore, proposed that the distribution of the fibrils was ordered and possibly that of an hexagonal lattice based on the structure of the cornea seen in the electron microscopy of Jakus (1954). It was already known that the fibrils were approximately parallel to each other within a lamella and had nearly the same diameters. If such fibrils were arranged in a lattice, each lamella might be expected to act as a three-dimensional diffraction grating. As the distance between diffracting regions (fibrils) is less than the wavelength of visible light (i.e. 400-800nm) only the zero order beam of such diffracting system would be transmitted.i.e. using the diffraction equation $d \sin \theta = n\lambda$ where d is the distance between the fibrils, 60nm, and is 600 nm, then $\sin \theta = n \times 10$, a condition which can only be satisfied if $n = 0$ when $\theta = 0$.

According to Payrau et al(1967), Caspersson and Engström (1946) have proposed that the refractive index does not change singularly at one point but that it changes slowly as the distance from each fibril is increased. Such a gradient of refractive indices would bend the light and not cause the light to be scattered according to Caspersson and Engström. However, the major objection to this theory is that it is thought unlikely that light could be 'bent' in this way over regions smaller than a wavelength of light (Maurice, 1957, Payrau et al, 1967).

Smith (1969) disagrees with Maurice's calculation that an irregular arrangement of the fibrils would scatter 95% of the incident light. Electron micrographs of Smith and Frame (1969) showed that 33% of the total volume of the stroma was occupied by collagen fibrils compared with the average of 7% found by Schwarz and Graf Keyserlingk (1966). It was also noted that the protein-polysaccharide chains attach to the collagen fibrils even after disintegration of the tissue. Hence the determination of the refractive index of the ground substance made by Aurell and Holmgren (1953) would be too low. Using these revised figures Smith (1969) calculates the refractive index of the fibrils and the ground substance and concludes that 96-97% of the incident light is transmitted by a random arrangement of fibrils. Swelling of the stroma leads to a large difference in the refractive indices which decreases the amount of transmitted light. Maurice's lattice theory is also criticised on the grounds that both the fibril diameter and the distance separating the fibrils is variable (Smith and Frame, 1969).

Evidence against the existance of an ordered hexagonal lattice is provided by the electron microscopy of Schwarz and Graf Keyserlingk, 1966; Goldman and Benedek, 1967; Goldman et al, 1968. These authors do not find ordered regions of fibrils. In direct constrast, Goldman and Benedek (1967) find that the Bowman's zone of the shark was formed from collagen fibrils in commplete disorder. Even so the cornea of the shark is transparent. Benedek (1971) proposes a theory in which the

regularity of the lattice of fibrils is not required. Only a partial correlation in position is needed to account for the measured transmission of light. The decrease in transmission on swelling is assumed to be due to the presence of lakes, non-collagenous areas, which scatter light more effectively than the fibrils because they are nearer to the size of a wavelength of light (Benedek, 1971).

Farrell and Hart (1969) and Cox et al (1970) have produced a more detailed mathematical model to accound for the transparency based on limited correlation in the position of the fibrils (described by a radial distribution function). Feuk (1970) has proposed that random fluctuations of the fibrils occurs about their mean lattic positions which would correspond to the lattice positions suggested by Maurice (1957).

The main difference between the model of Cox et al (1970) and Feuk (1970) is their predictions for the wavelength dependence of the scattered light. Feuk (1971) describes data showing that the light which is scattered is dependent on the inverse fifth power of the wavelength whereas Farrell et al (1973) find a dependence on the inverse third power for normal cornea. Swollen corneas depend on the inverse second power (Farrell et al, 1973). This is consistent with the lake theory of Benedek which also predicts this dependence.

II Theory of Transmission of light.

It is well known that when electromagnetic radiations travels

through matter it decreases exponentially with the thickness of the tissue. If I_o is the incident intensity and I_t the transmitted intensity then

$$I_t = I_o e^{-bd} \quad \text{(Jenkins and White, 1951)}$$

where d is the thickness and b is a constant depending on the tissue. The transmission, T, is defined as

$$T = I_t/I_o$$

When the corneal stroma swells, its structure alters i.e. the density of fibrils changes, at the same time as its thickness is increasing. This implies that both b and d in this equation are functions of the hydration of the tissue. The relation between the thickness and the hydration is linear because swelling takes place in one direction (Hedbys and Mishima, 1966). However, the theoretical relation between b and hydration depends on the model used to describe the stroma (Cox et al, 1970; Feuk, 1970 , 1971; Benedek, 1971).

Farrell et al (1973) found experimentally that the average transmission, T, decreased linearly with the hydration of the corneal stroma. Hence,

$$T = a_1 - a_2 \times H$$

where a_1 and a_2 are constants. In the experiments presented here, it is the absorbance of the corneal stroma which has been measured. This is related to the transmission by

$$T = 10^{-A}$$

where A is the absorbance. Hence, it is expected that the function 10^{-A} will decrease linearly with the hydration of the tissue. The rate of change of transmission with hydration is dT/dH where

$$dT/dH = - a_2 .$$

III Methods

(i) Material.

Dried corneal stroma were swollen in solutions of different ionic strength and pH as previously described (Chapter 2, section III). It was necessary to use stroma which had dried flat and were not wrinkled. Pieces of stroma were cut slightly larger than the central part of the cell through which the light beam travelled. This was to ensure that the light beam always went through an equivalent area of stromal surface and also to allow the tissue to be handled with tweezers without scratching the surface. It is necessary to scrape the epithelium off the fresh tissue because this tissue gives rise to a considerable loss of transparency during the initial stages of swelling (Payrau et al, 1967). However, this had to be done carefully in order to maintain the smooth surface of the stroma.

(ii) The Cell

A cell was designed which would fit in the cell holders in the sample compartment of the spectrophotometer. The cell used was basically similar to that used for the x-ray diffraction experiments i.e. it contained a small air-tight compartment for the stroma. However, the windows of the cells were made from quartz glass cover slips for measurements in the visible regions. Black masking tape was used to prevent the light beam passing through all but the central part of the cell containing the

the specimen.

(iii) The Spectrophotometer.

A Perkin-Elmer 402 uv double beam spectrophotometer was used to record the absorbance of the corneal stroma as a function of the wavelength of the incident light. (Fig. 1). This instrument disperses visible light into different wavelengths using a prism. A narrow slit which can transverse the prism defines the wavelength. The incident beam is spit into two parts of equal intensity. One part of the beam is directed onto the specimen cell while the other goes through the reference cell. These beams are recombined after passing though the sample chamber and are focusses onto a photomultiplier tube. The signal from the photomultiplier is amplified and fed to a pen recorder which moves linearly with the absorbance of the specimen. The absorbance is continuously recorded as a function of wavelength. In all experiments the fast wavelength scan was used as no sharp absorption edges are recorded from cornea in the visible region. Before a specimen was tested the sample and reference beams were adjusted in order to allow for any slight differences in the cells. Wavelengths in the range 390 - 830 nm were used to determine the dependence of the absorbance on the hydration of the sample.

(iv) Procedure.

Swollen corneal stroma were removed from the bathing solution

blotted and weighed. They were carefully placed in the centre of the cell so that they were flat. The whole cell was placed in the front of the sample beam in the spectrophotometer. The absorbance was recorded within 2 minutes so that the hydration was essentially unchanged by this procedure. The stroma was then immediately replaced in its bathing solution in order to obtain a higher value of hydration. Three corneas were used for each different solution. A range of pH values and ionic strengths were used similar to those used in the microelectrode experiments.

IV Results.

(i) General Properties.

In general, the transmission of the corneal stroma, swollen in the solutions used in the experiments presented here, decreases as the hydration of the tissue increases. However, the rate at which the transmission descreases as a function of the hydration depends to a large extent on the pH and on the ionic strength of the bathing solution. This dependence will be discussed in detail below. The transmission also depends on the wavelength of the incident light in such away that, in general, any decrease in the wavelength decreases the transmission.

The data presented in Figures 2-16 as transmission as a function of the hydration of the stroma includes readings from three wavelengths namely 450, 550 and 650 nm. A linear relation between the transmission

and the hydration of the tissue is seen to exist as suggested by Farrell et al (1973). The transmission is always least at 450 nm and largest at 650nm, at a given hydration, for all solutions. Linear regression fits are obtained at each wavelength for each solution. The details of these regressions are given in Tables 1,2 and 3. The data includes the slope of the regression which is proportional to the rate of decrease of transmission with hydration, dT/dH.

(ii) Behaviour at pH 4.

Corneal stromas swollen in solutions buffered at pH 4 show a faster decrease in transmission with hydration than stromas swollen at either higher or lower pH values (Figs 4 and 5). At μ = .06 and λ = 450 nm, the slope of the regression fit is - .311 $\pm$ .091 (Table 1) which is approximately four times the rate of decrease found with stroma swollen at pH 7 and μ = .15 (Table 1). Increasing the ionic strength to μ = .15 decreases the rate of decrease of transmission by approximately one half of the value at μ = .06 to -.159 $\pm$ .024 (at λ = 450 nm).

(iii) Behaviour at pH 2.

The transmission of stroma swollen in solutions at pH 2 is shown in Figs 2 and 3 as a function of hydration. The details of the regressions are given in Tables 1-3. At μ = .06, the rate of decrease is similar to that at higher pH values being - .067 $\pm$ .007. However, increasing the ionic strength to μ = .15, increases the rate of loss of transmission to - .107 $\pm$ .009 which is higher than other rates of decrease of transmission except those at pH 4. The

dependence of dT/dH on ionic strength is exactly the opposite to that found at pH 4 i.e. at pH 2 increasing the ionic strength increases the loss of transmission but at pH 4 increasing the ionic strength decreases the loss of transmission.

(iv) Behaviour at pH 6,7,8 and 10.

The data for the loss of transmission in the high pH range (6-10) is shown in Figs 6 - 16. The details of the regressions are shown in Tables 1 - 3. It can be seen immediately from Table 1 that the rate of loss of transmission decreases in magnitude as the pH of the bathing solution is increased. At μ = .15, the slope of the regression is .084 $\pm$ .006 at pH 6 (λ= 450 nm) compared with .052 $\pm$ .005 at pH 10. The values of the slopes at pH 7 and pH 8 decrease in size between the value at pH 6 and that at pH 10. This occurs at all wavelengths (Table 2 and 3). A similar decrease in rate of loss of transmission is seen when the stroma is swollen in solutions at μ = .02. The slope of the regression at pH 6 is .057 $\pm$ .004 and at pH 10 is .033 $\pm$ .003. At each pH value, the rate of loss of transmission is less at μ = .02 than at μ = .15 i.e. the same ionic strength dependence which is found at pH 2 (Fig. 18).

The dependence of the transmission on swelling at different ionic strengths at pH 7 shows a complicated relationship. The transmission decreases fastest at μ = .15 and slowest at μ = .25. In between these values, the rate of loss of transmission is in the order μ = .05, μ = .02 and μ = .1 (Table 1-3), the latter value having the lower value.

(v) Fresh Tissue.

The absorbance of fresh beef corneal stroma was measured as a function of wavelength of light. Eight different cornea were used. The individual data points are plotted in Fig. 17. The solid line is the curve through the average value of the absorbance at each wavelength. The values of the transmission are given on one axis. However, the absorbance is related to the logarithm of the transmission so the scale of the transmission axis is not linear.

V Discussion.

(i) Fresh Beef Corneal Stroma.

The absorbance measurements on fresh beef corneal stroma (Fig 17) give values which are low compared with the 94% transmission, at 550 nm, for fresh rabbit cornea (Maurice, 1957, 1969; Farrell et al, 1973). However, Payrau et al (1967) report a value of 81% for the transmission of light (wavelength not given) for calf cornea which have been dried over silica gel. This value is comparable with the transmission of 75% found, at 650 nm, for fresh beef stroma (Fig 17), although Payrau et al (1967) found, for rabbit cornea, that the transmission of fresh tissue is slightly increased compared with that of dehydrated tissue. It should be noted that Payrau et al (1967) conclude that the transmission is inversely related to the thickness of the cornea from a comparison of data from several species. Hence, the low values of the transmission found with fresh beef stroma, in Fig 17,

may be due to the thickness of beef cornea.

The two hour delay after ennucleation of the eye to arrival at the laboratory may be enough for the active mechanisms maintaining transparency to stop functioning and hence lead to a swelling of the stroma by imbibition of the fluid from the aqueous humour (Davson, 1955; Harris, 1957).

The transmission of dried stroma rehydrated to physiological hydration i.e. $H = 3.5$ is always lower than the transmission of fresh tissue e.g. the transmission of stroma rehydrated in a bathing solution at pH 7 and $\mu = .15$ is 48% compared with 75% for fresh tissue at $\lambda = 650$ nm (Table 3). The reason for this is unknown but may indicate that the loss in order of the fibril arrangement and or percentages of lakes is greater in rehydrated tissue than in fresh tissue possibly due to the large initial rate of hydration when dried stroma is placed in a salt solution.

(ii) The Dependence of the Transmission of Hydration and Wavelength.

In general, the transmission decreases with hydration as has been found before (e.g. Payrau et al, 1967, for review). The linear regression obtained from the data plotted as transmission as a function of hydration are all significant as seen by the values of the f-ratios (Table 1-3). This linear decrease with hydration is expected from the work of Farrell et al (1973). The slopes from the experimental data are negative indicating that the transparency of the corneal stroma is decreasing with increasing hydration.

During wavelength scans, at any given hydration, the absorbance always decreases with increasing wavelength i.e. the transmission increases. This is shown in any of the graphs (Figs 2-16) in which the transmission at 650 nm is always higher than that at 450 nm. This dependence on wavelength is also shown by the linear regression fits although the slope alone is not always largest at the lowest wavelength. The slopes are largest at λ = 450 nm and smallest at λ = 650 nm for most solutions other than those at pH 2 and pH 4 (Tables 1-3).

(iii) The Dependence of the Rate of Loss of Transmission on pH and Ionic Strength.

The rate of loss of tranmission with hydration, dT/dH, (which is estimated from the slope of the data for any given solution) is a function of both the pH and the ionic strength of the bathing solution. Maximum rate of loss of transmission and minimum value of the transmission are found at pH 4. This relation between the point of minimum swelling, pH 4, and minimum transparency was found by Loeven and van Walbeek (1954). The next highest rate of loss of transmission is found at pH 2 (μ = .15) (Fig 3).

With solutions buffered at pH 6,7,8 and 10, it is found that the higher the value of the pH the lower the rate of loss of transmission. This occurs at both the ionic strengths used i.e. μ = .02 and μ = .15 and at all three wavelengths (Tables 1-3).

The reason for this pH dependence is unknown. It is unlikely that 'lakes' are the principle cause of the loss of transparency at pH 4 and pH 2 because the total water content of the tissue is

so low in these solutions. The presence of electrovalent bonds between zwitterion pairs may change the structure causing a loss in transparency. These attractive forces have been discussed in Chapter 2, Section V, in order to explain the swelling behaviour at pH 4, in terms of polyelectrolyte gel theory (Katchalsky, 1954).

The dependence of the rate of loss of transmission on ionic strength is complex. At all pH values, except pH 4, dT/dH , at μ = .15, is larger than at μ = .02. At pH 4, the dependence is such that dT/dH at μ = .06 is larger than at μ = .15. It is noted that the rate of decrease of transmission with hydration decreases with increase in pH while the rate of increase of hydration, dH/dt, increases with increase in pH. The rate of decrease of transmission is also smaller at the lowest ionic strength, μ = .02, compared with μ = .15 whereas the swelling rate is smaller at the latter ionic strength. This inverse dependence on pH of the rate of swelling and the loss in transmission with hydration will discussed in more detail in Chapter 6, Section VII.

(iv) The Dependenc of Transmission of pH and Ionic Strength.

The transmission at physiological hydration has been calculated using the regression fits for several solutions (Table 4). At the low ionic strength, μ = .02, the maximum value of the transmission occurs at pH 7 for each of the three wavelengths. At the higher ionic strength, μ = .15, the maximum transmission occurs at pH 8. A decrease or increase in pH either side of the range pH 7 -8 seems to decrease the value of the transmission. Thus maximum transmission appears to occur at pH values around that expected

for physiological pH.

The ionic strength does not appear to influence the value of the transmission as at two pH values (6 and 8) the transmission is larger at μ = .15 to that at μ = .02 and at the other two pH values (7 and 10) the transmission at μ = .02 is larger than at μ = .15.

Table 1.

Details of regressions for Transmission as a function of Hydration.

$T = + a_1 - a_2 \times H$ at $\lambda = 450$ nm

Solution pH	Solution μ	$-a_2 \pm$ s.e.	a_1	N *	F-ratio **
2	.06	-.067 ±.007	.46	30	88
2	.15	-.107 ±.009	.53	30	149
4	.06	-.311 ±.091	.64	27	11.5
4	.15	-.159 ±.024	.54	33	44
6	.02	-.057 ±.004	.59	36	189
7	.02	-.053 ±.003	.63	39	252
8	.02	-.047 ±.003	.6	36	224
10	.02	-.033 ±.003	.52	36	137
6	.15	-.084 ±.006	.72	33	165
7	.15	-.074 ±.009	.66	51	65
8	.15	-.055 ±.005	.66	45	102
10	.15	-.052 ±.005	.55	36	92
7	.05	-.060 ±.004	.68	45	234
7	.1	-.049 ±.003	.53	45	235
7	.25	-.045 ±.004	.58	73	108

* N is the number of data points used to calculate the regression.

** An explanation of the f-ratio test is given in Appendix 1.

Table 2.

Details of regressions for Transmission as a function of Hydration.

$T = + a_1 - a_2 \times H$ at λ = 550 nm

Solution pH	Solution μ	$-a_2 \pm$ s.e	a_1	N *	F-ratio **
2	.06	-.073 ±.006	.54	30	124
2	.15	-.108 ±.009	.55	30	141
4	.06	-.331 ±.050	.72	27	14
4	.15	-.144 ±.020	.85	33	36
6	.02	-.06 ±.004	.69	36	201
7	.02	-.049 ±.003	.66	39	239
8	.02	-.045 ±.003	.64	36	229
10	.02	-.031 ±.003	.57	36	126
6	.15	-.070 ±.006	.72	33	103
7	.15	-.070 ±.007	.71	51	119
8	.15	-.050 ±.005	.68	45	92
10	.15	-.047 ±.005	.56	36	72
7	.05	-.053 ± .004	.71	45	146
7	.1	-.042 ±.003	.59	45	162
7	.25	-.038 ±.004	.59	73	72

* N is the number of data points used to calculate the regression.

** An explanation of the f-ratio test is given in Appendix 1.

Table 3.

Details of regressions for Transmission as a function of Hydration.

$$T = +a_1 - a_2 \times H \quad \text{at } \lambda = 650 \text{ nm}$$

Solution pH	Solution μ	$-a_2 \pm$ s.e.	a_1	N *	F-ratio **
2	.06	-.073 ±.006	.57	30	149
2	.15	-.108 ±.009	.62	30	118
4	.06	-.309 ±.09	.73	27	129
4	.15	-.124 ±.02	.83	33	26
6	.02	-.058 ±.004	.69	36	189
7	.02	-.046 ±.003	.67	39	210
8	.02	-.042 ±.003	.65	36	181
10	.02	-.028 ±.003	.57	36	102
6	.15	-.064 ±.008	.71	33	71
7	.15	-.067 ±.007	.71	51	80
8	.15	-.047 ±.005	.69	45	82
10	.15	-.043 ±.005	.56	36	63
7	.05	-.046 ±.005	.72	45	98
7	.1	-.037 ±.003	.58	45	117
7	.25	-.033 ±.004	.6	73	53

* N is the number of data points used to calculate the regression.

** An explanation of the f-ratio test is given in Appendix 1.

Table 4.

Transmission through Beef Corneal Stroma at H = 3.5

Solution		Transmission		
pH	μ	λ = 450 nm	λ = 550 nm	λ = 650 nm
6	.02	.391	.480	.487
7	.02	.445	.489	.509
8	.02	.436	.483	.503
10	.02	.405	.462	.472
6	.15	.426	.475	.486
7	.15	.401	.465	.476
8	.15	.468	.505	.526
10	.15	.368	.396	.410

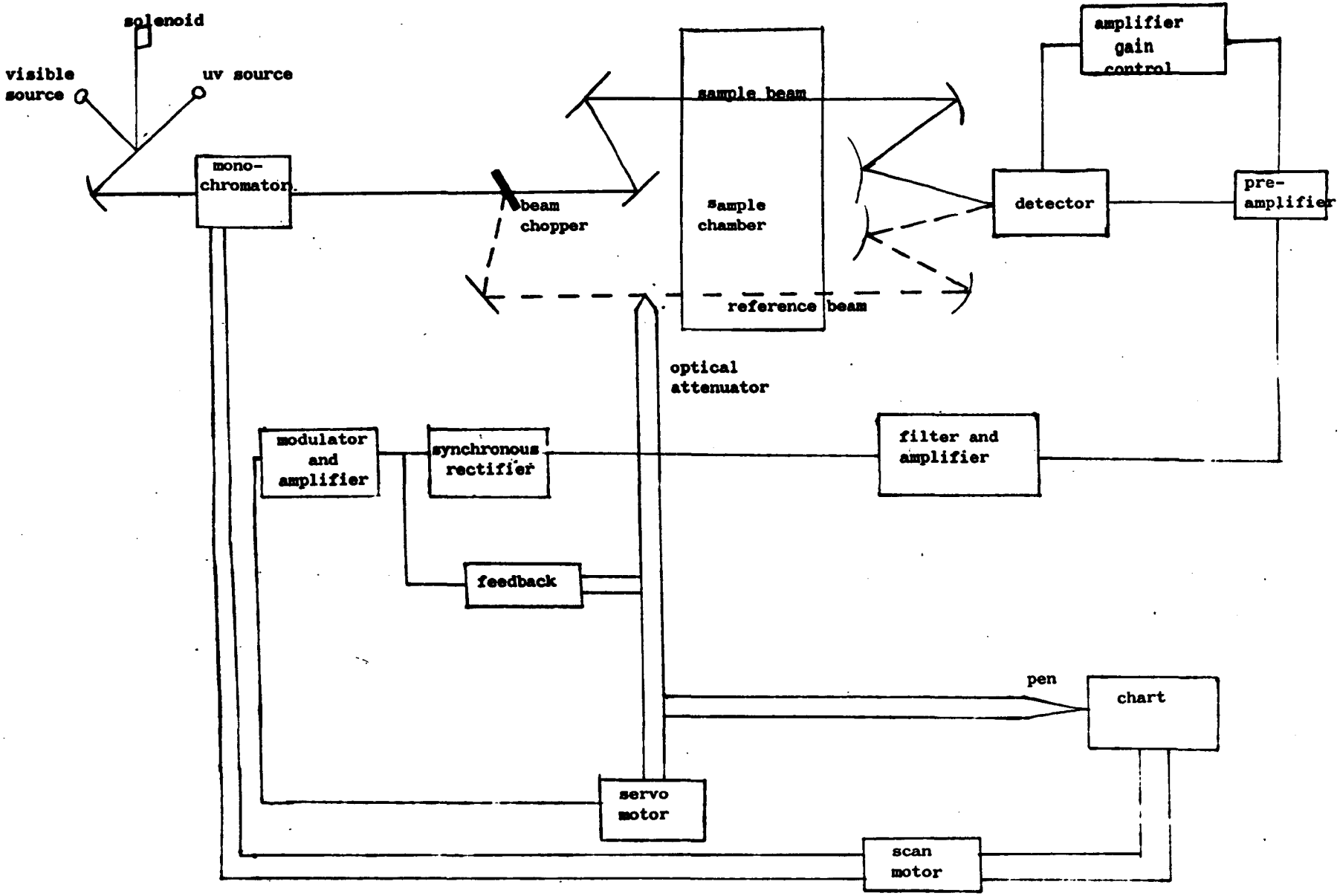

Fig. 1. Diagram of spectrophotometer circuit for measuring absorbance.

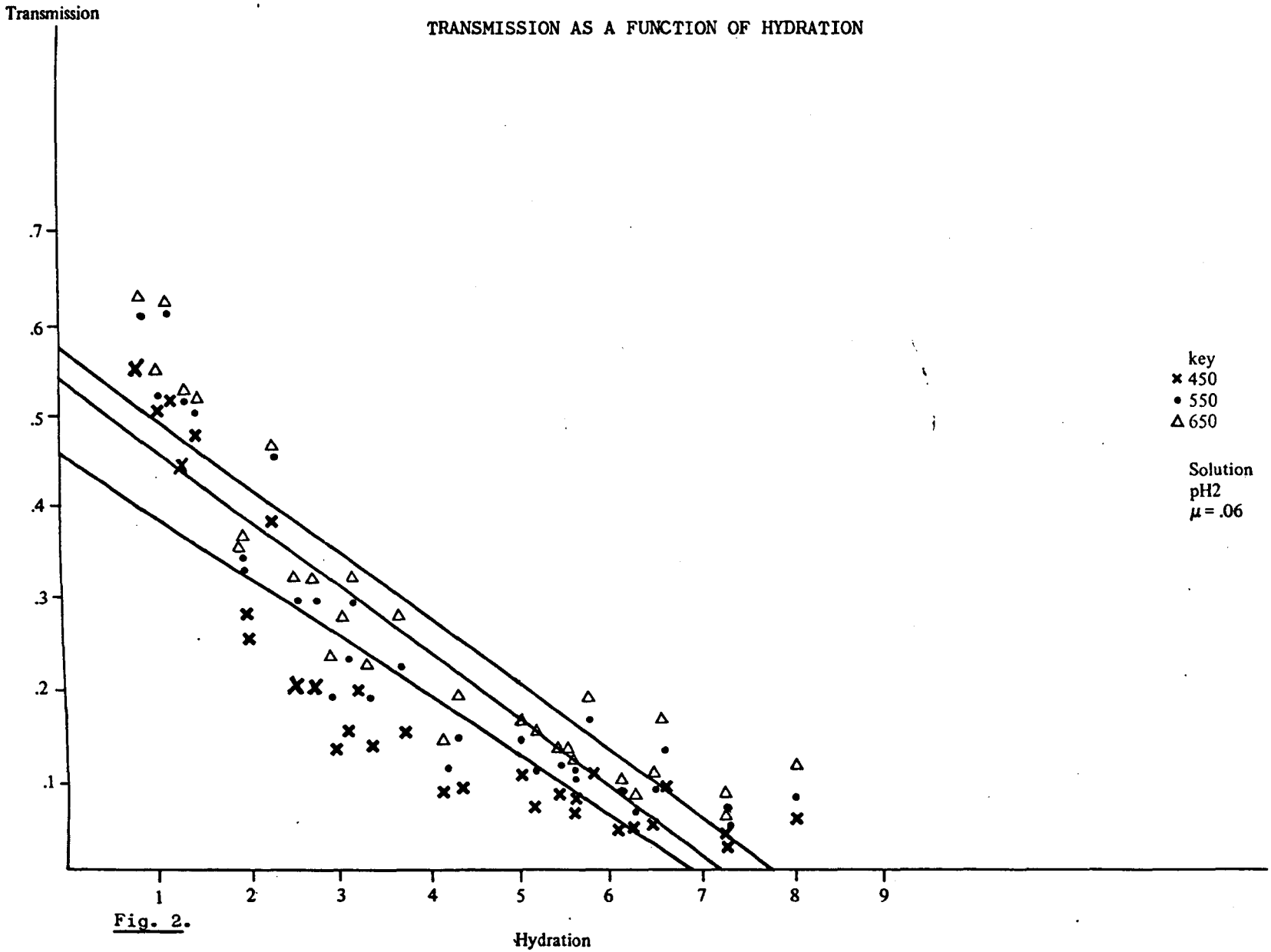
TRANSMISSION AS A FUNCTION OF HYDRATION
Transmission
.7
.6
.5
.4
.3
.2
.1
1
2
3
4
5
6
7
8
9
Hydration
key
× 450
• 550
△ 650
Solution
pH2
μ = .06

Fig. 2.

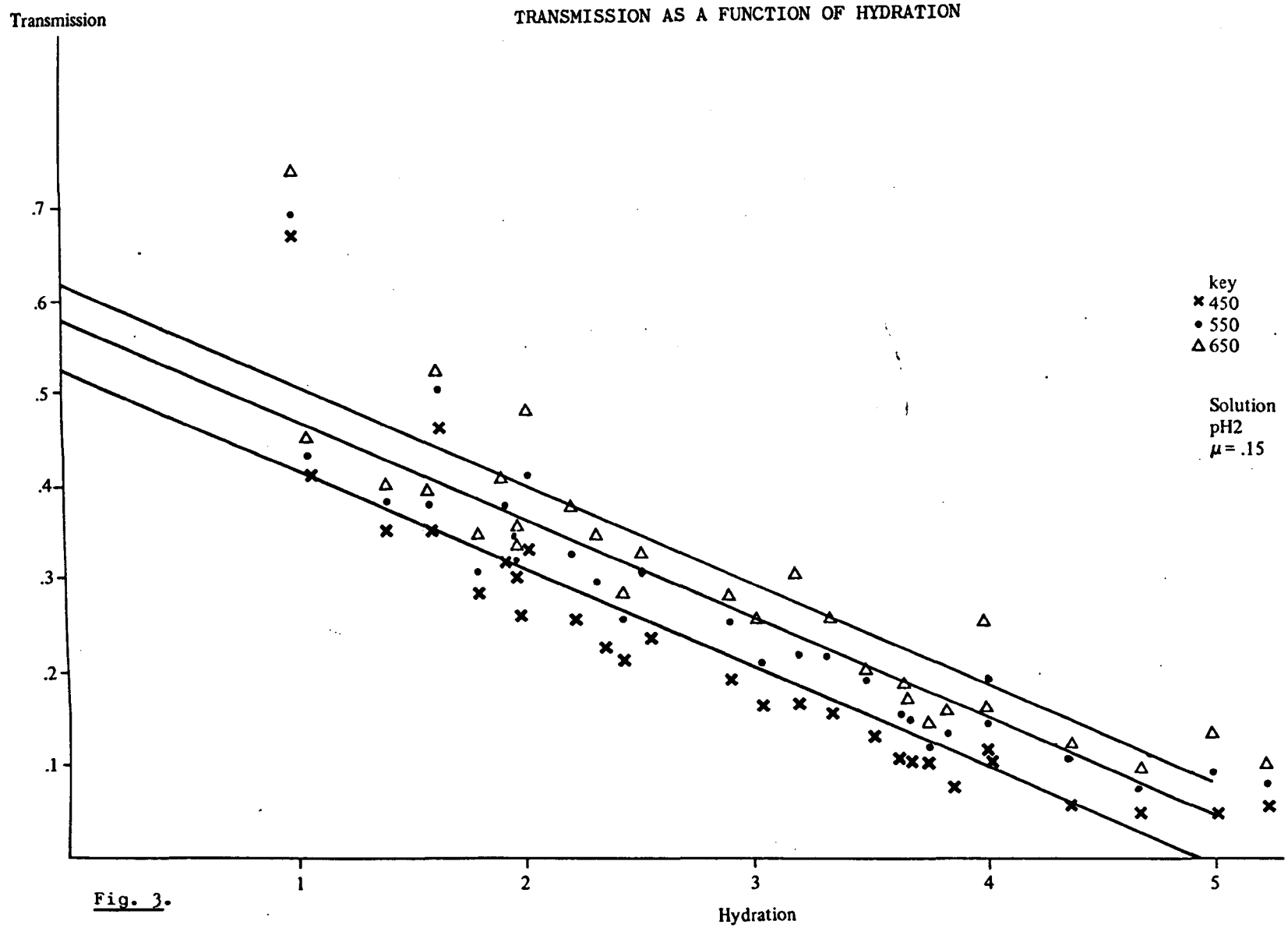
TRANSMISSION AS A FUNCTION OF HYDRATION
Transmission
.7
.6
.5
.4
.3
.2
.1
1
2
3
4
5
Hydration
key
× 450
• 550
△ 650
Solution
pH2
μ = .15

Fig. 3.

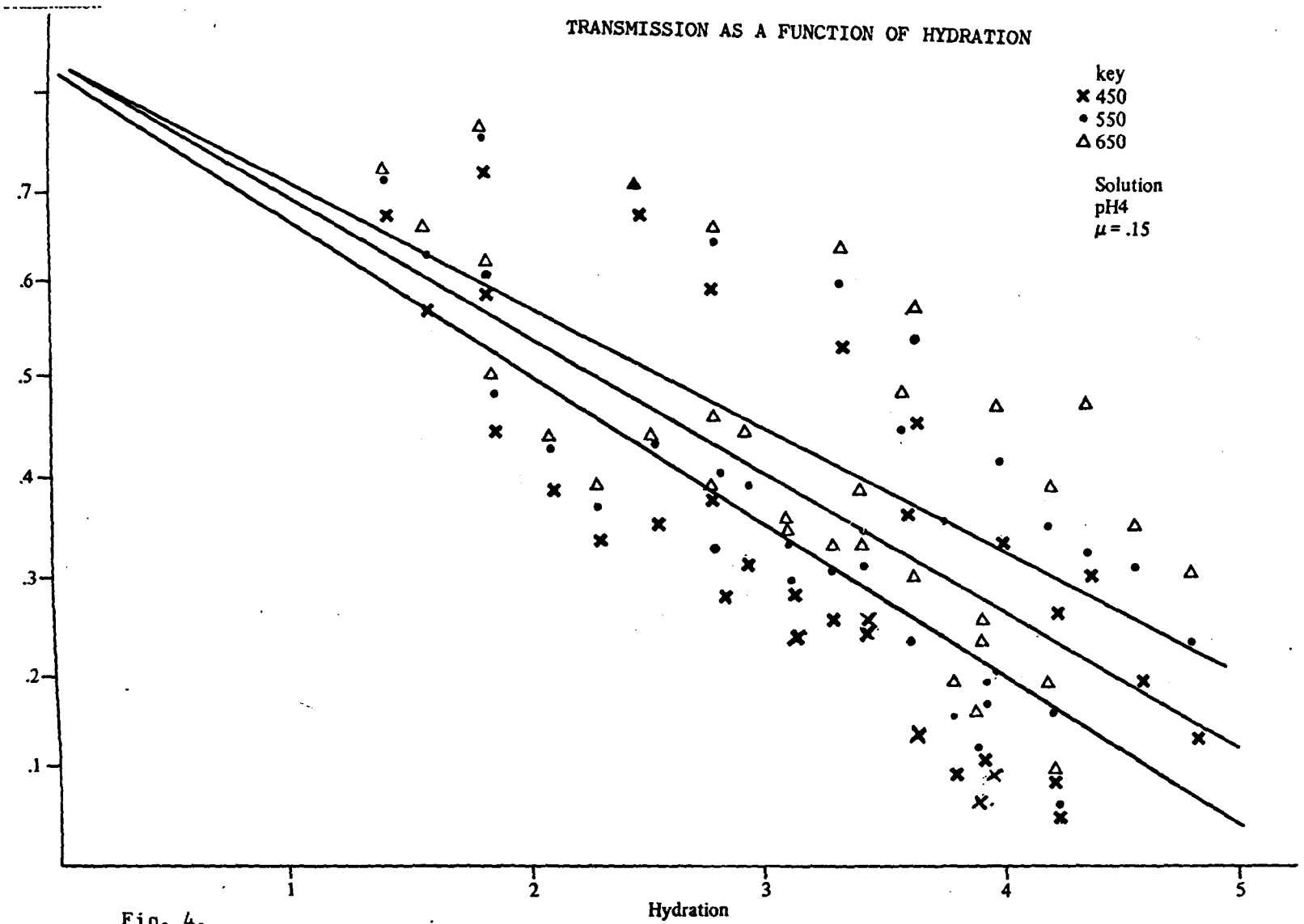
TRANSMISSION AS A FUNCTION OF HYDRATION
key
450
550
650
Solution
pH4
μ = .15
.7
.6
.5
.4
.3
.2
.1
1
2
3
4
5
Hydration

Fig. 4.

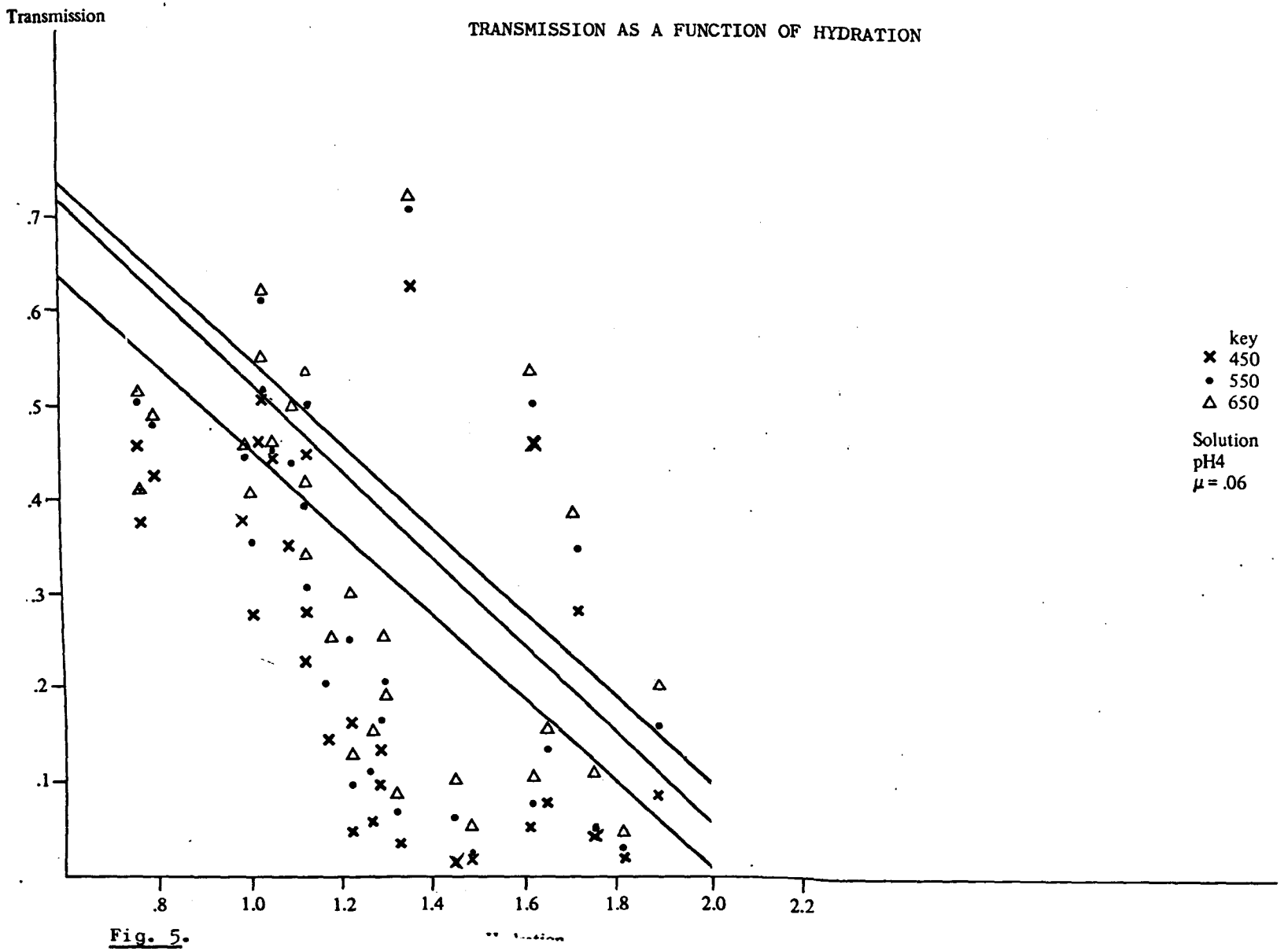
Transmission
TRANSMISSION AS A FUNCTION OF HYDRATION
.7
.6
.5
.4
.3
.2
.1
.8
1.0
1.2
1.4
1.6
1.8
2.0
2.2
key
× 450
• 550
△ 650
Solution
pH4
μ = .06

Fig. 5.

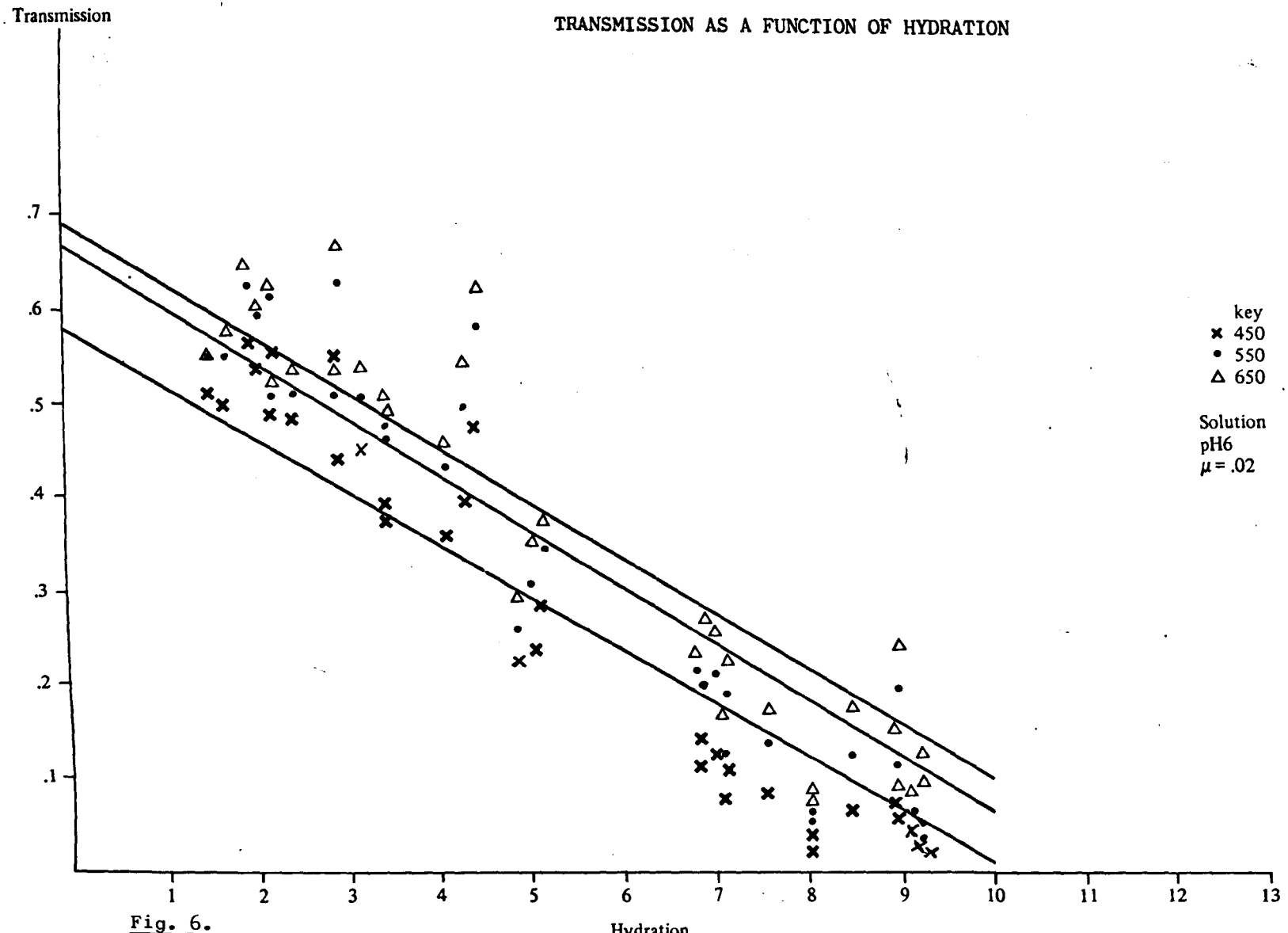
TRANSMISSION AS A FUNCTION OF HYDRATION
Transmission
.7
.6
.5
.4
.3
.2
.1
1
2
3
4
5
6
7
8
9
10
11
12
13
Hydration
key
× 450
• 550
△ 650
Solution
pH6
μ = .02

Fig. 6.

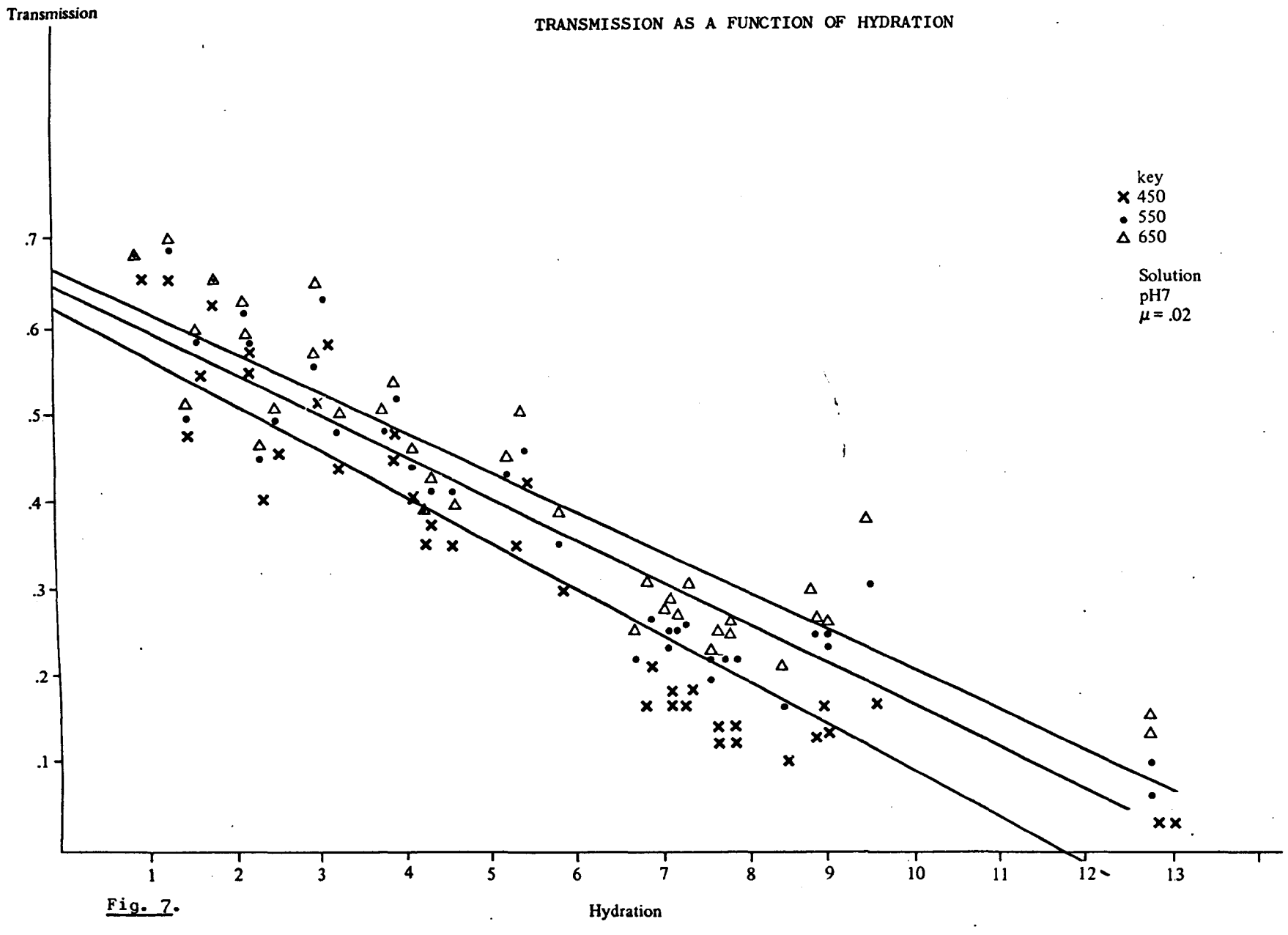
TRANSMISSION AS A FUNCTION OF HYDRATION
Transmission
.7
.6
.5
.4
.3
.2
.1
1
2
3
4
5
6
7
8
9
10
11
12
13
Hydration
key
× 450
• 550
△ 650
Solution
pH7
μ = .02

Fig. 7.

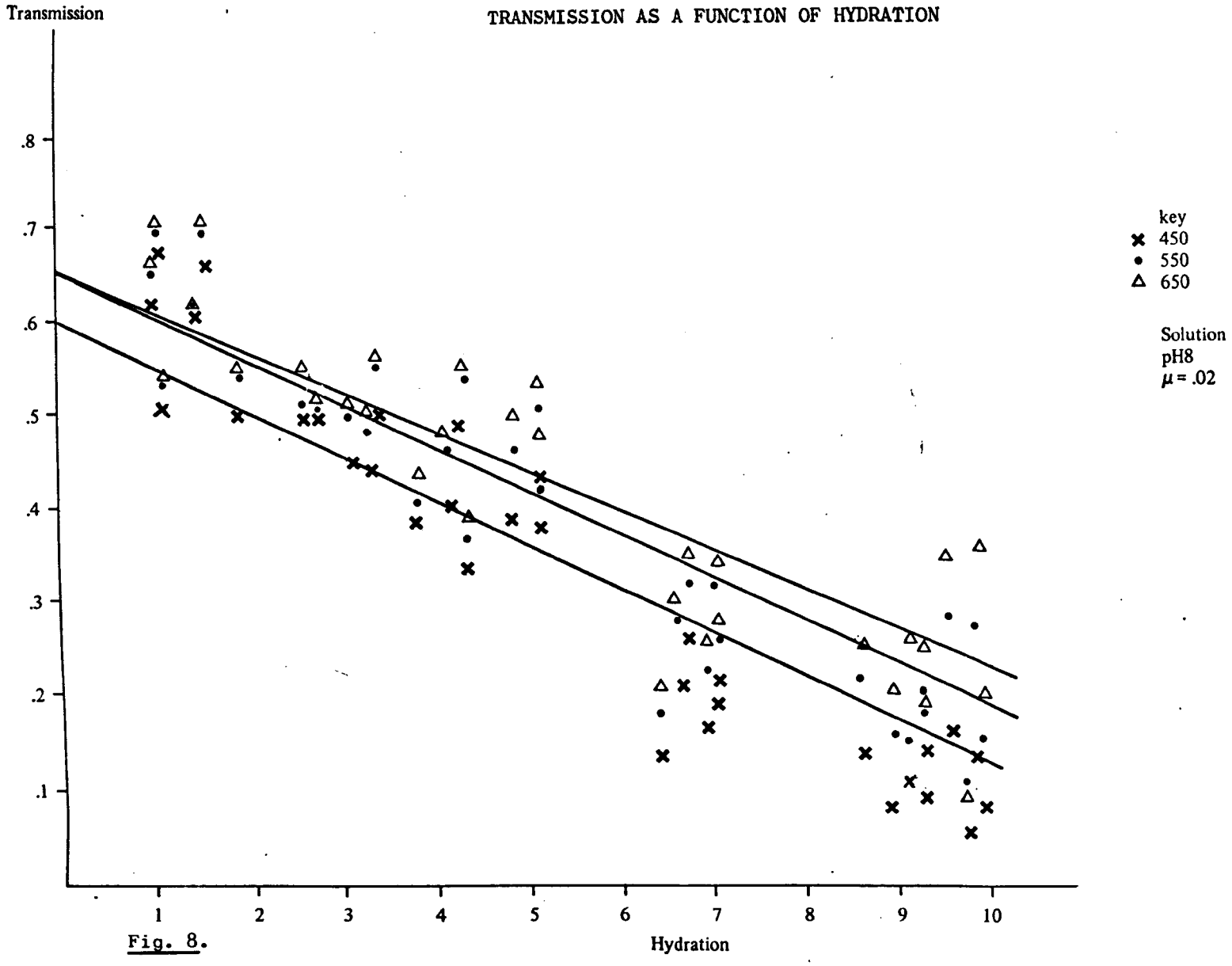
TRANSMISSION AS A FUNCTION OF HYDRATION
Transmission
.8
.7
.6
.5
.4
.3
.2
.1
1
2
3
4
5
6
7
8
9
10
Hydration
key
450
550
650
Solution
pH8
μ = .02

Fig. 8.

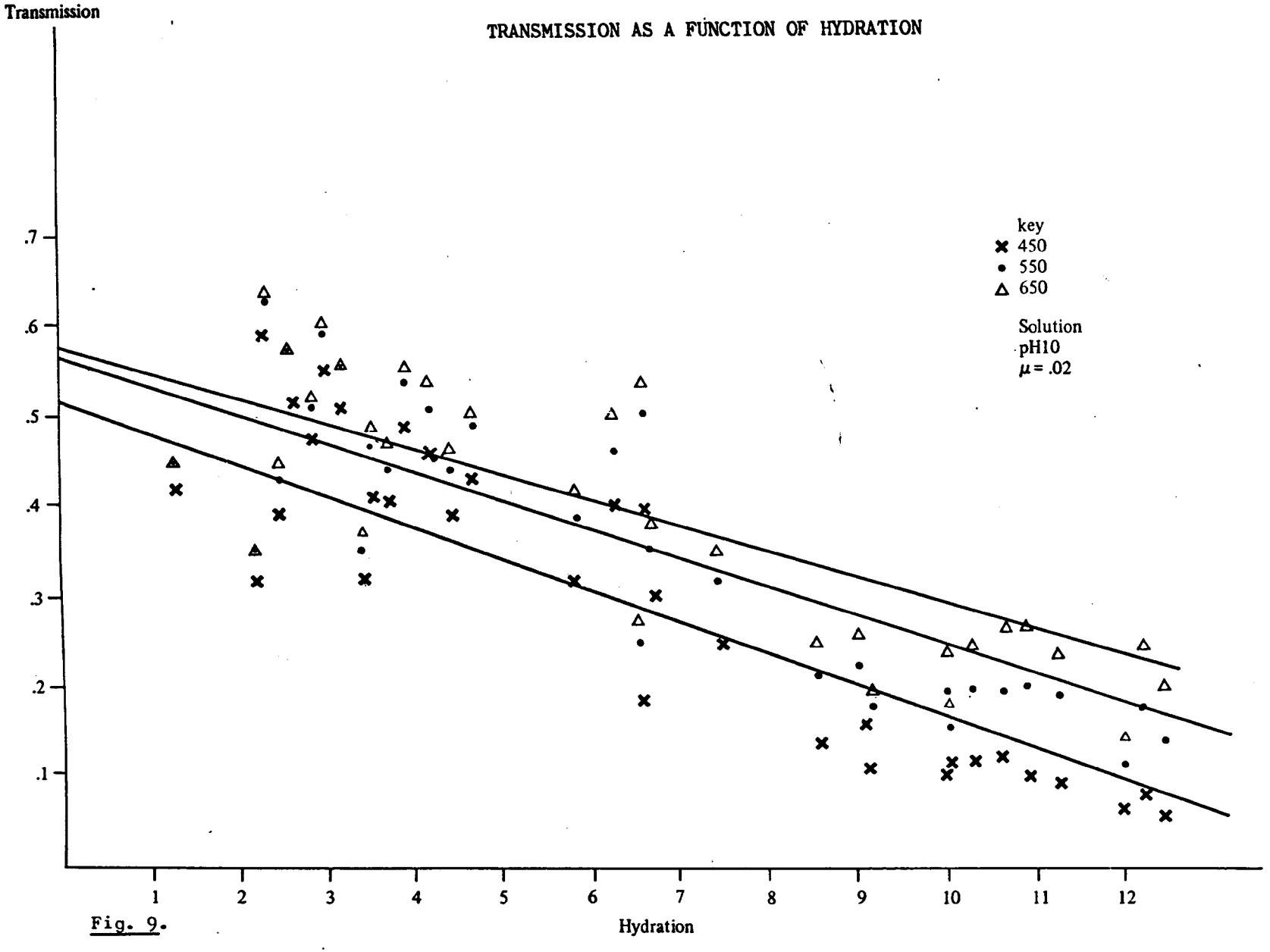
TRANSMISSION AS A FUNCTION OF HYDRATION
Transmission
.7
.6
.5
.4
.3
.2
.1
1
2
3
4
5
6
7
8
9
10
11
12
Hydration
key
450
550
650
Solution
pH10
μ = .02

Fig. 9.

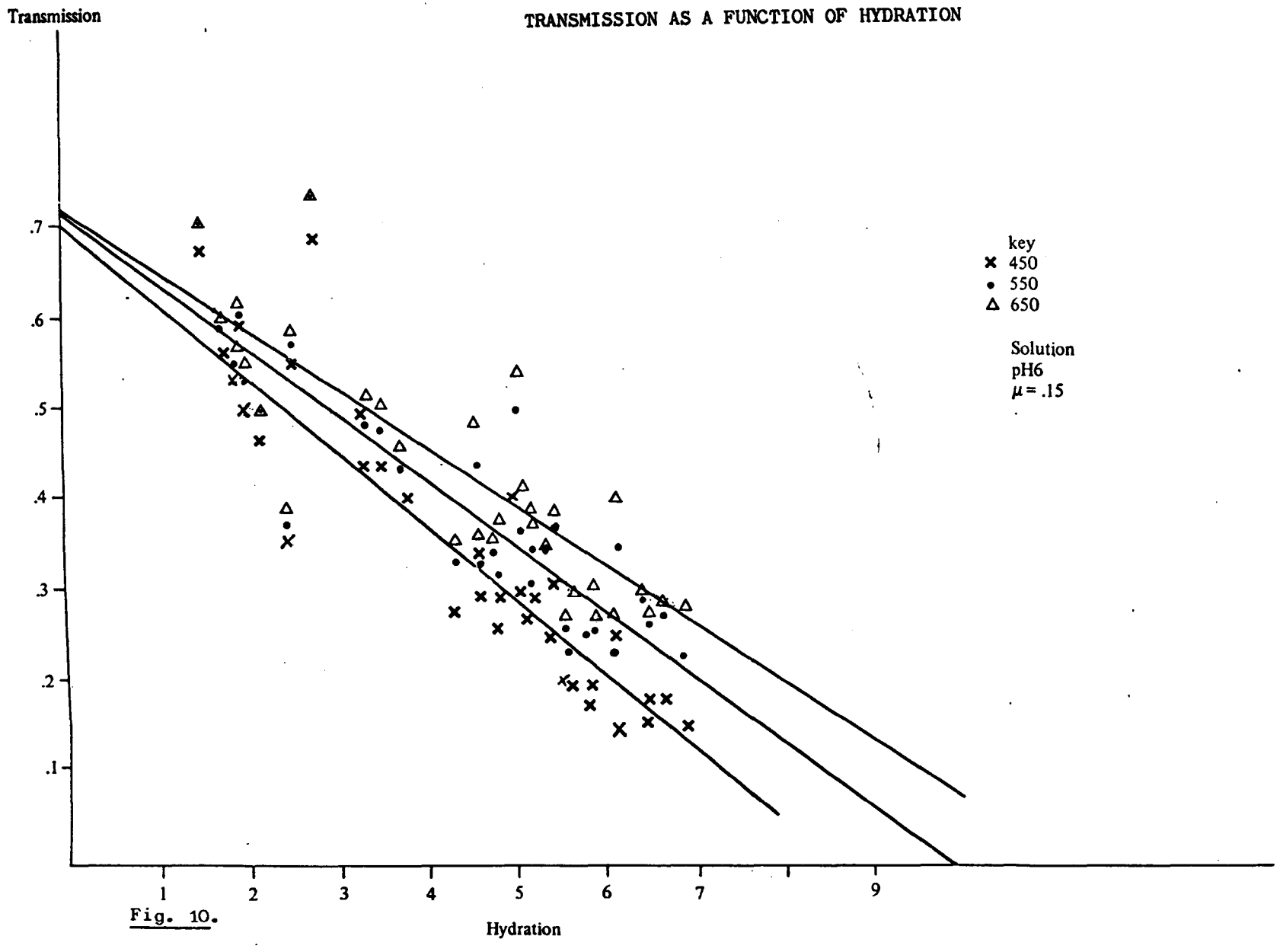
TRANSMISSION AS A FUNCTION OF HYDRATION
Transmission
.7
.6
.5
.4
.3
.2
.1
1
2
3
4
5
6
7
9
Hydration
key
× 450
• 550
△ 650
Solution
pH6
μ = .15

Fig. 10.

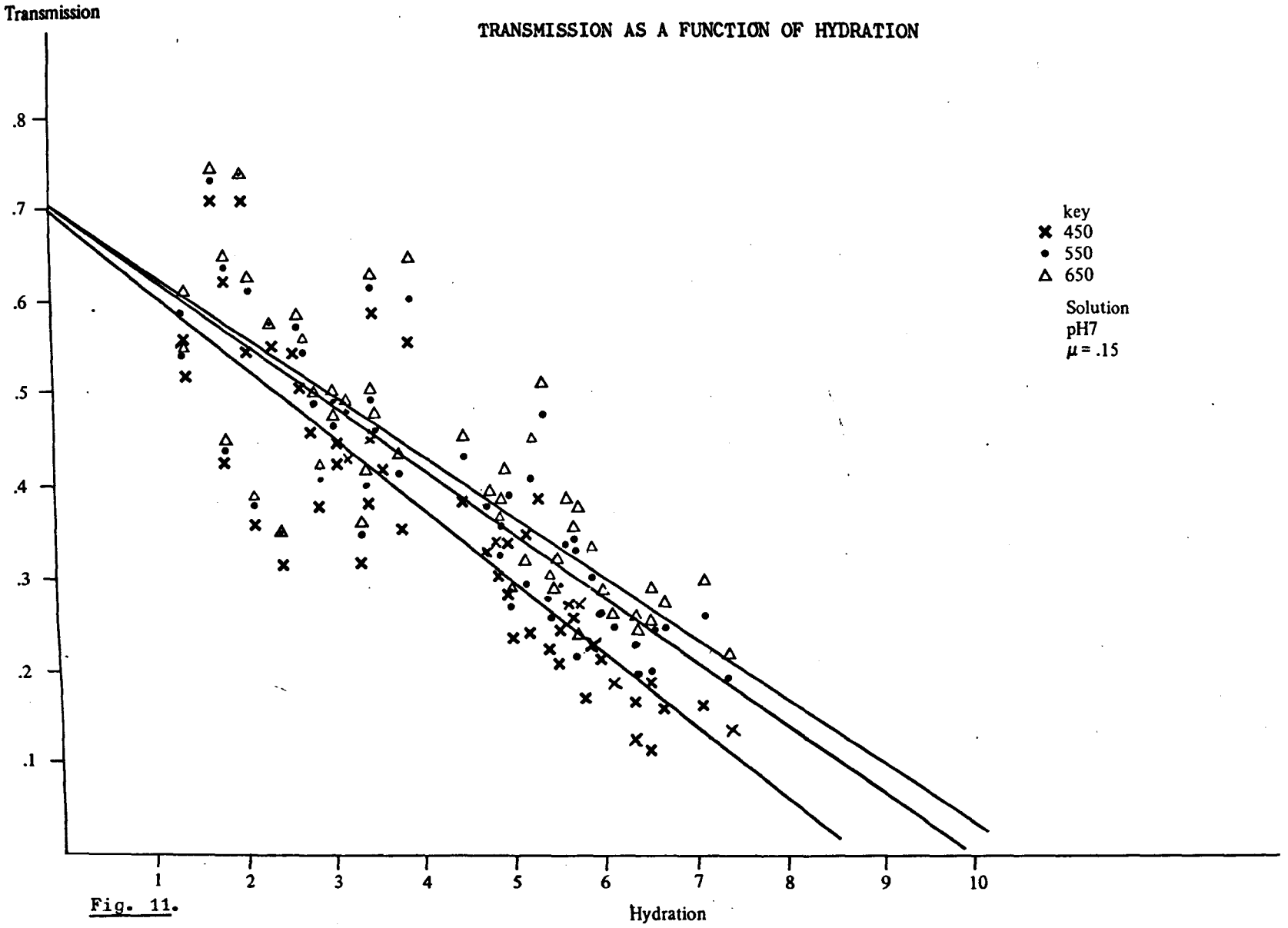
TRANSMISSION AS A FUNCTION OF HYDRATION
Transmission
.8
.7
.6
.5
.4
.3
.2
.1
1
2
3
4
5
6
7
8
9
10
Hydration
key
450
550
650
Solution
pH7
μ = .15

Fig. 11.

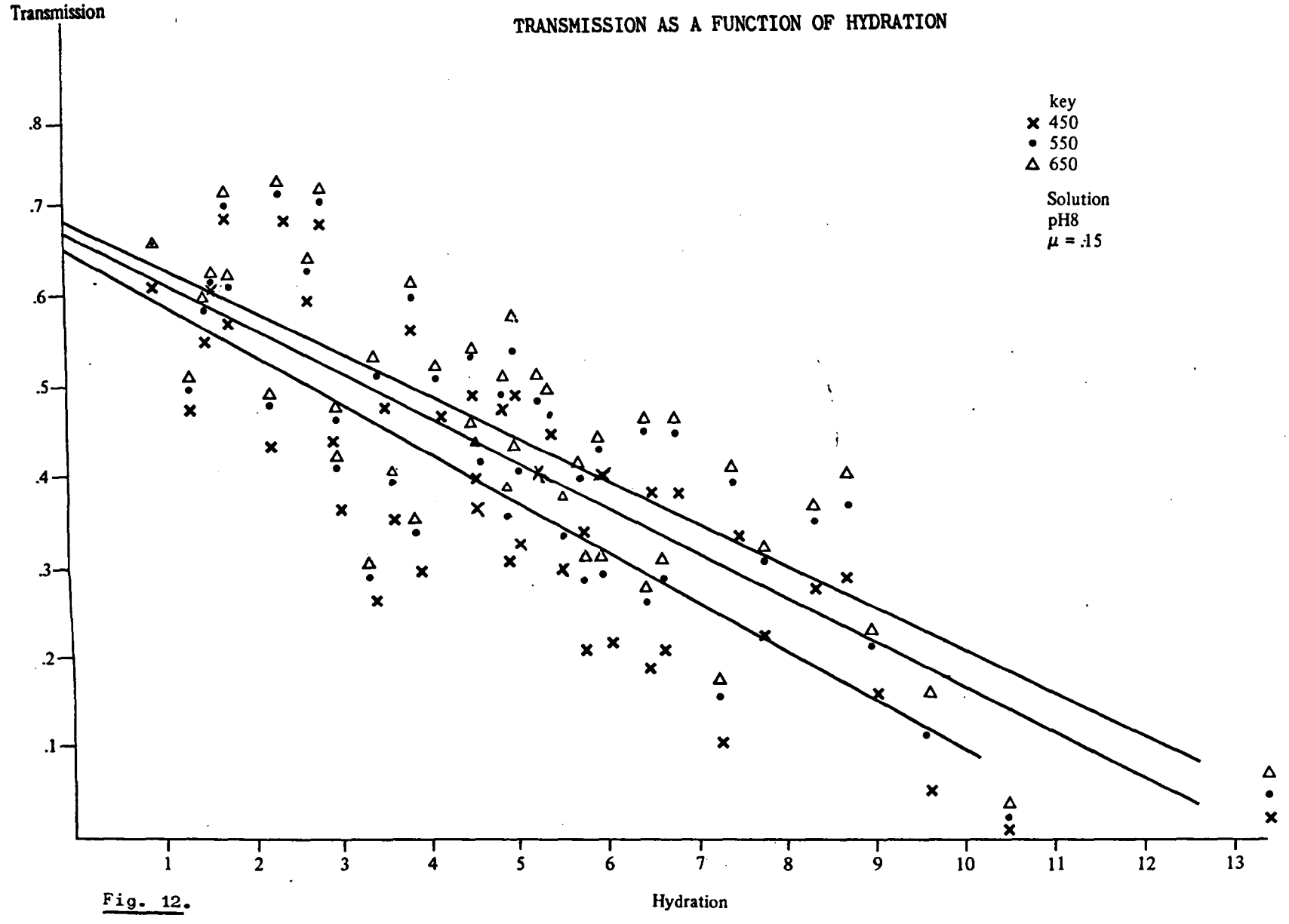
TRANSMISSION AS A FUNCTION OF HYDRATION
Transmission
.8
.7
.6
.5
.4
.3
.2
.1
1
2
3
4
5
6
7
8
9
10
11
12
13
Hydration
key
× 450
• 550
△ 650
Solution
pH8
μ = .15

Fig. 12.

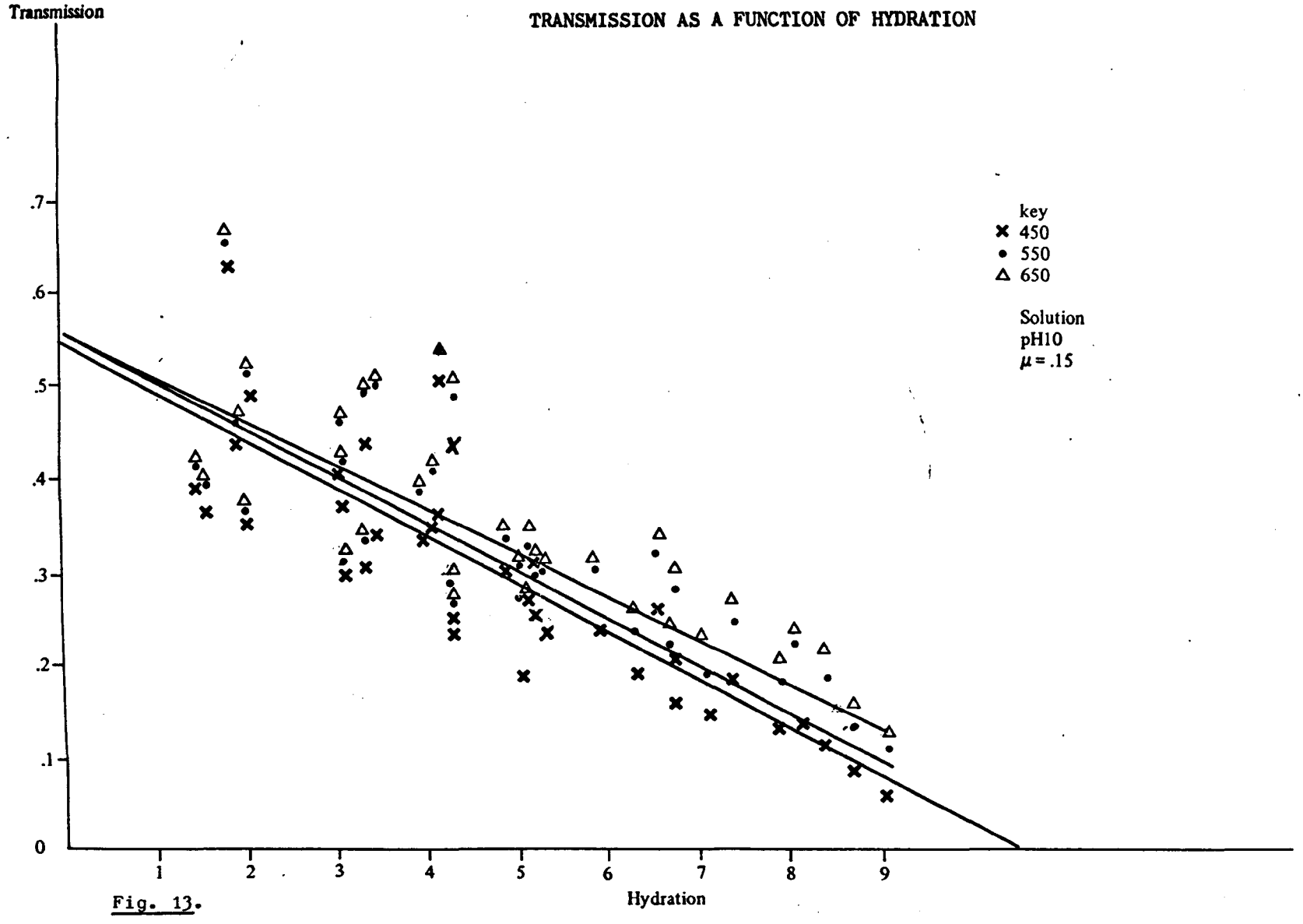
TRANSMISSION AS A FUNCTION OF HYDRATION
Transmission
.7
.6
.5
.4
.3
.2
.1
0
1
2
3
4
5
6
7
8
9
Hydration
key
450
550
650
Solution
pH10
μ = .15

Fig. 13.

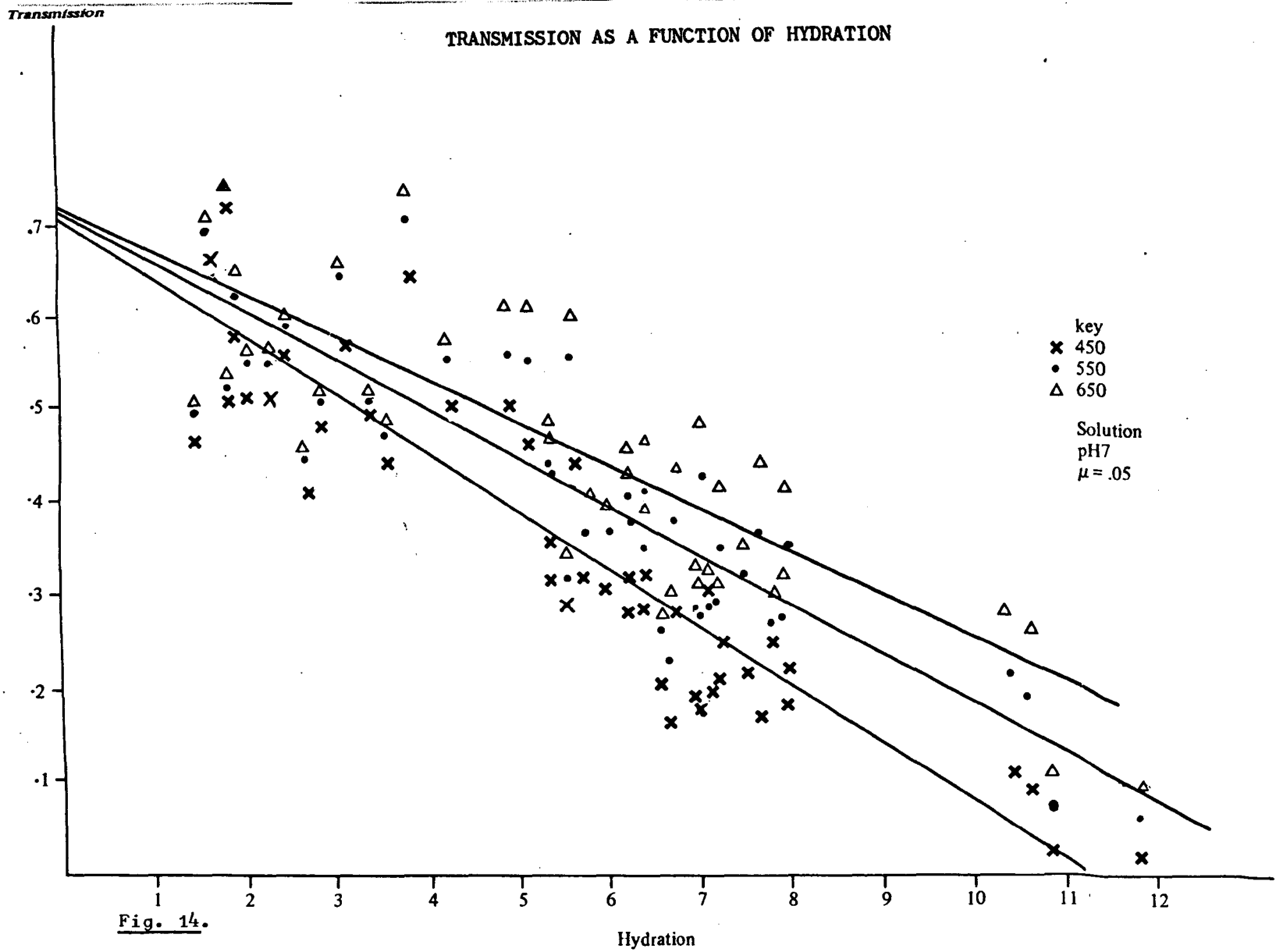
Transmission
TRANSMISSION AS A FUNCTION OF HYDRATION
.7
.6
.5
·4
·3
·2
·1
1
2
3
4
5
6
7
8
9
10
11
12
Hydration
key
450
550
650
Solution
pH7
μ = .05

Fig. 14.

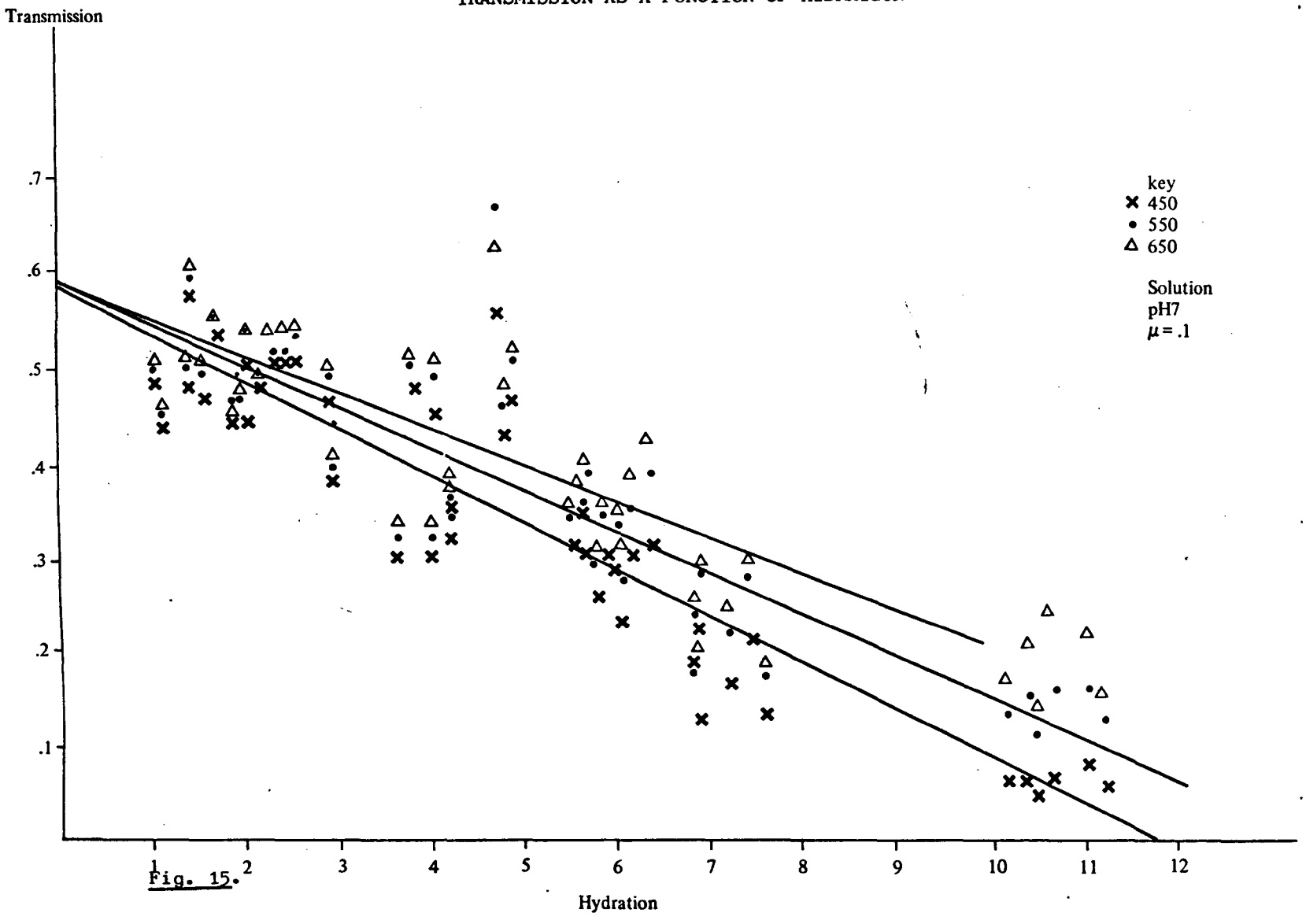
TRANSMISSION AS A FUNCTION OF HYDRATION
Transmission
.7
.6
.5
.4
.3
.2
.1
1
2
3
4
5
6
7
8
9
10
11
12
Hydration
key
× 450
• 550
△ 650
Solution
pH7
μ = .1

Fig. 15.

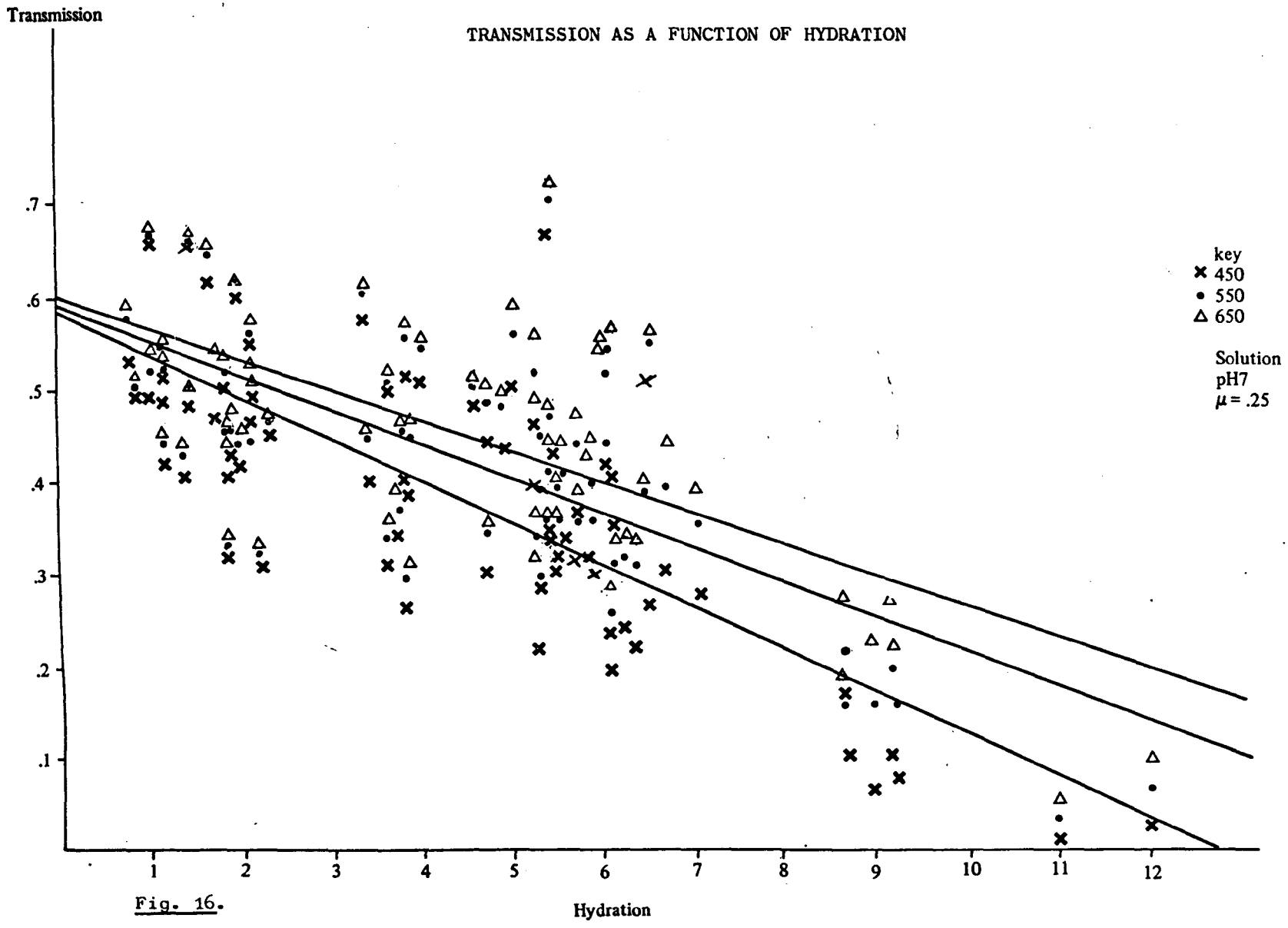
TRANSMISSION AS A FUNCTION OF HYDRATION
Transmission
.7
.6
.5
.4
.3
.2
.1
1
2
3
4
5
6
7
8
9
10
11
12
Hydration
key
× 450
• 550
△ 650
Solution
pH7
μ = .25

Fig. 16.

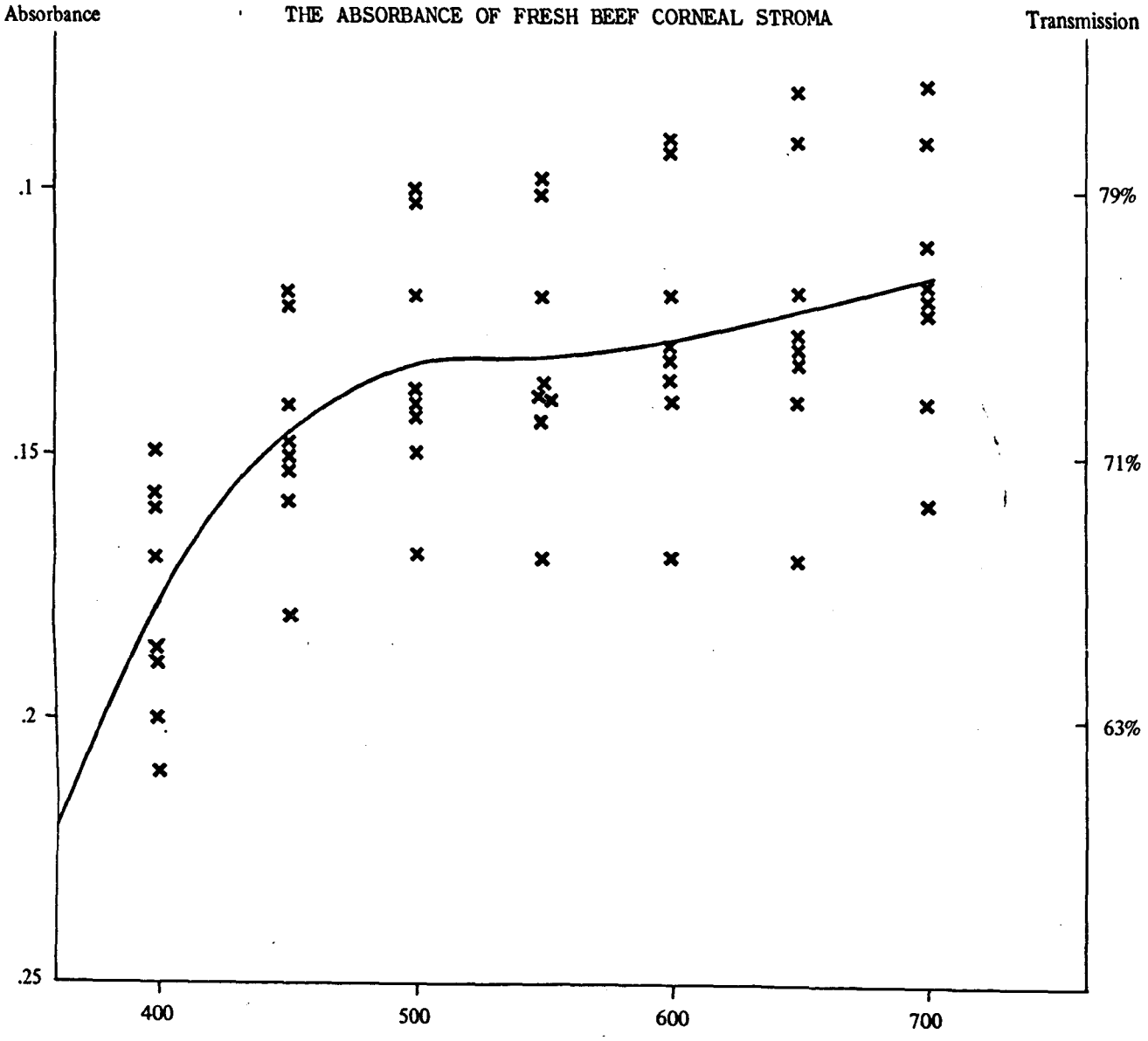
Absorbance
THE ABSORBANCE OF FRESH BEEF CORNEAL STROMA
Transmission
.1
.15
.2
.25
79%
71%
63%
400
500
600
700
Wavelength nm

Fig. 17.

RATE OF DECREASE OF TRANSMISSION WITH HYDRATION AS A FUNCTION OF pH.

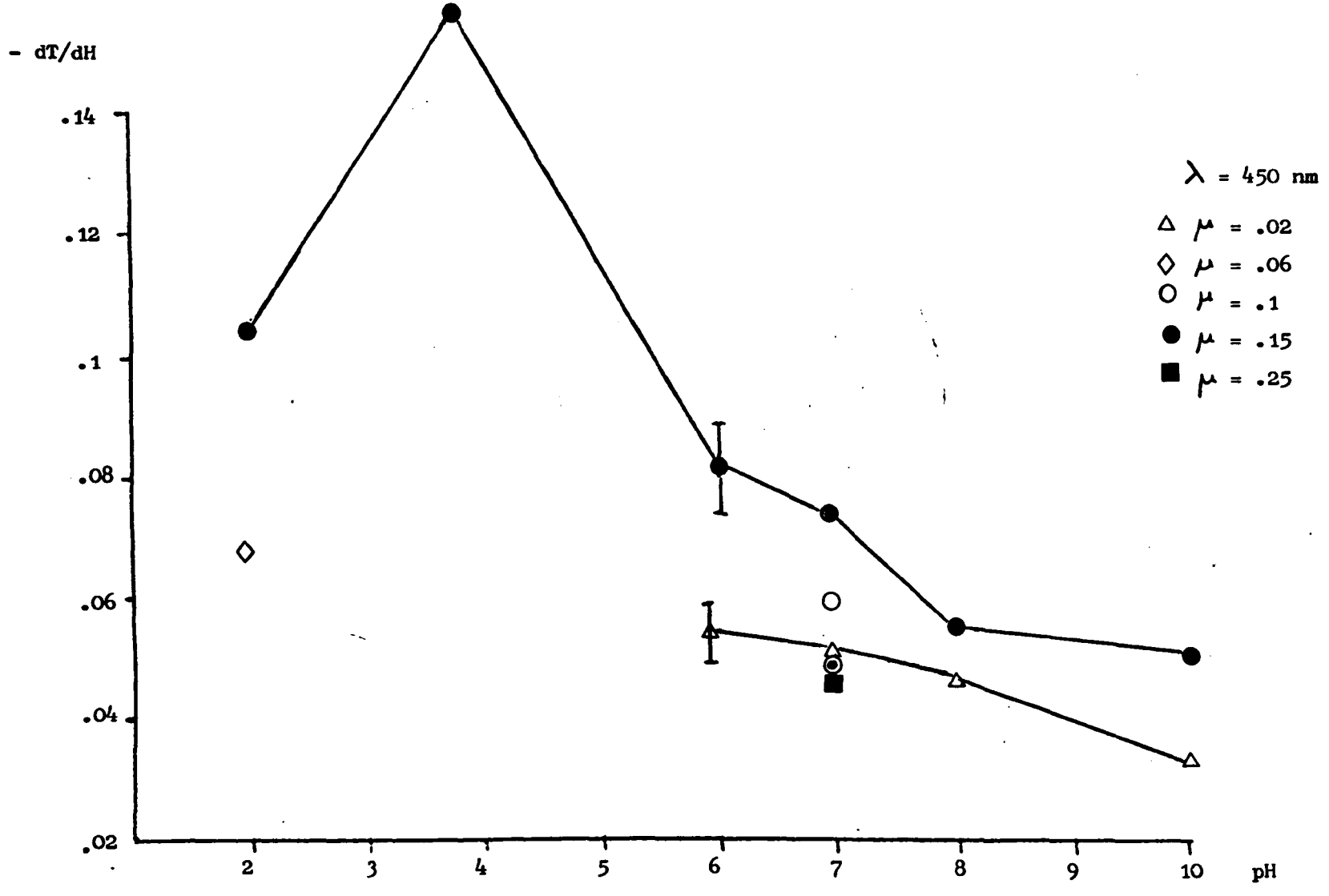

Fig. 18.

Chapter 6.

Discussion.

I General Comments.

Four different techniques are used, in this thesis, to study the structure and factors affecting the structure of the corneal stroma as it is allowed to swell freely in salt solutions of known pH and ionic strength. In this chapter, I should like to make comparisons between the corneal stroma and other biological systems as well as between specific measurements obtained from more than one technique e.g. the fixed charge concentration can be calculated from the microelectrode measurements as well as being estimated from the swelling results. Correlations between various parameters e.g. absorbance and percentage of the total water in 'lakes', rate of hydration and rate of decrease of transmission with hydration are also discussed below.

II Comparison with Other Tissues.

The results on the dependence of the swelling on both pH and ionic strength are consistent with the hypothesis that the fixed charge concentration is the most important parameter in regulating the swelling pressure. The fixed charge comes from the presence in the stroma of polyelectrolytes i.e. glycosaminoglycans and collagen which cause an unequal distribution of permeant ions in order to maintain electrical neautrality. The distribution of ions gives rise to an osmotic pressure difference and hence causes swelling.

Bungenberg de Jong (1949) has described systems, such as connective tissues, containing two oppositely charged polyelectrolytes as complex colloid systems. Such systems have maximum absorbance at the point of minimum swelling when the number of fixed positively charged groups is equal to the number of fixed negative groups (Loeven, 1955).

Thus the stroma is similar to other connective tissues e.g. cartilage and sclera except that there appears to be no force opposing the swelling. In cartilage, this force is elastic and due to cross-linking between the collagen fibrils (Maroudas, 1975). Other systems whose structure is dependent on the fixed charge from the presence of polyelectrolytes include myosin filaments of striated muscle and tobacco mosaic virus. Thus, they swell due to the osmotic pressure difference but reach equilibrium situations in which this repulsive force is balanced by an attractive force which may be due to the elastic cross-links or possibly to van der Waals forces (Elliott, 1968; Rome, 1968; Miller and Woodhead-Galloway, 1971). Because no equilibrium is reached in the swelling of the corneal stroma (in the pH region 6-10) it appears that any attractive forces must be very weak especially at high hydrations when the distance between the fibrils is large. At low hydrations, the osmotic pressure is likely to be very high because the concentration of fixed charge becomes large and thus it may swamp any attractive force which can exist when the fibrils are fairly close together.

III Organisation of the Corneal Collagen.

The arrangement of the collagen fibrils has been shown to give rise to the interfilament spacing indicating that some correlation in the positions of the fibrils exists. This could possibly be

a quasi-ordered quasi-random arrangement as proposed by Farrell and Hart (1969) where there is thought to be correlation in the position of nearest neighbours. Information about any further order is not available from the present x-ray data because of the lack of any other orders of the interfilament spacing. In section III, chapter 3, it was shown that even if a d_{11} spacing of a hypothetical hexagonal lattice existed, it would be very much weaker than the d_{10} spacing so that it might not be seen on film.

The other systems of charged cylindrical polyelectrolytes mentioned previously (myosin filaments in striated muscle and TMV) give rise to a more detailed x-ray pattern in which d_{11} spacings can be seen. In muscle, the low-angle x-ray diffraction pattern is due to both the myosin filaments in the A-band and the fraction of the actin filaments which are interdigitating with the myosin (Elliott et al, 1963). Myosin filaments from rabbit psoas muscle have a diameter of around 120 nm (Huxley, 1963) and a centre-to-centre distance of 380 nm (i.e. the ratio of diameter to distance apart is approximately the same as for the collagen fibrils in the cornea) so that their transform and hence intensity would be expected to fall off fairly rapidly with higher orders. However, the position (at the trigonal points of the myosin lattice) and the size (6 nm) (Huxley, 1963) of the actin filaments are such that they contribute to the d_{11} reflection and increase its intensity. Thus the d_{11} reflection is readily seen in muscle but does not appear in the x-ray pattern from the cornea.

Another technique for looking at the order in the collagen lattice, and possible decrease on swelling, is the measurement of the line-widths of the reflections. The line-width is found from the microdensitometer trace of the x-ray pattern on film and is a measure of the intensity of

the reflection to its width. Thus a sharp reflection, small linewidth, would be expected from an ordered system. On swelling, when the lattice is likely to become more disordered, the line-width would increase i.e. the reflection becomes more diffuse. It has not been found possible to undertake this experiment with the apparatus at present available. The line-width of the reflection from fresh tissue can just be measured but only with a large experimental uncertainty. The fall-off in the intensity of the reflection, even at d_{10} = 60 nm, merges into the back-stop scatter so that the overall shape of the intensity cannot be recorded. At larger spacings the reflection becomes smaller in size so that even more of the overall shape is lost behind the back-stop scatter. This may partly be due to the loss in resolution obtained by using film and a micro-densitometer to record the intensity profile.

In order to measure the line-widths at these large spacings it will be necessary to use a very long specimen to film distance with a mirror-monochromator camera. However, the exposure time for such an experimental set up is long and much background scatter will occur. The use of more intense x-ray sources, which are now available, may help solve this problem. Finally the intensity profile may be found directly by the use of a position-sensitive proportional counter from which the number of quanta reaching a given point along the wire is recorded and shown on a screen. The line-width can be found directly from the data. Thus, it might be possible to monitor the change in the line-width on the interfilament reflection as a function of the hydration of the tissue.

IV Absence of the First Order of the Collagen Pattern

The absence of the first order of the collagen pattern is surprising because in most collagens this reflection is very intense relative to other orders (e.g. Tomlin and Worthington, 1956). The Patterson function suggests that regions of high electron density exist at distances of .24D and .38D apart (Chapter 3, section III). The reason for this is not known but may be due to the interaction of the glycosaminoglycans at specific sites along the collagen repeat distance, D. The absence of this first order has been confirmed by the light diffraction of electron micrographs (fig. 24, Chapter 3).

Experiments to verify this hypothesis, that the interaction of the glycosaminoglycans with the collagen is the reason for the lack of the first order, must involve the separation of the glycosaminoglycans from the collagen and the corresponding appearance of the first order, 66nm reflection. A possible method involves the use of enzymic digestion to remove the glycosaminoglycans. Although chondroitin sulphatase is commercially available, its substrate is only chondroitin sulphates and not keratan sulphate, which is the major glycosaminoglycan in the corneal stroma (Chapter 1, section IV, iv). Keratan sulphatase is not readily available

V Comparison of the Measurements of Fixed Charge Concentration.

The fixed charge concentration in the stroma has been measured by the use of microelectrodes (Chapter 4) and estimated from the use of the Donnan theory of swelling to interpret the

swelling data. It can be seen that although quantitatively there is a discrepancy in the magnitude of the two sets of results (table 7, Chapter 2 and table 2, chapter 4), there is a large measure of agreement between these results on the dependence of the fixed charge concentration on pH and ionic strength.

The swelling results indicate that increasing the pH tends, in general, to increase the estimated value of fixed charge concentration at physiological hydration i.e. H = 3.5 (Table 7, Chapter 2). The microelectrode data indicates the same general dependence on pH at both μ = .02 and μ = .15 the only two ionic strengths studied (table 2, Chapter 4).

The dependence of the fixed charge on the ionic strength of the bathing solution is more complex. The swelling results indicate that the fixed charge concentration at H = 3.5, at pH 7, increases from 17 $\pm$.3 mequivl^{-1} at μ = .05, to 18 $\pm$ .5 mequivl^{-1} at μ = .02, 22 $\pm$ .6 mequivl^{-1} at μ = .1, 29 $\pm$ 1.2 mequivl^{-1} at μ = .25 and 33 $\pm$ .9 mequivl^{-1} at μ = .15. A similar dependence on ionic strength is seen with the fixed charge concentration directly from the potential. The lowest fixed charge concentration is found at μ = .02, the next at μ = .05, then μ = .25 and the largest at μ = .15.

A better quantitative agreement can be obtained using activity coefficients instead of the concentrations alone. In section V, vii, Chapter 4, it is shown that the use of activity coefficients for the counterion (i.e. sodium) reduces the fixed charge concentration because of the expected decrease in activity of sodium ions in the presence of negatively charged polyelectrolyte (Katchalsky, 1954). No

measurements of the activities of the counterions has been made for the stroma but this experiment is possible using ion-selective microelectrodes.

The use of activities in the derivation of the theory in Chapter 2, section II will increase the value of the fixed charge concentration although it is difficult to predict the amount in the absence of experimental values for the activities.

VI Comparison of the Rate of Loss of Transmission with the Rate of Hydration.

The rate of hydration, dH/dt, is found to be very strongly dependent on the solution in which the corneal stroma is bathing (Chapter 2). In general, it is found that an increase in the pH of the bathing solution increases the rate of hydration in the 'high' pH range. At low pH, a final constant values of the hydration is maintained after about 10-20 hours. With this swelling behaviour in mind, it is interesting to compare the rate of loss of transparency with hydration, dT/dH, in different solutions, with the rate of hydration of the stroma, in the same solution.

The greatest value of dT/dH is found when the stroma is swollen in solutions at pH 4. At μ = .06, dT/dH is equal to .311 $\pm$ .091 (at λ = 450 nm). This is approximately four times greater in magnitude than dT/dH at pH 7, μ = .15. On increasing the ionic strength to μ = .15, at pH 4, dT/dH decreases to .159 $\pm$ .024 (Chapter 4, table 1 The swelling of the corneal stroma, at pH 4, is least at μ = .06 and increases with increasing ionic strength. Thus it can be seen

that the bathing solution which produces the smallest amount of swelling causes the greatest loss of transmission with hydration.

This behaviour is consistent with that expected from the complex colloid systems of Bungenberg de Jong (1949) and found for 'model systems' of connective tissues (i.e. mixtures of gelatin and chondroitin sulphate) by Loeven (1955).

Swelling of the corneal stroma at pH 2 also give rise to a constant final value of the hydration which decreases in value with increasing ionic strength of the bathing solution. At pH 2, μ = .06, the value of dT/dH is equal to .067 $\pm$ .007 which is similar to that in solutions of high pH value. Increasing the ionic strength to μ = .15 increases the rate of loss of transmission to .107 $\pm$ .009. Thus, the rate of loss of hydration is increasing with increasing ionic strength although the value of the final hydration is decreasing. Again, we find that the smaller amount of swelling is giving rise to the largest drop in transparency with hydration.

In the high pH range, the loss of transparency, dT/dH, decreases as the pH is increased from 6 to 10. At μ = .02, dT/dH is equal to .057 $\pm$ .004, at pH 6, and decreases to . 033 $\pm$ .003, at pH 10 (λ = 450 nm) (table 1, Chapter 5). Increasing the pH of the bathing solution was found to increase the rate of hydration (Chapter 2). Therefore we must associate a high loss of transparency with hydration dT/dH, with a small rate of hydration. A similar relation is found at μ= .15. However, at this ionic strength the rate of hydration, for a given pH, is known to be less than at μ = .02 (Chapter 2) whereas the values of dT/dH for a give pH, are higher at μ = .15 than at

μ = .02. Again, a higher rate of hydration is associated with a lower value of dT/dH.

The behaviour of the rate of loss of transparency with changing ionic strength, at a constant pH of 7, does not show a complete inverse dependence on the rate of swelling. dT/dH at μ = .15 is larger than at μ = .02 and μ = .05 which is consistent with inverse dependence on the rate of swelling. However, the swelling rate of μ = .25 and μ = .1 is known to be less than at u = .15 (Chapter 2) for a given pH but the rate of loss of transparency is greater at the latter ionic strength than at μ = .25 and μ = .1 (Chapter5, table 1).

It can be concluded that there appears to be, in general, a correlation of high rate of loss of transparency with a small rate of hydration although exceptions occur when the ionic strength dependencies of dT/dH and dH/dt are considered. The reason for such a correlation is not known although it appears that the rate of loss of transparency with time dT/dt (assumed equal to the product of dT/dH and dH/dt) must be approximately constant, for a given ionic strength if dT/dH decreases with pH and dH/dt increases with pH i.e. dT/dt is independent of pH of the bathing solution.

VII Correlation of Transmission with the Percentage of 'Lakes'.

In chapter 3, it was shown that the percentage of water not in the lattice of fibrils and, therefore, possibly in 'lakes' as described by Benedek (1971) is a function of the pH of the bathing solution. In particular, it was seen that the minimum percentage of the total water content which was in the form of 'lakes' occurs

when the bathing solution is buffered at pH 7 (i.e. near physiological pH) for three out of four ionic strengths. It was noted Chapter 5, section V, that the maximum transmission occurs at pH 7 at μ = .02 and at pH 8 at μ = .15 for all wavelengths i.e. near physiological pH. Thus, it appears that there may be some correlation between the percentage of water in the 'lakes' and the transmission of the stroma such that maximum transmission occurs in a solution which produces the smallest percentage 'lakes'.

VIII Suggestion for Further Work.

The studies presented in the last four chapters suggest further work which could be undertaken either to improve the techniques used in these studies or using different techniques.

(i) A more detailed study of the amount of swelling with ionic strength of the bathing solution especially between μ = .1 and μ = .15 to find the exact minimum and maximum in the swelling curve.

(ii) Studies on the time dependence of the swelling changes as the pH is increased slightly above the point of minimum swelling would be interesting in order to find at what pH continuous swelling begins (i.e. when there are little or no attractive forces opposing the osmotic pressure).

(iii) Refinement of the theory presented in Chapter 2 would be possible if the relationship between the Onsager coefficient L_{pd} and hydration was known for a wide range of hydrations. This would make the deduction from the measurements of flow conductivity unnecessary.

(iv) The X-ray diffraction results do not cover a very large range of hydration because the interfilament spacing which we can measure

is limited by the apparatus to a maximum around 90 nm. Such a spacing corresponds to a relatively low hydration i.e. under H = 10 and it can be seen from Chapter 2 that much higher hydrations can occur within several hours. Thus, x-ray diffraction results are obtained only over a narrow range of hydrations. This limitation means that hydrations at which one would expect a possible large volume of non-lattice water was not studied.

A technique which could prove useful in extending the x-ray diffraction data is that of neutron diffraction. With neutrons, larger spacings can be measured because of the large range of energies (and hence wavelengths) which are possible, the high intensity available and the long specimen-to-detector distance which can be used. It may also prove possible to use the line-width of the neutron reflections in a similar way to that proposed for x-ray reflections (section III, this chapter). However, the usual wavelength spread for neutrons is around 7% so that a special monochromator would be needed to decrease the spread to 1% with a consequential loss in intensity of the neutron beam. The Biophysics group have applied for facilities to carry out this work on the ILL neutron camera at Grenoble.

(v) In chapter 3, laser light diffraction patterns from electron micrographs were obtained. Fig. 22 (Chapter 3) shows that such diffraction patterns from corneal tissue, at approximately normal hydration initially, showed three diffraction rings which might possibly correspond to d_{10} , d_{20} and d_{22} of an hexagonal lattice. The number of orders of diffraction could possibly be improved by making a mask of the electron micrograph by punching holes at the exact positions of the fibrils but of a smaller size than the fibrils on the electron micrograph. Thus, the overall shape of the trans-

form is changed such that is should decrease more slowly.

(vi) The reliability of the microelectrode results depend on the accurate knowledge of the tip potential and resistance of the microelectrode. Relatively little is known about tip potentials at present so that the restriction involved in Chapter 4 in which electrodes with tip potential, which are constant in the range 10 to 100 mMol NaCl, are employed must be carefully adhered to. The standard error of the results are large, often being as much as 25% and may be improved by increasing the number of data points. It would be useful to know the activities of the permeant ions. This could be accomplished using ion-selective microelectrodes. Further more it would be useful to find out whether there is a resistivity change in the electrode when it penetrates the tissue. This would mean modification of the existing apparatus.

APPENDIX 1.

The Significance of the Linear Regressions - F-ratio.

The significance of the linear relation obtained from the regression fit of the data is conveniently given in the form of a f-ratio whose value can be compared with that from statistical tables in order to determine whether the linear fit is significant. The f-ratio is the ratio of the variances of two samples of different size from the same population. If the f-ratio is significant, then it is unlikely that the two samples are from the same normal population or from normal populations of equal variance. The details about the f-ratio test, given in this appendix, can be found in Weatherburn (1968).

The significance of a regression function is defined as the ratio of the variance of the regression function from the average value of the function to the deviation of the regression function from the measured values. If we have N pairs of x_i, y_i variables whoses means are $\bar{x}$, $\bar{y}$, respectively, then the variation of the regression function is $\sum_i (Y_i - \bar{y})^2$ where Y_i is the value of y_i given by the regression function. The deviation of the regression function from the experimental data is $\sum (y_i - Y_i)^2$. These two expression can be written in terms of the correlation coefficient, r, which is defined as

$$r = \frac{\sum f_i (x_i - \bar{x})(y_i - \bar{y})}{(\sum f_i (x_i - \bar{x})^2)^{\frac{1}{2}} (\sum f_i (y_i - \bar{y})^2)^{\frac{1}{2}}}$$

where f_i is the frequency of each x_i, y_i and is equal to 1/N in this case. It can be shown that (Weatherburn, 1968)

$$\sum(Y_i - \bar{y})^2 = Nr^2S_y^2$$

where S_y^2 is equal to $\sum (y_i - \bar{y})^2/N$. The sum $\sum(y_i - Y_i)^2$ can also be written in terms of r and S_y^2 so that

$$\sum(y_i - Y_i)^2 = \sum N S_y^2 (1 - r^2).$$

It is also necessary to known that number of degrees of freedom for both the sum $\sum (Y_i - \bar{y})^2$ and $\sum(y_i - Y_i)^2$. The number of degrees of freedom of the former summation is one and of the latter sum is N - 2. Thus the f-ratio is given by

$$F = NS_y^2r^2/N\ S_y^2(1-r^2)/(N-2) = (N-2)r^2/(1-r^2)$$

where the number of degrees of freedom of the numerator and the denominator are 1 and N-2 respectively.

A value of F below the 5% points, given in the tables, is not significant. A value between 5% and 1% points is significant only at the 5% level. If the value of F is higher than the 1% level, it can be regarded as highly significant. (Weatherburn, 1968).

The 1% point for F varies from 11.26 for 8 degrees of freedom, i.e. 8 pairs of data are used to calculate the regression fit, to 7.31 for 40 pairs of data (Hodgman, 1959).

REFERENCES.

Abramowitz, M. and Stegun, I.A. (1970). Handbook of Mathematical Functions, New York, Dover Publications.

Adler, H. J., Gross, S.T. and Lambert, J.M. (1949). Science, 109, 383-384.

Adrian, R.H. (1956). J. Physiol., 133, 631-658.

Agarwal, L.P., Chand, D., Mishra, R.K. and Khosla, P.K. (1972). Orient. Arch. Ophthal., 10, 238-245.

Anderson, B., Hoffman, P. and Meyer, K. (1963). Biochim. biophys. Acta, 74, 309-311.

Anderson, B., Hoffman, P. and Meyer, K. (1965). J. biol. Chem., 240, 156-167.

Anseth, A. (1961). Expl Eye Res., 1, 106-115.

Anseth, A. and Laurent, T.C. (1961). Expl Eye Res., 1, 25-38.

Aurell, G. and Holmgren, H. (1941). Z. mikro-anat. Forsch., 50, 446-457.

Aurell, G. and Holmgren, H. (1953). Acta Ophthal, Kbh., 31, 1-27.

Azaroff, L.V. (1968). Elements of X-ray crystallography, New York, McGraw-Hill.

Bailey, A.J. and Peach, C. (1969). Biochem. J., 111, 12P.

Banga I. (1966). Structure and Function of Elastin and Collagen, Budapest, Akademiai Kiado.

Bear, R.S. (1942). J. Am. Chem. Soc., 64, 727

Bear, R.S. (1944). J. Am. Chem. Soc., 66, 1297-1305.

Bear, R.S. (1952). Adv. Protein Chem., 7, 69-160.

Benedek, G.B. (1971). Applied Optics, 10, 459-473.

Berman, E.R. and Saliternik-Givant, S. (1968). In 'Symposium of the eye', Tutzing, 1966, Basel, Karger, 29-42.

Bernal, J.D. and Fankucken, I. (1941). J. gen. Physiol., 25, 111-120.

Bettelheim, F.A. and Vinciguerra, M.J. (1969). Biochim. biophys. Acta, 177, 259-264.

Bhavanandan, V.P. and Meyer, K. (1966). Science, 151, 1404-1405.

Bhavanandan, V.P. and Meyer, K. (1967). J. biol. Chem., 242, 4352-4359.

Bito, L.Z. and Saraf, S. (1973). Expl Eye Res., 16, 315-325.

Bleckmann, H. and Wollensak, J. (1974). Albrecht v Graefes Arch. klin. exp. Ophthal., 189, 71-80.

Blümke, S. and Morgenroth, K. jr. (1967). J. Ultrastruct. Res. 18, 502-528.

Boettner, E.A. and Wolter, J.R. (1962). Invest. Ophthal., 1, 776-783.

Bolková, A. and Čejková, J. (1971). Ophthal. Res., 2, 126-131.

Bowes, J.H. and Kenten, R.H. (1950). Biochem. J., 46, 1-8.

Brenner, S.L. and McQuarrie, D.A. (1973). J. Theor. Biol., 39, 343-361.

Brenner, S.L. and Parsegian, V.A. (1975). Expl Eye Res., In Press.

Brophy, J.J. (1966). Basic Electronics for Scientists, New York, McGraw-Hill.

Brown, S.I. and Hedbys, B.O. (1965). Invest. Ophthal., 4, 216-221.

Bungenberg de Jong, H.G. (1949). In 'Colloid Science, II,'. Ed. Kruyt, H.R., New York, Elsevier.

Burge, R.E. and Randall, J.T. (1955). Proc. Roy. Soc. London, 233, 1-16.

Caspersson, T. and Engström, A. (1949). Nord. Med., 30, 1279-1282.

Castellani, A.A. (1967). Biochem. J., 104, 16P.

Castillo, del J. and Katz, B. (1955). J. Physiol., 128, 396-411.

Čejkova, J. and Bolkova, A. (1970). Ophthal. Res., 1, 273-278.

Čejkova, J. and Brettschneider, I. (1969). Histochemie, 17, 327-336.

Chandross, R.J. and Bear, R.S. (1973). Biophys. J., 13, 1030-1048.

Chapman, J.A. and Steven, F. (1966). In 'Biochemie and Physiologie du Tissu Conjontif.', Ed. Comte, P., Lyon, Societe Ormeco.

Cogan, D.C. (1951). Trans. Am. Acad. Ophthal. oto-lar, 55, 329-359.

Cogan, D.C. and Kinsey, V.E. (1942). Arch. Ophthal., Chicago, 27, 466-476.

Collins, E.W. and Edwards, C. (1971). Am J. Physiol., 221, 1130-1132.

Coulombre, A.J. and Coulombre, J.L. (1958). J. Cell Comp. Physiol., 51, 1-11.

Coulombre, A.J. and Coulombre, J.L. (1961). In ' The Strucure of the Eye', Ed. Smelser, G.K., New York and London, Academic Press, 405-419.

Cox, J.L., Farrell, R.A., Hart, R.W. and Langham, M.E. (1970). J. Physiol., 210, 610-616.

Curtis, H.J. and Cole, K.S. (1942). J. Cell. Comp. Physiol., 19, 135-144.

Cox, R.W., Grant, R.A. and Horne, R.W., (1967). J. R. Microsc. Soc., 87, 123-142.

Davis, T.L., Jackson, J.W., Day, B.E., Shoemaker, R.L. and Rehm, W.S. (1970). Am J. Physiol., 219, 178-183.

Davson, H. (1949). Brit. J. Ophthal., 33, 175-181.

Davson, H. (1955). Biochem. J., 59, 24- 28.

Dawson, R.M.C., Elliott, D.C., Elliott, W.H. and Jones, K.M. (1969). Data for Biochemical Research. Oxford, Clarendon, 2nd Ed., chapter 20.

Disalvo, J. and Schubert, M. (1966). Biopolymers, 4, 247-258.

Dohlman, C.H. and Anseth, A. (1957). Acta Ophthal., 35, 73-84.

Dohlman, C.H. and Balazs, E. (1955). Archs. Biochem., 57, 445-457.

Dohlman, C.H. and Balazs, E. (1957). Acta Ophthal., 35, 454-460.

Dohlman, C.H., Hedbys, B.O. and Mishima, S. (1962). Invest. Ophthal., 1, 158-162.

Donn, A. (1962). Invest. Ophthal., 1, 170-177.

Doyle. B.B., Hukins, D.W.L., Hulmes, D.J.S., Miller, A., Rattew, C.J. and Woodhead-Galloway, J. (1974a). Biochem.Biophys. Res. Commun., 60, 858-864.

Doyle, B.B., Hulmes, D.J.S., Miller, A., Parry, D.A.D., Piez, K.A., and Woodhead-Galloway, J. (1974b). Proc. R. Soc. London, B, 186, 67-74.

Duane, T.D. (1949). Am. J. Ophthal., 32, 203-207.

Ehlers, N. (1966). Acta Ophthal., 44, 620-630.

Ehlers, N. (1973). Expl Eye Res., 15, 553-565.

Elliott, G.F. (1960). PhD. Thesis, University of London.

Elliott, G.F. (1968). J. Theor. Biol., 21, 71-87.

Elliott, G.F., Lowy, J. and Worthington, C.R. (1963). J. Mol. Biol., 6, 295-305.

Ericson, L.G. and Tomlin, S.G. (1959). Proc. R. Soc. A, 252, 197-216.

Farber, S.J. and Schubert, M. (1957). J. Clin. Invest., 36, 1715-1722.

Farrell, R.A. and Hart, R.W. (1969). Bull. Math. Biophys., 31, 727-759.

Farrell, R.A., McCally, R.L. and Tatham, P.E.R. (1973). J. Physiol., 233, 589-612.

Fatt, I and Goldstick, T.K. (1965). J. Colloid Sci., 20, 962.

Fatt, P. (1961). In ' Methods of Medical Research 9'. Ed. Quastel, G.H., Chicago, Year Book Medical Publication, 381-404.

Feeney, M.L. and Garron, L.K. (1961). In ' The Structure of the Eye'. Ed. Smelser, G.K., New York, Academic Press, 367-380.

Feuk, T. (1970). IEEE Trans. Biomed. Eng. BME-17, 186-190.

Feuk, T. (1971). IEEE Trans. Biomed. Eng. BME-18, 92-95.

Feuk, T. and McQueen, D. (1971). Invest. Ophthal., 10, 294-299.

Fisher, F.P. (1933). Arch. Augenheilk., 107, 295-318.

François, J. and Rabaey, M. (1956). Arch. Ophthal., Kbh., 34, 45-62.

François, J. and Rabaey, M. (1960). In 'The Transparency of the Cornea, a symposium'. Ed. Duke-Elder, S. and Perkins, E.S., Oxford, Blackwell.

François, J., Rabaey, M. and Vandermeerssche, G. (1954). Ophthalmologica, Basel, 127, 74-85.

Franks, A. (1955). Proc. Phys. Soc. B, 68, 1054-1068.

Fransson, L-Å. and Anseth, A. (1967). Expl Eye Res., 6, 107-119.

Freeman, I.L., Steven, F.S. and Jackson, D.S. (1968). Biochim. Biophys. Acta, 154, 252-254.

Friedman, E. and Kupfer, C. (1960). Arch. Ophth., 64, 892-896.

Friedman, M.H. (1971). J. Theor. Biol., 30, 93-109.

Friedman, M.H. and Green, K. (1971a). Am. J. Physiol., 221, 356-362.

Friedman, M.H. and Green, K. (1971b). Expl Eye Res., 12, 239-250.

Friedman, M.H., Kearns, J.P., Michenfelder, C.J. and Green, K.

(1972). Am. J. Physiol., 222, 1565-1570.

Garzino, A. (1955). Rass. ital. Ottal., 24, 118-157.

Goldman, J.N. and Benedek, G.B. (1967). Invest. Ophthal., 6, 574-599.

Goldman, J.N., Benedek, G.B., Dohlman, C.H.,and Kravitt, B. (1968). Invest. Ophthal., 7, 501-519.

Gould, B.S. (1968). Treatise on Collagen, Vol. 2. London, Academic Press.

Grant, M.E., Freeman, I.L., Schofield, J.D. and Jackson, D.S. (1969). Biochim. Biophys. Acta, 177, 682-685.

Grant, R.A., Cox, R.W. and Horne, R.W. (1967). J. R. Microsc. Soc., 87, 143-155.

Green, K. and Friedman, M.H. (1971). Am. J. Physiol., 221, 363-367.

Green, K. Hastings, B. and Friedman, M.H. (1971). Am. J. Physiol., 220, 520-525.

Greilung, H. and Stuhlsatz, H.W. (1966). Hoppe-Seyler's Z. Physiol. Chem., 345, 236-248.

Greilung, H., Stuhlsatz, H,W. and Kisters, R. (1967). Hoppe- Seyler's Z. Physiol. Chem., 348, 970-978.

Harris, J.E. (1957). Am. J. Ophthal., 44, 262-280.

Hart, R.W. and Farrell, R.A. (1971). Bull, Math.Biophys., 33, 165-186.

Hart, R.W., Farrell, R.A. and Langham, M.E. (1969). APL Technical digest.

Hedbys, B.O. (1961). Expl Eye Res., 1, 81-91.

Hedbys, B.O. and Dohlman, C.H. (1963). Expl Eye Res., 2, 122-129.

Hedbys, B.O. and Mishima, S. (1962). Expl Eye Res., 1, 262-275.

Hedbys, B.O. and Mishima, S. (1966). Expl Eye Res., 5, 221-228.

Hedbys, B.O., Mishima, S. and Maurice, D.M. (1963). Expl Eye Res., 2, 99-111.

Helfferich, F. (1962). Ion Exchange. New York, McGraw-Hill.

Heringa, G.C., Leyns, W.F. and Weidinger,A. (1940). Acta neerl. Morph., 3, 196-201.

Hertel, E. (1933). Archiv für Augenheilk., 107, 260-293.

His, W. (1856). Beiträge zur normalen und pathologischen Histologie der Cornea. Basel, Schweighauser.

Hodge, A.J. and Schmitt, F.O. (1960). Proc. natn Acad. Sci., USA, 46, 186-197

Hogkin, A.L. and Huxley, A.F. (1962). J. Physiol., 116, 449-472.

Hogman, C.D. (1959). Mathematical Tables from Handbook of Chemistry and Physics. Cleveland, Chemical Rubber Publishing Co..

Hodson, S. (1968). Expl. Eye Res., 7, 221-224.

Hodson, S. (1971). J. Theor. Biol., 33, 419-427.

Hodson, S. and Meenan, A. (1969). Separatum Experientia, 25, 1305.

Hulmes, D.J.S., Miller, A., Parry, D.A.D., Piez, K.A. and Woodhead-Galloway, J. (1973). J. Mol. Biol., 79, 137-148.

Huxley, H. E. (1963). J. Mol. Biol., 7, 281-308.

Itoi, M. (1961). Expl Eye Res., 1, 92-97.

Iwamoto, T. and Smelser, G.K. (1965). Invest. Ophthal., 4, 270-284.

Jakus, M.A. (1954). AM. J. Ophthal., 38, 40-53.

Jakus, M.A. (1956). J. biophys. biochem. Cytol. Suppl, 2, 241-252.

Jakus, M.A. (1962). Invest. Ophthal., 1, 202-225.

Jakus, M.A. (1964). Ocular Fine Structure Selected Electron Micrographs. London, Churchill.

James, R.W. (1962). The Optical Principles of the Diffraction of X-rays. Ed. Sir L. Bragg, London, Bell and Sons, Ltd..

Jenkins, F.A. and White, H.E. (1951). Fundamentals of Optics, 2nd. Ed., London, McGraw-Hill.

Kaesberg, P. and Shurman, M.M (1953). Biochim. Biophys. Acta, 11, 1-6.

Kanai, A. and Kaufman, H. (1973a). Annals Ophthal., 5, 178-190.

Kanai, A. and Kaufman, H. (1973b). Annals Ophthal., 5, 667-674.

Kapfhammer, J. (1942). Albrecht v Graefes Arch. Ophthal., 144, 182-185.

Kaplan, D. and Bettelheim, F.A. (1972). Expl Eye Res., 13, 219-226.

Katchalsky, A. (1954). J. Polymer Sci., 12, 159-184.

Katchalsky, A. and Curran, P.F. (1967). Nonequilibrium Thermodynamics. Cambridge, Mass., Havard University Press.

Kaye, G.I., Pappas, G.D. and Donn, A. (1961). Anat. Rec., 139, 244-245.

Kaye, G.I., Pappas, G.D., Donn, A. and Mallett, N. (1962). J. Cell Biol., 12, 481-501.

Kennard, D.W. (1958). In 'Electronic Apparatus for Biological Research'. Ed. Donaldson, P.E.K., London, 534-567.

Kern, H.L. and Brassil, D. (1967). Archs. Biochem. Biophys., 118, 115-121.

Kikkawa, Y. (1958). Jap. J. Physiol., 8, 138-147.

Kikkawa, Y. (1960). Jap. J. Physiol., 10, 292-302.

Kikkawa, Y. (1964). Expl Eye Res., 3, 132-140.

Kikkawa, Y, (1966). Expl Eye Res., 5, 31-36.

King, J.H. and McTigue, J.W. (1965). The Cornea - World Congress, Washington, Butterworths.

Kinoshita, A., Manabe, R. and Kikkawa, Y. (1965). Jap. J. Ophthal., 9, 48-52.

Kinsey, V.E. (1948). Archs. Ophthal., 39, 508-513.

Kinsey, V.E. and Cogan, D.G. (1942). Arch. Ophthal., 28, 272-284.

Klyce, S.D. (1972). J. Physiol., 226, 407-429.

Klyce, S.D. (1973). Expl Eye Res., 15, 567-575.

Krause, A.C. (1934). The Biochemistry of the Eye. New York, John Hopkins Press.

Kühn, K. (1969). Essays in Biochemistry, 5, 59-87.

Langham, M.E., Hart, R.W. and Cox, J. (1969). In 'The Cornea: Macromolecular Organisation of the Corneal Connective Tissue'. Ed. Langham, M.E., Baltimore, John Hopkins Press, 157-183.

Langham, M.E. and Taylor, I.S. (1956). Brit. J. Ophthal., 40, 321-340.

Laurent, T.C. (1968). In The Chemical Physiology of Mucopolysaccharides'. Ed. Quintavelli, G., Boston, Little, Brown & Co.

Laurent, T.C. and Anseth, A. (1961). Expl Eye Res., 1, 99-105.

Lavallée, M. (1964). Circulation Res., 15, 185-193.

Lewis, M.S., Dubin, M.W. and Aandahl, V.A. (1967). Expl Eye Res., 6, 57-69.

Leydhecker, W., Akiyama, K. and Neumann, H.G. (1958). Klin. Mbl. Augenheilk., 133, 662-670.

Leyns, W.F., Heringa, G.C. and Weidinger, A. (1940). Acta Brev. Neerland, 10, 25-26.

Ling, G. and Gerard, R.W. (1949). J. Cell. Comp. Physiol., 34, 382-396.

Loeven, W.A. (1955). Acta Anat., 24, 217-244.

Loeven, W.A. and Van Walbeek, K. (1954). Biochim. biophys. Acta, 14, 471-481.

Lowther, D.A. and Natarajan, M. (1972). Biochem. J., 127, 607-608.

McTigue,J.W. (1965). In 'The Cornea : World Congress', Eds. King, J.H. and McTigue, J.W., Washington, Butterworths, 49-60.

Mallard, E. (1884). Traite de Crystallographie, 2, Chapter 8, Paris, Di mond.

Maroudas, A. (1975). J. Biorheology, In Press.

Maroudas, A. and Thomas, H. (1970). Biochim. biophys. Acta, 215, 214-216.

Mathews, M.B. (1965). Biochem. J., 96, 710-716.

Mathews, M.B. (1967). In 'Connective Tissue', Eds Wagner, B.M. and Smith, D.E., Baltimore, Williams and Wilkins, 309-329.

Mathews, M.B. (1970). In 'Chemistry and Molecular Biology of the Intercellular matrix', Ed. Balazs, E.A., New York, Academic Press, 1155-1169.

Mathews, M.B. and Cifonelli, J.A. (1965). J. biol. Chem.,240, 4140-4145.

Mathews, M.B. and Decker, L. (1968). Biochem. J., 109, 517-526.

Maurice, D.M. (1957). J. Physiol., 136, 263-286.

Maurice, D.M. (1962). In 'The Eye', Ed. Davson, H., London, Academic Press , Vol. 1.

Maurice, D.M. (1967). In 'The Cornea', a symposium, Kyoto, 1967, Ed. Langham, M.E., Vol. 1, 193-204.

Maurice, D.M. (1969). In 'The Eye', Ed. Davson, H., 2nd Ed., London, Academic Press.

Maurice, D.M. and Giardini, A.A. (1951). Brit. J. Ophthal., 35, 791-797.

Maurice, D.M. and Riley, M.V. (1970). In 'Biochemistry of the Eye', Ed. Graymore, C.N., London, Academic Press.

Meyer, K., Linker, A., Davidson, E.A. and Weissmann, B. (1953). J. biol. Chem., 205, 611-616.

Miller, A. and Woodhead-Galloway, J. (1971). Nature (London), 229, 470.

Miller, A. and Wray, J.S. (1971). Nature, 230, 437-439.

Moczar, E., Moczar, M. and Robert, L. (1967). Biochem. biophys. Res.,Commun., 28, 380 - 389.

Modrell, R.W. and Potts, A.M. (1959). Am. J. Ophthal., 48, 834-842.

Muir, H. (1958). Biochem. J., 69, 195-204.

Myers, D.B., Highton, T.C. and Rayns, D.G. (1969). J. Ultrastruct. Res., 28, 203-213.

Myers, D.B., Highton, T.C. and Rayns, D.G. (1973). J. Ultrastruct. Res., 42, 87-92.

Nastuk, W.L. (1953). J. Cell. Comp. Physiol., 42, 249-272.

Nastuk, W.L. and Hodgkin, A.L. (1950). J. Cell. Comp. Physiol., 35, 39-73.

Naylor, W.G. and Merrillees, N.C.R. (1964). J. Cell Biol., 22,533-550.

Nemetschek, T. (1965). Z. Naturfors., 20, 77-79.

Obenberger, J., Čejková, Bolková, A. and Babický, A. (1971). Ophthal. Res., 2, 266-272.

Obrink, B. (1973). Eur. J. Biochem., 33, 387-400.

Oster,G. and Riley, D.P. (1952). Acta Cryst., 5, 272-276.

Otori , T. (1967). Expl Eye Res., 6, 356-367.

Overbeek, J. Th. G. (1956). Prog. Biophys. & Biophys Chem., 6, 58-84.

Partridge, S.M. (1948). Biochem. J., 43, 387-397.

Pau, H. (1954). Graefes Archiv. fur Ophthal., 154, 579-602.

Payrau, P. (1968). In 'Biochemistry of the Eye, a Symposium', Tutzing, 1966, Basel, Karger, 1-19.

Payrau, P. and Pouliquen, Y. (1960). Ann. d'Oculist, 193, 309-345.

Payrau, P., Pouliquen, Y., Faure, J.P., Bisson, J. and Offret, G. (1965). Arch. Ophthal., Paris, 25, 745-754.

Payrau, P., Pouliquen, Y., Faure, J.P. and Offret, G. (1967). La Transparence de la Cornée. Les Mecanismes de ses Alterations. Paris, Masson et c^ie.

Pemrick, S.M. and Edwards, C. (1974). J. gen Physiol., 64, 551-567.

Pirie, A. (1947). Biochem. J., 41, 185-190.

Polack, F.M. (1961). Am. J. Ophthal., 51, 1051-1056.

Polatnick, J., Tessa, A.J.La, and Katzim, H.M. (1957a). Biochim. biophys. Acta, 26, 361-364.

Polatnick, J., Tessa, A.J.La and Katzim, H.M. (1957b). Biochim. biophys. Acta, 26, 365-369.

Potts, A.M. and Friedman, B.C. (1959). Am. J. Ophthal., 48, 480-487.

Potts, A.M, and Moddrell, R.W. (1957). Am. J. Ophthal., 44, 284 - 289.

Ramachandran, G.N. (1962). In 'Collagen', Ed. Ramanathan, N., New York, Wiley, p3.

Ramachandran, G.N. (1967). In 'Treatise on Collagen, Vol I',New York, Academic Press.

Ranvier, L.A. (1881). Lecons d'anatomie generale faites au College de France, 9^eme lecon, 135-150, Paris, Baillère & fils.

Remé, Ch., Mueller, F.O.,and Bannasch, P. (1972). Albrecht v Graefes Arch. klin. exp. Ophthal., 185, 189-205.

Robert, B., Parlebas, J. and Robert, L. (1963). C.R. Acad. Sci., 256, 323-325.

Robert, L, and Dische, Z. (1963). Biochem. Biophys. Res. Commun., 10, 209-214.

Robert, L., Oudea, P., Zweibaum, A., Parlebas, J. and Robert, B. (1964). Protides of Biological Fluids, 12, 110-116.

Robert, L. and Robert, B. (1967). Protides of Biological Fluids, 15, 143

Robinson, R.A. and Stokes, R.H. (1959). Electrolyte Solutions. 2nd Ed., London, Butterworths.

Rome, E. (1968). J. Mol. Biol., 37, 331-344.

Saliternik-Givant, S. and Berman, E.R. (1965). Israeli J. Chem., 3, 103P.

Salzmann, M. (1912). In 'The Anatomy and Histology of the Human Eyeball in the Normal state, its Development and senscence', Trs. Brown, E.V.L., Chicago, University Press.

Sandler, S. (1974). J. Theor. Biol., 48, 207-213.

Schaefer, C. (1909). S.B. Preuss, Akad. Wiss., 31, 326-345.

Schanne , O.F. , Lavallée, M., Laprade, R. and Gagné, S. (1968). Proc. of I.E.E.E., 56, 1072-1082.

Schmitt, F.O., Hall. C.E. and Jakus, M.A. (1942). J. Cell. Comp. Physiol., 20, 11-33.

Schofield, J.D., Freeman, I.L. and Jackdon, D.S. (1971). Biochem. J., 124, 467-473.

Schubert, M. (1966). Fedn Proc. Fedn Am. Socs. Exp. Biol., 25, 1047-1052.

Schwarz, W. (1953). Z. Zellforsch., 38, 26-49.

Schwarz, W. and Graf Keyserlingk, D. (1966). Z. Zellforsch., 73, 540-548.

Seno, N., Meyer, K., Anderson, B. and Hoffmann, P. (1965). J. biol. Chem., 240, 1005-1010.

Small, J.V. and Squire, J.M. (1972). J. Mol. Biol., 67, 117-149.

Smelser, G.K. (1962). Invest. Ophthal., 1, 11-32.

Smelser, G.K. and Ozanics, V. (1965). In 'The cornea: World Congress'. Eds. King, J.H. and McTigue, J.W., Washington, Butterworths, 1-20.

Smith, J.W. (1968). Nature, 219, 157-158.

Smith, J.W. (1969). Vision Res., 9, 393-396.

Smith, J.W. and Frame, J. (1969). J. Cell Sci., 4, 421-436.

Smits, G. (1957). Biochim. biophys. Acta, 25, 542-548.

Speakman, J.S. (1959). Archs. Ophthal., N.Y., 62, 882-888.

Stanworth, A. and Naylor, E.J. (1953). J. exp. Biol., 30, 160-163.

Svedbergh, B. and Bill, A. (1972). Acta Ophthal, 50, 321-336.

Tasaki, I. and Singer, I. (1968). Ann N.Y. Acad. Sci., 148, 36-53.

Tomlin, S.G. and Worthington, C.R. (1956). Proc. R. Soc., 235, 189-201.

Toole, B.P. and Lowther, D.A. (1968). Biochem. J., 109, 857-866.

Topping, J. (1962). Errors of Observation and their Treatment. 3rd Ed., London, Chapman and Hall.

Trelstad, R.L. and Kang, A.H. (1974), Expl Eye Res., 18, 395-406.

Trenberth, S.M. and Mishima, S. (1968). Invest. Ophthal., 7, 44-52.

Tripathi, R.C. and Tripathi, B.J. (1972). Contact Lens, 3, 10-15.

Urrets-Zavalia, A. (1963). Bull. Soc. frac. Ophthal., 76, 547-554.

Van den Hoof, A. (1952). Proc. Kan. Ned. Ak. v. Wet., Ser.C., 55 628-633.

Van Walbeek, K. and Neumann, H. (1951). Arch. Ophthal., 46, 482-487.

Virchow, H, (1910). In 'Graefe-Saemisch Handbuch derGesamten Augenheilkunde', Leipzig, Engelmann, 37-183.

Weatherburn, C.E. (1968). A First Course in Mathematical Statistics. Cambridge, University Press, 196-200 and 223-226.

Weiss, R.M., Lazzara, R. and Hoffman, B.F. (1967). Nature, London, 215, 1305-1307.

Witz., J. (1969). Acta Cryst., A25, 30-42.

Wolpers, C. (1944). Virchow's Archiv. f. Path., 312, 292-302.

Wood, G.C. (1960). Biochem. J., 75, 605-612.

Woodin, A.M. (1952). Biochem. J., 51,319-330.

Woodin, A.N. (1954). In XVII Int. Ophthal. Congress, 1, 475-581.

Wortman, B. (1964). Biochim. biophys. Acta, 83, 288-295.

Yamamoto, K., Nobuto, F. and Kobashi, T. (1965). Folia Ophthal. jap., 16, 554-559.

Yannas, I.V. (1972). J. Macromol. Sci. Revs. Macromol. Chem., C7 (i), 49-104.